

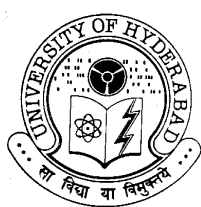
# **Synthesis and Reactions of Tröger Base Derivatives**

A Thesis

Submitted for the Degree of  
**DOCTOR OF PHILOSOPHY**

By

**Sundaram Suresh**



**SCHOOL OF CHEMISTRY**  
**UNIVERSITY OF HYDERABAD**  
**HYDERABAD-500046**  
**INDIA**  
**June-2016**

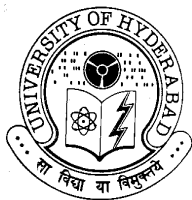
**To**  
**My Mother**

## Contents

<b>Statement</b>	i
<b>Certificate</b>	iii
<b>Acknowledgements</b>	v
<b>Abbreviations</b>	vii
<b>Abstract</b>	ix
<b>1. Introduction</b>	1
1.1 Synthesis of Tröger base derivatives	4
1.2 Chirality of Tröger base derivatives	5
1.2.1 Resolution of Tröger base derivatives	9
1.2.2 Diastereoselective synthesis of Tröger base derivatives	14
1.3 Reactions of Tröger base derivatives	15
1.3.1 Quaternary ammonium salts of Tröger base derivatives	16
1.3.2 Functionalization of benzylic methylene unit of Tröger base	17
1.3.3 Reactions of methylene bridge of Tröger base	18
1.3.4 Effect of diazocine bridgehead of Tröger base on the torsion balance	22
1.4 Applications of Tröger base transition–metal complexes	22
1.5 Applications of Tröger base and its derivatives in asymmetric transformations	23
1.6 Synthesis of various tetrasubstituted Tröger base derivatives	25
1.7 Previous methods for resolution of racemic mixtures developed in this laboratory	27
<b>2. Results and Discussion</b>	29
2.1 Resolution of dimethyl Tröger base: (±)-2,4,8,10-tetramethyl-6H,12H-5,11-methanodibenzo[b,f][1,5]diazocine	29
2.2 Resolution of dibromo Tröger base: (±)-2,8-dibromo-4,10-dimethyl-6H,12H-5,11-methanodibenzo[b,f][1,5]diazocine	36
2.3 Resolution of 4,10-dibromo Tröger base: (±)-4,10-dibromo-2,8-dimethyl-6H,12H-5,11-methanodibenzo[b,f][1,5]diazocine	41
2.4 Resolution of dimethoxy Tröger base: (±)-4,10-dimethoxy-2,8-dimethyl-6H,12H-5,11-methanodibenzo[b,f][1,5]diazocine	47

2.5	Synthesis of 5,11-substituted Tröger base derivatives	52
2.5.1	Exchange of the methylene bridge of Tröger base with dimethylformamide	52
2.5.2	Diastereoselective synthesis of Tröger base derivatives	58
2.5.3	Epimerization of Tröger base derivatives	64
2.5.4	Stereoselective exchange of methylene bridge of Tröger base with formamides	70
2.6	Reaction of Tröger base with aryne intermediates	75
2.7	Hydroboration of prochiral olefins using chiral Tröger base-borane complexes	85
2.7.1	Asymmetric Hydroboration using chiral amine borane complexes	85
2.7.2	Iodine activation of chiral amine borane complexes	86
2.7.3	Hydroboration of prochiral olefins using chiral <i>ortho</i> -substituted Tröger base borane complexes	89
2.7.4	Hydroboration of prochiral olefins using chiral <i>para</i> -substituted Tröger base borane complexes under iodine activation	91
2.8	Charge transfer complexes of Tröger base derivatives	94
2.9	Conclusions	123
<b>3.</b>	<b>Experimental section</b>	125
	<b>References</b>	177
	<b>Appendix I (Representative spectra)</b>	191
	<b>Appendix II (X-Ray crystallographic data)</b>	235
	<b>Appendix III Synthesis and application of poly(<i>N</i>-methylaniline)</b>	249
	<b>List of publications</b>	271





School of Chemistry  
University of Hyderabad  
Central University P. O.  
Hyderabad 500 046  
India

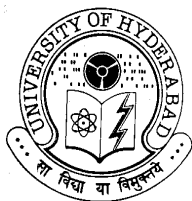
---

## Statement

I hereby declare that the matter embodied in this thesis is the result of investigations carried out by me in the School of Chemistry, University of Hyderabad, Hyderabad, under the supervision of **Professor M. Periasamy**.

In keeping with the general practice of reporting scientific observations, due acknowledgement has been made wherever the work described is based on the findings of other investigators.

**SUNDARAM SURESH**



School of Chemistry  
University of Hyderabad  
Central University P. O.  
Hyderabad 500 046  
India

---

## Certificate

Certified that the work embodied in this thesis entitled “**Synthesis and Reactions of Tröger Base Derivatives**” has been carried out by **Mr. Sundaram Suresh** under my supervision and the same has not been submitted elsewhere for a Degree.

**PROFESSOR M. PERIASAMY**  
(THESIS SUPERVISOR)

**DEAN**  
**SCHOOL OF CHEMISTRY**

## Acknowledgements

With profound respect, I wish to express my heartfelt gratitude and indebtedness to my thesis supervisor **Prof. M. Periasamy** for his constant guidance, inspirations, encouragements and morale support throughout my tenure here. I owe my sincere thanks for suggesting historic problems.

My sincere thanks to Prof. D. Basavaiah, Prof. M. V. Rajasekharan and Prof. M. Durga Prasad Deans, School of Chemistry, for providing all the necessary facilities to carry out my research work.

I would like to thank Prof. Surya Prakash Rao, Department of Chemistry, Pondicherry University, for his inspiring teaching during my M.Sc chemical sciences. I also thank all the other faculty members of the chemistry department for their excellent teaching. I take this opportunity to thank V. C. Senthil kumar for his inspiring teaching during my B.Sc and his friends Dr. A. Chandrakumar and Dr. Sivaraj for their motivational talk.

I am thankful to my doctoral committee members Dr. Muralidharan and Dr. A. K. Sahoo for their generous support. I wish to thank my senior colleague Dr. Sakilam Satishkumar for his help during the initial stages of my research. I extend my sincere thanks to my past and present labmates Dr. P. Vairaprakash, Dr. Shaik Anwar, Dr. S. Selva Ganesan, Dr. M. Nagaraju, Dr. Mallesh Beesu, Dr. N. Sanjeeva Kumar, Dr. Guru Brahmam, Dr. Manasi Dalai, Dr. A. Laxman, Dr. P. Obula Reddy, Mr. M. Shanmugaraja, Mr. A. Edukondalu, Mr. Ramusagar, Mr. V. Harish, Mr. G. Ananda rao, Mr. B. Uday Kumar, Mr. I. Satyanarayana, Mr. L. Mohan, Mr. E. Ramesh, Mr. Yesu and Mr. Srinivas for creating a pleasant working atmosphere.

All the research scholar of the school of chemistry have been extremely helpful, I thank them all. I specially thank Mr. Krishnachary, Mr. Suresh, Ms. P. Srujana, Dr. Bharat Kumar Tripuramallu, Dr. Gangadhar, Dr. Ramesh, Dr. Ragavaiah, Dr. Chandrashekar, Dr. Thirupathi reddy, Dr. Naveen, Mr. Siva reddy, Dr. Srinivasa rao, Mr. Obaiah, A to Z are to mention. I also thank all my Tamil friends of University of Hyderabad.

I thank Dr. P. Raghavaiah and Ms. Lakshmi for their help in X-ray data collection. All the non-teaching staff of the School has been helpful, I thank them all. Mr. Shetty, Mr. S.

Satyanarayana, Mrs. Vijaya Lakshmi, Mr. V. Bhaskar Rao, Mr. Asia Parwez, Mr. Vijaya Bhaskar, Mr. K. R. V. Prasad, Mr. Ramana, Mr. Joseph, Mr. Santosh and, Mr. Sambasiva Rao are a few to mention.

I specially thank my M.Sc classmates Dr. K. Durga Prasad, Dr. Sanatan nayak, Dr. Avinash Desai, Dr. Veerabhadrrao Avula, Dr. Periyaraja, Dr. Ganesh majji, Mr. Rama raju jella, Dr. Srikanth peddireddy, Dr. Anil Kumar, Dr. M. Ravi, Mr. Raveendra kumar, Mr. Rama Krishna, Mr. Ranga Prasad, Mr. Yasodha krishna sunkari, Mr. Yasoda krishna sajja, Mr. Srinivasarao kondaparla, Mr. L. Seva Naik, Mr. Mekka sudhakar, Ms. Sireesha Kanuri and Ms. Lakshmi Aparna Nallapati.

I wish to express my gratitude to my parents Mr. R. Sundaram and Mrs. S. Periyammal and my brother S. Raja and my grandmother for their affections and caring at each and every stage of my life. I specially thank my wife M. Savithri for her affection and caring.

I wish to extend my sincere thanks to the University authorities for providing all the necessary facility for this work. The X-ray crystallography data were collected in the National Single Crystal X-ray facility funded by DST, New Delhi.

Finally, I would like to thank the CSIR, New Delhi for the financial support during my tenure. Also, financial assistance from the research grant of DST-J.C BOSE National fellowship of Prof. M. Periasamy is gratefully acknowledged.

**Sundaram Suresh**

## Abbreviations

$[\alpha]_{\text{D}}^{25}$	specific rotation at 25 °C, $\lambda = 589$ nm.
Ac	acetyl
anhyd.	anhydrous
aq.	aqueous
Ar	aryl
BINAP	2,2'-bis(diphenylphosphino)-1,1'-binaphthyl
Bn	benzyl
br	broad (in spectroscopy)
Bu	butyl
Bz	benzoyl
conf	configuration
cp	cyclopentadienyl
CIAT	crystallization induced asymmetric transformation
CSA	10-camphorsulfonic acid
d	doublet (in spectroscopy)
dba	dibenzylideneacetone
DBTA	<i>O,O</i> -dibenzoyltartaric acid
de	diastereomeric excess
DEPT	distortionless enhancement by polarization transfer
DMF	<i>N,N</i> -dimethylformamide
DEF	<i>N,N</i> -diethylformamide
DMSO	dimethyl sulfoxide
dr	diastereomeric ratio
ee	enantiomeric excess
EI	electron impact (in mass spectrometry)
equiv.	equivalent
Et	ethyl
h	hour(s)
HPLC	high performance liquid chromatography
<i>i</i>	iso
IPA	2-propanol
IR	infrared

<i>J</i>	coupling constant (in NMR spectroscopy)
m	multiplet (in spectroscopy)
Me	methyl
min	minute(s)
mp	melting point
MS	mass spectrum
NMR	nuclear magnetic resonance
Nu	nucleophile
ORTEP	Oak Ridge Thermal Ellipsoid Plot
Pent	pentyl
Ph	phenyl
PNMA	poly( <i>N</i> -methylaniline)
ppm	parts per million
Pr	propyl
q	quartet (in spectroscopy)
ref	reference number
rt	room temperature
s	singlet (in spectroscopy)
sat.	saturated
<i>sec</i>	secondary
SET	single electron transfer
soln	solution
T	temperature
<i>t</i>	tertiary
t	triplet (in spectroscopy)
TB	Tröger base
ETB	ethylene bridged Tröger base
TFA	trifluoroacetic acid
TFAA	trifluoroacetic anhydride
THF	tetrahydrofuran
TMEDA	<i>N,N,N',N'</i> -tetramethylethylenediamine
TMS	trimethylsilyl
Uv	ultraviolet

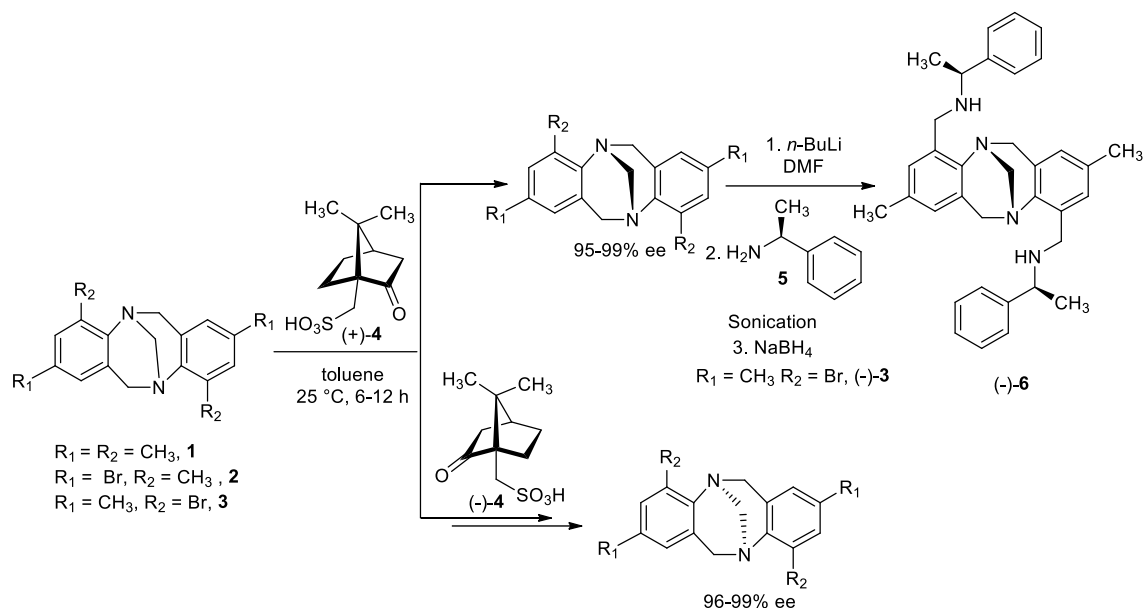
## Abstract

This thesis describes, “**Synthesis and Reactions of Tröger Base Derivatives**”. It comprises of three chapters. 1) **Introduction**, 2) **Results and Discussion** and 3) **Experimental Section**. The work described in this thesis is exploratory in nature.

The first chapter describes a brief review on the development of Tröger base chemistry. The second chapter deals with the results and discussion on the resolution methods developed for tetrasubstituted Tröger base derivatives and studies on their reactions.

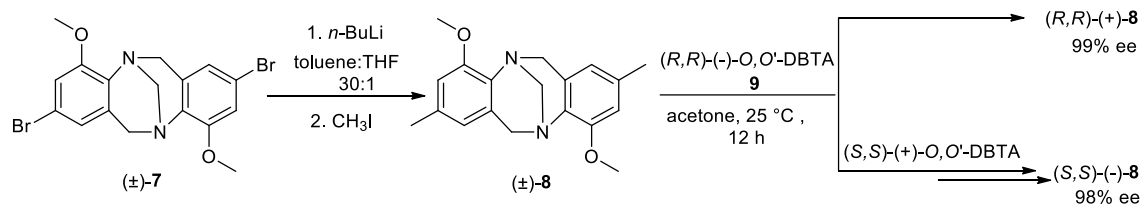
Chiral tetramethyl and dibromo-dimethyl substituted Tröger base derivatives (**1-3**) are readily prepared in enantiomerically pure forms using camphorsulfonic acid **4** (CSA) as a resolving agent. The (*S,S*)-isomers of these derivatives were obtained with 95-99% ee by precipitation using (1*S*)-(+)-10-camphorsulfonic acid and the partially resolved samples present in the mother liquor were enriched by treatment with (1*R*)-(-)-10-camphorsulfonic acid to obtain the (*R,R*)-isomers of tetrasubstituted Tröger base derivatives with 96-99% ee. In the case of 2,8-dibromo-4,10-dimethyl derivative, the (*R,R*)-isomer was obtained with 96-97% ee from the filtrate fraction after the (*S,S*)-enantiomer precipitated out. The dibromo derivative is readily functionalized to access a new chiral amine system containing chiral phenylethylamine moiety. The configurations of nitrogen centers of (+)-**1** and (+)-**2** were assigned as 5*S*,11*S* by single crystal X-ray analysis of the precipitated diastereomeric salts and the configuration of (-)-**3** was determined as 5*S*,11*S* by the single crystal X-ray analysis of the product (-)-**6** (Scheme 1).

## Scheme 1



We have also prepared the racemic *ortho*-methoxy Tröger base **8** by lithiation of the corresponding bromo compound followed by quenching with iodomethane. It was readily resolved *via* the preparation of diastereomeric salts using chiral dibenzoyl-L-tartaric acid **9** (Scheme 2).

## Scheme 2

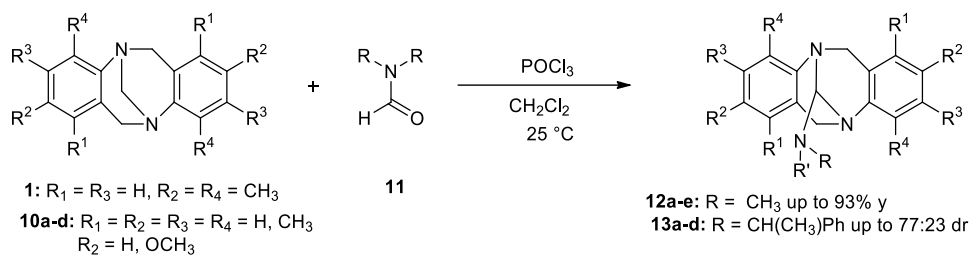


We have observed that the methylene bridge of *rac*-Tröger base derivatives exchanges by reaction with formamide in the presence of  $\text{POCl}_3$ . The reaction using chiral  $(S,S)$ -*N,N*-bis( $\alpha$ -methylbenzyl)formamide as a carbonyl partner gave the corresponding methano Tröger base derivatives **13a-13d** with the diastereomeric ratio of up to 77:23 (Scheme 3). The configurations of the stereogenic nitrogen centers were assigned as



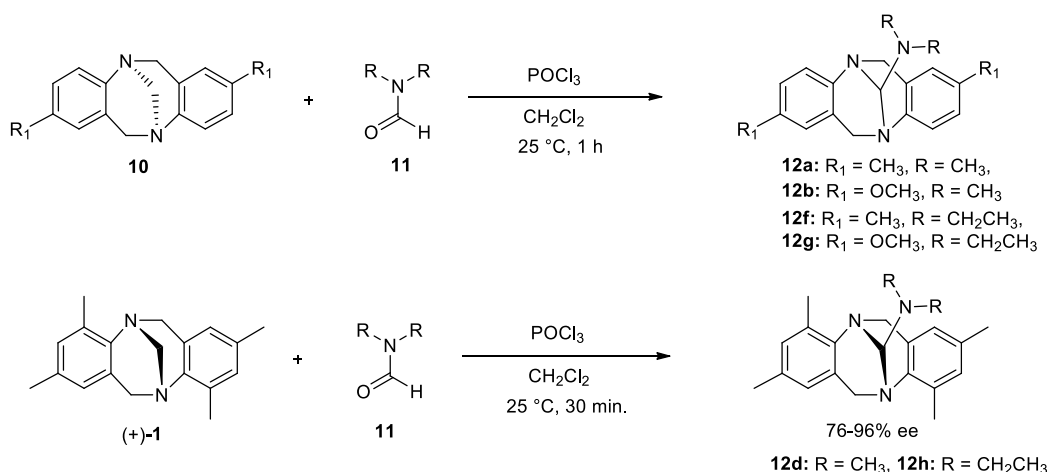
5*R*,11*R* by single crystal analysis. It was also observed that the Tröger base derivative with *ortho*-methyl groups is configurationally more stable compared to compounds without substituents in the aromatic rings.

### Scheme 3



Whereas the reaction of chiral *para*-substituted Tröger base **10** with formamides gives the corresponding methylene bridge substituted products as a racemic mixture, reaction of *ortho*-substituted derivative **1** gives the product **12d** with up to 96% ee (Scheme 4). The results are discussed considering mechanisms involving ring inversion of the corresponding cyclic intermediates.

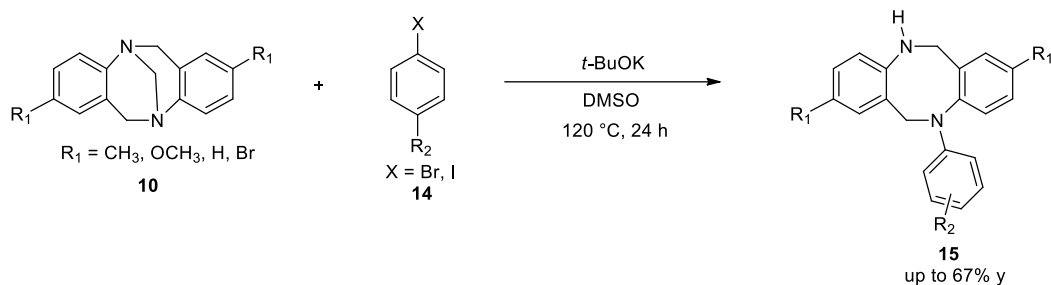
### Scheme 4



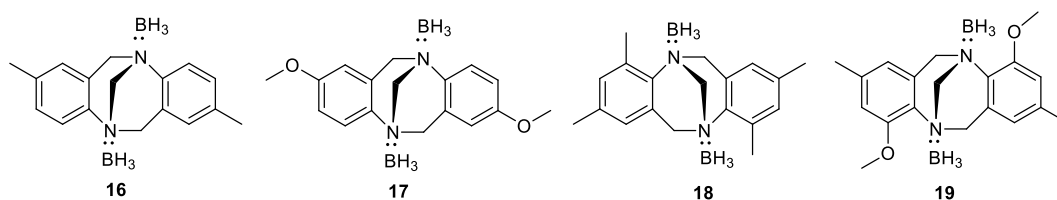
We have developed a method for ring opening of Tröger base **10** with concomitant N-arylation in the presence of *t*-BuOK/DMSO reagent system. The regioisomers were obtained in 1:1 ratio using *para*-substituted aryl halides **14**. During the course of the

reaction, the methylene bridge is cleaved by aryne intermediate formed *in situ* leading to the N-arylated product **15** in up to 67% yield (Scheme 5).

### Scheme 5



Studies were undertaken on the hydroboration reaction of prochiral olefins using chiral Tröger base-borane complexes **16-19**. The corresponding alcohols were obtained with up to 5% ee under iodine activation (Figure 1). The results are discussed considering different possible mechanisms.



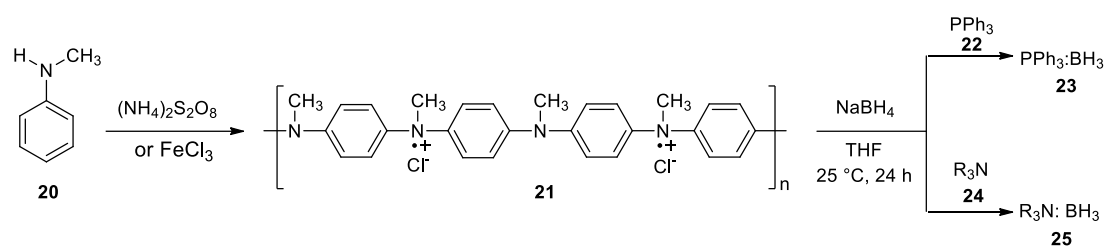
**Figure 1**

We have briefly studied the electron transfer reaction of Tröger base derivatives with chloranil. The nature of the charge transfer and electron transfer complexes formed were investigated by UV-Visible and esr spectroscopic methods.

The experimental details are described in the third chapter. The physical constant data (mp), IR,  $^1\text{H}$  NMR,  $^{13}\text{C}$  NMR, mass spectral data, HPLC data and elemental analysis are presented.

We have also briefly investigated the synthesis and reactions of N-methyl polyaniline. Results of these studies are described in the Annexure III. A method for estimation of oxidative doping level in poly(*N*-methylaniline) using NaBH<sub>4</sub> in THF is described. This method is also useful for the preparation of borane Lewis base complexes (Scheme 6).

**Scheme 6**




---

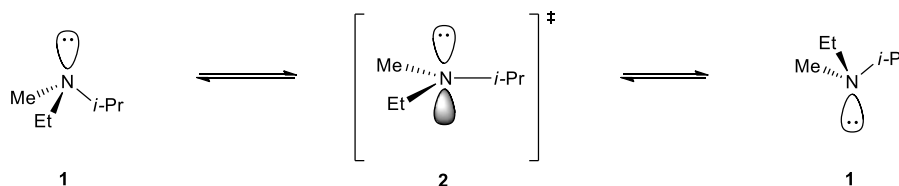
**Note:** Scheme numbers and compound numbers given in this abstract are different from those given in the chapters.

# 1. Introduction

---

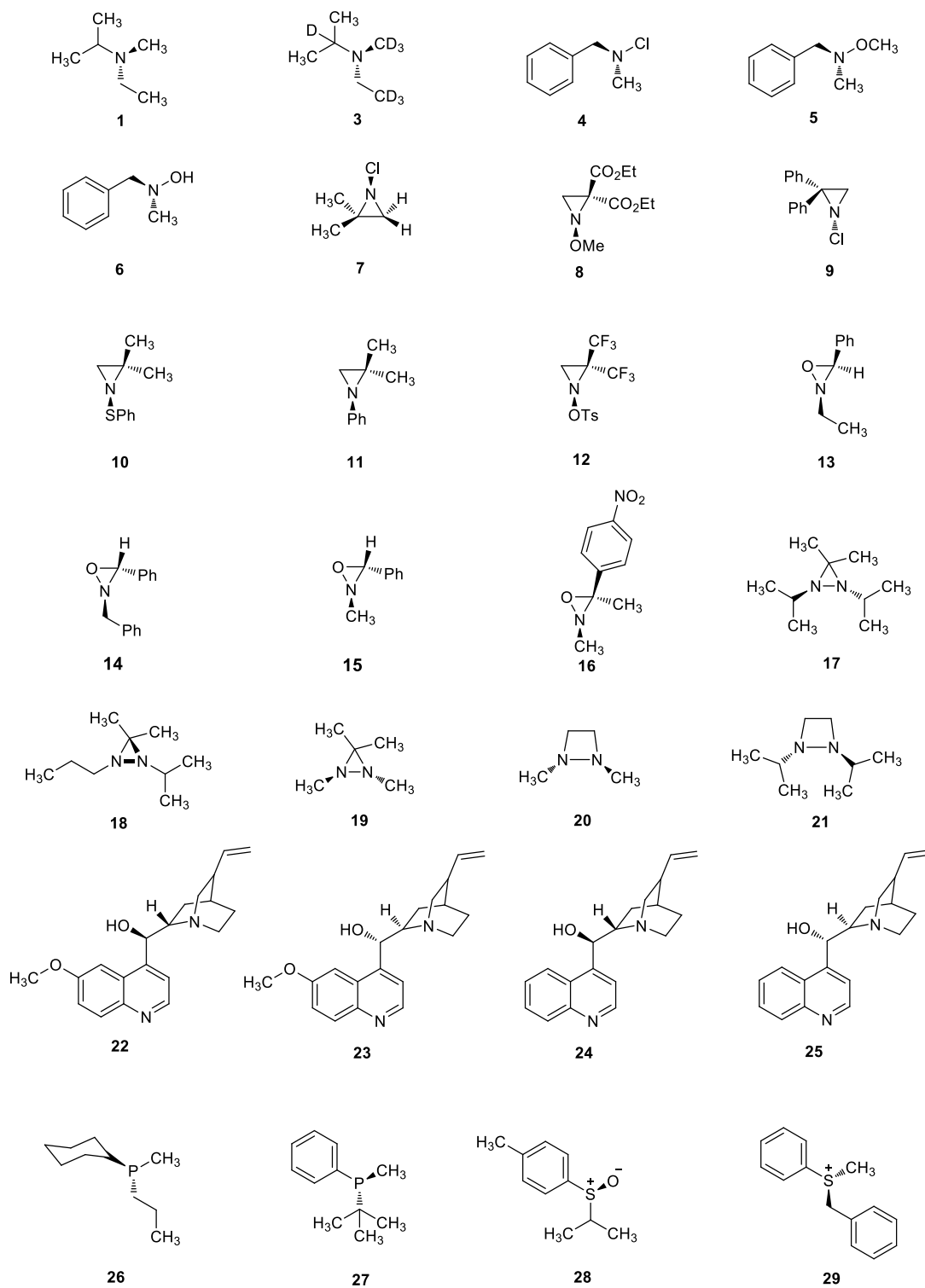
Stereochemistry of organic molecules containing a hetero atom as a stereogenic center is relatively less explored in organic chemistry compared to that with carbon centers. Hetero atoms such as nitrogen, phosphorus and sulfur with three different substituents are well-known stereogenic centers in modern organic chemistry. Due to the pyramidal inversion of nitrogen, the acyclic amines **1**, **3-6** with three different substituents are not optically active at room temperature.<sup>1</sup> Such asymmetrically substituted acyclic amine derivatives were studied only by dynamic nuclear magnetic resonance spectroscopy or by acid/base complexation with a suitable host acid.<sup>2</sup>

**Scheme 1**



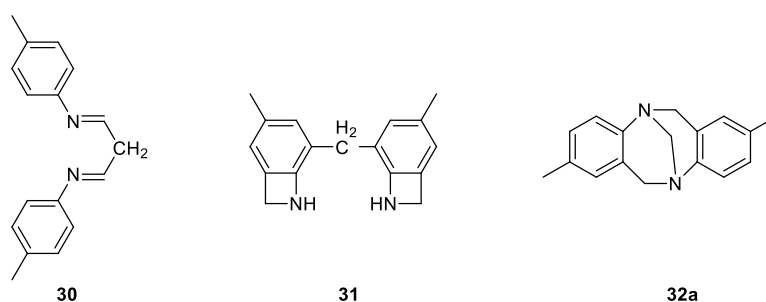
Incorporation of an electronegative element on the nitrogen increases the racemization barrier to some extent.<sup>3</sup> Also, nitrogen atom of the three or four member ring systems **7-21** has higher racemization barrier because of the higher activation energy required for the planar transition state (Scheme 1).<sup>4</sup> Whereas the angle strain is less for the nitrogen atom of a five or six member ring leading to rapid inversion, systems with other hetero atoms such as phosphorus and sulphur centers **26-29** are configurationally more stable.<sup>5</sup> However, molecules with bridgehead nitrogen atoms are configurationally stable because here racemization can take place only by breaking a bond in such cases.

Figure 1.



### Figure 1

Tröger base **32a**<sup>6</sup> is one such molecule with bridgehead stereogenic nitrogen atoms. This molecule with an empirical formula of C<sub>17</sub>H<sub>18</sub>N<sub>2</sub> was first isolated from the condensation reaction of dimethoxymethane with *p*-toluidine in aqueous HCl solution by Tröger in 1887. The structure **30** was assigned by Tröger but other structures were also proposed without considering the empirical formula.<sup>7</sup> For instance, Eisner and Wagner<sup>8</sup> suggested a tentative structure **31** for Tröger base. However, the correct structure **32a** was assigned as 2,8-dimethyl-6H,12H-5,11-methanodibenzo[b,f][1,5]diazocine by Spielman only in 1935 (Figure 2).<sup>9</sup>



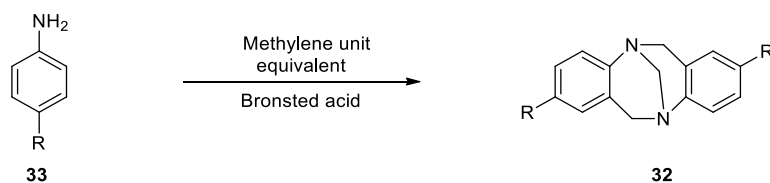
**Figure 2**

Previously, *para*-substituted Tröger base derivatives were synthesized and resolved by using dibenzoyl-L-tartaric acid as a resolving agent from this laboratory.<sup>10</sup> These derivatives were used as chiral host in the chiral recognition studies of carboxylic acids and also as ligand in dihydroxylation reactions of *trans*-stilbenes.<sup>11</sup> Also, methods were reported in recent years for resolution, synthesis and applications of Tröger base derivatives. Therefore, a brief review of reports on the Tröger base chemistry would facilitate further discussion.

## 1.1 Synthesis of Tröger base derivatives

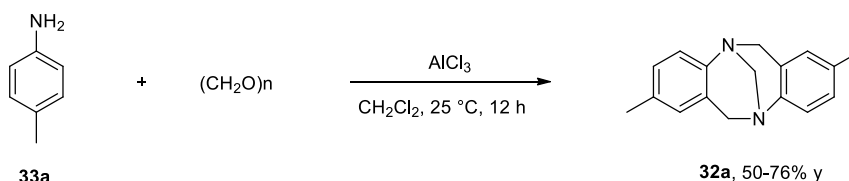
A general approach for the synthesis of Tröger base derivatives involves condensation reaction of a suitable substituted aniline with a methylene equivalent compound in the presence of Bronsted acids. Various methylene unit equivalent compounds used are formaldehyde, paraformaldehyde, hexamethylenetetramine and DMSO in AcOH/HCl media.<sup>12</sup> Bronsted acids such as aqueous or alcoholic HCl solution,<sup>13</sup> trifluoroacetic acid (TFA)<sup>14</sup> and methanesulfonic acid<sup>15</sup> are generally used in the Tröger base synthesis (Scheme 2). Among all, TFA/paraformaldehyde combination was used widely for the synthesis of derivatives with electron donating as well as withdrawing substituents.<sup>16</sup> Also, diglycolic acid in combination with polyphosphoric acid was also reported as an acidic medium.<sup>17</sup>

### Scheme 2



A method using Lewis acid AlCl<sub>3</sub> was developed in this laboratory for the synthesis of Tröger base **32a** with paraformaldehyde as methylene unit equivalent (Scheme 3).<sup>10a</sup>

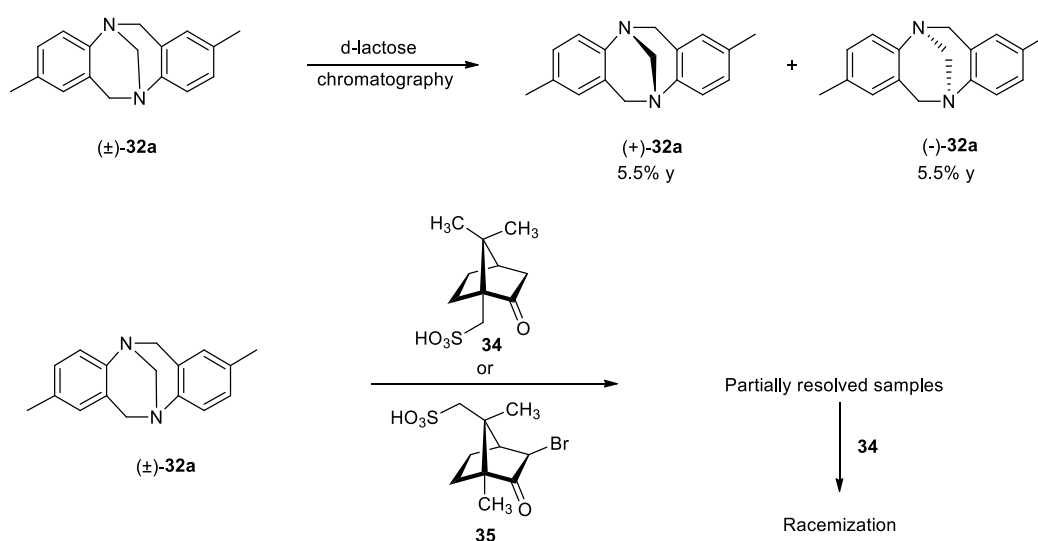
### Scheme 3



## 1.2 Chirality of Tröger base derivatives

The pyramidal inversion of trivalent nitrogen atoms was suggested to be a possible reason for the racemization of tertiary amines with different substituents even at room temperature.<sup>18</sup> Unlike stereogenic carbon atom, the nitrogen atom undergoes rapid inversion at room temperature. Therefore, the separation of stereo isomers of molecule with stereogenic nitrogen atom is a challenging task. It has been speculated for several years that Tröger base could be a chiral molecule because of the bridgehead N-atoms. Prelog and Wieland were able to separate the enantiomers of Tröger base for the first time by chromatography on *d*-lactose column in 1944.<sup>19</sup> They were able to isolate both isomers in 5.5% yield using 6 g of *rac*-Tröger base and 270 g of *d*-lactose in a column. This chiral resolution established that not only the carbon but also nitrogen atom can be a stereogenic center in a molecule (Scheme 4). Prelog also reported, unsuccessful attempts to resolve **32a** via the diastereomeric salt formation using (1*R*)-(-)-10-camphorsulfonic acid **34** or (1*R*)-(endo,anti)-(+)-3-bromo-camphor-8-sulfonic acid **35**.<sup>19</sup>

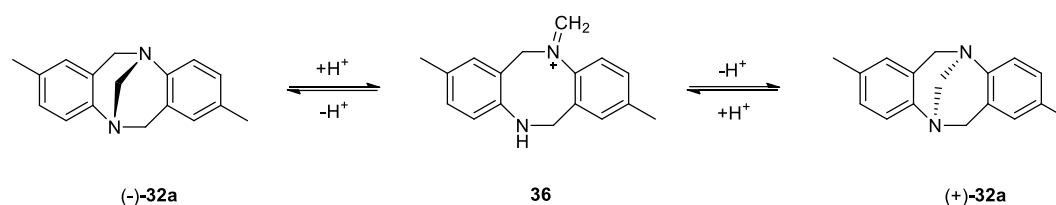
**Scheme 4**





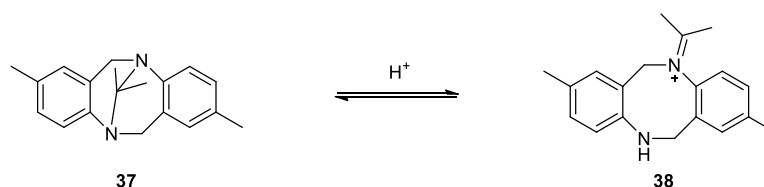
However, Prelog observed racemization of partially resolved samples in dilute acidic medium, and suggested that proton catalyzed formation of iminium ion **36** as an intermediate in the racemization process. Due to this racemization, it was believed for several years that the resolution of **32a** *via* the diastereomeric salt formation would not be practicable (Scheme 5).<sup>19</sup>

**Scheme 5**



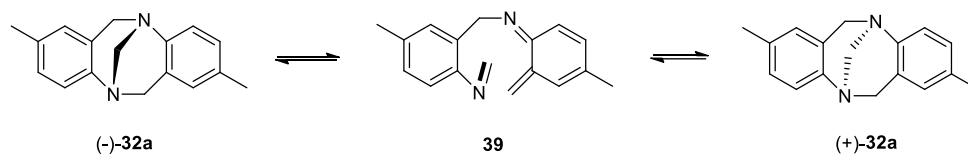
Later, investigation on the mechanism of acid promoted racemization by NMR spectroscopy did not give evidence for the iminium ion intermediate **36**.<sup>20</sup> It was speculated that the intermediate would be present in a very low concentration to be detected by NMR spectroscopy studies.<sup>20</sup> The inversion observed for **32a** in dilute acidic medium indicated that proton exchange between two bridgehead nitrogen atoms is rapid on the NMR time scale. However, the UV spectroscopy studies of **37** in concentrated acid gave evidence for the formation of **38**. The iminium ion **38** was also confirmed by  $^{13}C$  NMR spectroscopy studies of **37** in concentrated acid (Scheme 6).<sup>20</sup>

**Scheme 6**



Trapp and Schurig<sup>21</sup> reported that Tröger base **32a** racemizes under inert gas helium at ambient temperature. A retro-hetero-Diels-Alder ring opening followed by hetero-Diels-Alder ring closure was invoked for this racemization (Scheme 7).

## Scheme 7



The epimerization studies of bis-Tröger base derivatives **40** and **41** in the gaseous state using ion-mobility mass spectrometry were reported by Schroder and co-workers.<sup>22</sup> These authors concluded that proton-catalyzed ring-opening sequence as a more probable mechanism than the above discussed Diels-Alder type mechanism for the epimerization of Tröger base derivatives **40** and **41** (Figure 3).

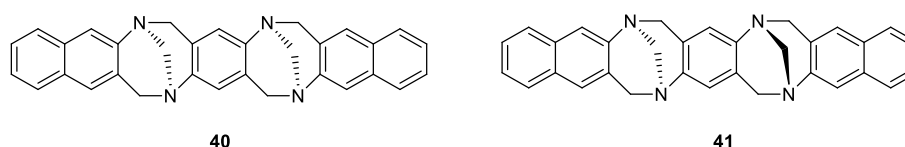
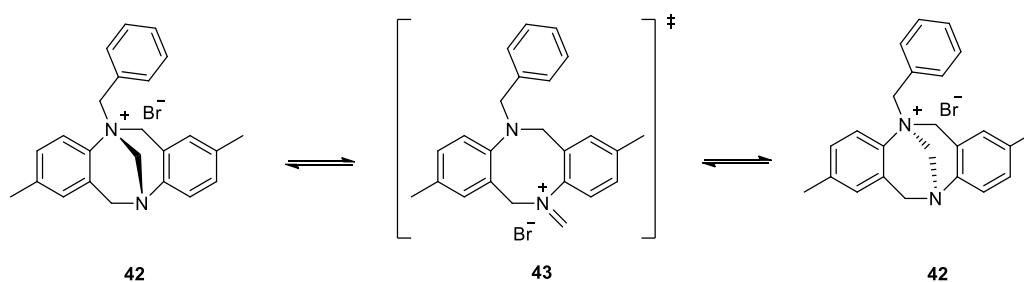


Figure 3

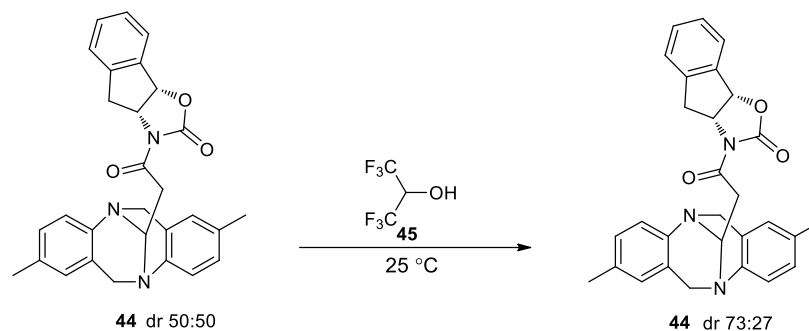
Dynamic enantioselective electrokinetic chromatography method was used to study the stereointegrity of TB **32a** and the monobenzyl derivative **42** using hydroxypropyl- $\beta$ -cyclodextrin as a chiral mobile additive.<sup>23</sup> It was found that the presence of positive charge in the monobenzylated derivative decreases the racemization barrier significantly (Scheme 8).<sup>23</sup>

## Scheme 8



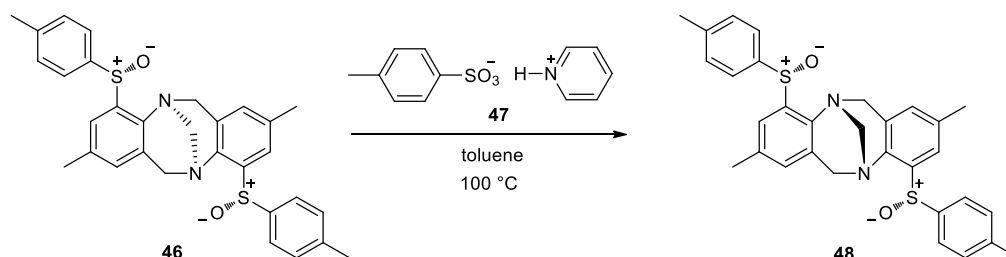
Cvengros *et al.*<sup>24</sup> reported that the diastereoselectivity was improved to 73:27 from 50:50 by stirring of the diastereomeric mixture **44** in hexafluoroisopropanol **45** (HFIP) solvent (Scheme 9).

#### Scheme 9



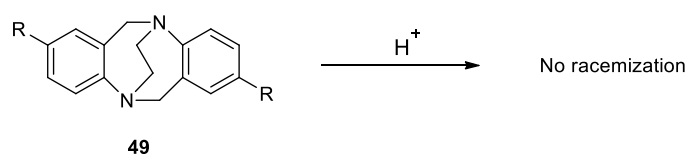
Tröger base **46** was isomerized to its diastereomer **48** by heating at 100 °C in the presence of pyridinium *p*-toluenesulfonate **47** in toluene. It was also reported that the sulfur centers did not undergo isomerization in this experiment (Scheme 10).<sup>25</sup>

#### Scheme 10



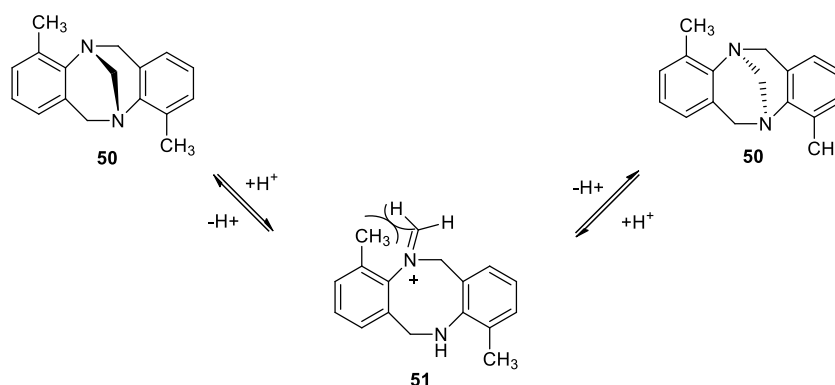
Chiral ethylene-bridged Tröger base derivative **49** is configurationally stable in acidic medium. The ethylene bridged Tröger base does not racemize in acidic medium because the acid promoted formation of iminium ion cannot take place as in the case of the parent TB **32a** (Scheme 11).<sup>26</sup> This observation also supports the formation of iminium ion proposed by Prelog.

#### Scheme 11



Lenev *et al.*<sup>27</sup> reported that steric effect of *ortho*-methyl groups increases racemization barrier as revealed by quantum-mechanical (DFT) calculations. The racemization takes place by ring-opening followed by interconversion of the monocyclic intermediate **51**. The steric hindrance of *ortho*-methyl groups significantly increases the energy of this intermediate **51** (Scheme 12). As a result, the racemization barrier of *ortho*-methyl substituted Tröger base **50** in acidic media is raised by 30 kJmol<sup>-1</sup> relative to that of the parent compound **32a**.

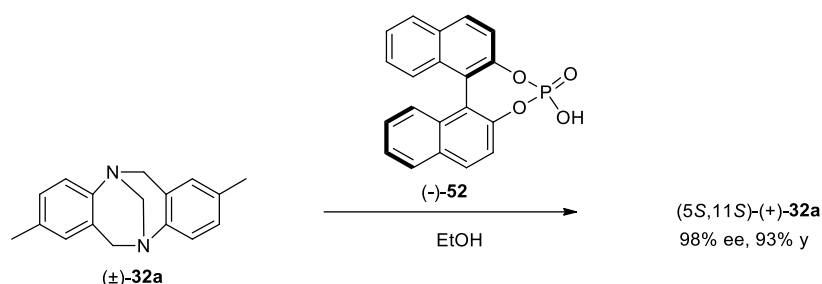
**Scheme 12**



### 1.2.1 Resolution of Tröger base derivatives

Due to the acid-promoted racemization, it was postulated that the chiral resolution of **32a** *via* the diastereoisomeric salts formation with chiral acids is not feasible. However, the isolation of enantiomerically pure (>98% ee) **32a** with the aid of (–)-1,1'-binaphthalene-2,2'-dihydrogen phosphate **52** was reported by Wilen and co-workers.<sup>28</sup> Only one isomer was isolated under the experimental conditions, and the (–)-isomer was completely isomerised to (+)-isomer during this process (Scheme 13). Wilen assigned the configuration of (+)-**32a** as 5*S*,11*S*. Indeed, this process is a crystallization-induced asymmetric transformation (CIAT).

## Scheme 13



Crystallization of 1:1 mixture of **53** and **54** from diethyl ether was reported to give the pure crystals of **53**.<sup>29</sup> For example, upon treatment of diastereomer **54** with aqueous HCl in methanol gave the **53** with >99% de. This crystallization-induced asymmetric transformation (CIAT) was driven by (*S*)-1-phenylethyl group (Figure 4).<sup>29</sup>

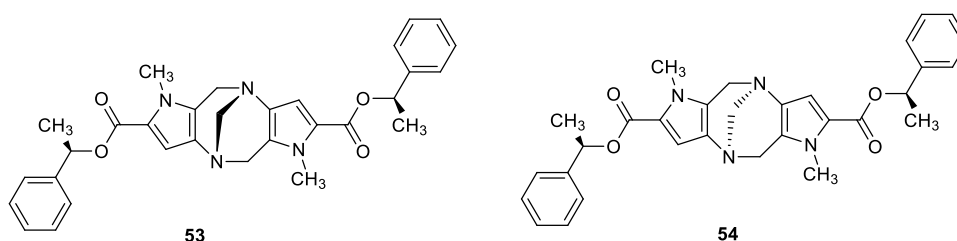
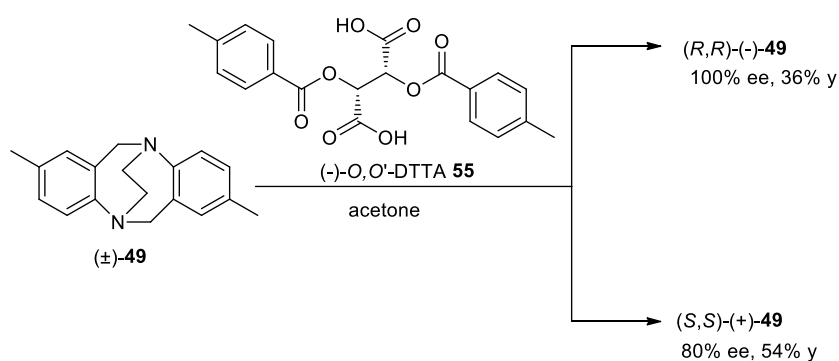


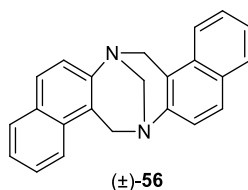
Figure 4

Hamada *et al.*<sup>26</sup> reported a method for the resolution of configurationally stable ethylene bridged TB **49** using (–) and (+)-di-*p*-toluoyl-tartaric acid **55** as resolving agents. The base and acid were dissolved in hot acetone and allowed to stand for crystallization (Scheme 14). The configuration of nitrogen atoms was assigned by comparison of CD spectra with chiral TB **32a**.

## Scheme 14



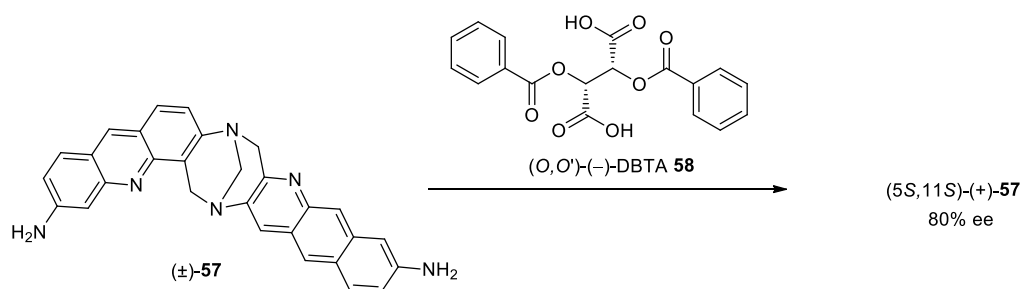
Later, Margitfalvi<sup>30</sup> followed the above strategy for the resolution of naphthyl TB derivative **56**. It was reported that the use of dry acetone under argon atmosphere is crucial for this resolution to obtain the enantiomers with 98 and 100% ee.<sup>30</sup> The enantiomers of TB **56** were also separated by manual separation of racemic conglomerate obtained from routine crystallization using methanol solvent (Figure 5).<sup>31</sup>



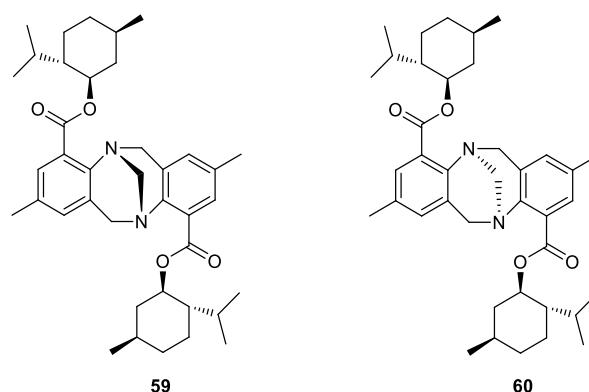
**Figure 5**

The acridinamine TB **57** was resolved by crystallization of the corresponding 2,3-*O,O'*-dibenzoyltartrate salts to give the TB **57** in 80% ee as calculated by an NMR spectroscopy technique. The formation of salt was believed to be with more basic N-atom of the acridine ring in **57**. Circular dichroism data were used to assign the configurations of the stereogenic bridgehead nitrogen atoms (Scheme 15).<sup>32</sup>

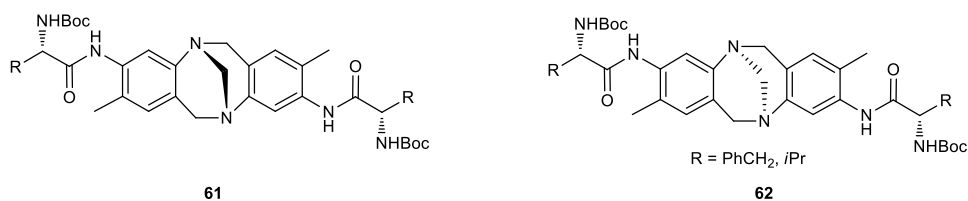
**Scheme 15**



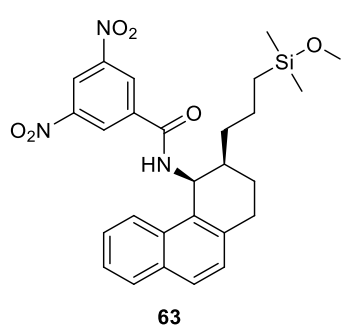
The 1:1 diastereomeric mixture of **59** and **60** was readily separated by silica gel column chromatography. The mixture of **59** and **60** was also separated by crystallization from diethyl ether. Whereas (5*S*,11*S*)-**59** was obtained as colourless crystals, the diastereomer (5*R*,11*R*)-**60** was isolated as yellow oil (Figure 6).<sup>33</sup>

**Figure 6**

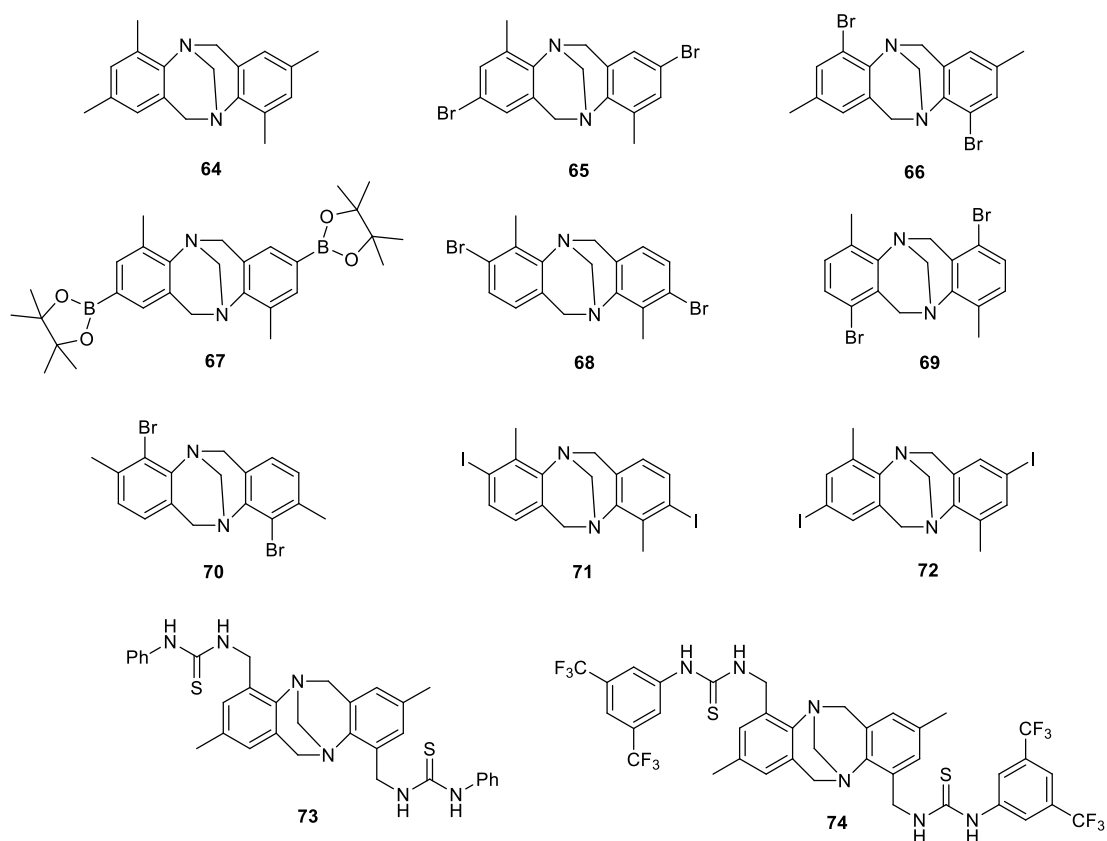
Later, the enantiomers of amino-substituted TB derivative were separated by preparation of 1:1 diastereomeric mixture using amino acid (L-phenylalanine or L-valine) as a chiral auxiliary. The 1:1 mixture of **61** and **62** was separated by using column chromatography separation method. It was pointed out that the configurations of nitrogen atoms are not clear and tentatively assigned as 5*S*,11*S* for (+)-isomer. The  $t_{1/2} = 12$  h was found in 1.5 M HCl/EtOH for the racemization of amino-substituted derivative (Figure 7).<sup>34</sup>

**Figure 7**

The resolution methods discussed so far are not applicable for *ortho*-disubstituted derivatives. Hence, only HPLC resolution methods have been used widely to obtain the chiral derivatives.<sup>35</sup> The polymer Whelk O1 with covalently bound 3,4-disubstituted 1,2,3,4-tetrahydrophenanthrene **63** as a chiral stationary phase (CSP) has extensively been used for the resolution of *ortho*-disubstituted TB derivatives in semi preparative quantities (Figure 8).

**Figure 8**

For example, the TB derivatives with *ortho*-methyl, *ortho*-bromo and thiourea derivatives were resolved in semi preparative quantities (Chart 1).<sup>36</sup> The chiral stationary phase **63** is more compatible with high polar and chlorinated solvents, but the polysaccharide coated CSP is found to leach off with the use of chlorinated solvents. Also, the separation was a lengthy process. Representative examples of tetrasubstituted derivatives resolved in this way are shown in the Chart 1.

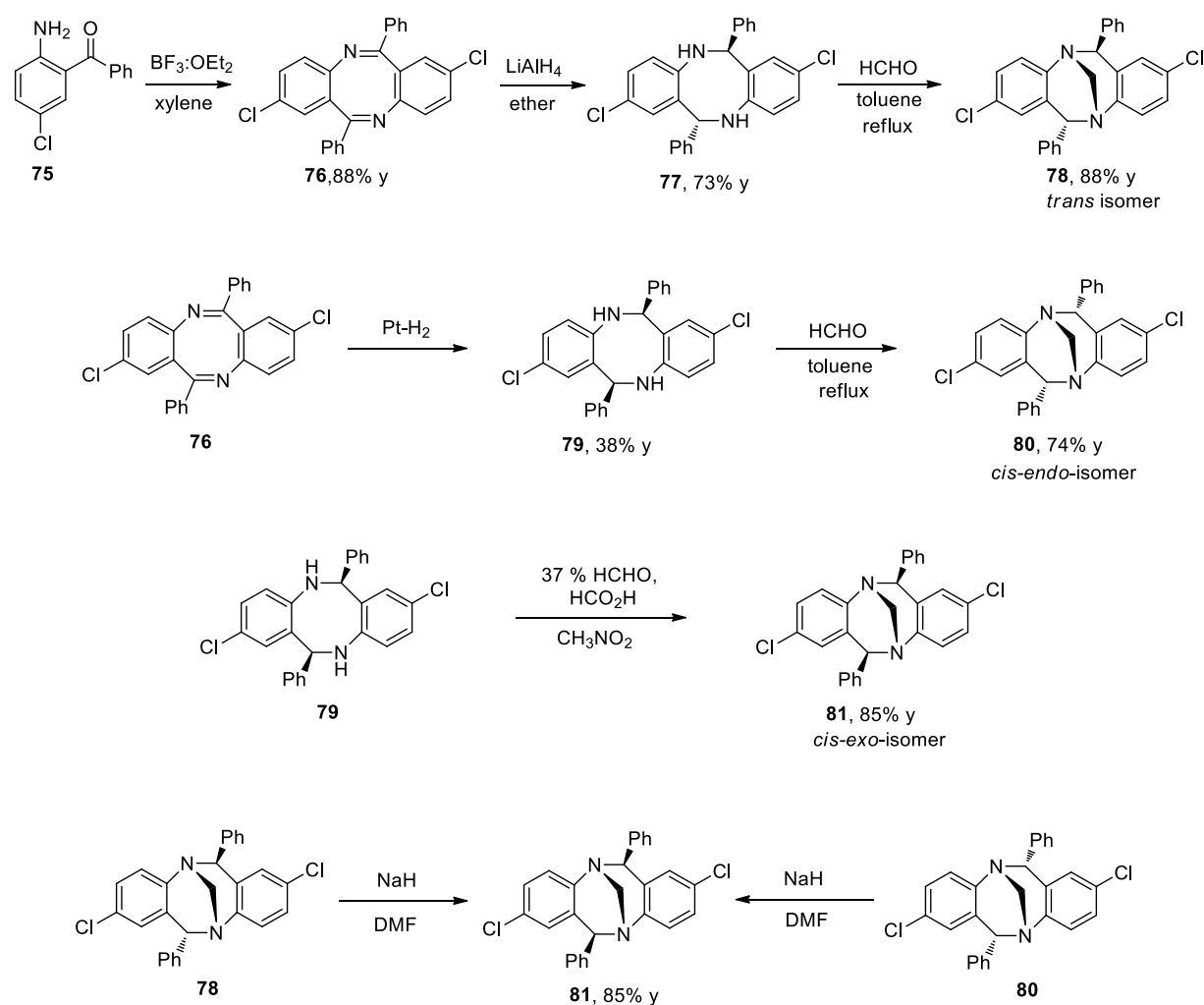
**Chart 1**



### 1.2.2 Diastereoselective synthesis of Tröger base derivatives

Upon condensation of *cis* or *trans* tetrahydro-diphenyl[1,5]diazocine **79** or **77** with formaldehyde, the diastereomerically pure Tröger base derivatives are obtained depending on the reaction conditions (Chart 2).<sup>37</sup> Rearrangement of *trans* **78** and *cis-endo* **80** isomers to *cis-exo* **81** isomer was also reported in the presence of NaH in DMF.

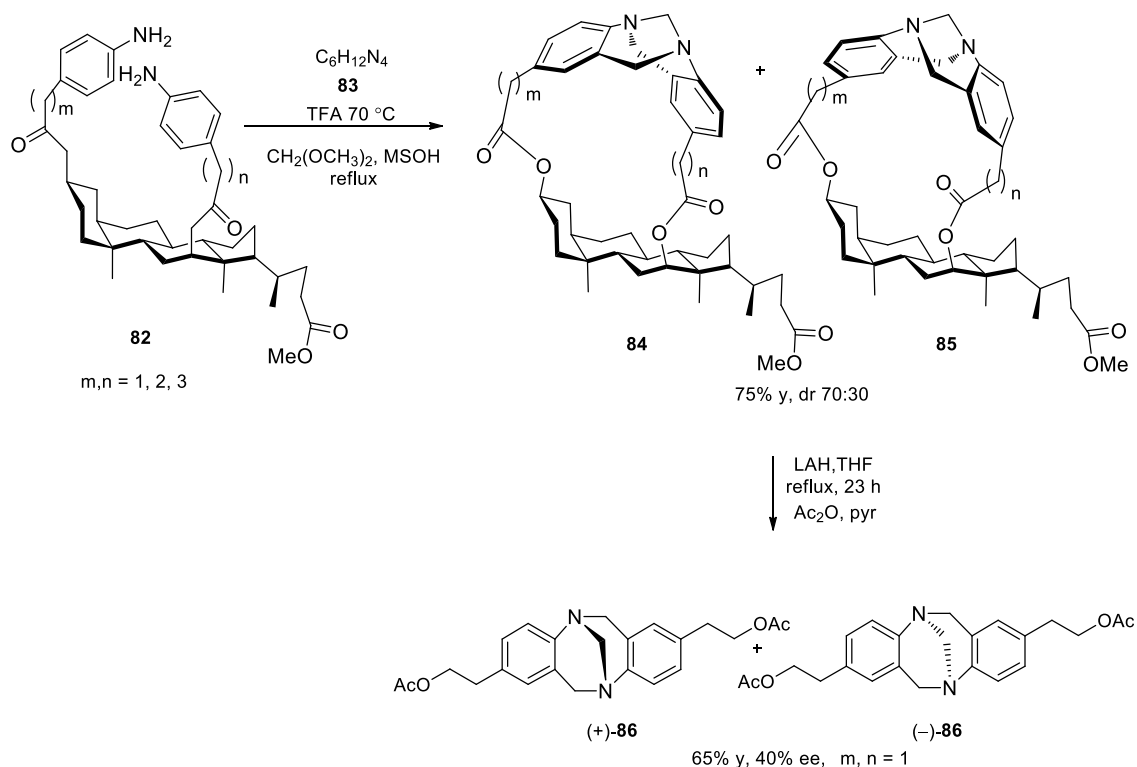
**Chart 2**



Maitra *et al.*<sup>38</sup> reported the asymmetric synthesis of TB derivative with 40% ee using deoxycholic acid as a chiral template, which was removed by reduction with  $\text{LiAlH}_4$  (Scheme 16). Later, the effect of spacer length on the diastereoselectivity was also reported. The spacer length of  $m = 1$  and  $n = 2$  gave the better selectivity 70:30 dr.<sup>39</sup> The

diastereomeric mixture was separated only by slow crystallization process. Also, it was found that the mixture could not be separated even by chiral HPLC methods.

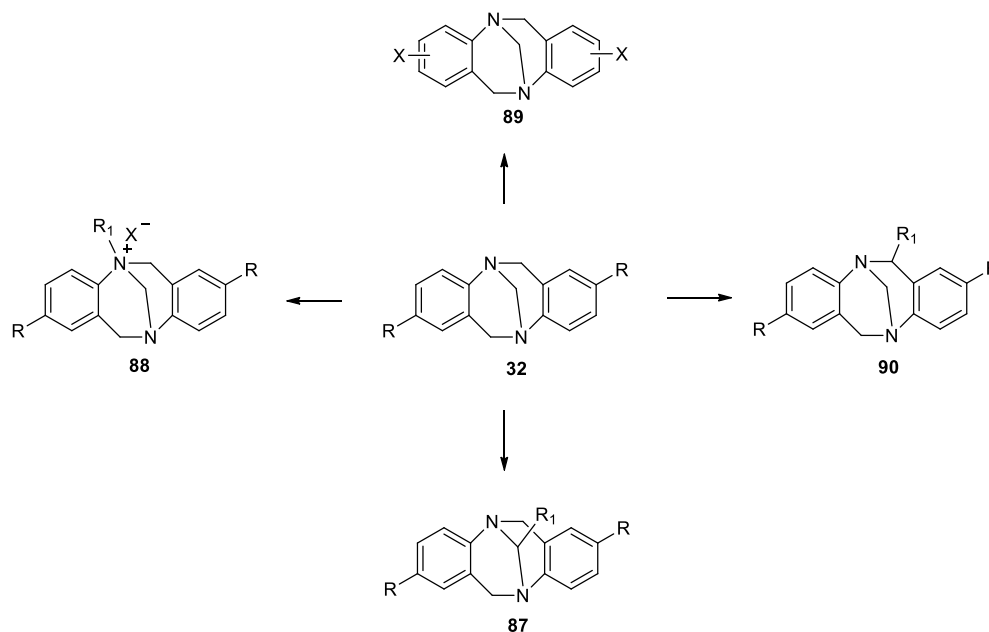
### Scheme 16



### 1.3 Reactions of Tröger base derivatives

Many structurally diverse Tröger base derivatives were synthesized with synthetic alterations on aromatic core as well as the saturated aliphatic core (Figure 9).<sup>40</sup> Aromatic electrophilic substitution reactions of Tröger base derivatives could be compared to *N, N'*-dimethylaniline for their structural similarity of aromatic ring. A recent theoretical study revealed that Tröger base derivatives are relatively sluggish towards reaction with the electrophiles compared to *N, N*-dimethylaniline but more reactive than benzene.<sup>41</sup> Halogenation<sup>42</sup> and cross-coupling reactions such as Suzuki-Miyaura,<sup>43</sup> Corriu-Kumada,<sup>44</sup> Sonogashira,<sup>45</sup> Stille<sup>46</sup> and Negishi<sup>46</sup> were reported for the functionalization of aromatic rings. Ullmann<sup>47</sup> and Buchwald-Hartwig<sup>48</sup> aminations were also reported for the carbon-

heteroatom bond formation. Functionalization of aliphatic saturated core involves the reactions of benzylic methylene unit, methylene bridge and nitrogen itself.



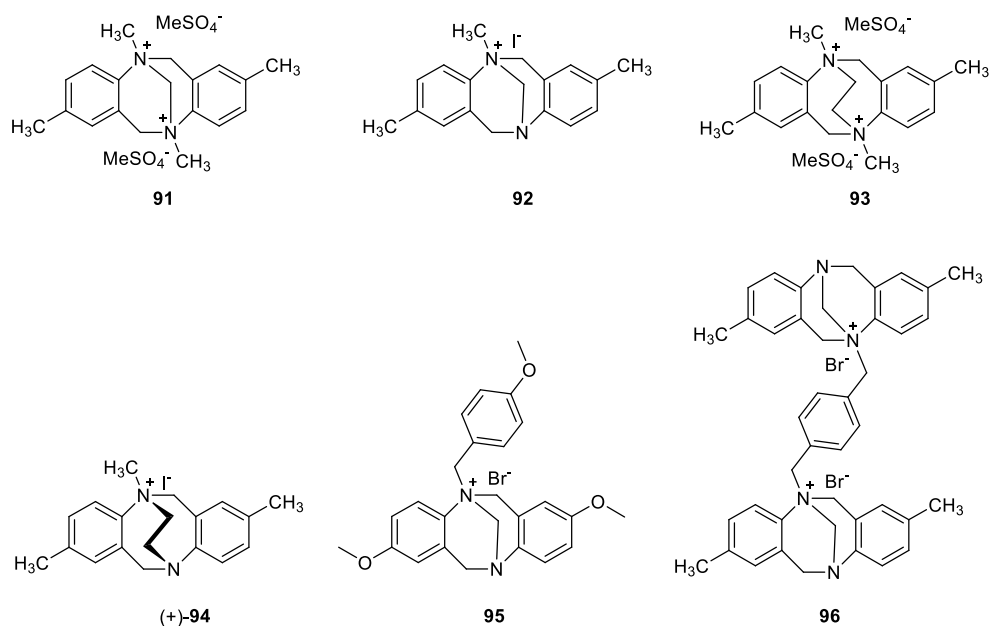
**Figure 9**

In recent years, functionalization of methanodiazocine ring has attracted considerable attention because it leads to molecular diversity. We briefly review here the reports on the reactions of aliphatic saturated core as these are relevant to our current research efforts.

### 1.3.1 Quaternary ammonium salts of Tröger base derivatives

The quaternary ammonium salts of TB were synthesized by reaction with appropriate halides or with dimethyl sulphate. Due to its V shape TB derivatives were used as a host in molecular recognition studies. Formation of inclusion compound was reported for host **92** and dioxane in 1:2 stoichiometry ratio.<sup>49</sup> The inclusion compound of (+)-**94** with benzene was also reported (Chart 3).<sup>50</sup>

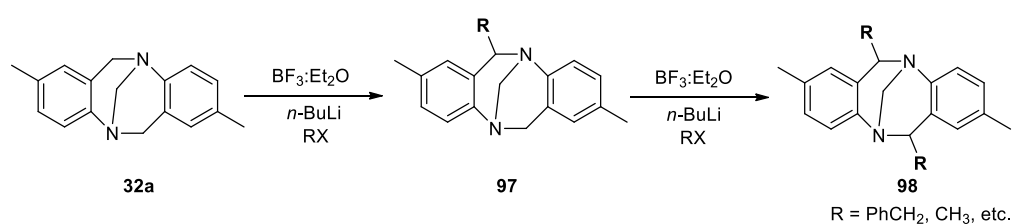
## Chart 3



## 1.3.2 Functionalization of benzylic methylene unit of Tröger base

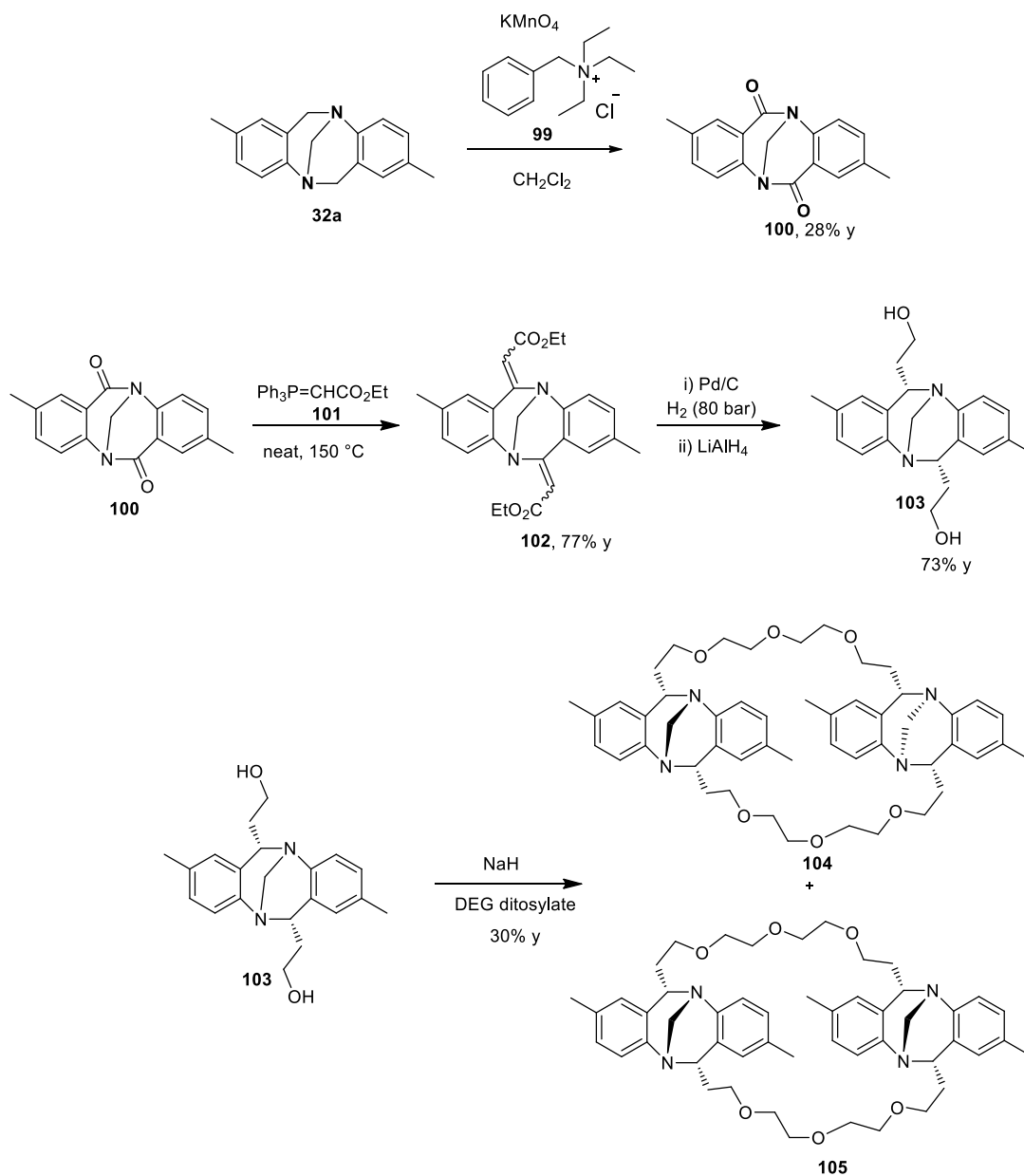
The first benzylic functionalization of TB was reported by Harmata and co-workers in 1996.<sup>51</sup> The new derivatives **97** and **98** were synthesized by metalation using  $\text{BF}_3\cdot\text{OEt}_2$  and  $n\text{-BuLi}$  followed by quenching with an electrophile (Scheme 17).

## Scheme 17



Very recently, a lactam derivative of TB **100** was synthesized by oxidation using 3 equiv. of  $\text{KMnO}_4$  and benzyltriethylammonium chloride **99** in  $\text{CH}_2\text{Cl}_2$  at reflux.<sup>52</sup> The compound **100** was transformed to bis-TB crown ether derivatives **104** and **105** via the sequence of reactions involving Wittig reaction in a key step (Chart 4).<sup>53</sup>

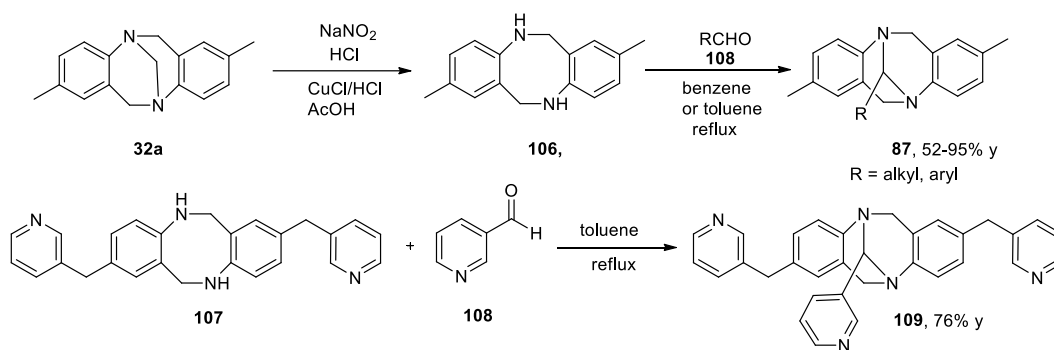
Chart 4



### 1.3.3 Reactions of methylene bridge of Tröger base

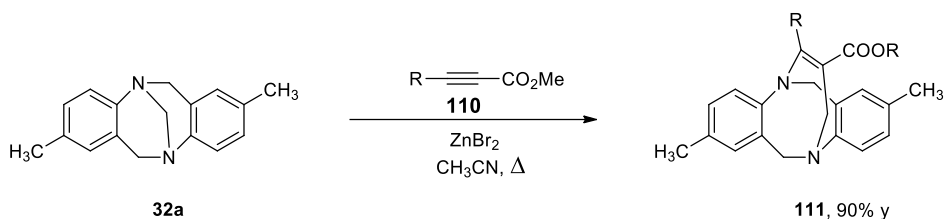
The first methylene bridge substitution was achieved by Cooper and co-workers<sup>54</sup> *via* multistep reactions. The TB **32a** was first converted into the cyclic di-secondary amine **106** followed by condensation with an aromatic aldehyde (Scheme 18). Later, the same approach was used for the synthesis of other TB derivatives.<sup>55</sup>

## Scheme 18



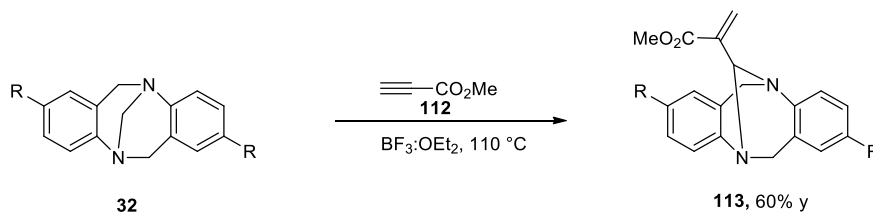
Kim *et al.*<sup>56</sup> reported the synthesis of the unusual cyclic enaminone ester **111** from TB **32a** and conjugated esters **110** in the presence of  $\text{ZnBr}_2$  under heating conditions in  $\text{CH}_3\text{CN}$ . Although these authors have reported the formation of bridge with three carbon atoms, the structure of product was not established by X-ray diffraction method (Scheme 19).

## Scheme 19



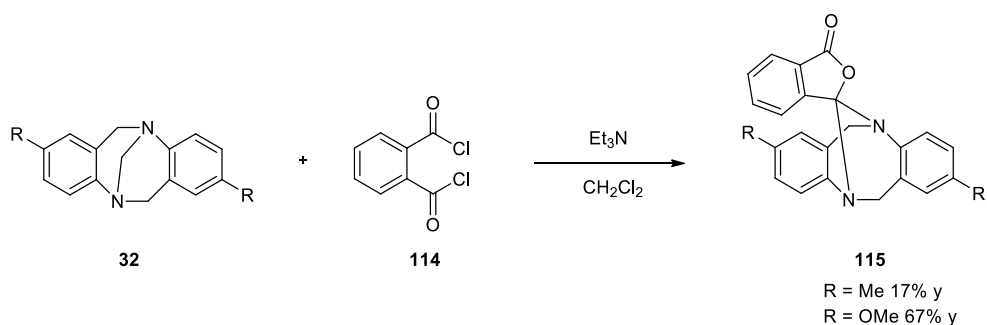
Later, Lenev and co-workers<sup>57</sup> reported the same reaction in the presence of  $\text{ZnBr}_2$  as well as  $\text{BF}_3\cdot\text{OEt}_2$  to obtain the corresponding methylene bridged TB derivatives **113**. The structure was unambiguously confirmed by X-ray structural analysis. Thus, the addition product of TB with activated acetylene was established as **113** and not **111** (Scheme 20).

## Scheme 20



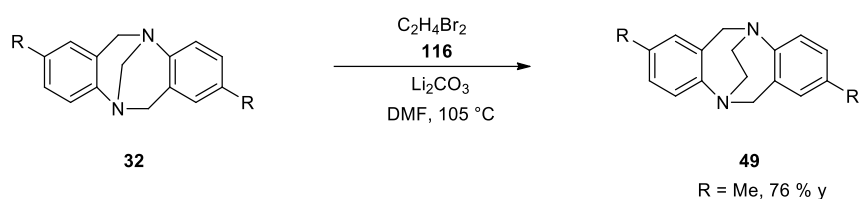
A new class of TB derivatives **115** bearing spiro lactone as methylene bridge were synthesized by the reaction of TB **32** with phthaloyl dichloride **114** in  $\text{CH}_2\text{Cl}_2$ . The methoxy derivative was obtained in higher yield in this reaction (Scheme 21).<sup>58</sup>

**Scheme 21**



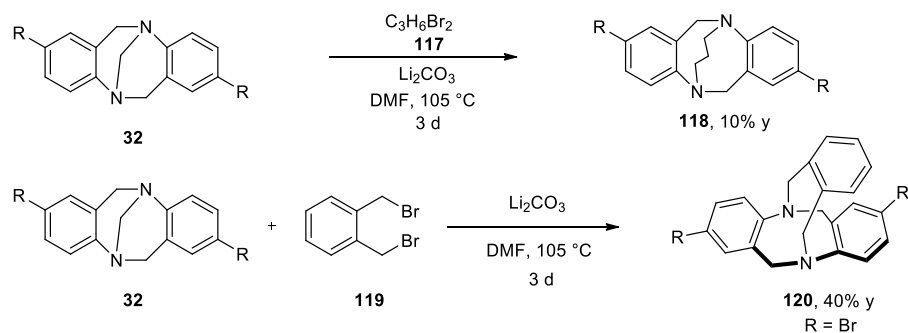
Hamada and co-workers<sup>26</sup> reported the reaction of TB **32a** and ethylene bromide in the presence of  $\text{Li}_2\text{CO}_3$  that gives the ethylene bridge derivatives **49** with two seven membered rings as aliphatic saturated bicyclic core (Scheme 22).

**Scheme 22**



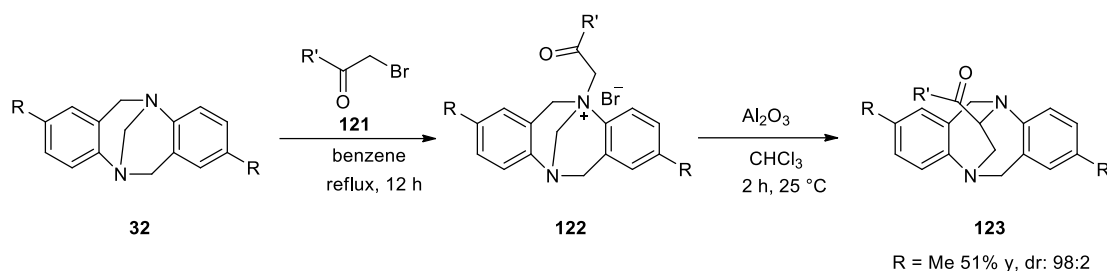
Tröger base derivatives with three and four atoms bridge were reported to result in dramatic change of the shape of the molecules. Aromatic rings are flattened out in **118** and dihedral angle was determined to be  $134.7^\circ$ , while the corresponding angle for **120** is  $127.0^\circ$ . These derivatives are not ‘V’ shaped like the parent TB **32** with dihedral angle of  $90.0^\circ$  (Scheme 23).<sup>59</sup>

**Scheme 23**



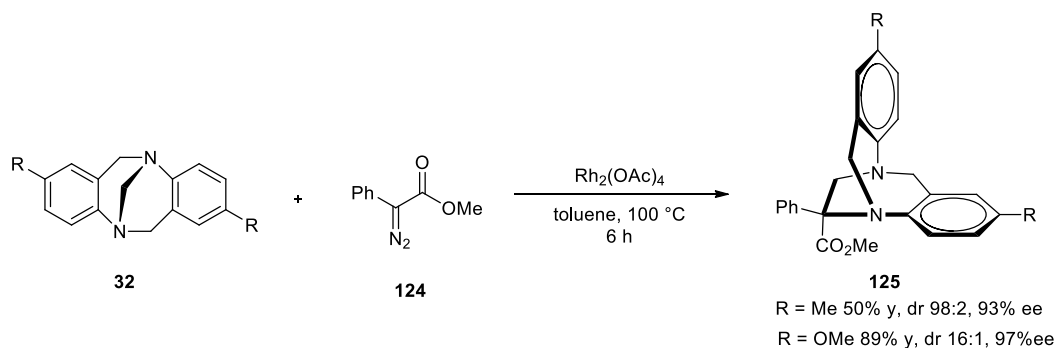
Lacour and co-workers<sup>60</sup> reported a method for the stereoselective synthesis of ethylene bridged derivatives **123** in moderate yields with diastereoselectivity of up to 98:2 by using the [1,2]-Stevens rearrangement. A simple alkylation and rearrangement were carried out separately in two steps (Scheme 24).

**Scheme 24**



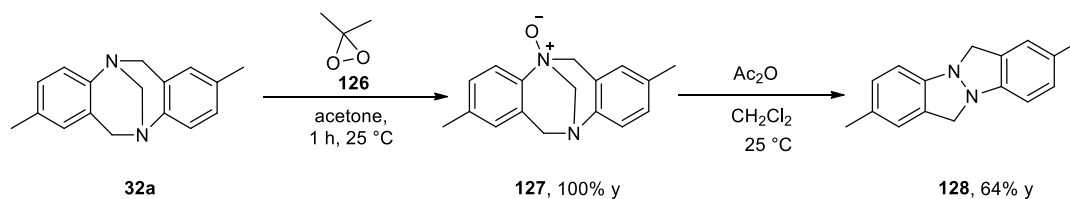
Later, a one-step rhodium(II)-catalyzed asymmetric synthesis of configurationally stable ethylene bridged derivatives **125** was also reported by Lacour and co-workers (Scheme 25).<sup>61</sup>

**Scheme 25**



Polonovski reaction of Tröger base N-oxide **127** leads to the corresponding hydrazine **128**.<sup>62</sup> It was also reported that the corresponding *ortho*-methyl substituted derivative did not give the desired hydrazine product in this reaction (Scheme 26).<sup>62</sup>

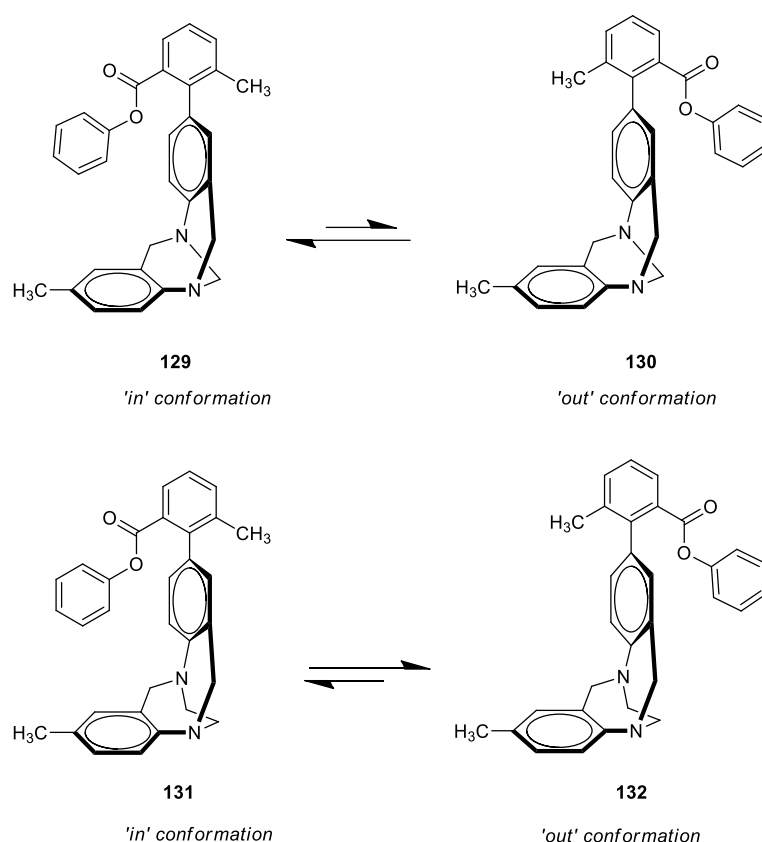
**Scheme 26**





### 1.3.4 Effect of diazocine bridgehead of Tröger base on the torsion balance

Wilcox torsion balance is a useful tool to measure the edge-to-face aromatic interactions.<sup>63</sup> The molecular torsion balance study revealed that TB with methylene bridge prefers ‘folded’ conformation **129**, but TB with ethylene bridge prefers ‘out’ conformation **132**. It was suggested that the steric repulsion dominates over an attractive interaction in the case of ethylene bridged Tröger base (ETB) (Figure 10).<sup>64</sup>



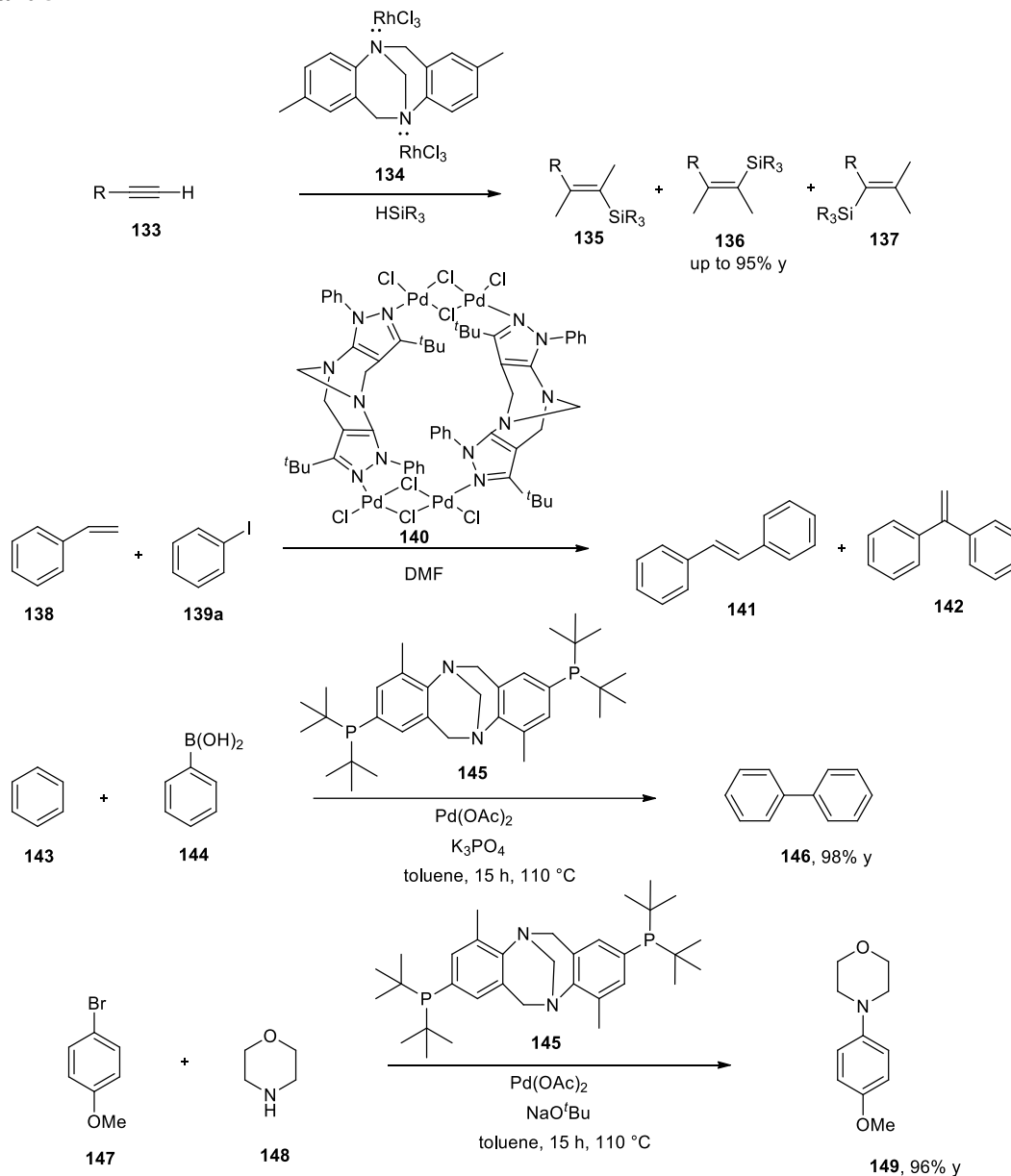
**Figure 10**

### 1.4 Applications of Tröger base-transition metal complexes

The first synthesized transition metal complex of TB was the TB. $2\text{RhCl}_3$  complex **134**. The 1:2 complex formed is well characterized by NMR and elemental analysis. It is air stable and used for the hydrosilylation of terminal alkynes.<sup>65</sup> A dimeric palladium complex **140** of pyrazole TB derivative was used as a catalyst in the Mizoro-Heck C-C

coupling reaction.<sup>66</sup> Recently, the TB phosphine derivative **145** along with Pd(OAc)<sub>2</sub> was used as a catalyst in C-C and C-N bond forming reactions (Chart 5).<sup>67</sup>

**Chart 5**



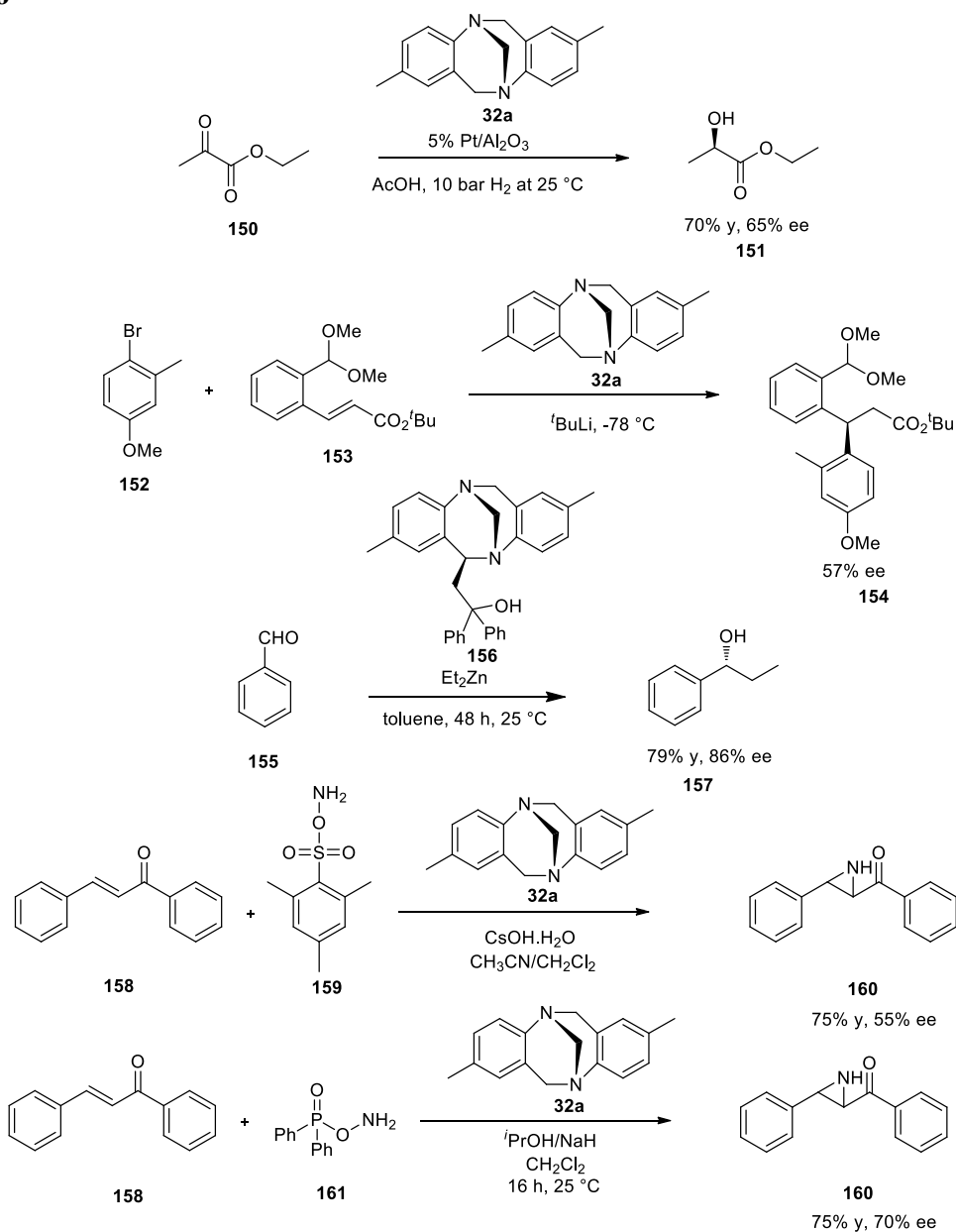
### 1.5 Applications of Tröger base and its derivatives in asymmetric transformations

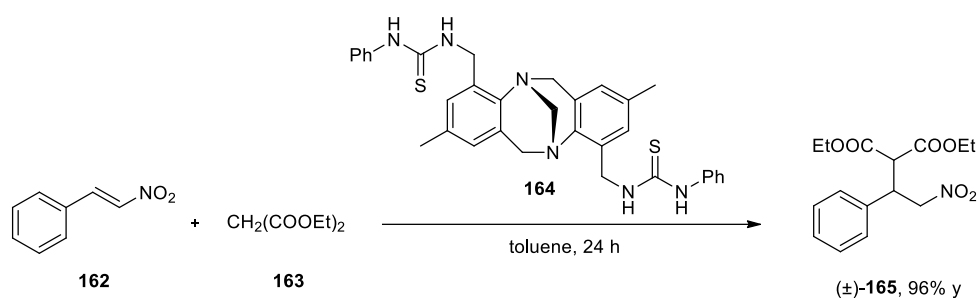
Tröger base or its derivatives are still not well developed as ligands in asymmetric transformations. However, a few transformations were reported with moderate enantioselectivity. For example, enantioselective hydrogenation of ethyl pyruvate **150** and 1,4-addition of aryllithium were reported to give 65% and 57% ee.<sup>68</sup> The selectivity of

86% ee was observed in the  $\text{Et}_2\text{Zn}$  addition to benzaldehyde **155** using **156** as a ligand.<sup>69</sup>

The catalytic asymmetric aziridination of chalcone **158** using TB **32a** and *O*-mesitylhydroxylamine (MSH) **159** was reported by Shi and co-workers<sup>70a</sup> to obtain the product **160** in 55% ee. Tröger base **32a** promoted aziridination of chalcone using  $\text{DppoNH}_2$  **161** was reported to give a product in 70% ee from this laboratory. Thiourea derivative **164** as organo catalyst gave only racemic mixture in Michale addition reaction<sup>36c</sup> (Chart 6).

**Chart 6**

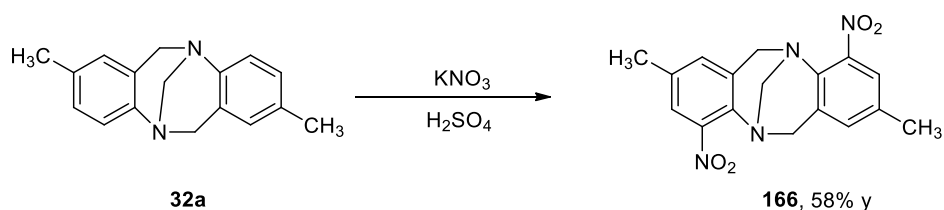




### 1.6 Synthesis of various tetrasubstituted Tröger base derivatives

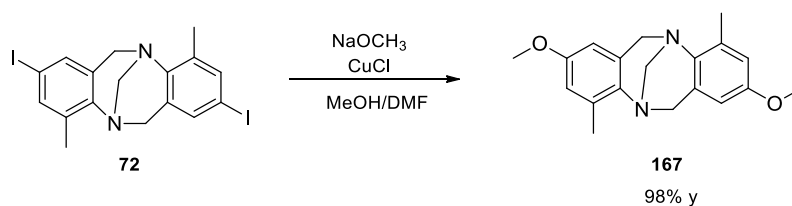
Regioselective nitration of TB **32a** was reported using potassium nitrate in sulphuric acid to introduce nitro groups to *ortho*-positions with respect to bridgehead nitrogen atoms (Scheme 27).<sup>71</sup>

**Scheme 27**



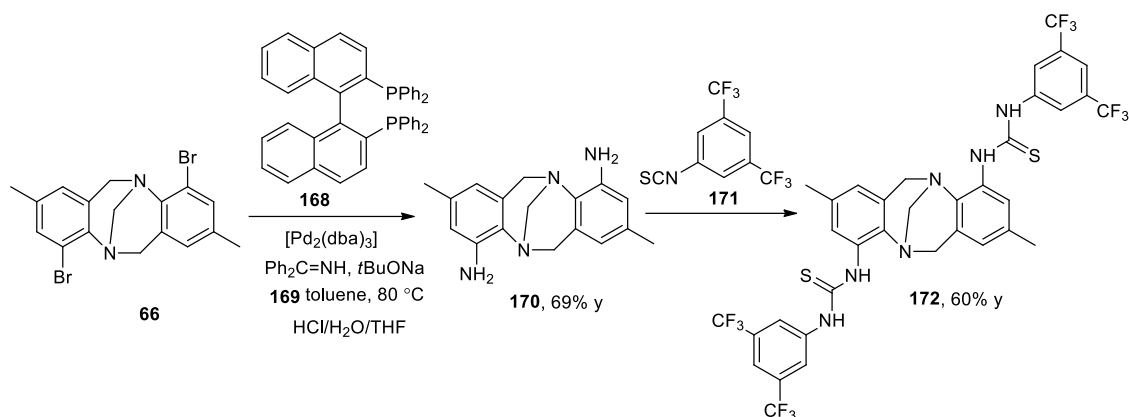
The C-O bond formation *via* a transition-metal-catalyzed reaction was reported in the synthesis of *para*-methoxy derivative **167** by employing the Ullmann reaction conditions (Scheme 28).<sup>47</sup>

**Scheme 28**



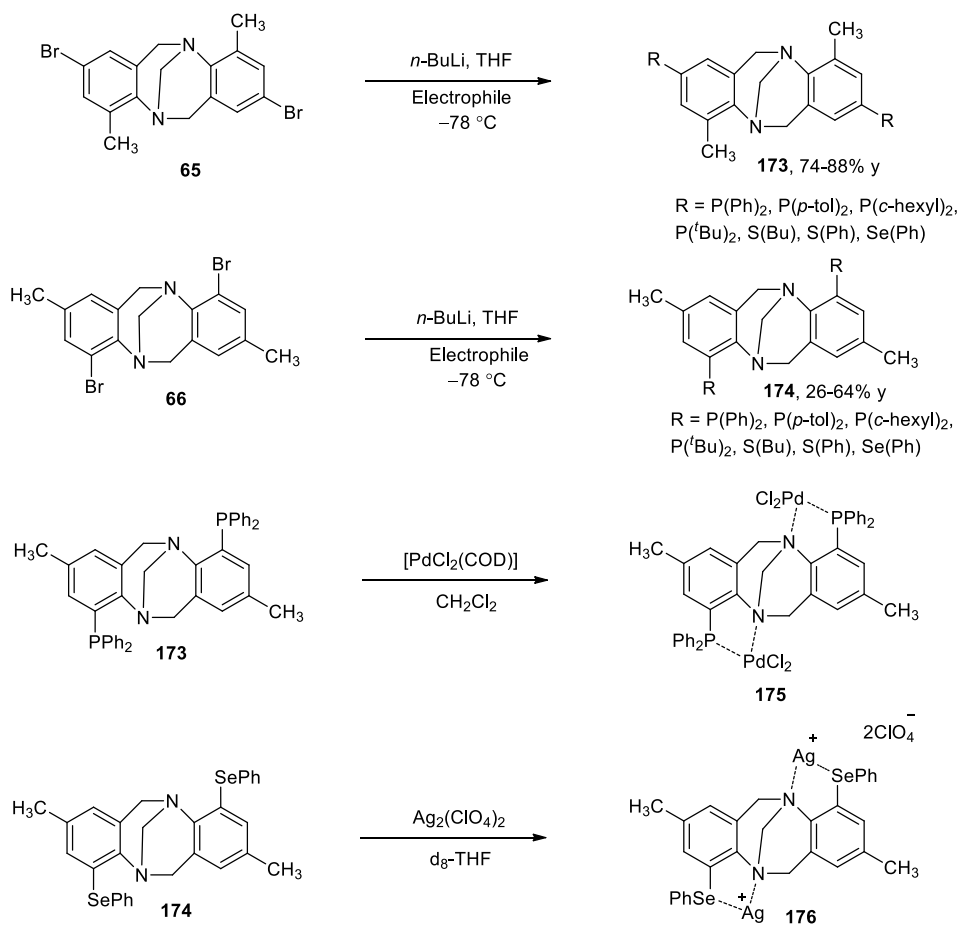
Buchwald-Hartwig amination of TB derivative **66** was reported using benzophenone imine in the presence of  $[\text{Pd}_2(\text{dba})_3]$ , (±)-2,2'-bis(diphenylphosphino)-1,1'-binaphthalene (BINAP), and *t*-BuONa at 80 °C.<sup>48</sup> The TB **172** derivative was obtained from the corresponding amino derivative **170** (Scheme 29).<sup>48</sup>

## Scheme 29



Cvengros *et al.*<sup>72</sup> reported the synthesis of various new Tröger base derivatives *via* lithiation of bromo compounds. These *ortho*-substituted TB derivatives were used as bidentate ligands to obtain the corresponding coordination complexes (Chart 7).

## Chart 7

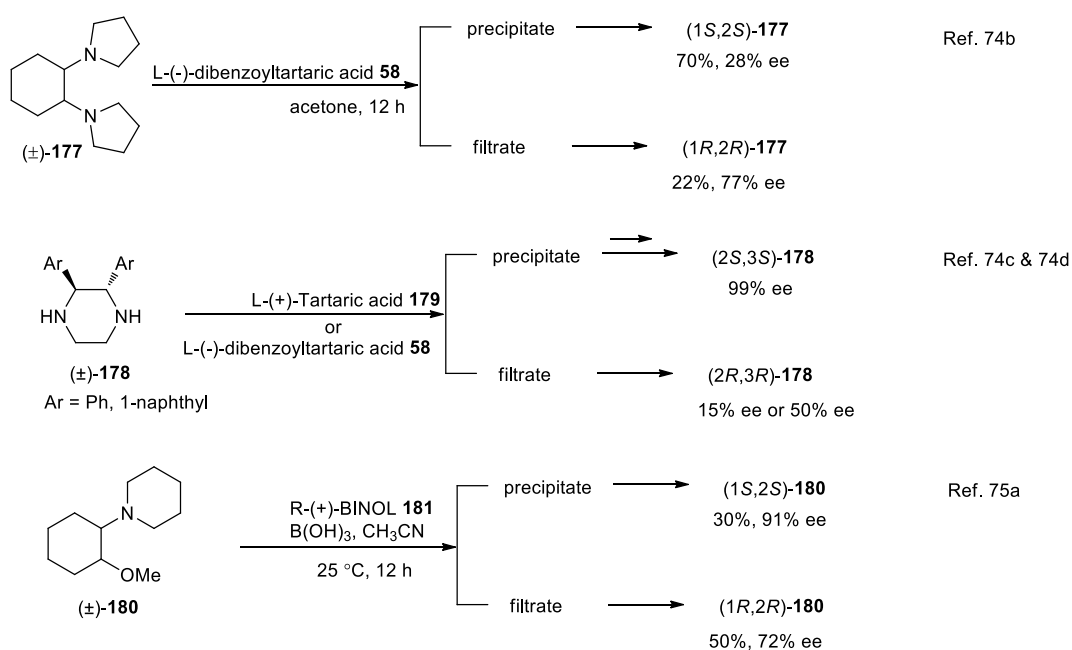


Although, chiral amines were well developed as chiral ligands,<sup>73</sup> amines with stereogenic nitrogen atoms are not well explored as ligands in organic synthesis. *Ortho*-substituted Tröger base derivatives offer new opportunities as bidentate ligands. However, these derivatives were synthesized only as a racemic mixture *via* lithiation reactions, followed by quenching of organometallic intermediates using suitable electrophiles. Therefore, developing new resolution procedures to access such derivatives in enantiomerically pure form are expected to be useful in organic synthesis.

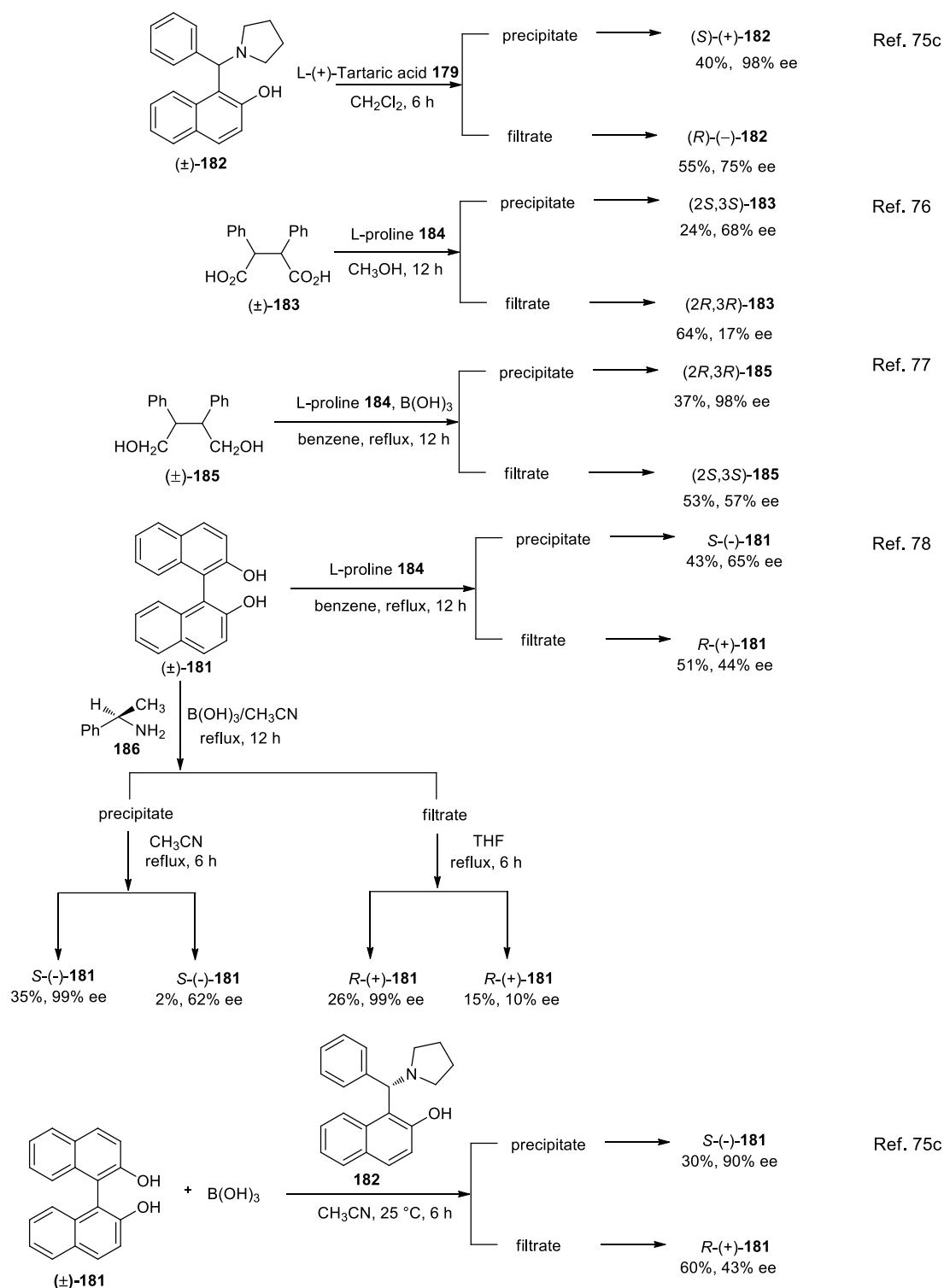
### 1.7 Previous methods for resolution of racemic mixtures developed in this laboratory

Several resolution procedures have been developed in this laboratory to access important chiral amines,<sup>74</sup> amino alcohols,<sup>75</sup> diacids<sup>76</sup> and alcohols<sup>77</sup> using commercially available resolving agents such as L-(+)-tartaric acid, chiral *O,O'*-dibenzoyltartaric acid (DBTA) and L-proline. Methods have also been developed for the resolution of an axially chiral bi-2-naphthol (Chart 8).<sup>78</sup>

**Chart 8**



## Chart 8 cont...



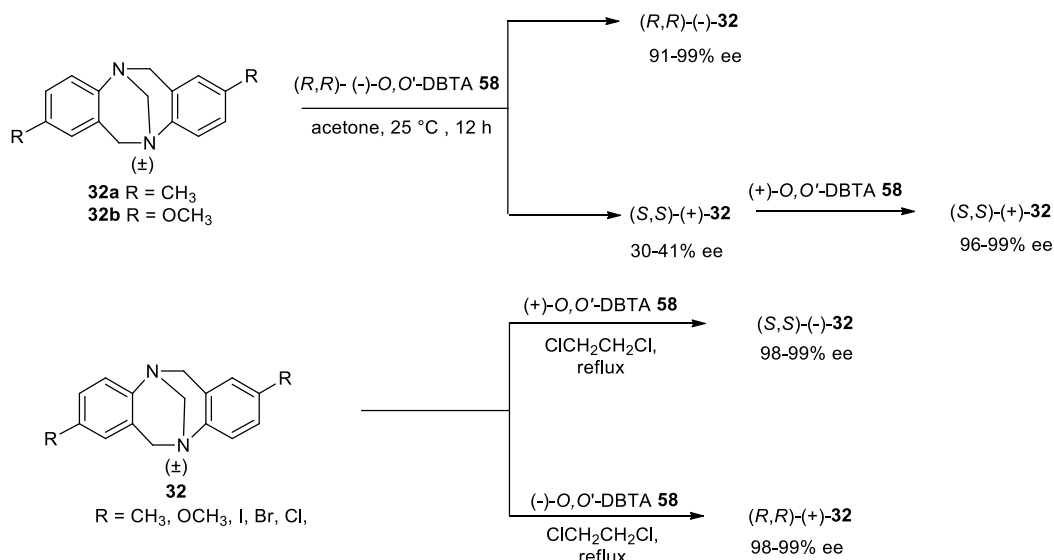
We have undertaken efforts to readily access the chiral tetrasubstituted Tröger base derivatives. The results are discussed in the next section.

## 2. Results and Discussion

### 2.1 Resolution of dimethyl Tröger base: ( $\pm$ )-2,4,8,10-tetramethyl-6H,12H-5,11-methano dibenzo[b,f][1,5]diazocine **64**

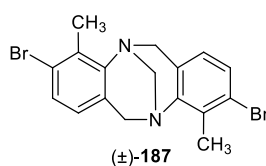
Previously, methods have been developed in this laboratory for the resolution of TB **32a** and **32b** using commercially available dibenzoyl-L-tartaric acid (DBTA) as a resolving agent.<sup>10</sup> Whereas TB **32a** forms hydrogen bonded complex with dibenzoyl-L-tartaric acid, the corresponding methoxy Tröger base derivative **32b** forms a salt. More recently, Jameson *et al.*<sup>79</sup> reported a general method for the resolution of *para*-substituted TB derivatives *via* crystallization-induced asymmetric transformation (CIAT) by heating TB derivatives with DBTA in dichloroethane (Scheme 30).

**Scheme 30**

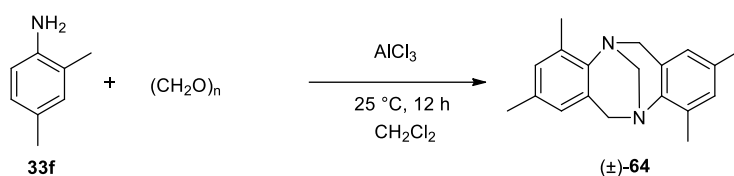


As outlined in the introductory section, most of the methods of resolution reported are for the *para*-substituted Tröger base derivatives. Although, HPLC resolution methods for *ortho*-substituted derivatives were reported, it would be difficult to obtain the isomers in larger quantities following the HPLC method. The enantiomers of TB **187** were separated by manual separation of racemic conglomerate in 20 mg scale but such methods cannot be generalized for other derivatives (Figure 11).<sup>80</sup>

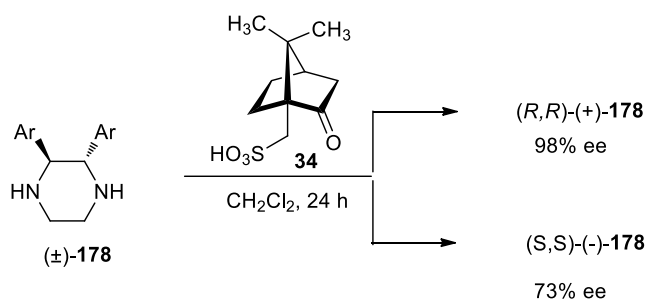


**Figure 11**

The 2,4,8,10-tetramethyl substituted Tröger base derivative (±)-**64** is easily accessed by the reaction of the corresponding aniline derivative with paraformaldehyde in the presence of  $\text{AlCl}_3$  following a procedure reported previously (Scheme 31).<sup>81</sup>

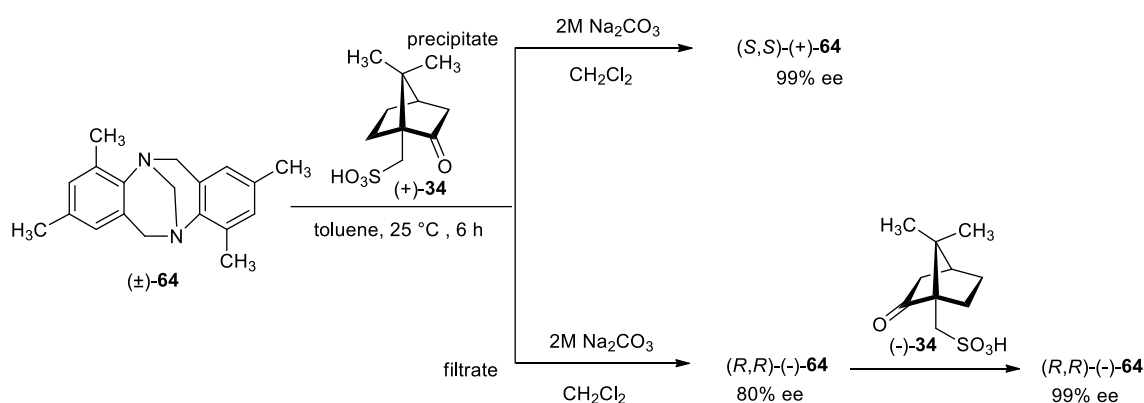
**Scheme 31**

We examined the resolution of the Tröger base compound (±)-**64** using dibenzoyl-L-tartaric acid as a resolving agent in acetone following a procedure previously reported for Tröger base and methoxy Tröger base,<sup>10</sup> but we did not observe the formation of a salt. Unlike the parent Tröger base, compound **64** has a sterically hindered *ortho*-methyl group with respect to the bridgehead nitrogen atoms. Previously, the resolution of a relatively hindered racemic 2,3-diphenylpiperazine derivative was reported using camphorsulfonic acid in  $\text{CH}_2\text{Cl}_2$  (Scheme 32).<sup>82</sup> Therefore, it was thought that the use of a stronger acid such as camphorsulfonic acid would facilitate the resolution.

**Scheme 32**

Accordingly, we have carried out the resolution in  $\text{CH}_2\text{Cl}_2$  and other solvents such as acetone and THF. However, the expected diastereomeric salt could not be separated in this run. Therefore, we turned our attention toward the use of less polar solvents. Fortunately, the salt is formed which can be also fractionated in toluene (Scheme 33). The results are summarized in Table 1. Optimum results were obtained using 2 equiv. of resolving agent in toluene (Table 1, entry 3). The volume of the solvent plays a crucial role in this resolution (Table 1, entries 1-3). The work-up of precipitate fraction using 2M aq  $\text{Na}_2\text{CO}_3$  gave the (*S,S*)-isomer with 99% ee and the (*R,R*)-isomer was obtained in 80% ee from the filtrate fraction. This resolution method is also applicable on a 20 mmol scale and the Tröger base compound (*S,S*)-**64** was obtained with 95% ee in this run (Table 1, entry 4). One crystallization of this (*S,S*)-**64** sample with 95% ee from hexane gave the sample of (*S,S*)-**64** with >99% ee. The (*R,R*)-isomer sample with 80% ee was enriched to 99% ee using 2 equiv. of (–)-camphorsulfonic acid in toluene at 25 °C (Table 1, entry 5).

### Scheme 33



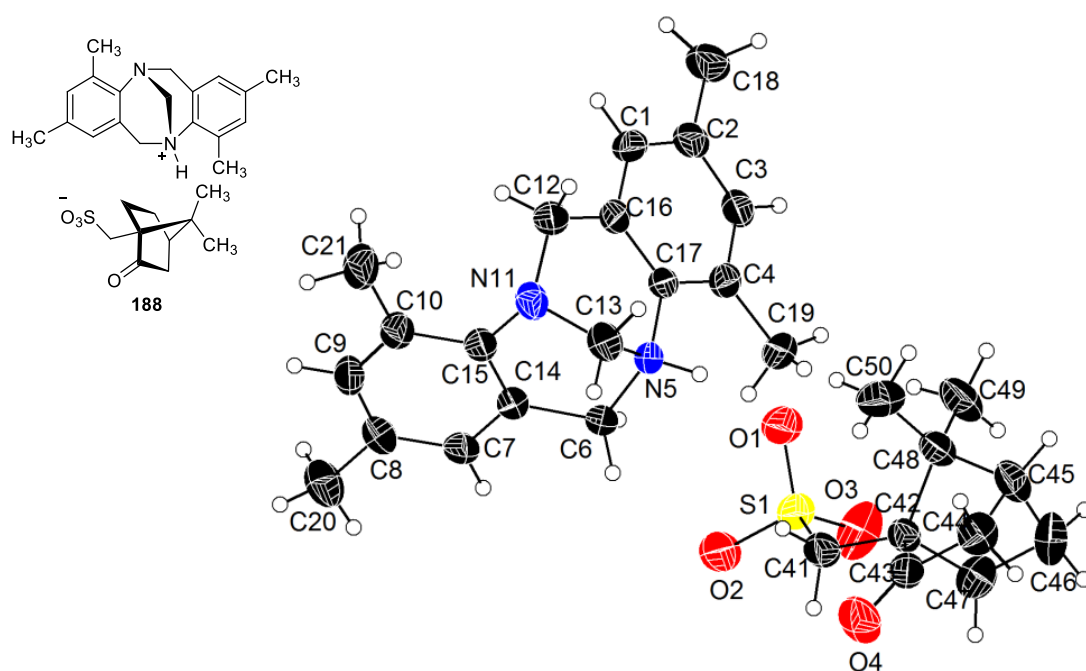
**Table 1.** Resolution of 2,4,8,10-tetramethyl-6H,12H-5,11-methanodibenzo[b,f][1,5]diazocine ( $\pm$ )-**64** using (+)-camphorsulfonic acid **34**.

entry	( $\pm$ )- <b>64</b> mmol (% ee)	acid <b>34</b> mmol	toluene (mL)	Tröger base obtained from			
				precipitate		filtrate	
				fraction		fraction	
				%ee <sup>a</sup> / conf	yield <sup>b</sup> (%)	%ee <sup>a</sup> / conf	yield <sup>b</sup> (%)
1	5 (00)	10	60	63 (S,S)	55	79 (R,R)	40
2	5 (00)	10	80	92(S,S)	49	85 (R,R)	48
3	5 (00)	10	100	99 (S,S)	45	80 (R,R)	49
4	20 (00)	40	400	95 (S,S)	46	81 (R,R)	48
5 <sup>c</sup>	5 (80)	10	40	99 (R,R)	77	67 (R,R)	17

<sup>a</sup>Enantiomeric purities are based on the HPLC analysis by using Chiralcel-OJ-H column. <sup>b</sup>Yields are of isolated Tröger base. <sup>c</sup>(-)-Camphorsulfonic acid was used as a resolving agent.

Single crystals suitable for X-ray analysis were obtained by recrystallization of the precipitated diastereomeric salt **188**[(+)-camphorsulfonic acid•(+)-**64**] from toluene. The X-ray structural analysis of salt **188** revealed that it was an 1:2 complex of the Tröger base compound **64** and (+)-camphorsulfonic acid. The asymmetric unit of the crystal structure contains two molecules of Tröger base, four molecules of camphorsulfonic acid and two water molecules (Figure 13). Interestingly, only one molecule of the camphorsulfonic acid is involved in the salt formation while the other camphorsulfonic acid is involved in the hydrogen bonding with water molecules through OH and C=O groups. Due to hydrogen bonding interactions, Tröger base compound **64** and camphorsulfonic acid are packed as a linear chain (Figure 14). The bond lengths between bridgehead nitrogens and the methylene bridge of Tröger base in the salt are N<sub>5</sub>-C<sub>13</sub> = 1.518 Å and N<sub>11</sub>-C<sub>13</sub> = 1.419 Å, indicating that

the proton transfer from (+)-camphorsulfonic acid to one of the Tröger base nitrogens and the other nitrogen is not involved in the salt formation (Figure 12). The bond lengths for the  $\text{SO}_3^-$  and  $\text{SO}_3\text{H}$  groups are  $\text{S}_1\text{-O}_1 = 1.457 \text{ \AA}$ ,  $\text{S}_1\text{-O}_2 = 1.465 \text{ \AA}$ ,  $\text{S}_1\text{-O}_3 = 1.437 \text{ \AA}$ ,  $\text{S}_3\text{-O}_{12} = 1.427$ ,  $\text{S}_3\text{-O}_{13} = 1.418$  and  $\text{S}_3\text{-O}_{14} = 1.536 \text{ \AA}$  (Table 2). The configurations of stereogenic nitrogen centers of (+)-**64** were determined as (5*S*,11*S*) by single crystal X-ray analysis (Figure 12).

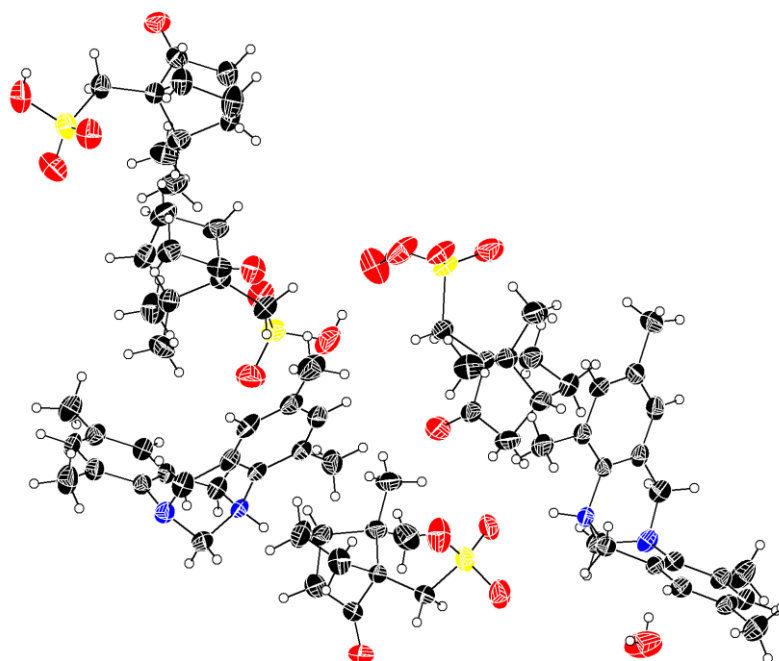


**Figure 12.** ORTEP representation of **188** (Thermal ellipsoids are drawn at 50% probability).

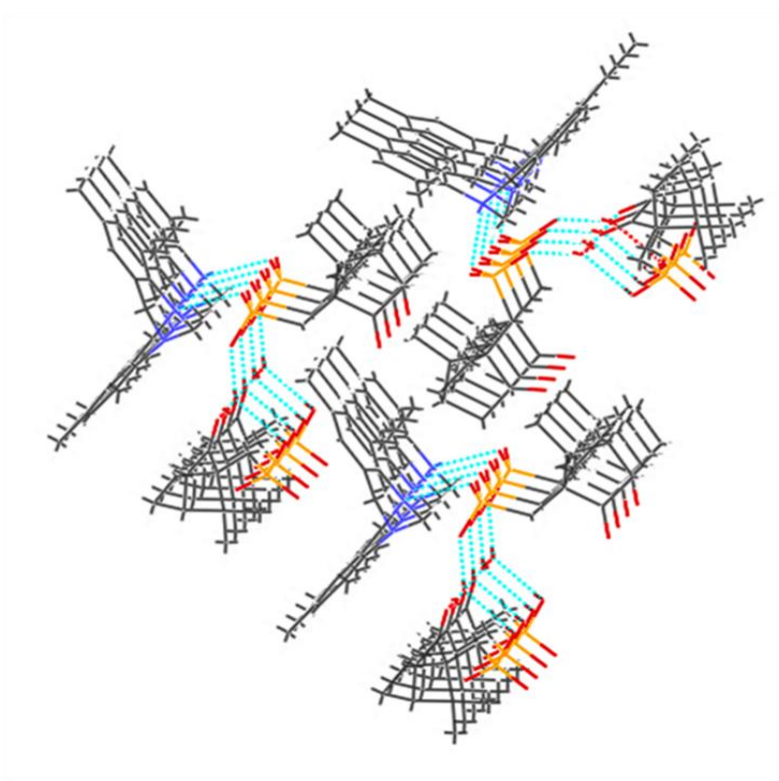
**Table 2.** Selected Bond lengths [ $\text{\AA}$ ] for **188**.

N(5)-C(13)	1.518(5)
N(11)-C(13)	1.419(5)
S(1)-O(3)	1.437(4)
S(1)-O(1)	1.457(3)
S(1)-O(2)	1.465(3)
S(3)-O(13)	1.418(3)
S(3)-O(12)	1.427(3)
*S(3)-O(11)	1.536(3)

\* S-OH bond length



**Figure 13.** ORTEP representation of the asymmetric unit of the crystal structure of diastereomeric salt **188** (Thermal ellipsoids are drawn at 50% probability).



**Figure 14.** Packing diagram of **188**, indicates the hydrogen bonding interactions.

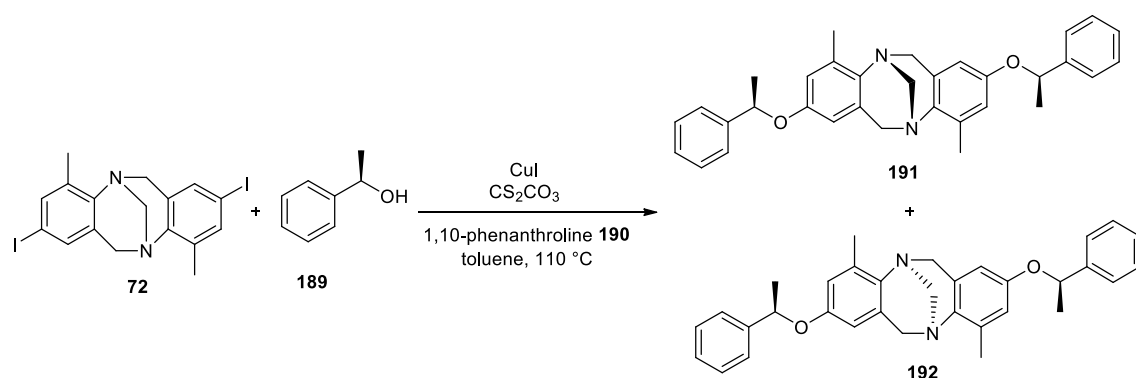
**Table 3. Crystal data and structure refinement for 188.**

Identification code	<b>188</b>	
Empirical formula	C <sub>39</sub> H <sub>56</sub> N <sub>2</sub> O <sub>9</sub> S <sub>2</sub>	
Formula weight	760.98	
Temperature	293(2) K	
Wavelength	1.54184 Å	
Crystal system	Triclinic	
Space group	p1	
Unit cell dimensions	a = 8.1082(5) Å	α = 82.616(6)°.
	b = 10.4833(8) Å	β = 82.762(6)°.
	c = 23.0502(18) Å	γ = 89.988(6)°.
Volume	1927.3(2) Å <sup>3</sup>	
Z	2	
Density (calculated)	1.311 Mg/m <sup>3</sup>	
Absorption coefficient	1.719 mm <sup>-1</sup>	
F(000)	816	
Crystal size	0.36 x 0.24 x 0.12 mm <sup>3</sup>	
Theta range for data collection	3.90 to 65.09°.	
Index ranges	-8 ≤ h ≤ 9, -12 ≤ k ≤ 12, -24 ≤ l ≤ 27	
Reflections collected	11196	
Independent reflections	7587 [R(int) = 0.0184]	
Completeness to theta = 65.09°	98.2 %	
Absorption correction	Semi-empirical from equivalents	
Max. and min. transmission	0.8203 and 0.5766	
Refinement method	Full-matrix least-squares on F <sup>2</sup>	
Data / restraints / parameters	7587 / 3 / 969	
Goodness-of-fit on F <sup>2</sup>	1.032	
Final R indices [I > 2σ(I)]	R1 = 0.0412, wR2 = 0.1093	
R indices (all data)	R1 = 0.0437, wR2 = 0.1120	
Absolute structure parameter	0.019(13)	
Largest diff. peak and hole	0.263 and -0.291 e.Å <sup>-3</sup>	

## 2.2 Resolution of dibromo Tröger base: ( $\pm$ )-2,8-dibromo-4,10-dimethyl-6H,12H-5,11-methanodibenzo[b,f][1,5]diazocine **65**

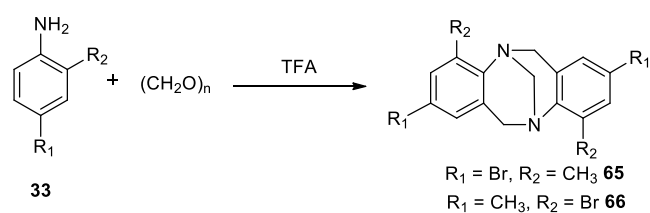
Lutzen and co-workers<sup>83</sup> reported attempts to resolve TB **72** and the corresponding bromo derivative **65** under various conditions using DBTA, DTTA or CSA as a chiral resolving agent but these attempts were not successful. However, they reported the preparation of the diastereomeric mixture **191** and **192** by Ullmann cross-coupling and separation of the diastereomers by a HPLC method (Scheme 34).

**Scheme 34**



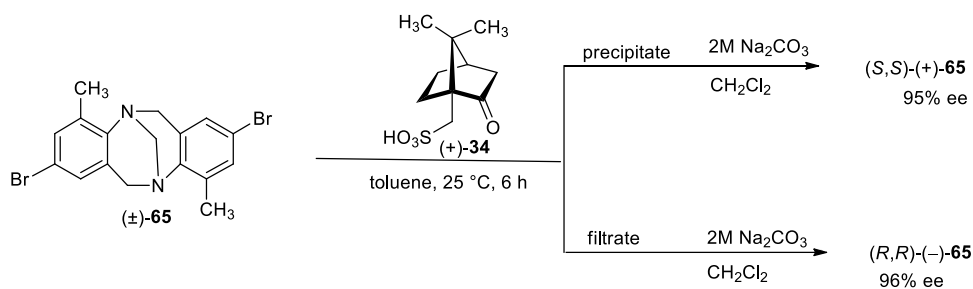
It was of interest to examine the efficacy of our method for the resolution of structurally similar derivatives such as dibromo-dimethyl Tröger base compound **65** since such derivatives could be readily functionalized following reported methods. We selected the bromo Tröger base compounds ( $\pm$ )-**65** and ( $\pm$ )-**66** for our studies since these Tröger base derivatives can be readily accessed by condensation of the corresponding substituted anilines and paraformaldehyde in the presence of trifluoroacetic acid (Scheme 35).<sup>84</sup>

**Scheme 35**



We observed that the racemic mixture ( $\pm$ )-**65** could be resolved using 2 equiv. of (+)-camphorsulfonic acid in toluene (Scheme 36). The results are summarized in Table 4. Reaction of the isolated salt with aqueous  $\text{Na}_2\text{CO}_3$  gave the (*S,S*)-isomer with 95% ee, and the (*R,R*)-isomer was obtained with 96% ee from the filtrate fraction (Table 4, entry 1). Similar treatment of the crystals of **193** [(+)-camphorsulfonic acid•(+)-**65**] obtained from  $\text{CH}_2\text{Cl}_2$  gave (*S,S*)-**65** with 98% ee. Thus, both isomers were obtained in enantiomerically pure form (Table 4). We also observed that the (*R,R*)-enantiomer was isolated in enantiomerically pure form from the filtrate fraction in all experiments, and the (*S,S*)-isomer was obtained in 82-95% ee from the precipitate fraction (Table 4, entry 1-4).

### Scheme 36



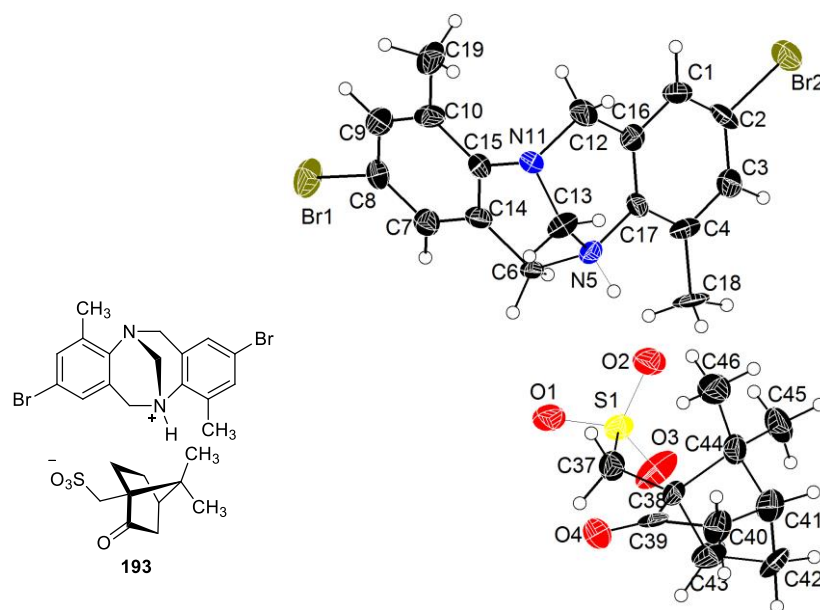
**Table 4.** Resolution of 2,8-dibromo-4,10-dimethyl-6H,12H-5,11-methanodibenzo[b,f][1,5] diazocine ( $\pm$ )-**65** using (+)-camphorsulfonic acid.

entry	( $\pm$ )- <b>65</b> mmol (% ee)	acid <b>34</b> mmol	toluene (mL)	Tröger base obtained from			
				precipitate		filtrate	
				fraction		fraction	
				%ee <sup>a</sup> / conf	yield <sup>b</sup> (%)	%ee <sup>a</sup> / conf	yield <sup>b</sup> (%)
1	5 (00)	10	100	95 ( <i>S,S</i> )	48	96 ( <i>R,R</i> )	49
2	5 (00)	10	80	92( <i>S,S</i> )	49	96 ( <i>R,R</i> )	48
3	5 (00)	10	60	92 ( <i>S,S</i> )	45	97 ( <i>R,R</i> )	49
4	5 (00)	10	40	82 ( <i>S,S</i> )	52	97 ( <i>R,R</i> )	42

<sup>a</sup>Enantiomeric purities are based on the HPLC analysis by using Chiralcel-OJ-H column. <sup>b</sup>Yields are of isolated Tröger base.



The  $^1\text{H}$  NMR spectra and single crystal X-ray structural analysis of the salt **193** revealed that it was a 1:2 complex. Bond length differences ( $\text{N}_5\text{-C}_{13} = 1.519 \text{ \AA}$ , and  $\text{N}_{11}\text{-C}_{13} = 1.435 \text{ \AA}$ ) were also observed between bridgehead nitrogens and methylene bridge in the salt **193** as in the case of **188**. Also,  $\text{SO}_3^-$  and  $\text{SO}_3\text{H}$  groups are present in the crystal structure (Table 5, Figure 16, 17). The configurations at the stereogenic nitrogen centers were assigned as (5*S*,11*S*) for the (+)-isomer by single crystal X-ray analysis (Figure 15).

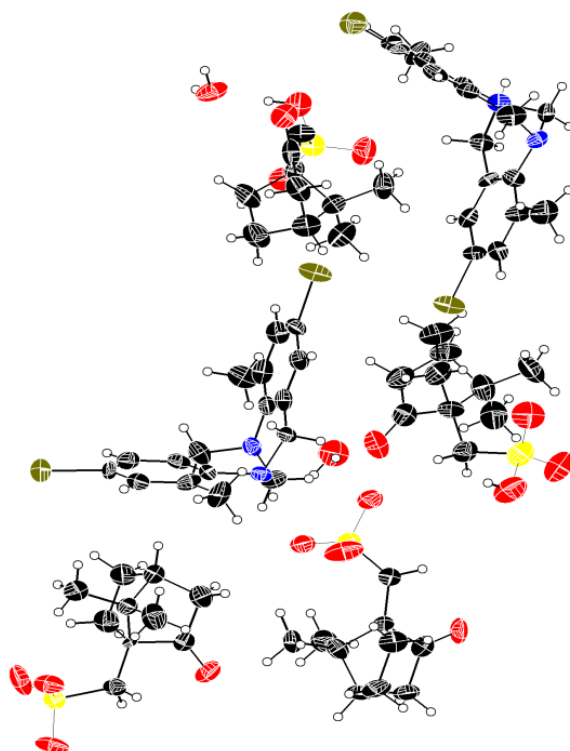


**Figure 15.** ORTEP representation of **193** (Thermal ellipsoids are drawn at 50% probability).

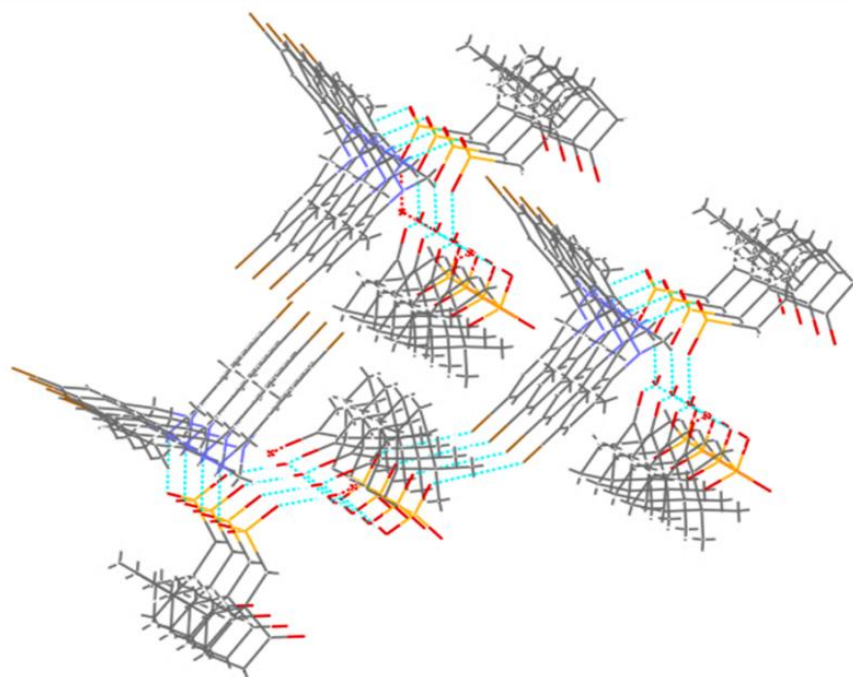
**Table 5.** Selected Bond lengths [ $\text{\AA}$ ] for **193**.

N(5)-C(13)	1.519(5)
N(11)-C(13)	1.435(5)
S(1)-O(1)	1.478(3)
S(1)-O(2)	1.472(3)
S(1)-O(3)	1.447(3)
S(3)-O(15)	1.431(3)
S(3)-O(13)	1.439(3)
*S(3)-O(14)	1.530(3)

\*S-OH bond length



**Figure 16.** ORTEP representation of the asymmetric unit of the crystal structure of diastereomeric salt **193** (Thermal ellipsoids are drawn at 50% probability).



**Figure 17.** Packing diagram of **193**, indicates the hydrogen bonding interactions

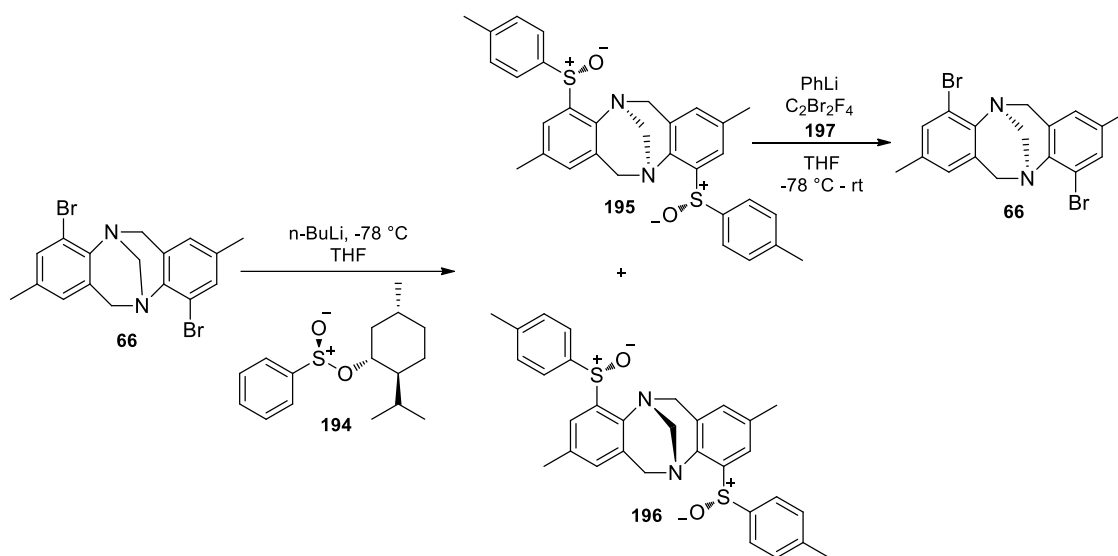
**Table 6. Crystal data and structure refinement for 193.**

Identification code	<b>193</b>	
Empirical formula	$C_{74}H_{98}Br_4N_4O_{18}S_4$	
Formula weight	1779.44	
Temperature	100(2) K	
Wavelength	0.71073 Å	
Crystal system	Triclinic	
Space group	P1	
Unit cell dimensions	$a = 7.9994(3)$ Å	$\alpha = 82.673(4)^\circ$ .
	$b = 10.3222(5)$ Å	$\beta = 82.277(3)^\circ$ .
	$c = 23.2240(9)$ Å	$\gamma = 89.954(4)^\circ$ .
Volume	$1884.47(14)$ Å <sup>3</sup>	
Z	1	
Density (calculated)	1.568 Mg/m <sup>3</sup>	
Absorption coefficient	2.319 mm <sup>-1</sup>	
F(000)	918	
Crystal size	0.30 x 0.24 x 0.20 mm <sup>3</sup>	
Theta range for data collection	2.50 to 30.36°.	
Index ranges	-11 ≤ h ≤ 11, -14 ≤ k ≤ 14, -32 ≤ l ≤ 32	
Reflections collected	37013	
Independent reflections	19243 [R(int) = 0.0513]	
Completeness to theta = 71.62°	99.9 %	
Absorption correction	Semi-empirical from equivalents	
Max. and min. transmission	0.6541 and 0.5429	
Refinement method	Full-matrix least-squares on F <sup>2</sup>	
Data / restraints / parameters	19243 / 6 / 955	
Goodness-of-fit on F <sup>2</sup>	1.048	
Final R indices [I > 2σ(I)]	R1 = 0.0521, wR2 = 0.1038	
R indices (all data)	R1 = 0.0611, wR2 = 0.1097	
Absolute structure parameter	0.001(5)	
Largest diff. peak and hole	1.300 and -0.636 e.Å <sup>-3</sup>	

### 2.3 Resolution of 4,10-dibromo Tröger base: ( $\pm$ )-4,10-dibromo-2,8-dimethyl-6H,12H-5,11-methanodibenzo[b,f][1,5]diazocine **66**

Previously, the chiral 2,8-dimethyl-4,10-dibromo derivative **66** was synthesized by a multi-step process involving bromination of disulfoxide **195** using PhLi and 1,2-dibromo-1,1,2,2-tetrafluoroethane **197** in dry THF in a crucial step (Scheme 37).<sup>25</sup>

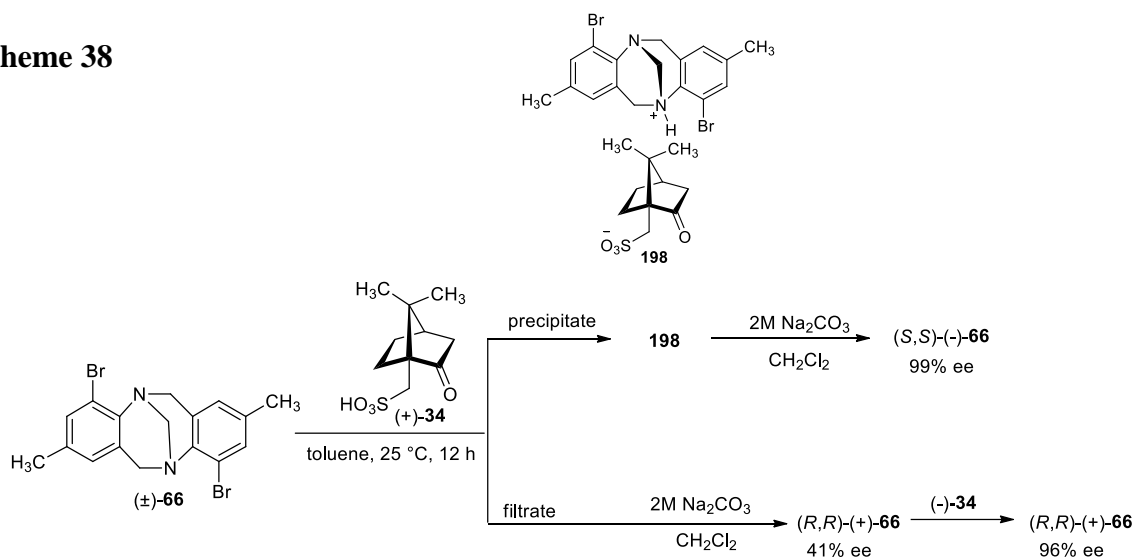
**Scheme 37**



We carried out the resolution of ( $\pm$ )-**66** under the experimental conditions followed for the resolution of the Tröger base derivatives ( $\pm$ )-**64** and ( $\pm$ )-**65** (Scheme 38). In these runs, only the camphorsulfonic acid precipitated out along with trace amounts of Tröger base. Fortunately, use of 1 equiv. of (+)-camphorsulfonic acid in toluene fractionated the salts formed. The results are summarized in Table 7. The (*S,S*)-isomer could be isolated in 99% ee from the precipitate fraction and the (*R,R*)-isomer was obtained with 41% ee from the filtrate fraction (Table 7, entry 2). The (*R,R*)-isomer sample of 41% ee was enriched to 96% ee using 1 equiv of (–)-camphorsulfonic acid in toluene. The 1:1 composition of the complex **198** [(+)-camphorsulfonic acid•(–)-**66**] was confirmed by NMR analysis. The crystals suitable for X-ray analysis could not be obtained for this salt by recrystallization using various solvents.

However, we obtained the crystals of enantiomerically pure (–)-**66** by crystallization of the salt **198** using EtOH as solvent (Figure 18).

**Scheme 38**



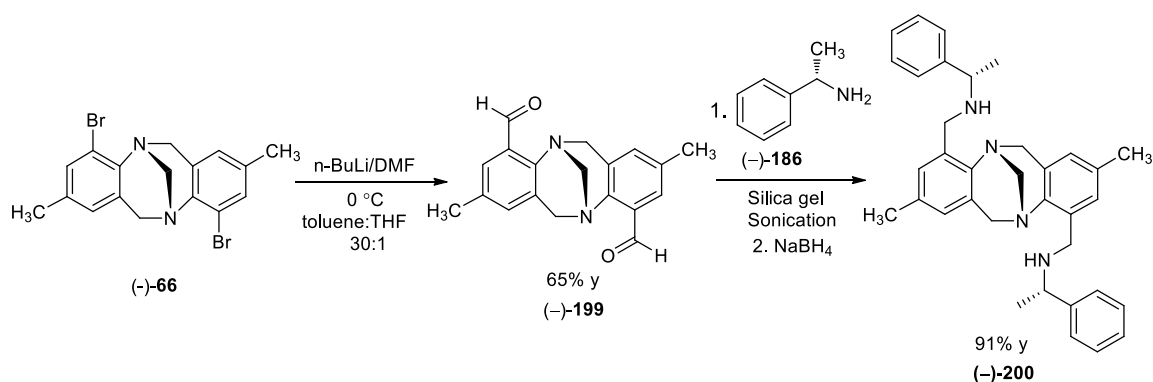
**Table 7.** Resolution of 4,10-dibromo-2,8-dimethyl-6H,12H-5,11-methanodibenzo[b,f][1,5] diazocine (±)-**66** using (+)-camphorsulfonic acid.

entry	(±)- <b>66</b> mmol (% ee)	acid <b>34</b> mmol	toluene (mL)	Tröger base obtained from			
				precipitate		filtrate	
				fraction		fraction	
				%ee <sup>a</sup> / conf	yield <sup>b</sup> (%)	%ee <sup>a</sup> / conf	yield <sup>b</sup> (%)
1	5 (00)	5	20	99 (S,S)	21	24 (R,R)	78
2	5 (00)	5	15	99(S,S)	29	41 (R,R)	68
3 <sup>c</sup>	5(00)	5	15	95(S,S)	28	38 (R,R)	70
4	10 (00)	10	50	96 (S,S)	26	31 (R,R)	73
5 <sup>d</sup>	5 (41)	5	15	96 (R,R)	25	10 (R,R)	71

<sup>a</sup>Enantiomeric purities are based on the HPLC analysis by using chiralcel-OJ-H column. <sup>b</sup>Yields are of isolated Tröger base. <sup>c</sup>Resolution was carried out for 6 h. <sup>d</sup>(–)-Camphorsulfonic acid was used as a resolving agent.

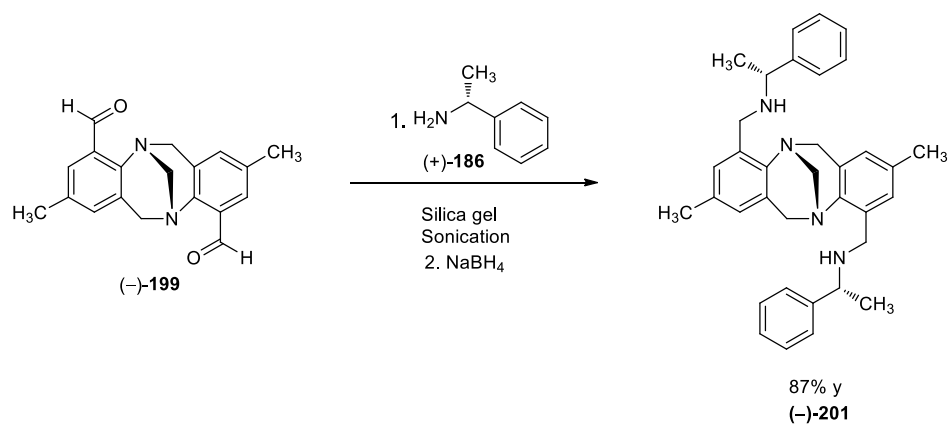
The presence of bromo groups in (–)-**66** is useful for further functionalization. Thus, we converted the bromo group to an aldehyde *via* a lithiation reaction. The resulting aldehyde was condensed with chiral amine **186** under sonication in the presence of silica gel to obtain the imine derivative, which upon reduction with sodium borohydride gave chiral amine **200** in 91% yield (Scheme 39). Recrystallization of the amine **200** from acetone gave crystals suitable for single crystal X-ray structural analysis. The configurations of nitrogen centers of (–)-**66** were determined as (5*S*,11*S*) by single crystal X-ray analysis (Figure 19).

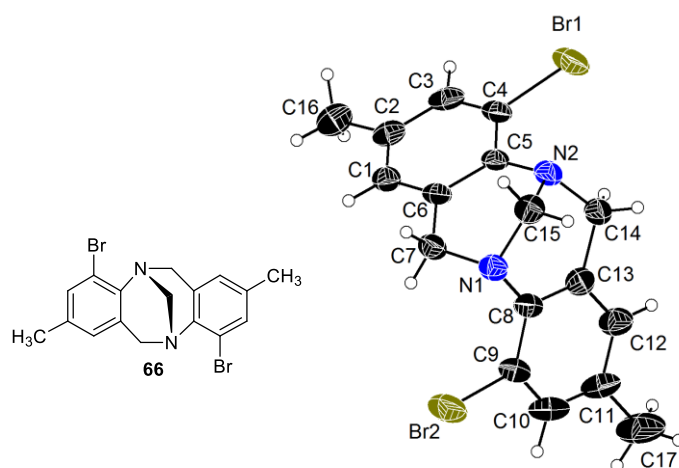
Scheme 39



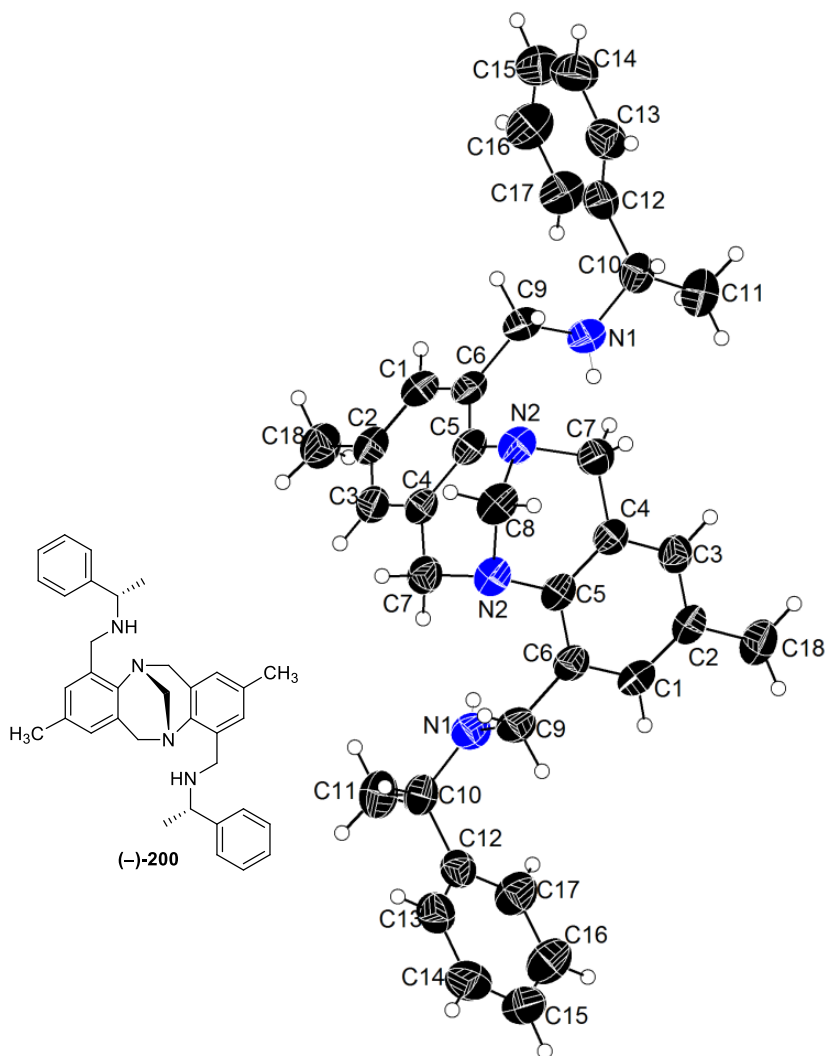
The *R*-(+)- $\alpha$ -methylbenzylamine was also used in the condensation reaction to obtain the corresponding chiral derivative **201** in 87% yield (Scheme 40).

Scheme 40





**Figure 18.** ORTEP representation of (-)-**66** (Thermal ellipsoids are drawn at 50% probability).



**Figure 19.** ORTEP representation of (-)-**200** (Thermal ellipsoids are drawn at 50% probability).

**Table 8. Crystal data and structure refinement for 66**

Identification code	<b>66</b>	
Empirical formula	C <sub>17</sub> H <sub>16</sub> Br <sub>2</sub> N <sub>2</sub>	
Formula weight	408.14	
Temperature	293(2) K	
Wavelength	1.54184 Å	
Crystal system	Monoclinic	
Space group	P21	
Unit cell dimensions	a = 7.7330(2) Å	α = 90°.
	b = 8.4737(3) Å	β = 95.968(2)°.
	c = 12.1573(3) Å	γ = 90°.
Volume	792.32(4) Å <sup>3</sup>	
Z	2	
Density (calculated)	1.711 Mg/m <sup>3</sup>	
Absorption coefficient	6.433 mm <sup>-1</sup>	
F(000)	404	
Crystal size	0.36 x 0.24 x 0.12 mm <sup>3</sup>	
Theta range for data collection	3.66 to 71.40°.	
Index ranges	-4 ≤ h ≤ 9, -8 ≤ k ≤ 10, -14 ≤ l ≤ 14	
Reflections collected	2819	
Independent reflections	2120 [R(int) = 0.0287]	
Completeness to theta = 71.40°	98.0 %	
Max. and min. transmission	1.00000 and 0.37637	
Refinement method	Full-matrix least-squares on F <sup>2</sup>	
Data / restraints / parameters	2120 / 1 / 193	
Goodness-of-fit on F <sup>2</sup>	1.080	
Final R indices [I > 2σ(I)]	R1 = 0.0447, wR2 = 0.1176	
R indices (all data)	R1 = 0.0449, wR2 = 0.1180	
Absolute structure parameter	0.01(3)	
Extinction coefficient	0.066(3)	
Largest diff. peak and hole	0.547 and -0.685 e.Å <sup>-3</sup>	



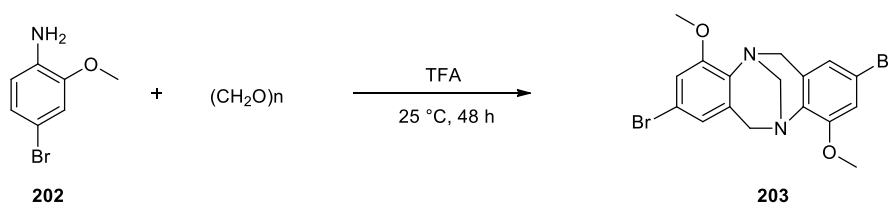
**Table 9. Crystal data and structure refinement for 200.**

Identification code	<b>200</b>	
Empirical formula	C <sub>35</sub> H <sub>40</sub> N <sub>4</sub>	
Formula weight	516.71	
Temperature	298(2) K	
Wavelength	1.54184 Å	
Crystal system	Monoclinic	
Space group	C2	
Unit cell dimensions	a = 18.660(4) Å	$\alpha = 90^\circ$ .
	b = 5.3434(4) Å	$\beta = 119.033(10)^\circ$ .
	c = 16.5853(19) Å	$\gamma = 90^\circ$ .
Volume	1445.9(4) Å <sup>3</sup>	
Z	2	
Density (calculated)	1.187 Mg/m <sup>3</sup>	
Absorption coefficient	0.535 mm <sup>-1</sup>	
F(000)	556	
Crystal size	0.22 x 0.20 x 0.18 mm <sup>3</sup>	
Theta range for data collection	3.05 to 71.57°.	
Index ranges	-20 ≤ h ≤ 22, -6 ≤ k ≤ 2, -20 ≤ l ≤ 15	
Reflections collected	2656	
Independent reflections	1702 [R(int) = 0.0160]	
Completeness to theta = 71.57°	96.5 %	
Refinement method	Full-matrix least-squares on F <sup>2</sup>	
Data / restraints / parameters	1702 / 1 / 179	
Goodness-of-fit on F <sup>2</sup>	1.043	
Final R indices [I > 2σ(I)]	R1 = 0.0459, wR2 = 0.1280	
R indices (all data)	R1 = 0.0499, wR2 = 0.1320	
Absolute structure parameter	-0.2(9)	
Largest diff. peak and hole	0.258 and -0.220 e.Å <sup>-3</sup>	

## 2.4 Resolution of dimethoxy Tröger base: ( $\pm$ )-4,10-dimethoxy-2,8-dimethyl-6H,12H-5,11-methanodibenzo[b,f][1,5]diazocine **204**.

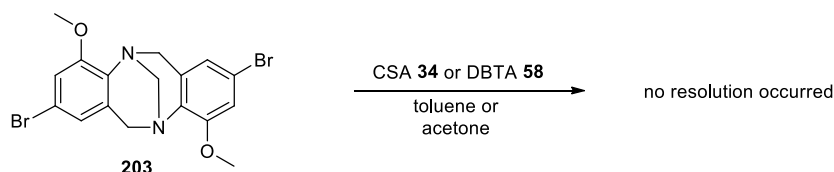
We envisaged that Tröger base **203** is structurally similar to other *ortho*-substituted derivatives (Scheme 36) resolvable using camphorsulfonic acid. Accordingly, we have prepared the compound **203** by following a reported procedure (Scheme 41).<sup>85</sup>

**Scheme 41**



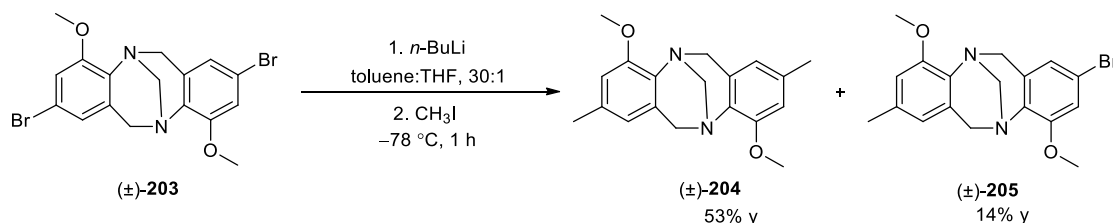
We carried out the resolution of compound **203** under the standard condition using CSA or DBTA. However, the expected salt was not formed in all these runs (Scheme 42).

**Scheme 42**



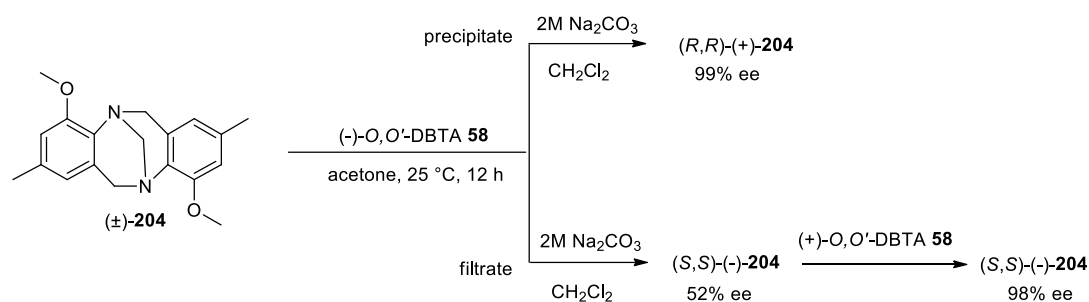
To understand further, we prepared the *ortho*-methoxy derivative **204** via a lithiation reaction followed by quenching with iodomethane. The Tröger base derivatives **204** and **205** were obtained in 53 and 14% yield respectively (Scheme 43).

**Scheme 43**



Initially, we carried out the resolution of Tröger base **204** using CSA as a chiral acid in toluene. Treatment of the isolated precipitate with aq  $\text{Na}_2\text{CO}_3$  gave only a racemic mixture in this run.

Scheme 44



Previously, it was reported that the *para*-methoxy derivative forms a salt with dibenzoyl-L-tartaric acid, while the parent Tröger base forms only hydrogen bonded aggregates.<sup>10</sup> Tröger base compound **204** is expected to be a strong base compared to other *ortho*-substituted derivatives resolved using CSA as a chiral resolving agent. Therefore, it was thought that a weak acid such as DBTA **58** could also be used as a chiral resolving agent (Scheme 44). Accordingly, we carried out the resolution studies in acetone. The results are summarized in Table 10. Treatment of the salts obtained using 1:1 ratio of base and chiral acid with aq  $\text{Na}_2\text{CO}_3$  gave the  $(R,R)$ -isomer with 92% ee. The  $(S,S)$ -isomer was obtained with 59% ee from the filtrate fraction (Table 10, entry 1). Optimum results were obtained using the base and chiral acid in 1:2 ratio (Table 10, entry 2). In this case, the  $(R,R)$ -isomer was obtained with 99% ee from precipitate fraction and the  $(S,S)$ -isomer with 52% ee was obtained from the filtrate fraction. Further, resolution using 3 equiv. of resolving agent also gave similar results (Table 10, entry 3). The  $(S,S)$ -isomer with 52% ee was readily enriched to obtain samples with 98% ee by repeating the resolution procedure using  $(+)$ -DBTA.

The  $^1\text{H}$  NMR analysis of diastereomeric salt revealed that it is an 1:1 complex of Tröger base **204** and  $(-)$ -DBTA **58**. Crystallization of diastereomeric salt **206** [ $(-)$ -DBTA  $\cdot$   $(+)$ -**204**] from ethyl acetate gave crystals suitable for the X-ray diffraction analysis. The crystal structure analysis confirmed that the salt is a 1:1 complex and the asymmetric unit contains one molecule of *ortho*-methoxy Tröger base **204** and dibenzoyl-L-tartaric acid **58**. The

ORTEP diagram is shown in Figure 20. It clearly shows proton transfer from (-)-DBTA to Tröger base **204**. The configurations of the stereogenic nitrogen centers of (+)-**204** were determined as 5*R*,11*R* by single crystal X-ray analysis (Figure 20).

**Table 10.** Resolution of Tröger base (±)-**204** using *O,O'*-dibenzoyl-L-tartaric acid

entry	(±)- <b>204</b> mmol (% ee)	acid <b>58</b> mmol	acetone (mL)	Tröger base obtained from			
				precipitate		filtrate	
				fraction		fraction	
				%ee <sup>a</sup> / config	yield <sup>b</sup> (%)	%ee <sup>a</sup> / config	yield <sup>b</sup> (%)
1	2 (00)	2	15	92 (R,R)	34	59 (S,S)	63
2	2 (00)	4	25	99 (R,R)	32	52 (S,S)	66
3	2 (00)	6	25	95 (R,R)	36	56 (S,S)	59
4 <sup>c</sup>	2 (52)	4	25	98 (S,S)	34	22 (R,R)	62

<sup>a</sup>Enantiomeric purities are based on the HPLC analysis by using Chiral-OJ-H column. <sup>b</sup>Yields are of isolated Tröger base. <sup>c</sup>(+)-Dibenzoyl-L-tartaric acid was used as resolving agent.

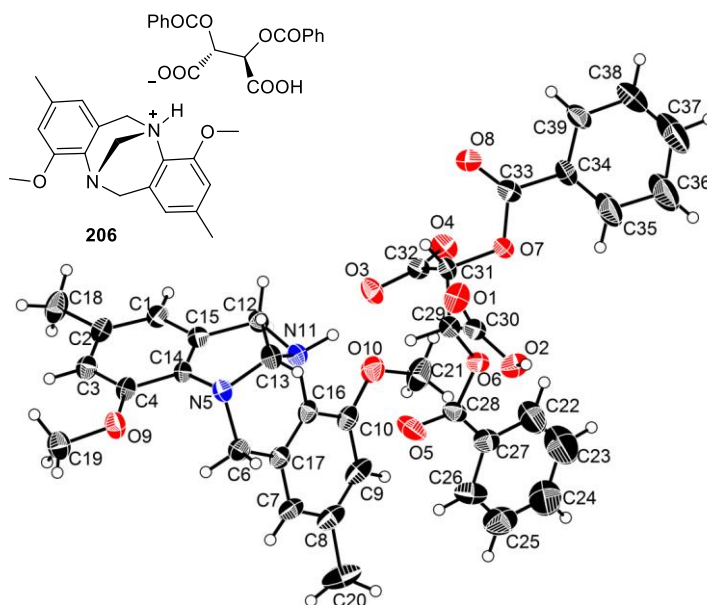
**Table 11.** Selected Bond lengths [Å] for **206**.

N(5)-C(13)	1.400(6)
N(11)-C(13)	1.504(6)
O(1)-C(30)	1.215(6)
O(2)-C(30)	1.284(6)
O(3)-C(32)	1.215(5)
*O(4)-C(32)	1.284(5)

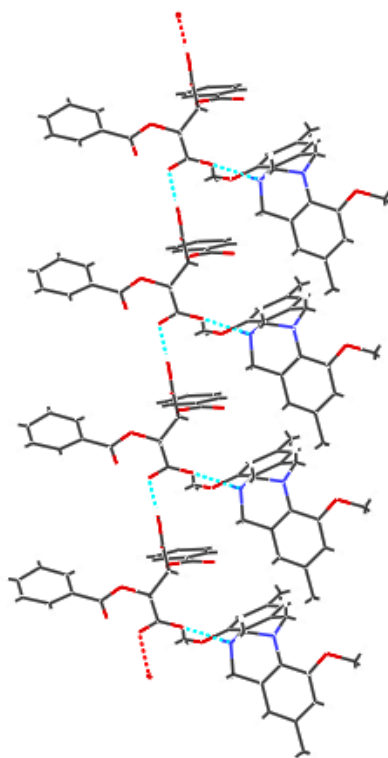
\*C-OH bond length

The selected bond lengths are given in Table 11. The diastereomeric salt **206** formation resulted in the bond lengths difference ( $N_5-C_{13} = 1.406$  and  $N_{11}-C_{13} = 1.504$  Å) between bridgehead nitrogens and methylene bridge of Tröger base compound **204**. The bond lengths of carboxylic acid and carboxylate groups are also given in Table 11. Tröger base and dibenzoyl-L-tartaric acid were packed as a linear chain (Figure 21) because of the strong O-H...O and N-H...O hydrogen bonding interactions ( $N-H\cdots O$ , 2.564 Å, 146°;  $O-H\cdots O$ , 2.534

Å, 167°). It is of interest to note that whereas the *ortho*-substituted derivative and chiral acid are packed as a linear chain in the diastereomeric salt, the *para*-substituted derivative and DBTA were packed as a helix in the diastereomeric salt (Figure 21).<sup>10</sup>



**Figure 20.** ORTEP representation of **206** (Thermal ellipsoids are drawn at 25% probability)



**Figure 21.** Packing diagram of **206**, indicates the hydrogen bonding interactions

**Table 12. Crystal data and structure refinement for 206.**

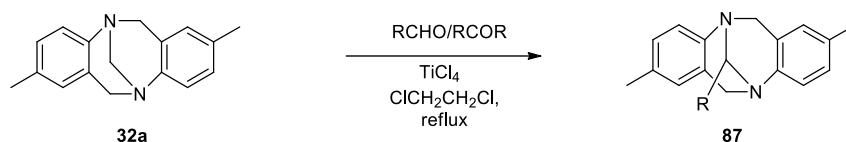
Identification code	<b>206</b>	
Empirical formula	C <sub>37</sub> H <sub>36</sub> N <sub>2</sub> O <sub>10</sub>	
Formula weight	668.68	
Temperature	293(2) K	
Wavelength	1.54184 Å	
Crystal system	Orthorhombic	
Space group	P21212	
Unit cell dimensions	a = 23.8296(9) Å	α = 90°.
	b = 21.2588(9) Å	β = 90°.
	c = 7.8763(3) Å	γ = 90°.
Volume	3990.0(3) Å <sup>3</sup>	
Z	4	
Density (calculated)	1.113 Mg/m <sup>3</sup>	
Absorption coefficient	0.675 mm <sup>-1</sup>	
F(000)	1408	
Crystal size	0.36 x 0.24 x 0.12 mm <sup>3</sup>	
Theta range for data collection	2.79 to 71.74°.	
Index ranges	-29 ≤ h ≤ 28, -26 ≤ k ≤ 24, -9 ≤ l ≤ 7	
Reflections collected	9407	
Independent reflections	6283 [R(int) = 0.0788]	
Completeness to theta = 71.74°	97.9 %	
Refinement method	Full-matrix least-squares on F <sup>2</sup>	
Data / restraints / parameters	6283 / 0 / 446	
Goodness-of-fit on F <sup>2</sup>	0.919	
Final R indices [I > 2σ(I)]	R1 = 0.0703, wR2 = 0.1696	
R indices (all data)	R1 = 0.1002, wR2 = 0.1938	
Absolute structure parameter	-0.1(3)	
Largest diff. peak and hole	0.209 and -0.201 e.Å <sup>-3</sup>	

## 2.5 Synthesis of 5,11-substituted Tröger base derivatives

### 2.5.1 Exchange of the methylene bridge of Tröger base with dimethylformamide (DMF)

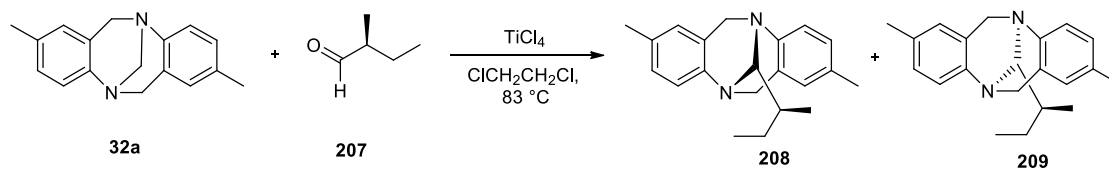
Previously, it was reported that the racemic Tröger base **32a** reacts with  $\text{TiCl}_4$  and carbonyl compounds to give the corresponding 5,11-substituted derivatives (Scheme 45).<sup>81</sup> Whereas use of  $\text{BF}_3\cdot\text{OEt}_2$  and  $\text{ZnBr}_2$  in the place of  $\text{TiCl}_4$  were not effective in the reaction with aromatic aldehydes, using  $\text{POCl}_3$  the 5,11-substituted Tröger base derivative was obtained in moderate yields (55-68%).

**Scheme 45**



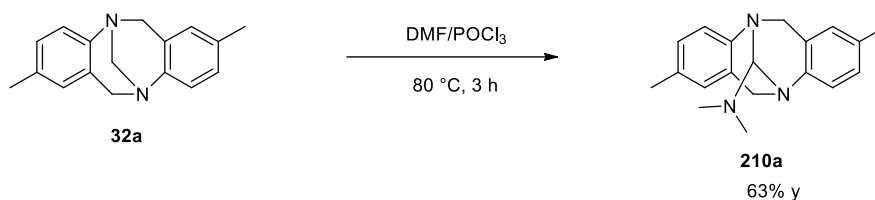
It is of interest to develop a method for the asymmetric synthesis of Tröger base derivatives by using chiral carbonyl compounds in the methylene bridge exchange reactions. However, we have observed that the reactions were not effective with camphor and menthone using  $\text{TiCl}_4$  or  $\text{POCl}_3$ . In these cases, only the starting Tröger base was recovered. As reported previously from this laboratory, we have obtained only diastereomeric mixture of products in the reaction of chiral (*S*)-2-butanal **207** with Tröger base **32a** in the presence of  $\text{TiCl}_4$  (Scheme 46).<sup>81</sup>

**Scheme 46**



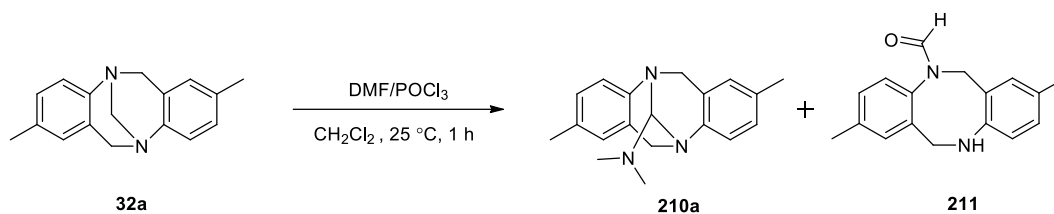
It was also reported that the dimethylformamide (DMF) can be used as a carbonyl partner in the reaction with  $\text{POCl}_3$  to obtain the corresponding 5,11-substituted product **210a** in a 63% yield (Scheme 47).<sup>81</sup>

## Scheme 47



We have also examined the reaction of TB with DMF in various solvents and reaction conditions. Optimum results were obtained using CH<sub>2</sub>Cl<sub>2</sub> as solvent (Scheme 48). In addition to the 5,11-substituted derivative **210a**, the ring opened product **211** was also obtained in small amounts (Table 13, Entry 2-9, Figure 22).

## Scheme 48

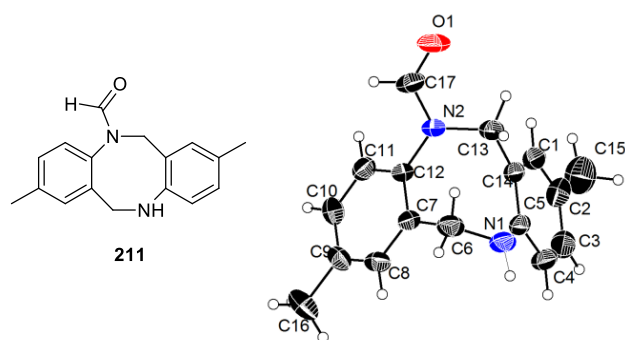


**Table 13.** Reaction of Tröger base with DMF in the presence of POCl<sub>3</sub><sup>a</sup>

Entry	POCl <sub>3</sub> (equiv)	Solvent	Yield (%) <sup>b,c</sup> <b>210a</b>	Yield (%) <sup>b,c</sup> <b>211</b>
1	1.75	DMF	63 <sup>d</sup>	0
2	1.75	DCM	93	Trace <sup>e</sup>
3	2.0	DCM	89	Trace <sup>e</sup>
3	1.5	DCM	91	5
4	1.25	DCM	74	12
5	1.5	DCM	70	19
6	1.75	CHCl <sub>3</sub>	56	7
7	1.75	DCE	42	9
8	1.75	Toluene	52	9
9	1.75	Acetonitrile	35	11
10	1.75	MeOH	0 <sup>f</sup>	0 <sup>f</sup>

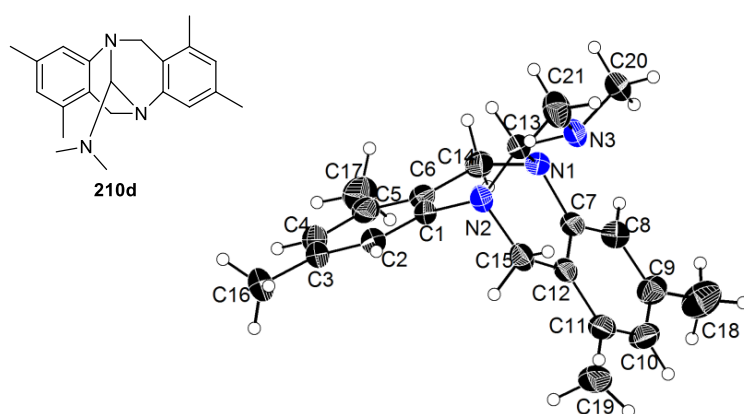
<sup>a</sup>Unless otherwise mentioned, all the reactions were carried out using racemic Tröger base (2 mmol), and DMF (2.1 mmol) in solvent (15 mL) at 25 °C for 1 h. <sup>b</sup>Yields are for isolated products. <sup>c</sup>Products were characterized by spectral data (IR, <sup>1</sup>H-NMR, <sup>13</sup>C-NMR). <sup>d</sup>Reaction was carried out using Tröger base (5 mmol) and POCl<sub>3</sub> (8.75 mmol) in 5 mL of DMF (5mL) at 0 °C and then heated at 80 °C 3 h. <sup>e</sup>Identified by <sup>1</sup>H NMR. <sup>f</sup>No reaction.





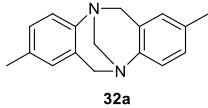
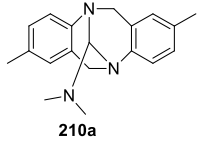
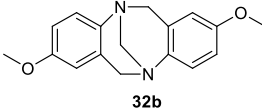
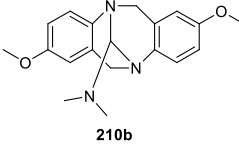
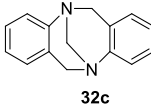
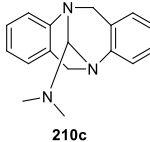
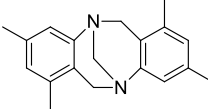
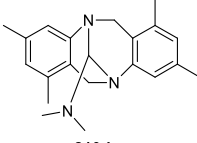
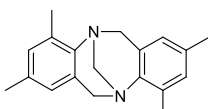
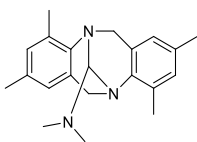
**Figure 22.** ORTEP representation of the crystal structure of compound **211**. (Thermal ellipsoids are drawn at 40% probability).

We have also examined the POCl<sub>3</sub> promoted reaction of other Tröger base derivatives with DMF. The results are summarized in Table 14. The reaction of methoxy Tröger base **32b** and DMF with POCl<sub>3</sub> gave the corresponding 5,11-substituted derivative **210b** in a 84 % yield (Table 14, entry 2). In order to further examine the scope of this reaction, we prepared other Tröger base derivatives without any substitution at the *ortho* and *para* positions with respect to the nitrogens (Table 14, entry 3 and 4, Figure 23). The steric effect of the *ortho* substitution by a methyl group seems to decrease the yield of the product significantly (Table 14, entry 5). A tentative mechanism can be considered to rationalize this transformation involving Vilsmeier iminium ion intermediates **212** (Scheme 49).

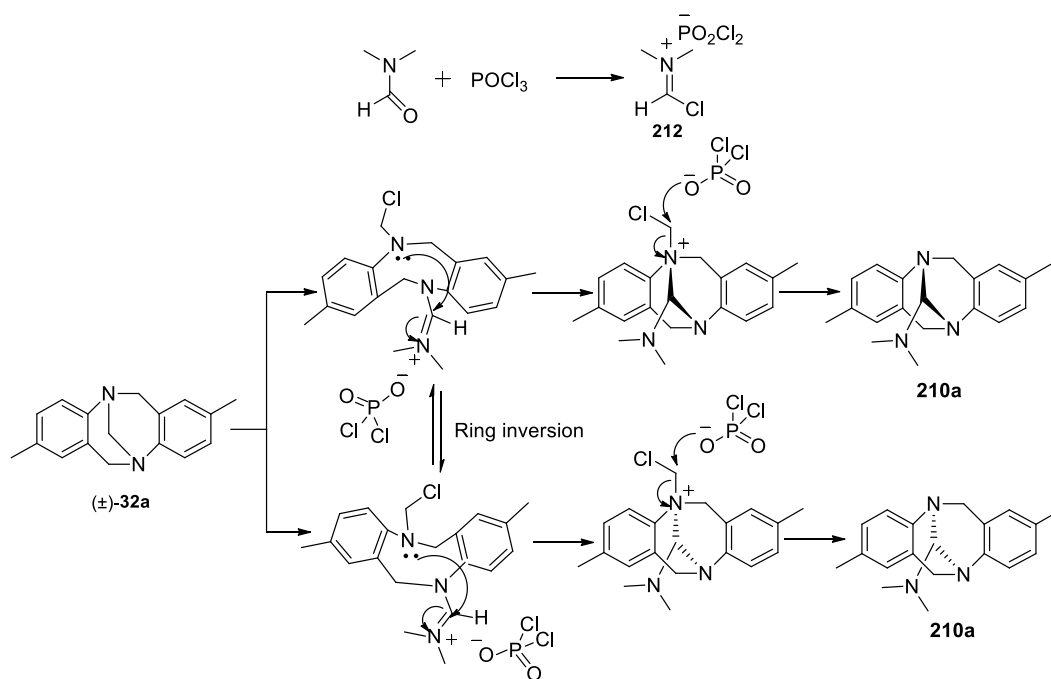


**Figure 23.** ORTEP representation of crystal structure of compound **210d**. (Thermal ellipsoids are drawn at 40% probability)

**Table 14.** Vilsmeier-Haack type reaction of Tröger base derivatives with DMF<sup>a</sup>

Entry	Substrate	Product	Yield (%) <sup>b,c</sup>
1	 32a	 210a	93
2	 32b	 210b	84
3	 32c	 210c	88
4	 32d	 210d	86
5	 64	 210e	65

<sup>a</sup>All reactions were carried out using racemic Tröger base derivatives (2 mmol), DMF (2.1 mmol) and POCl<sub>3</sub> (3.5 mmol) in dry CH<sub>2</sub>Cl<sub>2</sub> (15 mL). <sup>b</sup>Yields are for isolated products. <sup>c</sup>Products were characterized by spectral data (IR, <sup>1</sup>H-NMR, <sup>13</sup>C-NMR).

**Scheme 49**

**Table 15. Crystal data and structure refinement for 211**

Identification code	<b>211</b>	
Empirical formula	C <sub>17</sub> H <sub>18</sub> N <sub>2</sub> O	
Formula weight	266.33	
Temperature	298(2) K	
Wavelength	0.71073 Å	
Crystal system	Orthorhombic	
Space group	P2(1)2(1)2(1)	
Unit cell dimensions	a = 8.026(4) Å	α = 90°.
	b = 13.107(6) Å	β = 90°.
	c = 13.859(7) Å	γ = 90°.
Volume	1457.9(12) Å <sup>3</sup>	
Z	4	
Density (calculated)	1.213 Mg/m <sup>3</sup>	
Absorption coefficient	0.076 mm <sup>-1</sup>	
F(000)	568	
Crystal size	0.40 x 0.30 x 0.20 mm <sup>3</sup>	
Theta range for data collection	2.14 to 26.54°.	
Index ranges	-10 ≤ h ≤ 10, -16 ≤ k ≤ 16, -17 ≤ l ≤ 17	
Reflections collected	12556	
Independent reflections	2965 [R(int) = 0.1326]	
Completeness to theta = 26.54°	97.7 %	
Max. and min. transmission	0.9849 and 0.9701	
Refinement method	Full-matrix least-squares on F <sup>2</sup>	
Data / restraints / parameters	2965 / 0 / 187	
Goodness-of-fit on F <sup>2</sup>	1.011	
Final R indices [I > 2σ(I)]	R1 = 0.0788, wR2 = 0.1512	
R indices (all data)	R1 = 0.1345, wR2 = 0.1878	
Absolute structure parameter	0(4)	
Largest diff. peak and hole	0.189 and -0.191 e.Å <sup>-3</sup>	

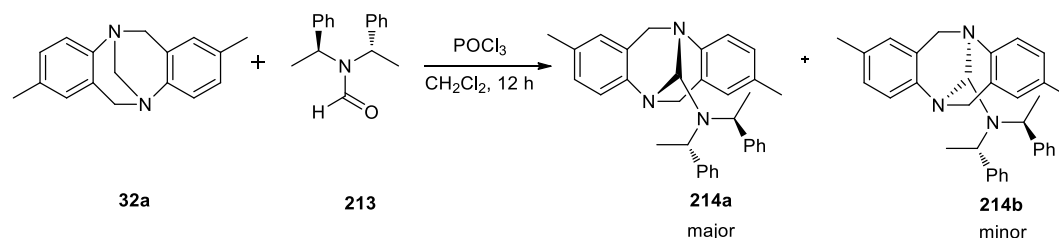
**Table 16. Crystal data and structure refinement for 210d.**

Identification code	<b>210d</b>	
Empirical formula	C <sub>21</sub> H <sub>27</sub> N <sub>3</sub>	
Formula weight	321.46	
Temperature	293(2) K	
Wavelength	0.71073 Å	
Crystal system	Monoclinic	
Space group	C2/c	
Unit cell dimensions	a = 16.088(4) Å	α = 90°.
	b = 9.615(3) Å	β = 107.906(4)°.
	c = 24.443(6) Å	γ = 90°.
Volume	3597.8(16) Å <sup>3</sup>	
Z	8	
Density (calculated)	1.187 Mg/m <sup>3</sup>	
Absorption coefficient	0.071 mm <sup>-1</sup>	
F(000)	1392	
Crystal size	0.22 x 0.20 x 0.18 mm <sup>3</sup>	
Theta range for data collection	1.75 to 25.97°.	
Index ranges	-19 ≤ h ≤ 19, -11 ≤ k ≤ 11, -29 ≤ l ≤ 30	
Reflections collected	17958	
Independent reflections	3531 [R(int) = 0.0314]	
Completeness to theta = 25.97°	99.8 %	
Refinement method	Full-matrix least-squares on F <sup>2</sup>	
Data / restraints / parameters	3531 / 0 / 217	
Goodness-of-fit on F <sup>2</sup>	1.375	
Final R indices [I > 2σ(I)]	R1 = 0.0885, wR2 = 0.2999	
R indices (all data)	R1 = 0.0954, wR2 = 0.3133	
Largest diff. peak and hole	0.425 and -0.284 e.Å <sup>-3</sup>	

## 2.5.2 Diastereoselective synthesis of Tröger base derivatives

We have envisaged the possibility of diastereoselective synthesis of Tröger base derivatives using the chiral formamide **213** instead of dimethyl formamide.

**Scheme 50**



**Table 17** Reaction of Tröger base with (*S,S*)-*N,N*-bis( $\alpha$ -methylbenzyl)formamide **213** in the presence of POCl<sub>3</sub><sup>a</sup>

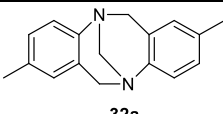
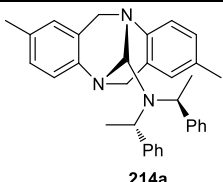
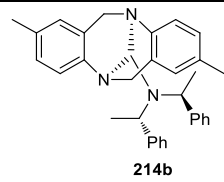
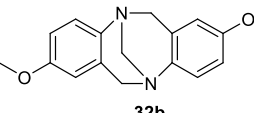
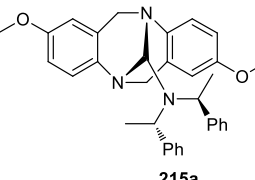
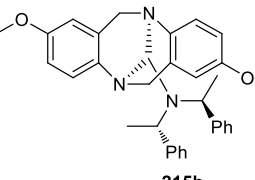
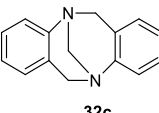
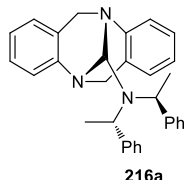
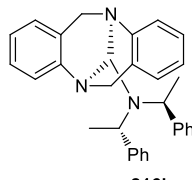
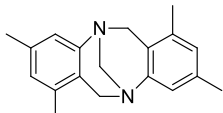
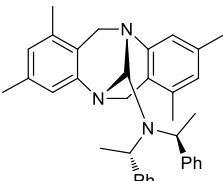
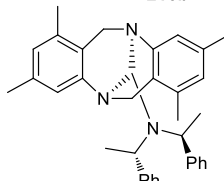
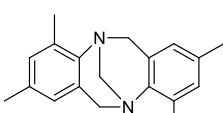
Entry	Solvent	Temperature (°C)	Yield(%) <sup>b,c</sup>	dr (%) <sup>d</sup>
1	DCM	25	75	75:25
2	CHCl <sub>3</sub>	25	40	75:25
3	Toluene	25	38	75:25
4	DCE	25	47	75:25
5	CH <sub>3</sub> CN	25	23	75:25
6	DCM	0	32	75:25
7	DCM	-10	trace <sup>e</sup>	-

<sup>a</sup>All reactions were carried out using racemic Tröger base **32a** (2 mmol) and (*S,S*)-*N,N*-bis( $\alpha$ -methylbenzyl)formamide **213** (2.1 mmol) and POCl<sub>3</sub> (3.5 mmol) in 15 mL DCM for 12 h. <sup>b</sup>Yields are of isolated products. <sup>c</sup>Products were characterized by spectral data (IR, <sup>1</sup>H NMR, <sup>13</sup>C NMR). <sup>d</sup>Diastereomeric ratios were estimated from <sup>1</sup>H NMR (400 MHz) data. Diastereomeric ratios 77:23 were also estimated by HPLC using chiral cell phenomenex cellulose-1 column. <sup>e</sup>dr not estimated.

Thus, we have examined the reaction of *rac*-**32a** and (*S,S*)-*N,N*-bis( $\alpha$ -methylbenzyl)formamide **213** as formyl partner in the presence of POCl<sub>3</sub> at 25 °C. In this reaction, the corresponding 5,11-substituted Tröger base derivative was obtained in 75% yield (Scheme 50). The <sup>1</sup>H NMR spectrum of the product showed that the product was a diastereomeric mixture in the ratio 75:25. The reaction was carried out using various solvents. Optimum results were obtained in dichloromethane solvent (Table 17, entry 1). Lowering the temperature to 0 °C did not improve the selectivity of the Tröger base formed (Table 17,

entry 6). Further, lowering of the temperature to -10 °C gave only a trace amount of the desired product (Table 17, entry 7). However, the diastereomers obtained could not be separated by chromatography or crystallization.

**Table 18.** Diastereoselective synthesis of various 5, 11-substituted methano bridged Tröger base derivatives<sup>a</sup>

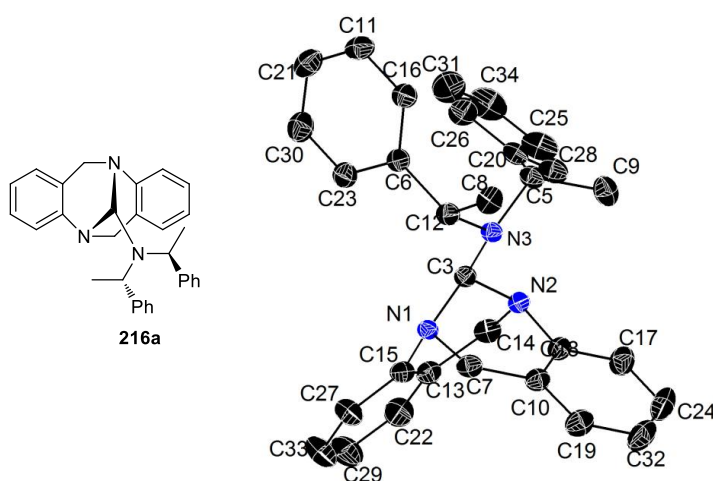
Entry	Substrate	Products	Yield (%) <sup>b,c</sup>	dr (%) <sup>d</sup>
1		 	75	75:25
2		 	66	75:25
3		 	68	75:25
4		 	52	58:42
5		No reaction	-	-

<sup>a</sup>All reactions were carried out using racemic Tröger base derivatives (2 mmol) and (*S,S*)-*N,N*-bis( $\alpha$ -methylbenzyl)formamide **213** (2.1 mmol) and POCl<sub>3</sub> (3.5 mmol) in 15 mL DCM at 25 °C for 12 h. <sup>b</sup>Yields are of isolated products. <sup>c</sup>Products were characterized by spectral data (IR, <sup>1</sup>H NMR, <sup>13</sup>C NMR). <sup>d</sup>Diastereomeric ratios were estimated from <sup>1</sup>H NMR (400 MHz) data. Diastereomeric ratios were also estimated for **214** (77:23), **215** (77:23), and **217** (60:40) by HPLC using chiralcel phenomenex cellulose-1 column.

We have also examined the POCl<sub>3</sub> promoted reaction of other Tröger base derivatives with (*S,S*)-*N,N*-bis( $\alpha$ -methylbenzyl)formamide. The results are summarized in Table 18. The reaction of Tröger base derivative **32c** and (*S,S*)-*N,N*-bis( $\alpha$ -methylbenzyl)formamide **213**

with POCl<sub>3</sub> gave the corresponding 5,11-substituted derivative **216** in 68% yield with a diastereomeric ratio of 75:25 (Table 18, entry 3). In this case, the diastereomeric mixture could not be isolated in pure form by column chromatography. However, crystallization of the product mixture **216** from acetone solvent gave the major diastereomer **216a** in pure form with a 51% yield. The Tröger base derivative **32d** gave the corresponding 5,11-substituted product **217** in a 52% yield with a diastereomeric ratio of 58:42 (Table 18, entry 4). In this case, the major diastereomer **217a** was also isolated in pure form with a 50% chemical yield by crystallization of product mixture **217** from acetone solvent.

X-ray structural analysis of a single crystal **216a** and **217a** revealed that the product was 5,11-substituted derivative with (*R,R*) configuration at the newly formed stereogenic nitrogen centers. The ORTEP diagrams for the major products are given in Figure 24 and Figure 25. The reaction of Tröger base derivative **64** with (*S,S*)-*N,N*-bis( $\alpha$ -methylbenzyl)formamide did not give the desired 5,11-substituted product (Table 18, entry 5) and the starting materials were recovered under the reaction conditions. Presumably, the *ortho* and *meta* methyl substituents greatly hinder this reaction.

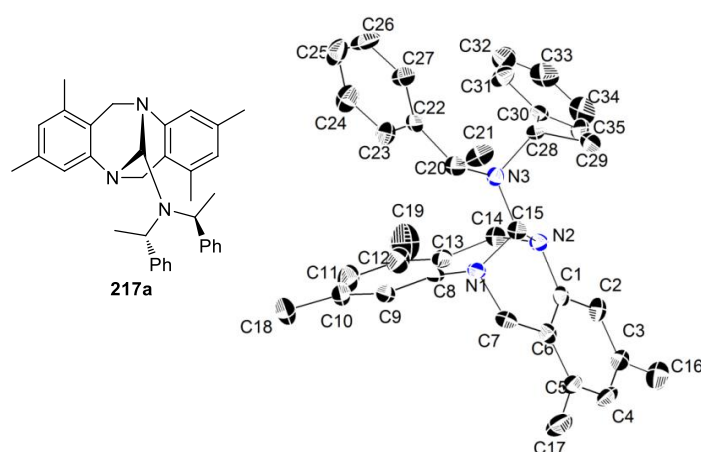


**Figure 24.** ORTEP representation of the crystal structure of compound **216a** (Thermal ellipsoids are drawn at 35% probability and all the hydrogen atoms are removed for clarity).

**Table 19. Crystal data and structure refinement for 216a.**

Identification code	<b>216a</b>	
Empirical formula	$C_{31} H_{31} N_3$	
Formula weight	445.59	
Temperature	293(2) K	
Wavelength	0.71073 Å	
Crystal system	Monoclinic	
Space group	P21	
Unit cell dimensions	$a = 11.5992(8)$ Å	$\alpha = 90^\circ$ .
	$b = 8.7862(5)$ Å	$\beta = 104.776(7)^\circ$ .
	$c = 12.5573(9)$ Å	$\gamma = 90^\circ$ .
Volume	1237.43(14) Å <sup>3</sup>	
Z	2	
Density (calculated)	1.196 Mg/m <sup>3</sup>	
Absorption coefficient	0.070 mm <sup>-1</sup>	
F(000)	476	
Crystal size	0.22 x 0.20 x 0.18 mm <sup>3</sup>	
Theta range for data collection	2.77 to 28.99°.	
Index ranges	$-12 \leq h \leq 15$ , $-10 \leq k \leq 10$ , $-12 \leq l \leq 16$	
Reflections collected	5455	
Independent reflections	4489 [R(int) = 0.0160]	
Completeness to theta = 28.99°	84.9 %	
Refinement method	Full-matrix least-squares on F <sup>2</sup>	
Data / restraints / parameters	4489 / 1 / 309	
Goodness-of-fit on F <sup>2</sup>	1.034	
Final R indices [I > 2sigma(I)]	R1 = 0.0451, wR2 = 0.0990	
R indices (all data)	R1 = 0.0560, wR2 = 0.1075	
Absolute structure parameter	-4(2)	
Largest diff. peak and hole	0.131 and -0.198 e.Å <sup>-3</sup>	

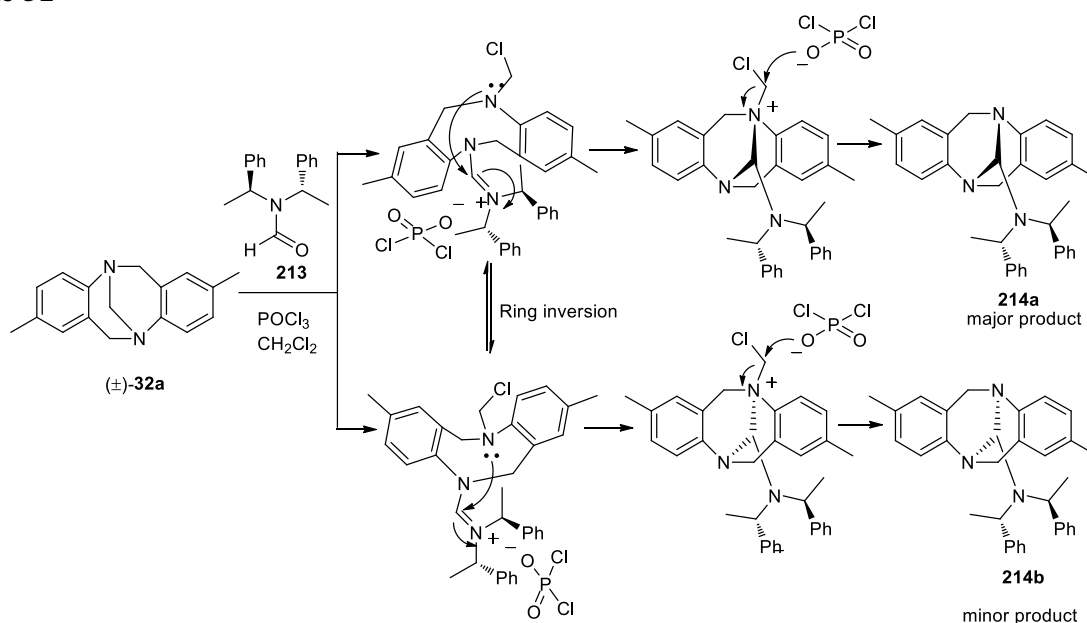




**Figure 25.** ORTEP representation of the crystal structure of compound **217a** (Thermal ellipsoids are drawn at 35% probability and all the hydrogen atoms are removed for clarity).

Asymmetric induction in the formation of the major product in the diastereoselective synthesis of Tröger base derivatives can be rationalized as outlined in Scheme 51. The reaction of racemic Tröger base **32a** with (*S,S*)-*N,N*-bis( $\alpha$ -methylbenzyl)formamide in the presence of  $\text{POCl}_3$  would lead to iminium ion intermediates, which are expected to be in equilibrium (Scheme 51). Invariant of the diastereomeric ratio (75:25) for unhindered substrates **32a**, **32b** and **31c**) would suggest thermodynamic control of the reaction.

**Scheme 51**



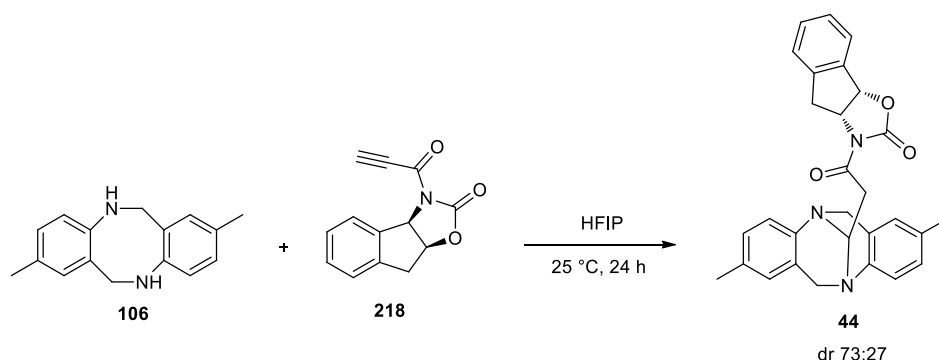
**Table 20. Crystal data and structure refinement for 217a.**

Identification code	217a		
Empirical formula	C <sub>35</sub> H <sub>39</sub> N <sub>3</sub>		
Formula weight	501.69		
Temperature	273(2) K		
Wavelength	0.71073 Å		
Crystal system	Orthorhombic		
Space group	P2(1)2(1)2(1)		
Unit cell dimensions	a = 9.3077(10) Å	α= 90°.	
	b = 14.8229(16) Å	β= 90°.	
	c = 20.866(2) Å	γ = 90°.	
Volume	2878.9(5) Å <sup>3</sup>		
Z	4		
Density (calculated)	1.158 Mg/m <sup>3</sup>		
Absorption coefficient	0.067 mm <sup>-1</sup>		
F(000)	1080		
Crystal size	0.22 x 0.20 x 0.18 mm <sup>3</sup>		
Theta range for data collection	1.69 to 25.00°.		
Index ranges	-11<=h<=11, -17<=k<=17, -24<=l<=24		
Reflections collected	27239		
Independent reflections	5069 [R(int) = 0.0700]		
Completeness to theta = 25.00°	100.0 %		
Refinement method	Full-matrix least-squares on F <sup>2</sup>		
Data / restraints / parameters	5069 / 0 / 349		
Goodness-of-fit on F <sup>2</sup>	1.360		
Final R indices [I>2sigma(I)]	R1 = 0.1079, wR2 = 0.2121		
R indices (all data)	R1 = 0.1172, wR2 = 0.2166		
Absolute structure parameter	-1(6)		
Largest diff. peak and hole	0.306 and -0.199 e.Å <sup>-3</sup>		

During the preparation of a manuscript of this work, reports have appeared describing  $\text{POCl}_3$  promoted exchange reaction of the methano bridge using achiral amides.<sup>86</sup> However, the methods described in our paper and here are generally applicable for aldehydes, ketones and amides. In addition, we have also devised a method for the diastereoselective synthesis of Tröger base derivatives using (*S,S*)-*N,N*-bis( $\alpha$ -methylbenzyl)formamide as carbonyl group partner.

Later, Cvengros *et al.*<sup>24</sup> reported a diastereoselective double aza-Michael conjugate addition of the cyclic secondary amine **106** to system containing chiral oxazolidinone as a chiral auxiliary to obtain a product **44** with up to 73:27 selectivity (Scheme 52). The diastereoselectivity observed in this reaction is similar to that realized in our methods (75:25).

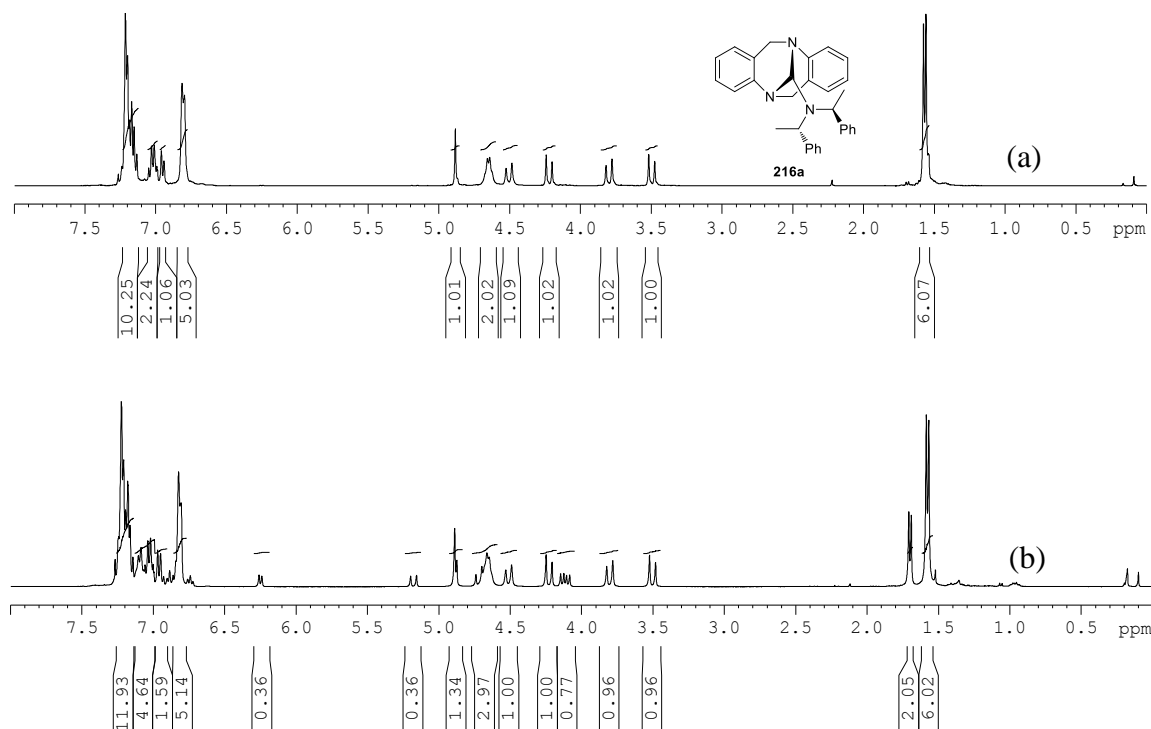
### Scheme 52



### 2.5.3 Epimerization of Tröger base derivatives

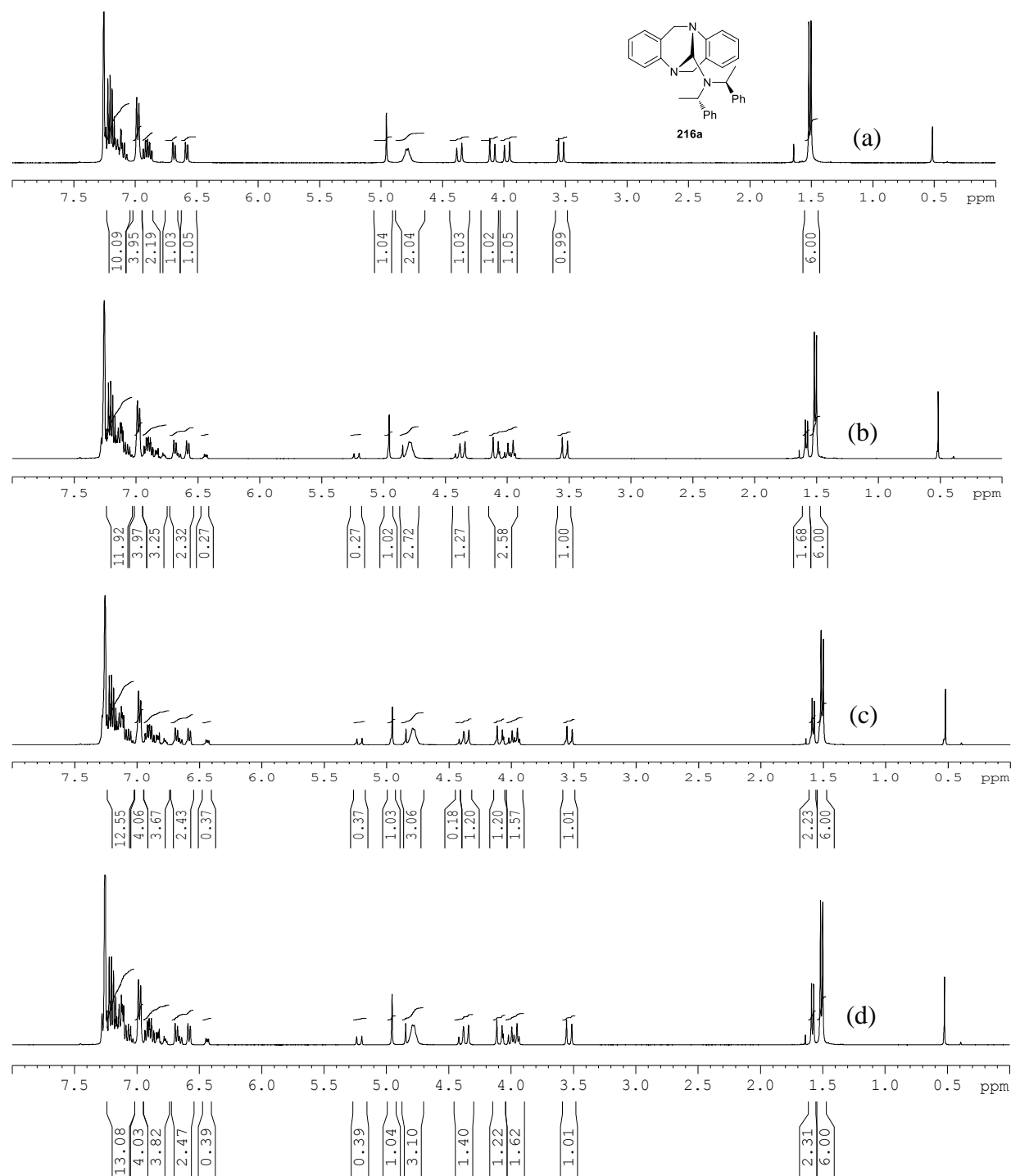
During the characterization of compounds by  $^1\text{H}$  NMR, it was observed that the epimerization of **216a** takes place in the solution. Initially, we used the  $\text{CDCl}_3$  purchased from the commercial sources for our studies. Later, we also used the pre-dried  $\text{CDCl}_3$  by

passing through a column containing anhydrous  $\text{K}_2\text{CO}_3$ . However, the epimerization was observed in all these cases (Figure 26).



**Figure 26.**  $^1\text{H}$  NMR spectra of **216a** using solvent  $\text{CDCl}_3$  at different time intervals (a) immediately (b) 1 day

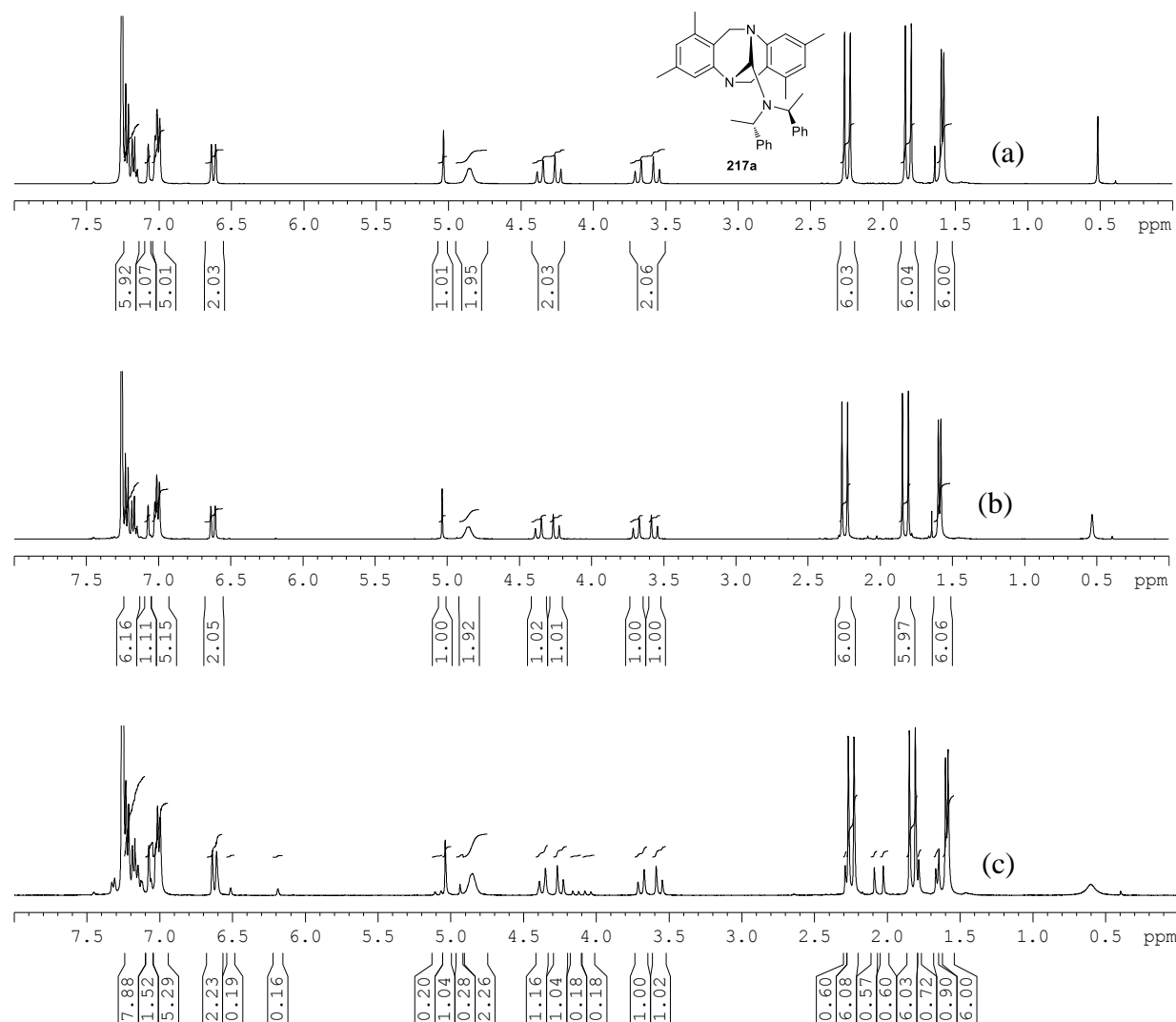
To understand further, we recorded the  $^1\text{H}$  NMR of compound **216a** using  $\text{C}_6\text{D}_6$  as a solvent at different time intervals. The results are presented in Figure 27. The  $^1\text{H}$  NMR of compound **216a** after 24 h indicated decrease in the diastereomeric ratio to 78:22.  $^1\text{H}$  NMR analysis after 48 h revealed decrease in ratio to 73:27. Further, experiments after three, four and five days did not show noticeable change in the diastereomeric ratios (Figure 27). Presumably, the chiral bis( $\alpha$ -methylbenzyl) moiety has influence over the epimerization.



**Figure 27.**  $^1\text{H}$  NMR spectra of **216a** using solvent  $\text{C}_6\text{D}_6$  at different time intervals (a) immediately (b) 1 day (c) 2 day (d) 3 day.

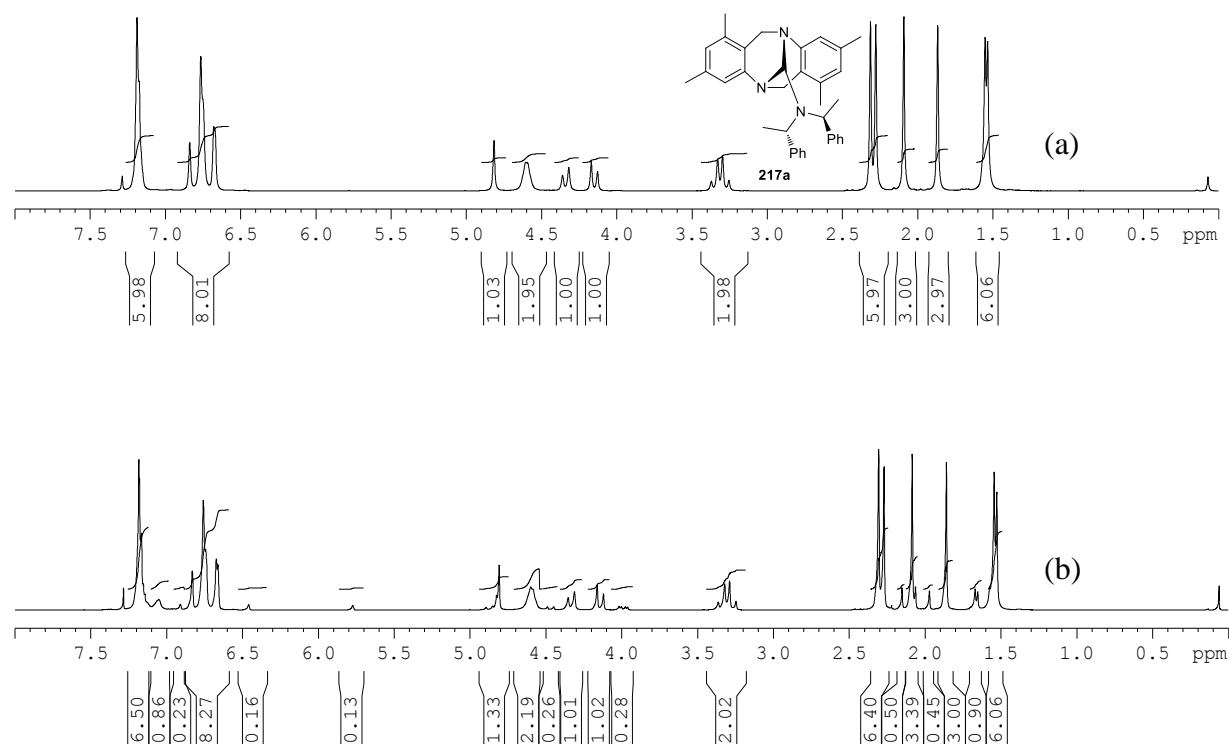
Similarly, we recorded the  $^1\text{H}$  NMR spectra of compound **217a** using  $\text{C}_6\text{D}_6$  to understand the epimerization. The results are presented in Figure 28. In this case, we did not observe the epimerization up to ten days. However, we observed that the diastereomeric ratio

decreased to 87:13 after twenty days. The slow epimerization observed could be attributed to steric hindrance to ring opening (Scheme 51) by the additional methyl groups in the aromatic rings.



**Figure 28.**  $^1\text{H}$  NMR spectra of **217a** using solvent  $\text{C}_6\text{D}_6$  at different time intervals (a) immediately (b) 10 day (c) 20 day

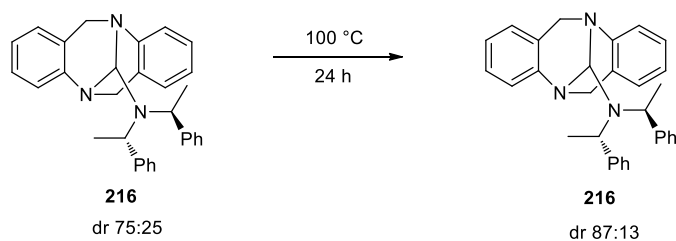
To understand the effect of solvent, we recorded the  $^1\text{H}$  NMR spectrum of compound **217a** in  $\text{CDCl}_3$  (Figure 29). In this case, we observed the epimerization as the dr ratio was decreased to 87:13. Also it should be pointed out that the epimerization is faster in  $\text{CDCl}_3$  compare to  $\text{C}_6\text{D}_6$ .

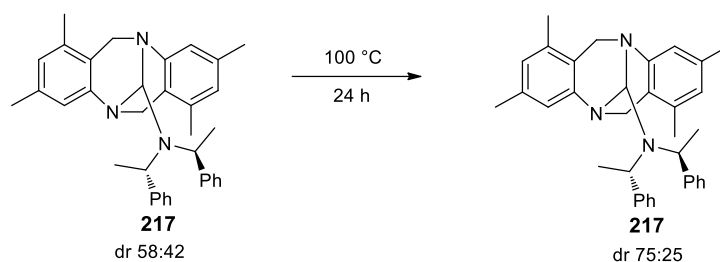


**Figure 29**  $^1\text{H}$  NMR spectra of **217a** using solvent  $\text{CDCl}_3$  at different time intervals (a) immediately (b) 1 day

The epimerization was also observed in the solid state at higher temperature (Scheme 53). Upon heating of a 75:25 mixture of compound **216** to  $100\text{ }^\circ\text{C}$ , the diastereomeric ratio increased to 87:13. In the case of the diastereomeric mixture of **217** with ratio 58:42, heating to  $100\text{ }^\circ\text{C}$  for 24 h gave a sample of **217** with 75:25 ratio.

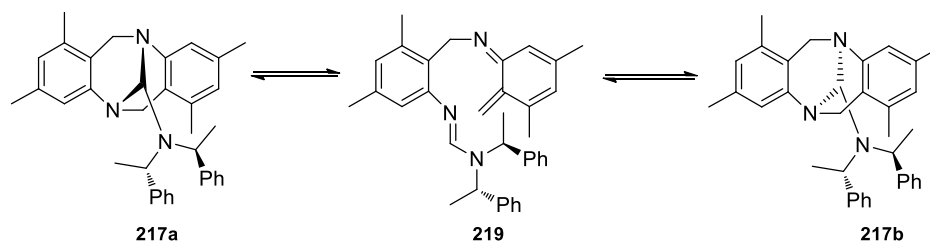
### Scheme 53





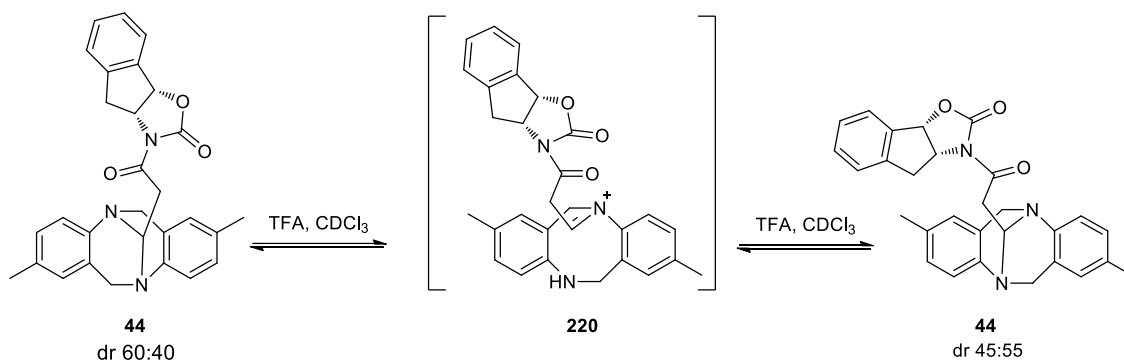
Since TB derivatives **216** and **217** undergo epimerization in solution as well as in the solid state, the epimerization could be rationalized by considering a retro-hetero-Diels-Alder ring opening followed by hetero-Diels-Alder ring closure mechanism (Scheme 54).

#### Scheme 54



However, a recent report on epimerization of larger Tröger base derivatives revealed that the proton catalyzed iminium ion formation as a probable mechanism.<sup>22</sup> Very recently, it was also reported that stirring of the diastereomeric mixture **44** in chloroform in the presence of TFA resulted in opposite selectivity. In this case, the iminium ion **220** was reported as intermediate (Scheme 55).<sup>24</sup>

#### Scheme 55

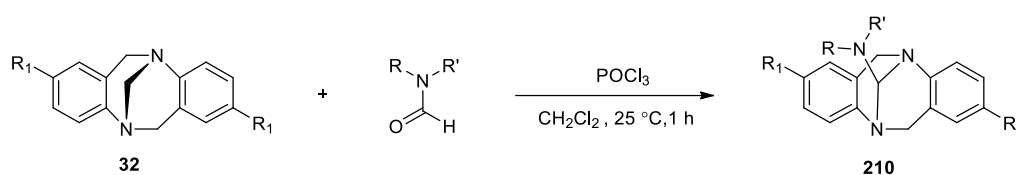




### 2.5.4 Stereoselective exchange of methylene bridge of Tröger base with formamides

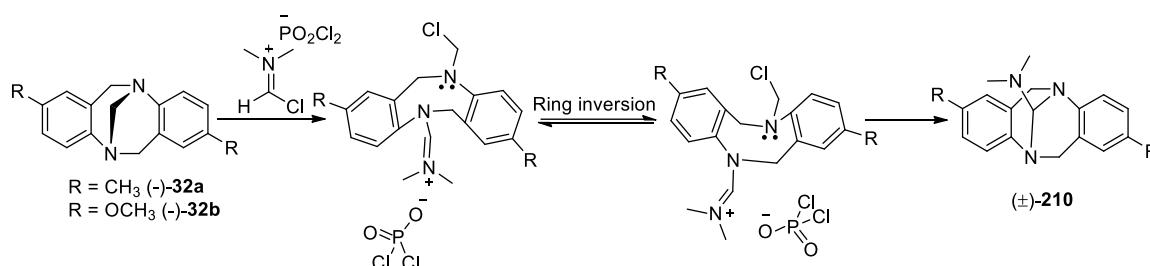
We have also examined the stereochemical integrity of various chiral Tröger base derivatives. Accordingly, we have carried out the exchange reaction of chiral Tröger base **32a** with DMF in the presence of POCl<sub>3</sub> and observed the formation of racemic mixture in 70% yield (Scheme 56, Table 21). Similar results were obtained using the chiral methoxy derivative **32b**.

**Scheme 56**



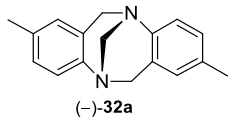
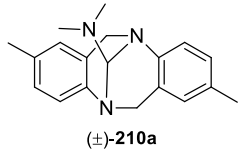
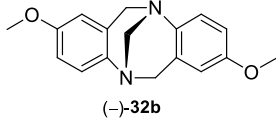
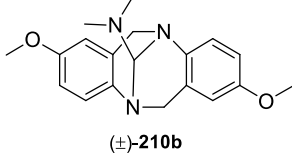
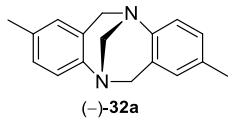
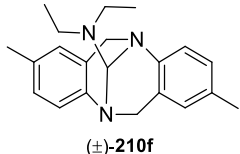
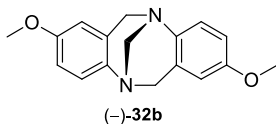
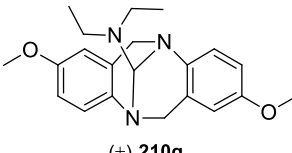
The formation of racemic mixtures could be rationalized by considering the ring inversion mechanism as outlined in Scheme 57.

**Scheme 57**



Previously, we have observed that Tröger base derivatives with *ortho* methyl substitutions greatly hinder the reaction (Table 14). It was also reported that the racemization barrier of bis-*ortho* methyl Tröger base derivative is higher (30 kJ mol<sup>-1</sup>) in acidic media compared to the *para*-substituted derivative.

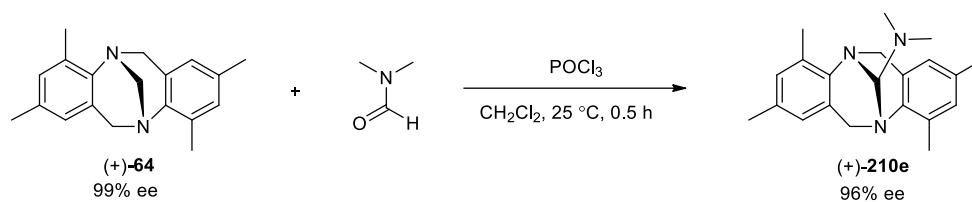
**Table 21** Reaction of chiral Tröger base with DMF in the presence of POCl<sub>3</sub><sup>a</sup>

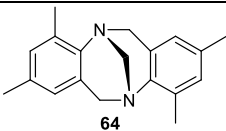
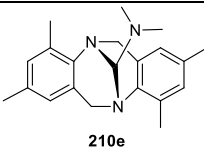
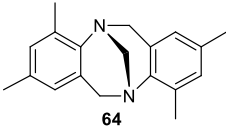
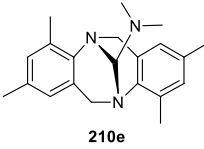
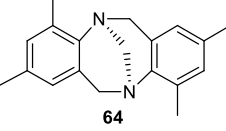
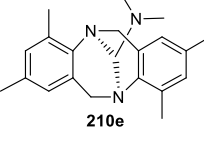
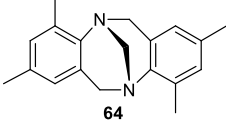
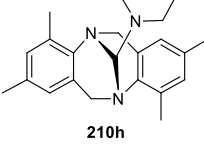
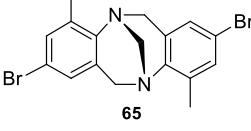
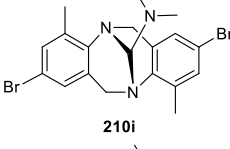
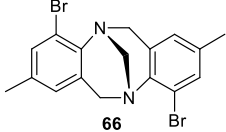
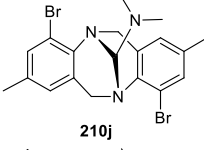
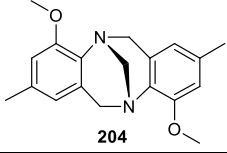
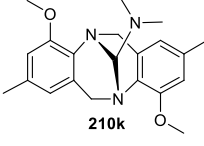
entry	substrate	product <sup>b</sup>	yield <sup>c</sup>
1	 (-)-32a	 (±)-210a	70
2	 (-)-32b	 (±)-210b	68
3	 (-)-32a	 (±)-210f	63
4	 (-)-32b	 (±)-210g	61

<sup>a</sup>All reactions were carried out using chiral Tröger base derivative (2 mmol), DMF (2.1 mmol) and POCl<sub>3</sub> (2.0 mmol) in dry CH<sub>2</sub>Cl<sub>2</sub> (15 mL) at 25 °C for 1 h. <sup>b</sup>Products were characterized by spectral data (IR, <sup>1</sup>H-NMR, <sup>13</sup>C-NMR). <sup>c</sup>Yields are of isolated products

Accordingly, it is of interest to utilize a chiral TB derivative with *ortho* methyl groups to examine the possibility of retention of configuration (Scheme 58). Accordingly, we have carried out the reaction of Tröger base derivative (+)-**64** with DMF (1 equiv) and POCl<sub>3</sub> (1 equiv) in CH<sub>2</sub>Cl<sub>2</sub> at 25 °C for 1 h. We have observed that Tröger base derivative (+)-**210e** is formed in 83% ee and 55% yield. In a reaction using 0.8 equiv POCl<sub>3</sub> gave (+)-**210e** in 93% ee and 42% yield (Table 22, entry 1). However, it was obtained with 96% ee and 25% yield in 0.5 h (Table 22, entry 2). Hence, Tröger base derivative (+)-**210e** obtained with 96% ee using (+)-**64** as a starting material indicates the retention of configuration in the bridge exchange reaction. Therefore, the configurations of stereogenic nitrogen centers were assigned tentatively as 5*S*,11*S* for (+)-isomer. The reaction of (-)-**64** with DMF also gave the product (-)-**210e** in 94% ee (Table 22, entry 3).

## Scheme 58

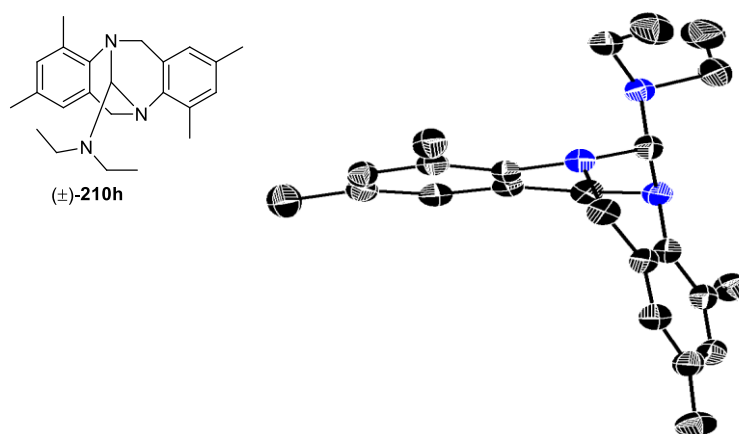
**Table 22.** Reaction of chiral *ortho*-Tröger base with DMF in the presence of  $\text{POCl}_3$ <sup>a</sup>

entry	substrate	Time (h)	product <sup>b</sup>	ee (%) <sup>c</sup>	yield (%) <sup>d</sup>
1		1		93	42
2		0.5		96	25
3		0.5		94	27
4		0.5		76	22
5 <sup>e</sup>		0.5		-	2
6		0.5		10	5
7		0.5		10	12

<sup>a</sup>All reactions were carried out using chiral Tröger base derivatives (2 mmol), DMF (2.1 mmol) and  $\text{POCl}_3$  (1.6 mmol) in dry  $\text{CH}_2\text{Cl}_2$  (15 mL) at 25 °C for 0.5 h. <sup>b</sup>Yields are of isolated products. <sup>c</sup>ee values calculated by HPLC analysis. <sup>d</sup>Isolated yield. <sup>e</sup>ee value was not determined.

We have also carried out the reaction of chiral **64** with diethylformamide (DEF). In this run, the product **210h** was obtained in 76% ee (Table 22, entry 4). Crystallization of the product gave only the crystals of racemic mixture. The ORTEP diagram is shown in Figure

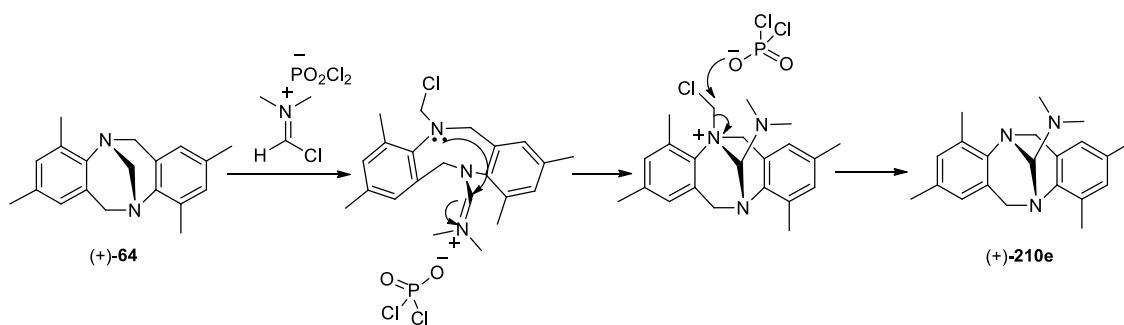
30. However, the compound obtained from the mother liquor was found to be 99% ee. The bromine substitution in TB greatly retards this reaction as the products were obtained only in 2% and 5% yield, respectively (Table 22, entry 5 and 6). Further, the reaction of DMF with Tröger base derivative **204** gave the product with 10% ee under the experimental condition (Table 22, entry 7).



**Figure 30.** ORTEP representation of the crystal structure of compound (±)-**210h** (Thermal ellipsoids are drawn at 30% probability and all the hydrogen atoms are removed for clarity).

The formation of product with retention of configuration could be rationalized by considering the mechanism as outlined in Scheme 59. The nucleophilic addition of Tröger base (+)-**64** to chloroiminium ion, followed by cyclization of iminium intermediate and dequaternarization would give the chiral Tröger base derivative (+)-**210e**. In this case, the ring inversion does not take place because of the steric hindrance of *ortho*-methyl group.

#### Scheme 59

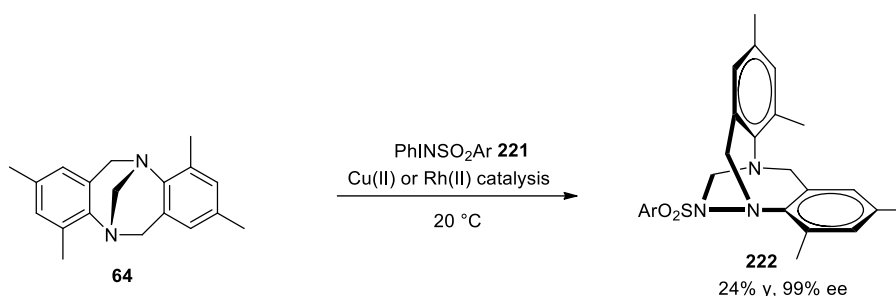


**Table 23. Crystal data and structure refinement for 210h.**

Identification code	<b>210h</b>		
Empirical formula	$C_{23} H_{31} N_3$		
Formula weight	349.51		
Temperature	293(2) K		
Wavelength	1.54184 Å		
Crystal system	Monoclinic		
Space group	P21/c		
Unit cell dimensions	$a = 14.9406(6)$ Å	$\alpha = 90^\circ$ .	
	$b = 8.0349(3)$ Å	$\beta = 102.530(4)^\circ$ .	
	$c = 17.3126(7)$ Å	$\gamma = 90^\circ$ .	
Volume	2028.81(14) Å <sup>3</sup>		
Z	4		
Density (calculated)	1.144 Mg/m <sup>3</sup>		
Absorption coefficient	0.514 mm <sup>-1</sup>		
F(000)	760		
Crystal size	0.22 x 0.20 x 0.18 mm <sup>3</sup>		
Theta range for data collection	3.03 to 71.98°.		
Index ranges	$-18 \leq h \leq 12$ , $-9 \leq k \leq 8$ , $-20 \leq l \leq 21$		
Reflections collected	7447		
Independent reflections	3898 [R(int) = 0.0159]		
Completeness to theta = 71.98°	98.1 %		
Refinement method	Full-matrix least-squares on F <sup>2</sup>		
Data / restraints / parameters	3898 / 0 / 241		
Goodness-of-fit on F <sup>2</sup>	1.055		
Final R indices [I > 2sigma(I)]	R1 = 0.0537, wR2 = 0.1589		
R indices (all data)	R1 = 0.0630, wR2 = 0.1690		
Largest diff. peak and hole	0.206 and -0.208 e.Å <sup>-3</sup>		

It is of interest to note that recently, Cu(II) or Rh(II) catalyzed nitrene insertion into C-N bond of Tröger base derivative was reported to give the product **222** with 99% ee and 24% yield (Scheme 60).<sup>87</sup>

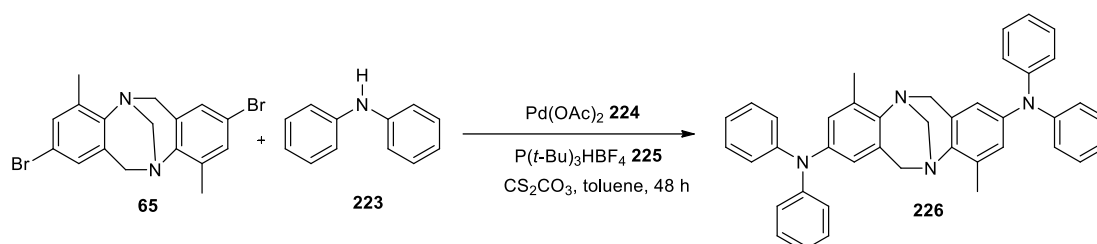
**Scheme 60**



## 2.6 Reaction of Tröger base with aryne intermediates

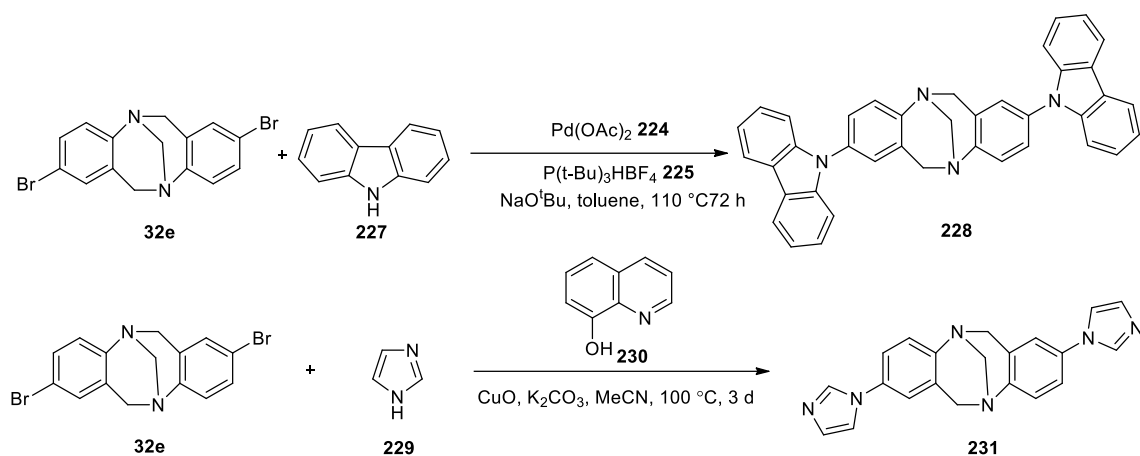
The N-arylation reactions are widely used for the synthesis of target molecules of pharmaceuticals, agrochemicals and organic functional materials.<sup>88</sup> The N-arylation of amines can readily be achieved by Ullmann-type<sup>89</sup>, Buchwald-Hartwig<sup>90</sup> and Chan-Lam<sup>91</sup> type coupling reactions. In recent years, C-N bond formation *via* C-H amination using transition metal catalysis or transition metal free C-N bond forming reactions were reported.<sup>92</sup> Triaryl amines are unique family of molecules widely used in optoelectronic devices. Synthesis of Tröger base derived triaryl amines **226** by using Pd(OAc)<sub>2</sub>/P(*t*-Bu)<sub>3</sub>HBf<sub>4</sub> catalyst system was reported (Scheme 61).<sup>93,94</sup>

**Scheme 61**



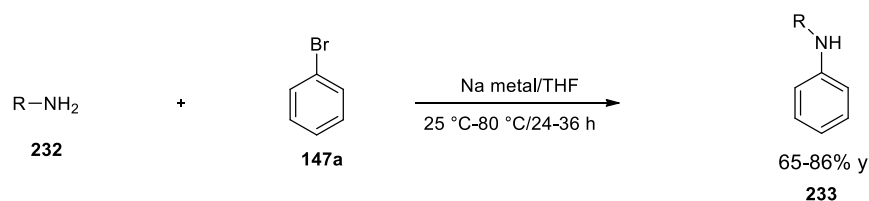
N-Arylation of bromo-substituted Tröger base derivative using NH-heterocycles as amine partner was reported using  $\text{Pd}(\text{OAc})_2/\text{P}(t\text{-Bu})_3\text{HBF}_4/\text{NaO}^t\text{Bu}$  or  $\text{CuO}/8\text{-hydroxyquinoline}/\text{K}_2\text{CO}_3$  reagent system (Chart 9).<sup>94,95</sup>

**Chart 9**



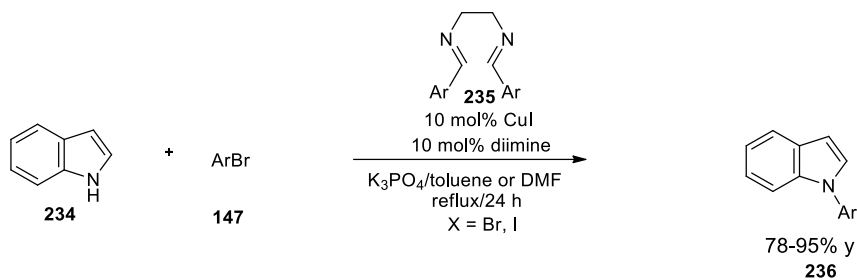
Over the years, several N-arylation methods were reported from this laboratory. For example, a straightforward method was developed in this laboratory for the N-phenylation of amines using sodium metal in THF under reflux condition to obtain the products in 65-86% yield (Scheme 62).<sup>96</sup>

**Scheme 62**



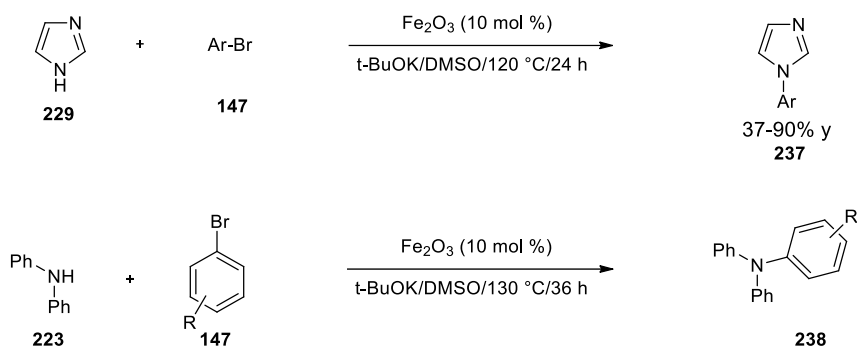
$\text{CuI}/\text{diimine}$  catalyzed N-arylation of indole was reported to give the N-arylated indoles in 78-95% yield (Scheme 63).<sup>97</sup>

## Scheme 63



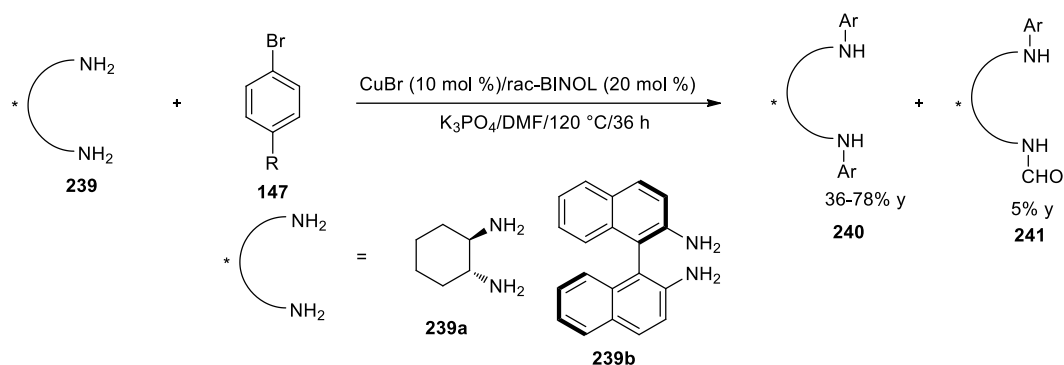
N-Arylation of imidazole and diphenylamine under  $Fe_2O_3$  catalytic system gave the corresponding C-N bond formed products in good yields (Scheme 64).<sup>98</sup>

## Scheme 64



Diamines were N-arylated in the presence of  $CuBr/rac-BINOL$  catalytic system under heating condition using  $K_3PO_4$  as a base in DMF (Scheme 65).<sup>99</sup>

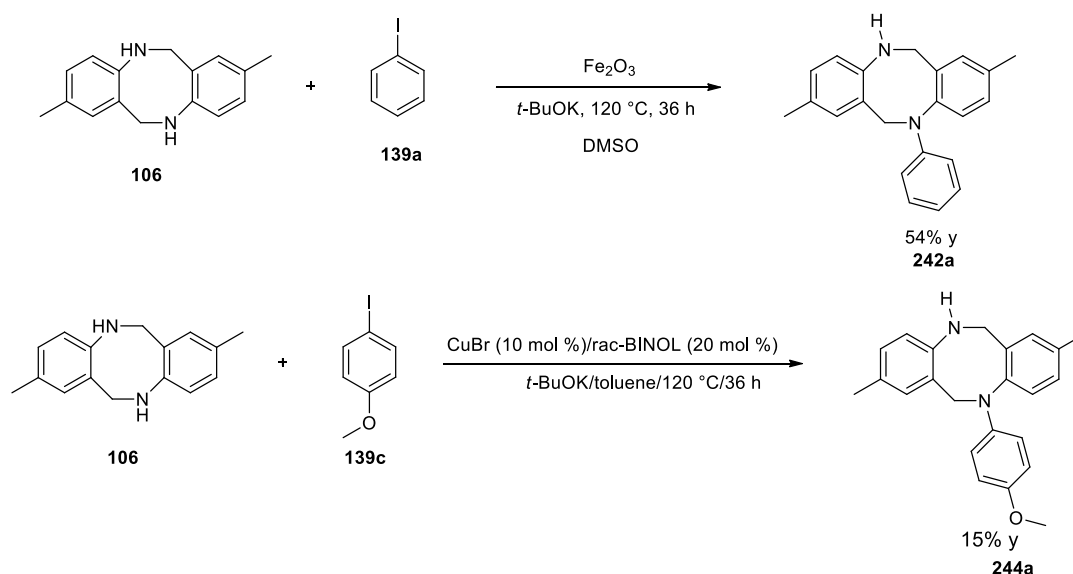
## Scheme 65





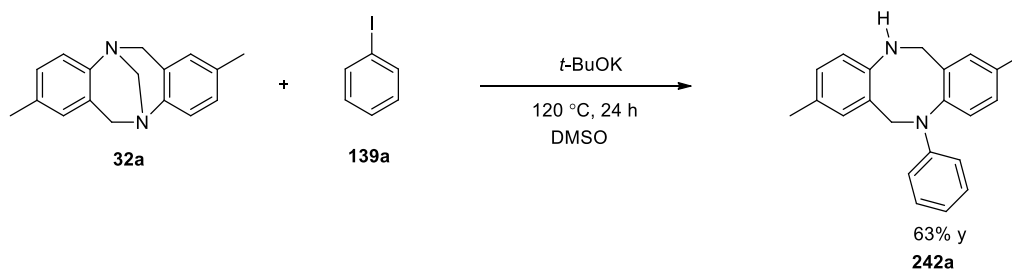
We have observed that N-arylation of the cyclic diamine **106** using  $\text{Fe}_2\text{O}_3/t\text{-BuOK}$  or  $\text{CuBr}/\text{rac-BINOL}$  system gives the corresponding N-arylated products in 54 and 15% yield respectively (Scheme 66).

**Scheme 66**



The diamine **106** was prepared by opening of the Tröger base (Scheme 18). We have observed that the reaction of Tröger base using iodobenzene and  $t\text{-BuOK}$  in the presence of  $\text{Fe}_2\text{O}_3$  in DMSO gave the N-arylated product **242a** in 63% yield (Scheme 67). Since the transformation could also follow benzyne mechanism,<sup>100</sup> we carried out the reaction without  $\text{Fe}_2\text{O}_3$ . Indeed, the N-phenyl product **242a** was obtained. The results are summarized in the Table 24. The structure of **242a** was confirmed by single crystal X-ray analysis. The ORTEP diagram of **242a** is shown in Figure 31.

**Scheme 67**

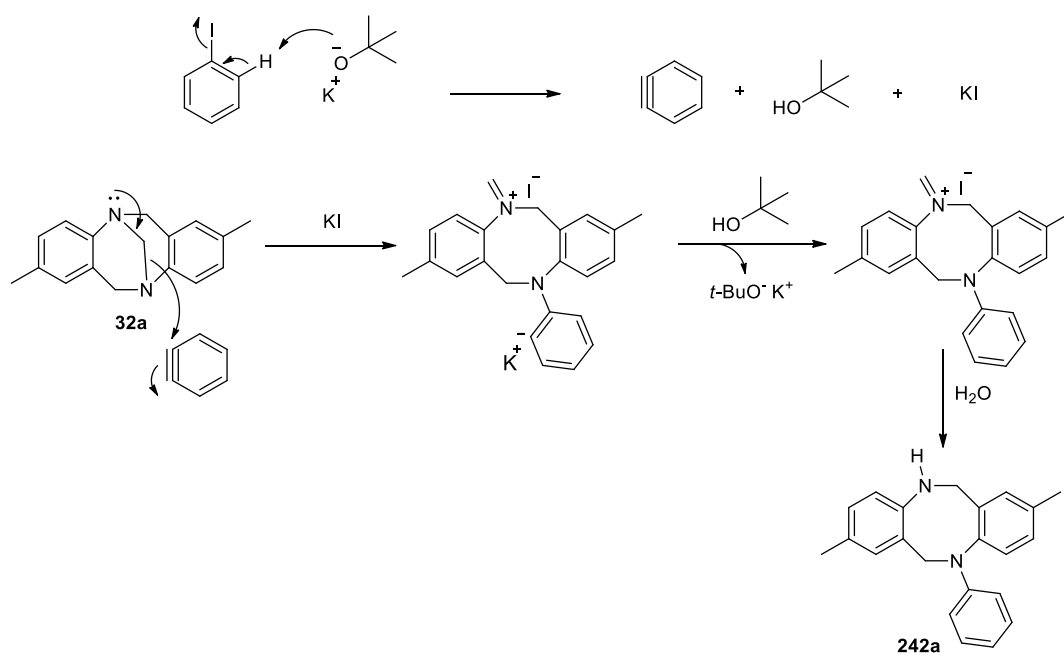


**Table 24.** Optimization of reaction of Tröger base with benzyne intermediate<sup>a</sup>

Entry	Base	Solvent	Time(h)	Temp(°C)	Yield(%) <sup>b,c</sup>
1	<i>t</i> -BuOK	DMSO	48	25	17
2	<i>t</i> -BuOK	DMSO	48	60	41
3	<i>t</i> -BuOK	DMSO	48	80	48
4	<i>t</i> -BuOK	DMSO	48	100	65
5	<i>t</i> -BuOK	DMSO	24	120	67

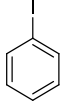
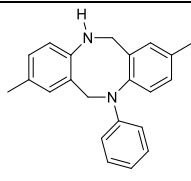
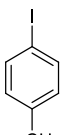
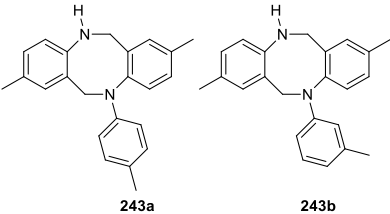
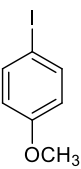
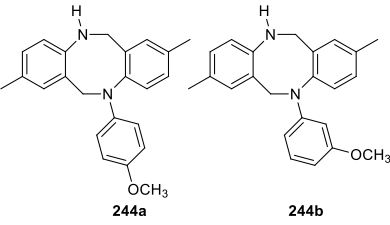
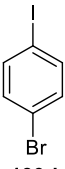
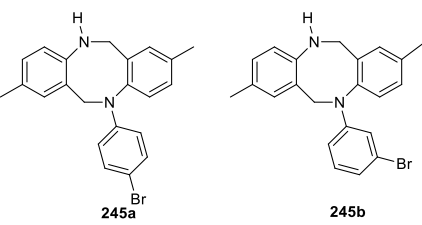
<sup>a</sup>All the reactions were carried out using *t*-BuOK (3 mmol), Iodobenzene (3 mmol) in DMSO (2 mL). <sup>b</sup>Product was identified by IR, <sup>1</sup>H-NMR, <sup>13</sup>C-NMR and mass spectral data. <sup>c</sup>Isolated yield.

The results may be explained by considering the mechanism as outlined in Scheme 68. The reaction of iodobenzene with *t*-BuOK would result in the formation of reactive benzyne intermediate, which upon reaction with Tröger base **32a** would give the methylene bridge cleaved iminium ion intermediate and water work up would finally give the product **242a**.

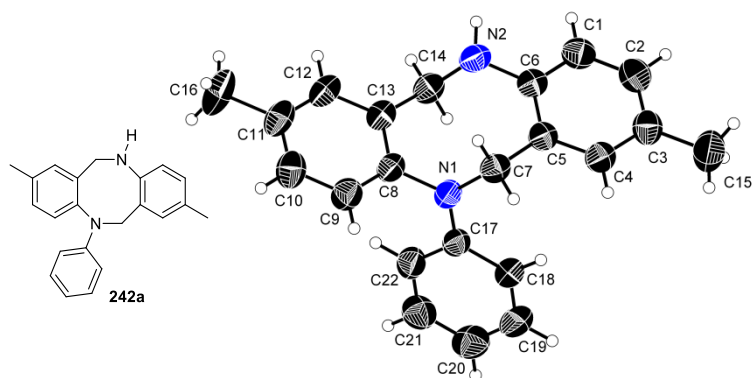
**Scheme 68**

We have observed that the reaction with 4-substituted aryl iodides gave the mixture of regioisomers, suggesting the involvement of aryne intermediate in the N-arylation of Tröger base (Table 25, Entry 2-4).

**Table 25.** Reactions of Tröger base with aryne intermediates<sup>a</sup>

Entry	Aryl halide	Product <sup>b</sup>	Yield <sup>c</sup>
1	 <b>139a</b>	 <b>242a</b>	65
2	 <b>139b</b>	 <b>243a</b> <b>243b</b>	50
3	 <b>139c</b>	 <b>244a</b> <b>244b</b>	60
4	 <b>139d</b>	 <b>245a</b> <b>245b</b>	44

<sup>a</sup>All the reactions were carried out using *t*-BuOK (3 mmol), aryl iodide (3 mmol) in DMSO (2 mL). <sup>b</sup>Product was identified by IR, <sup>1</sup>H-NMR, <sup>13</sup>C-NMR and mass spectral data. <sup>c</sup>Isolated yield.



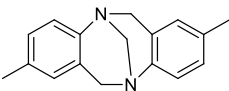
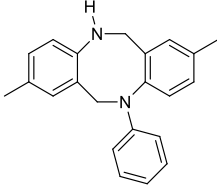
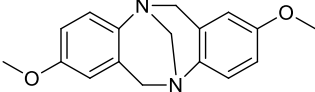
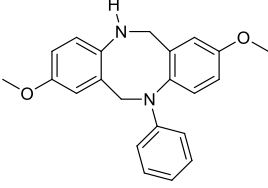
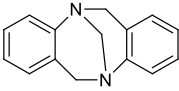
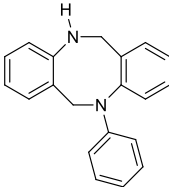
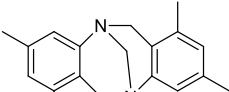
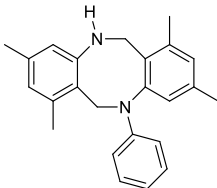
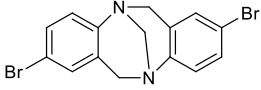
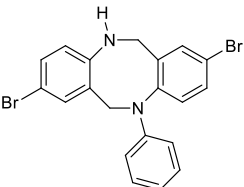
**Figure 31.** ORTEP representation of the crystal structure of compound **242a**. (Thermal ellipsoids are drawn at 50% probability).

**Table 26. Crystal data and structure refinement for 242a**

Identification code	<b>242a</b>	
Empirical formula	$C_{22} H_{22} N_2$	
Formula weight	314.41	
Temperature	295(2) K	
Wavelength	0.71073 Å	
Crystal system	Monoclinic	
Space group	C c	
Unit cell dimensions	$a = 15.260(4)$ Å	$\alpha = 90^\circ$ .
	$b = 17.280(4)$ Å	$\beta = 111.410(7)^\circ$ .
	$c = 7.2800(15)$ Å	$\gamma = 90^\circ$ .
Volume	$1787.2(7)$ Å <sup>3</sup>	
Z	4	
Density (calculated)	1.169 Mg/m <sup>3</sup>	
Absorption coefficient	0.068 mm <sup>-1</sup>	
F(000)	672	
Crystal size	0.28 x 0.22 x 0.18 mm <sup>3</sup>	
Theta range for data collection	2.357 to 27.537°.	
Index ranges	-19 ≤ h ≤ 19, -22 ≤ k ≤ 22, -9 ≤ l ≤ 9	
Reflections collected	13455	
Independent reflections	3785 [R(int) = 0.0292]	
Completeness to theta = 25.242°	98.8 %	
Refinement method	Full-matrix least-squares on F <sup>2</sup>	
Data / restraints / parameters	3785 / 2 / 221	
Goodness-of-fit on F <sup>2</sup>	0.632	
Final R indices [I > 2σ(I)]	R1 = 0.0427, wR2 = 0.1173	
R indices (all data)	R1 = 0.0566, wR2 = 0.1339	
Absolute structure parameter	-0.3(9)	
Extinction coefficient	n/a	
Largest diff. peak and hole	0.129 and -0.108 e.Å <sup>-3</sup>	

The reaction of iodobenzene with other Tröger base derivatives also gave the corresponding N-arylated products with 24-67% yield (Table 27).

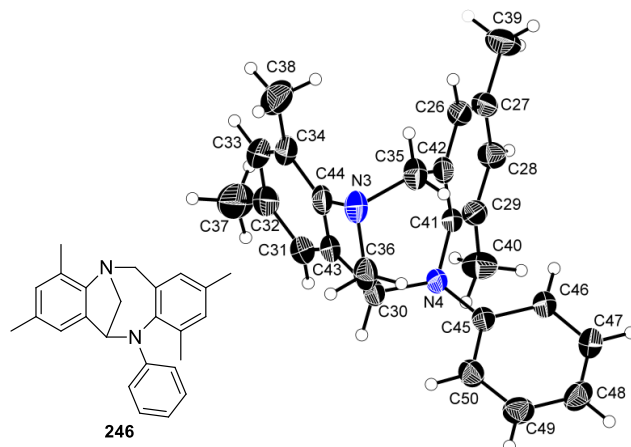
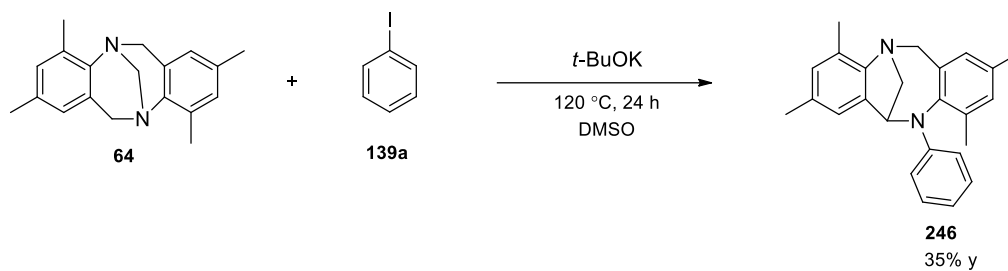
**Table 27.** Reactions of Tröger base derivatives with benzyne intermediate<sup>a</sup>

Entry	Tröger base	Product <sup>b</sup>	Yield <sup>c</sup>
1	 <b>32a</b>	 <b>242a</b>	67
2	 <b>32b</b>	 <b>242b</b>	50
3	 <b>32c</b>	 <b>242c</b>	59
4	 <b>32d</b>	 <b>242d</b>	55
5	 <b>32e</b>	 <b>242e</b>	24

<sup>a</sup>All the reactions were carried out using *t*-BuOK (3 mmol), aryl iodide (3 mmol) in DMSO (2 mL). <sup>b</sup>Product was identified by IR, <sup>1</sup>H-NMR, <sup>13</sup>C-NMR and mass spectral data. <sup>c</sup>Isolated yield.

Interestingly, the N-arylation of *ortho*-methyl Tröger base derivative **64** using iodobenzene as aryne precursor gave different N-arylated product **246** in 35% yield (Scheme 69). The structure of compound **246** was confirmed by X-ray structural analysis. The ORTEP diagram is shown in Figure 32.

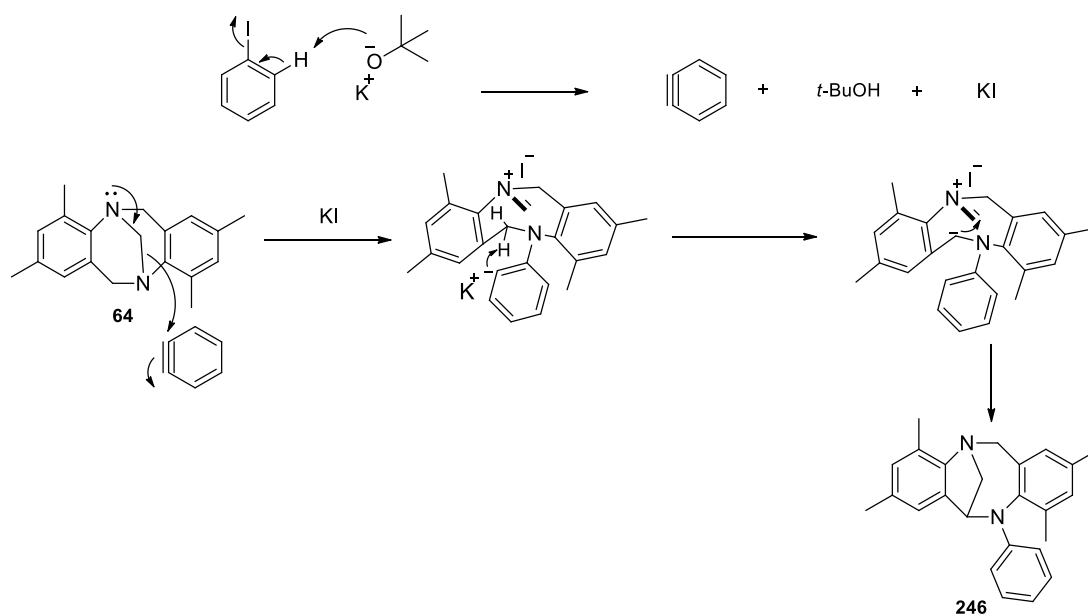
## Scheme 69



**Figure 32.** ORTEP representation of the crystal structure of compound **246**. (Thermal ellipsoids are drawn at 40% probability.)

The formation of product **246** can be explained by considering diversion of mechanism leading to formation of benzylic carbanion and ring closure to give the product **246** (Scheme 70).

## Scheme 70

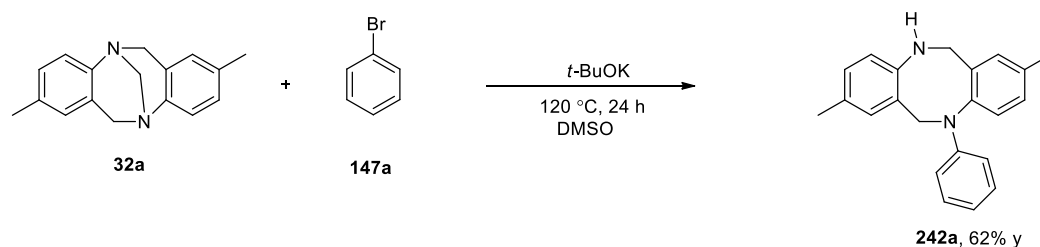


**Table 28. Crystal data and structure refinement for 246.**

Identification code	<b>246</b>	
Empirical formula	C <sub>50</sub> H <sub>52</sub> N <sub>4</sub>	
Formula weight	708.95	
Temperature	296(2) K	
Wavelength	0.71073 Å	
Crystal system	Triclinic	
Space group	P -1	
Unit cell dimensions	a = 12.7573(10) Å	α = 100.265(3)°.
	b = 13.2113(11) Å	β = 112.727(2)°.
	c = 13.9413(12) Å	γ = 104.576(3)°.
Volume	1995.1(3) Å <sup>3</sup>	
Z	2	
Density (calculated)	1.180 Mg/m <sup>3</sup>	
Absorption coefficient	0.069 mm <sup>-1</sup>	
F(000)	760	
Crystal size	0.22 x 0.24 x 0.26 mm <sup>3</sup>	
Theta range for data collection	2.702 to 27.556°.	
Index ranges	-16 ≤ h ≤ 16, -17 ≤ k ≤ 17, -18 ≤ l ≤ 18	
Reflections collected	93973	
Independent reflections	9191 [R(int) = 0.0460]	
Completeness to theta = 25.242°	99.7 %	
Refinement method	Full-matrix least-squares on F <sup>2</sup>	
Data / restraints / parameters	9191 / 0 / 488	
Goodness-of-fit on F <sup>2</sup>	1.049	
Final R indices [I > 2σ(I)]	R1 = 0.0603, wR2 = 0.1672	
R indices (all data)	R1 = 0.0834, wR2 = 0.1822	
Extinction coefficient	0.030(4)	
Largest diff. peak and hole	0.355 and -0.276 e.Å <sup>-3</sup>	

Finally, we have observed that use of bromobenzene as aryl halide partner, the corresponding N-arylated product **242a** was obtained in 62% yield (Scheme 71).

**Scheme 71**



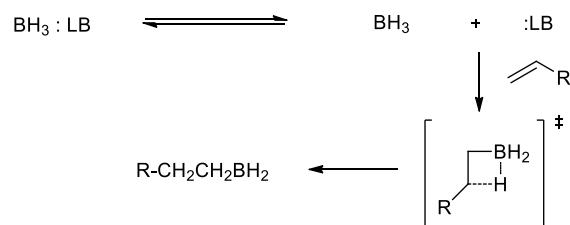
## 2.7 Hydroboration of prochiral olefins using chiral Tröger base-borane complexes

### 2.7.1 Asymmetric hydroboration using chiral amine borane complexes

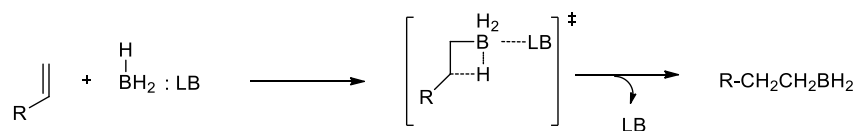
Three types of mechanism were proposed for the hydroboration of olefins (Scheme 72).<sup>101</sup>

**Scheme 72**

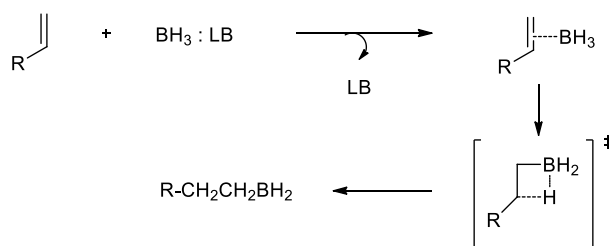
#### **S<sub>N</sub>1 type mechanism**



#### **S<sub>N</sub>2 type mechanism**



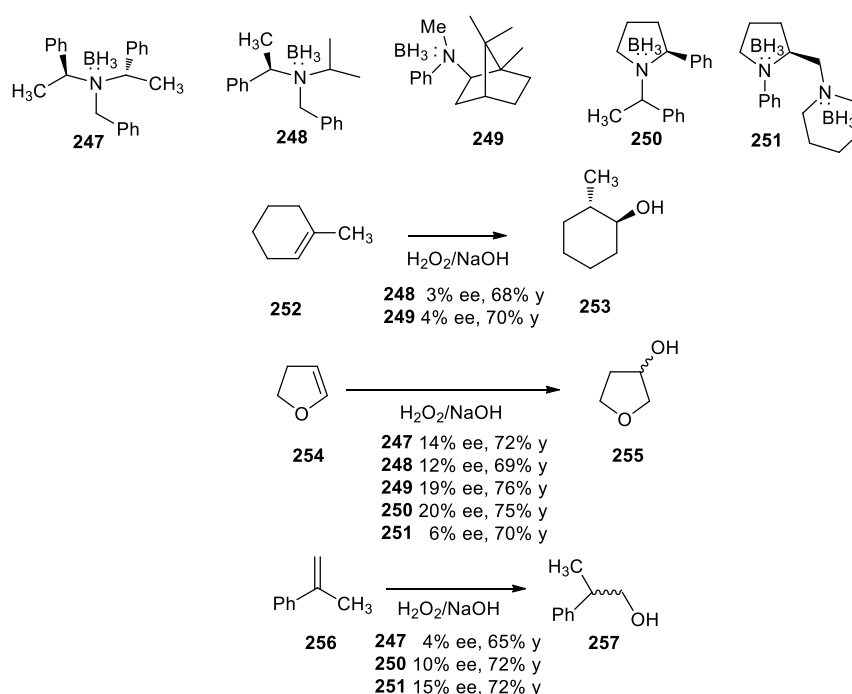
#### **S<sub>N</sub>2-type mechanism with π complex intermediate**





Previous efforts from this laboratory indicated that the  $S_N2$  type mechanism cannot be ruled out as hydroboration of prochiral olefins by various borane chiral amine complexes lead to the corresponding alcohols with 3-20% ee after  $H_2O_2/NaOH$  oxidation (Chart 10).<sup>102</sup> Poor enantioselectivity may be due to operation of a spectrum of mechanisms (Scheme 72).<sup>101</sup> Also, selectivity of the initial hydroboration by the amine- $BH_3$  complex and selectivity of further hydroboration by initially formed alkyl boranes ( $RBH_2$  and  $R_2BH$ ) may be different.

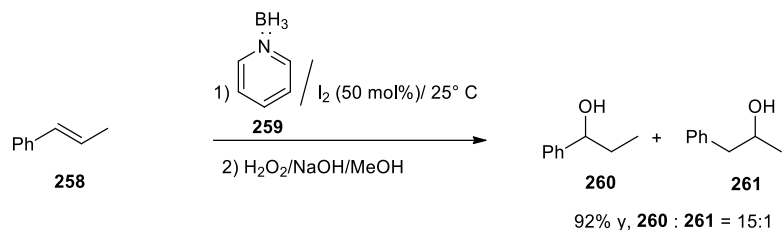
**Chart 10**



### 2.7.2. Iodine activation of chiral amine borane complexes

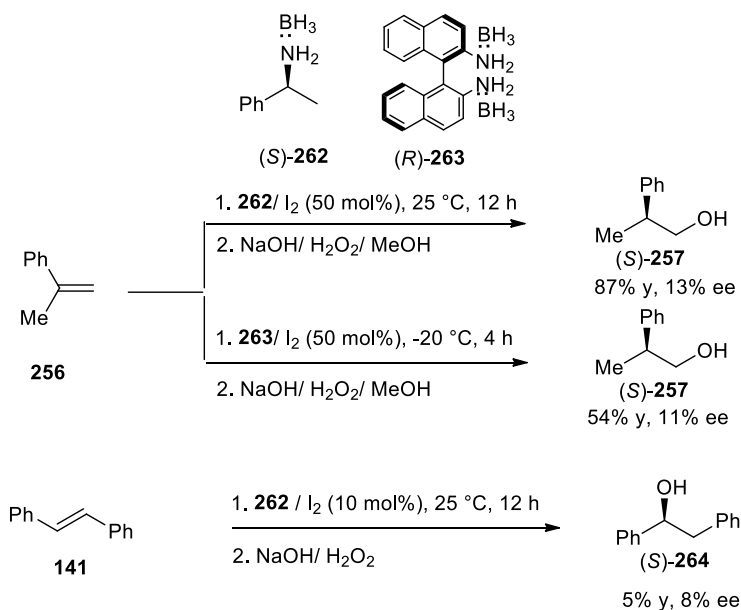
The hydroboration by iodine activation of strong amine- $BH_3$  complexes offers new opportunities for the asymmetric hydroboration as the  $BH_2I$  moiety is expected to be bonded with amines during the course of reaction with iodide behaving like a leaving group.<sup>103</sup> Vedejs *et al.*<sup>103</sup> reported a hydroboration reaction of  $\beta$ -methylstyrene **258** under iodine activation of pyridine borane complex **259** at 25 °C (Scheme 73).

## Scheme 73



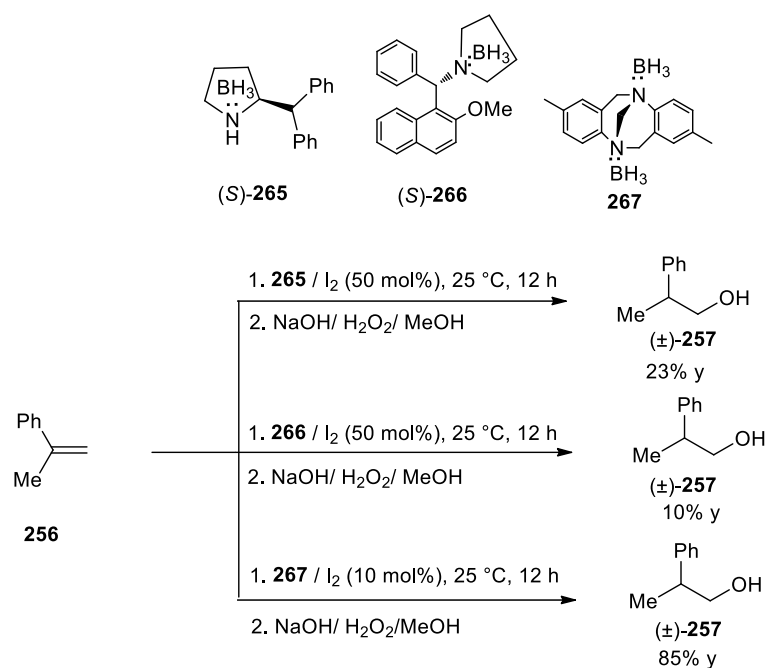
Chiral primary amine borane complexes such as  $\alpha$ -methylbenzylamine **262** and (*R*)-BINAM **263** were found to give the product **257** in 13% and 11% ee respectively, under iodine activation (Chart 11).<sup>104</sup> Also, the hydroboration reaction of *trans*-stilbene **141** using  $\alpha$ -methylbenzylamine-borane complex **262** with catalytic amount of iodine was reported to give the alcohol **264** in 5% yield and 8% ee (Chart 11).<sup>104</sup>

## Chart 11



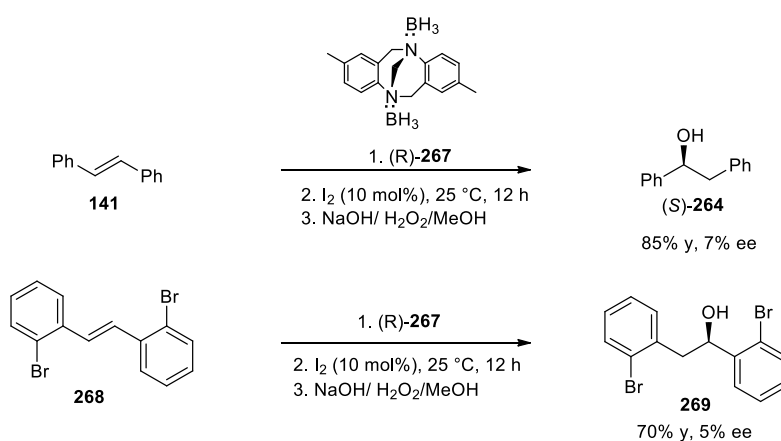
The hydroboration of  $\alpha$ -methylstyrene **256** using the secondary amine **265** and tertiary amine **266** borane complexes was reported to give only racemic alcohols under iodine activation. Further, the hydroboration reaction of  $\alpha$ -methylstyrene with the Tröger base borane **267** also resulted only in the formation of racemic mixture (Chart 12).<sup>104, 81</sup>

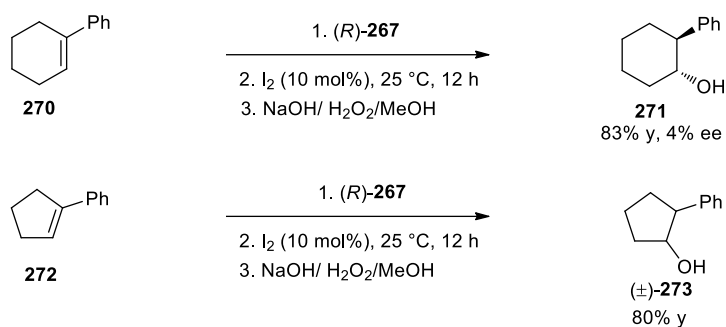
Chart 12



However, the hydroboration of different olefins using the chiral Tröger base-borane complex **267** with catalytic amount of iodine (10 mol%) gave the corresponding alcohols in 0-7% ee (Chart 13).<sup>81</sup>

Chart 13



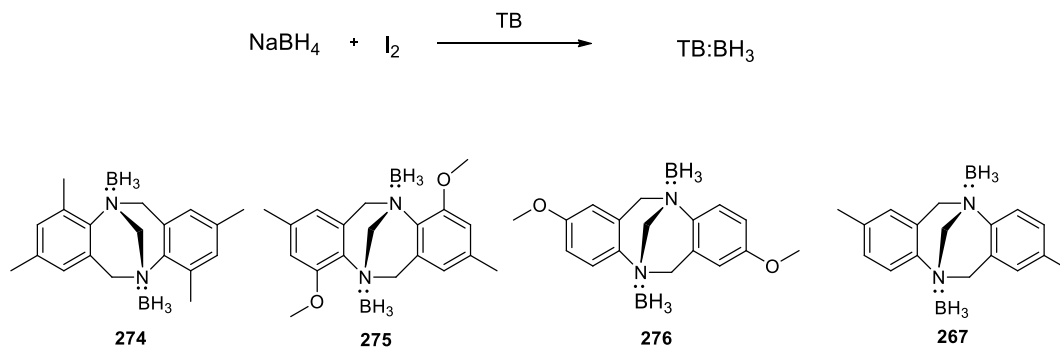


Since various chiral TB derivatives can be easily accessed *via* methods reported in previous sections, we became interested to examine the asymmetric hydroboration of prochiral olefins using various chiral TB-borane complexes.

### 2.7.3 Hydroboration of prochiral olefins using chiral *ortho*-substituted Tröger base borane complexes

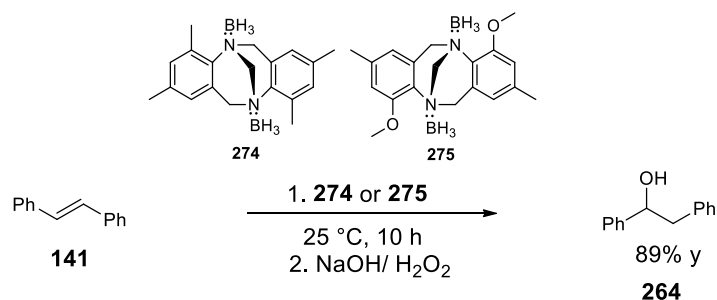
We have prepared the borane complexes by passing the B<sub>2</sub>H<sub>6</sub> gas generated from the reaction of NaBH<sub>4</sub> with I<sub>2</sub> in diglyme (Scheme 74).<sup>105</sup>

**Scheme 74**



The corresponding borane complex **274** showed a characteristic boron signal at -8.10 ppm. We carried out the hydroboration of prochiral olefins **141**, **256** and **277** using this borane complex at 25 °C. The corresponding alcohols isolated after oxidation were found to be racemic mixtures (Scheme 75, Table 29).

Scheme 75

**Table 29.** Hydroboration of prochiral olefins using chiral *ortho*-substituted Tröger base borane complexes<sup>a</sup>

Entry	Substrate	Borane complex	Product	Yield <sup>b,c</sup>
1	 141	 274	 264	89
2	 277	 274	 264	94
3	 256	 274	 257	91
4	 141	 275	 264	82
5	 277	 275	 264	91
6	 256	 275	 257	93

<sup>a</sup>All the reactions were carried out in 1 mmol scale at 25 °C for 10 h. <sup>b</sup>products were isolated after oxidation NaOH/H<sub>2</sub>O<sub>2</sub>. <sup>c</sup> HPLC analyses were carried out on chiral column OB-H; *n*-Hexane:*i*PrOH-97:3, 0.3 mL/min. and OD-H using *n*-Hexane:*i*PrOH-90:10, 0.5 mL/min.

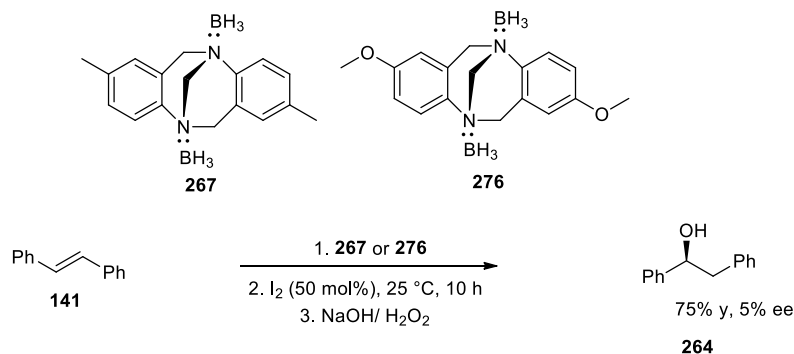
The Tröger base-borane complex **274** is expected to be weak borane complex due to the steric hindrance of the *ortho*-methyl group (Scheme 75 and Table 29). Since, hydroboration takes place at room temperature this may follow S<sub>N</sub>1 type mechanism (Scheme

77), in which the chiral amine ligand would depart while olefins approach the  $\text{BH}_3$ . We thought that the derivative **204** with *ortho*-methoxy substituents would form a stronger borane complex. Accordingly, we have prepared the borane complex **275** in toluene and carried out the hydroboration of olefins at 25 °C. The borane complex used in this reaction showed a characteristic boron peak at -8.9 ppm. However, in this case also the alcohols obtained were only racemic mixtures (Table 29, entries 4-6).

#### 2.7.4 Hydroboration of prochiral olefins using chiral *para*-substituted Tröger base borane complexes under iodine activation

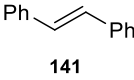
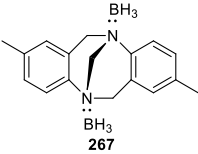
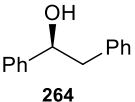
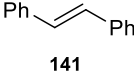
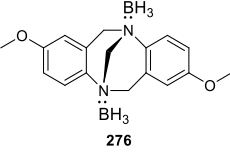
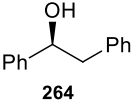
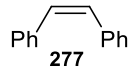
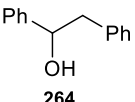
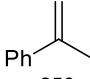
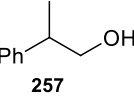
The borane complex **267** was prepared by passing the  $\text{B}_2\text{H}_6$  gas. It showed a characteristic  $^{11}\text{B}$  signal at -8.98. It was used for the hydroboration of *trans*-stilbene under iodine activation. The iodine activation was monitored by  $^{11}\text{B}$  NMR. A new peak at -13.69 ppm was observed. After the  $\text{H}_2\text{O}_2/\text{NaOH}$  oxidation the corresponding alcohol was obtained only in 5% ee (Scheme 76, Table 30).

**Scheme 76**

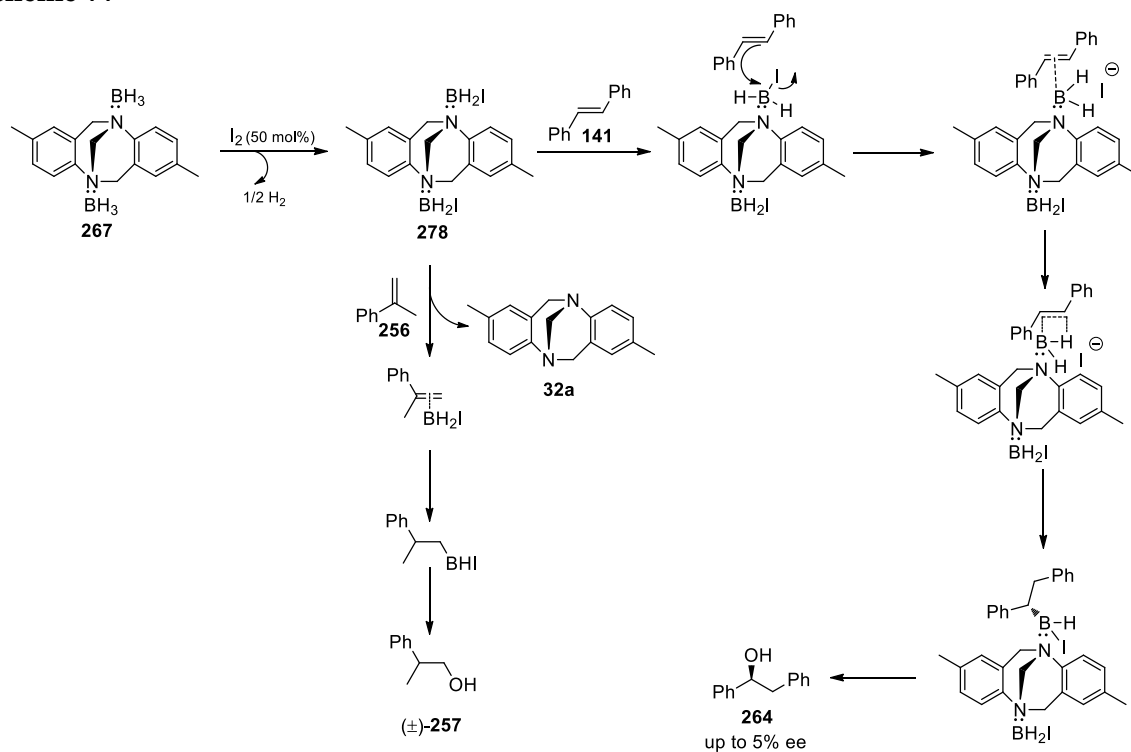


However, hydroboration of *cis*-stilbenes and  $\alpha$ -methylstyrene resulted only in the formation of racemic alcohols (Table 30, entry 3 and 4). We have also carried out the hydroboration of *trans*-stilbene under iodine activation of borane complex **276**. Again, the corresponding alcohol was isolated only in 4% ee after  $\text{H}_2\text{O}_2/\text{NaOH}$  oxidation.

**Table 30.** Hydroboration of prochiral olefins using chiral *para*-substituted Tröger base borane complexes under iodine activation<sup>a</sup>

Entry	Substrate	Borane complex	Product	% ee	Yield <sup>b,c</sup>
1	 <b>141</b>	 <b>267</b>	 <b>264</b>	5	75
2	 <b>141</b>	 <b>276</b>	 <b>264</b>	4	86
3	 <b>277</b>	<b>267 or 276</b>	 <b>264</b>	0	74
4	 <b>256</b>	<b>267 or 276</b>	 <b>257</b>	0	92

<sup>a</sup>All the reactions were carried out in 1 mmol scale at 25 °C for 10 h. <sup>b</sup>Products were isolated after oxidation NaOH/H<sub>2</sub>O<sub>2</sub>. <sup>c</sup>HPLC analyses were carried out on chiral column OB-H; *n*-Hexane:*i*prOH-97:3, 0.3 mL/min. and OD-H using *n*-Hexane:*i*prOH-90:10, 0.5 mL/min.

**Scheme 77**

The results obtained in hydroboration by borane complexes of chiral Tröger base derivatives can be rationalized by considering the mechanism as outlined in Scheme 77. The reaction of iodine with TB-BH<sub>3</sub> complexes would give the TB-BH<sub>2</sub>I complex **278** and hydrogen. In the reaction of olefin with TB-BH<sub>2</sub>I, if the iodide leaves, the chiral TB would be attached to the boron in the transition state leading to the optically active product. However, if chiral TB acts as a leaving group, the hydroboration reaction would lead to racemic mixtures. Unfortunately, studies undertaken to remove the iodide by using the AgBF<sub>4</sub> to prepare [Tröger base BH<sub>2</sub>]<sup>+</sup> did not improve the results (Table 31).

**Table 31.** Hydroboration of prochiral olefins using chiral *para*-substituted Tröger base borane complexes under iodine activation in the presence of additive<sup>a</sup>

Entry	Substrate	IBH <sub>2</sub> complex	Additive	Temperature (°C)	Product	% ee	Yield <sup>b,c</sup>
1			AgBF <sub>4</sub>	25		3	82
2			AgBF <sub>4</sub>	0		4	54
3			AgBF <sub>4</sub>	-20	-	-	-
4			AgBF <sub>4</sub>	25		0	62
5			AgBF <sub>4</sub>	-20	-	-	-

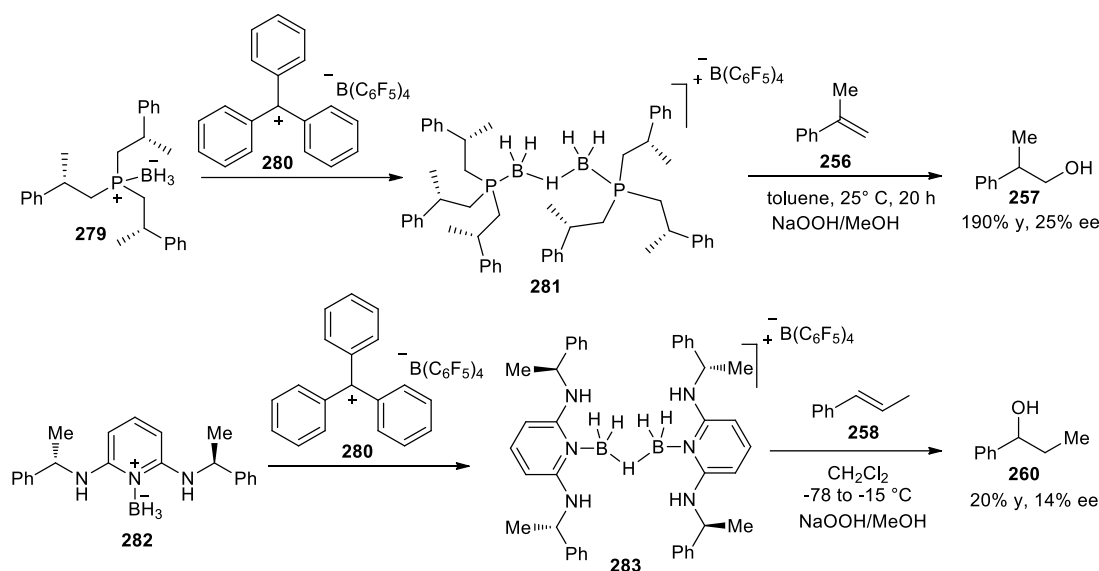
<sup>a</sup>All the reactions were carried out in 1 mmol scale for 12 h. <sup>b</sup>Products were isolated after oxidation NaOH/H<sub>2</sub>O<sub>2</sub>.

<sup>c</sup>HPLC analyses were carried out on chiral column OD-H using *n*-Hexane:*i*-PrOH-90:10, 0.5 mL/min. and OB-H; *n*-Hexane:*i*-PrOH-97:3, 0.3 mL/min.



Very recently, Vedejs *et al.*<sup>106</sup> reported that the asymmetric hydroboration of  $\alpha$ -methylstyrene **256** using C<sub>3</sub>-symmetric chiral phosphine-borane complex under trityl cation activation gave the corresponding alcohol in 190% yield and 25% ee. In another transformation using an amine-borane chiral system **283**, the alcohol product **260** was obtained in 14% ee (Scheme 78). Clearly, in these cases the Lewis base moiety is present in the hydroboration transition state (Scheme 72, S<sub>N</sub>2 Type Mechanism) to more extent.

**Scheme 78**



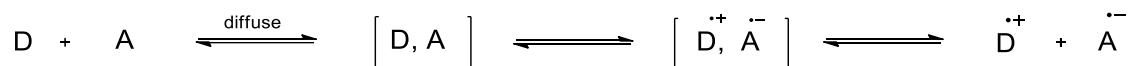
Therefore, studies on hydroboration of prochiral olefins using Tröger base-borane complexes under trityl cation activation may give fruitful results.

## 2.8 Charge transfer complexes of Tröger base derivatives

The Mulliken charge transfer (CT) complexes [D, A] are formed by diffusive interactions of electron donor (D) with electron acceptor (A).<sup>107</sup> In these complexes, two molecules, D and A, are weakly held together by nonbonding forces such as van der Waals forces, the molecules D and A remain unaltered, but new properties arise such as new absorption bands for the compound DA. The formation of ionic state (D<sup>+</sup>, A<sup>-</sup>) was not considered by Mulliken in those early days. Later, Bijl and co-workers<sup>108</sup> reported that the

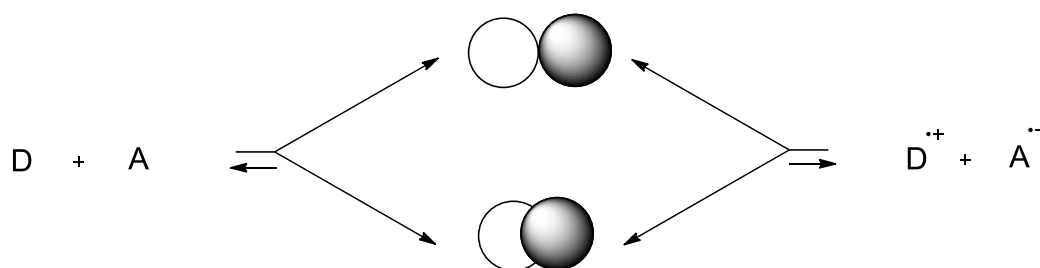
molecules with greater difference of electron affinity would have the ionic state as most populated at the room temperature. It was suggested that the ionic state  $D^{+\bullet}, A^{-\bullet}$  would be of biradical nature due to the presence of odd number of electron in the both donor and acceptor (Scheme 79).<sup>108</sup>

#### Scheme 79



Taube developed two separate mechanistic pathways, outer-sphere (OS) and inner-sphere (IS) mechanisms, for explaining the electron transfer in octahedral metal complexes.<sup>109</sup> Later, Marcus developed the intermolecular electron transfer in which activation energy was calculated by applying non-adiabatic or weakly adiabatic limitation between the encounter complexes (Scheme 80).<sup>110</sup>

#### Scheme 80



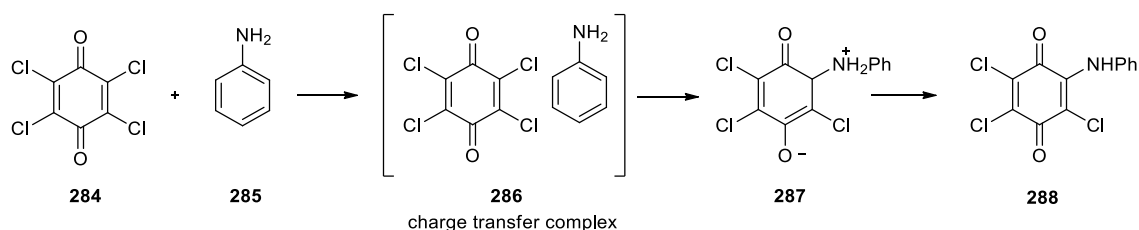
The outer-sphere complexes are expected to have loosely bound precursor and successor complexes. They show characteristic weak electronic absorption for electron-transfer processes.<sup>111</sup> In the classical inner-sphere mechanism, electronic couplings between donor/acceptor moieties are enhanced.<sup>112</sup>

In 2008, reports on electron-transfer reactions of organic electron donors and acceptors were reviewed by J. K. Kochi.<sup>113</sup> The outer-sphere/inner-sphere mechanism was extended to organic electron-transfer reactions, wherein donors and acceptors are not

considered as coordination spheres. Kochi *et al.*<sup>114</sup> proposed an alternative model based on distance dependence which is based on the van der Waals radii of electron donors and acceptors. The molecular interactions in outer-sphere processes are viewed as between donor and acceptor separated beyond their van der Waals radii. Whereas in inner-sphere complexes the distance between donor and acceptor is likely to be less than their van der Waals radii and hence in these complexes the donor/acceptor are packed closely with enhanced interactions.<sup>115</sup> Therefore, sterically hindered donor/acceptor complexes are expected to form outer-sphere complexes, while less sterically hindered donor and acceptor complexes would prefer to form inner-sphere complexes.<sup>116</sup>

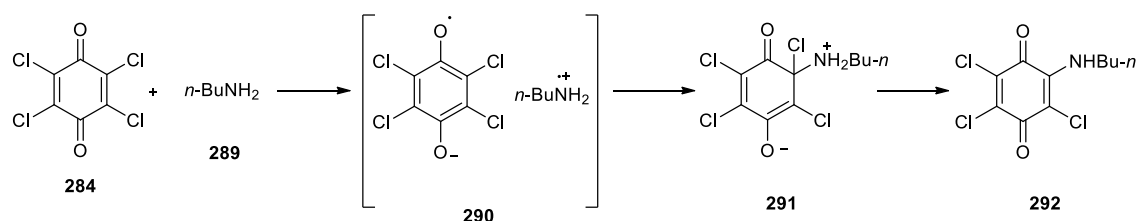
In 1969, Nagakura *et al.*<sup>117</sup> reported that the reaction of chloranil **284** with aniline **285** gives the charge transfer (CT) complex **286** (Scheme 81). Subsequently, the ionic diamagnetic intermediate **287** is formed before formation of the aminoquinone product **288**.

#### Scheme 81



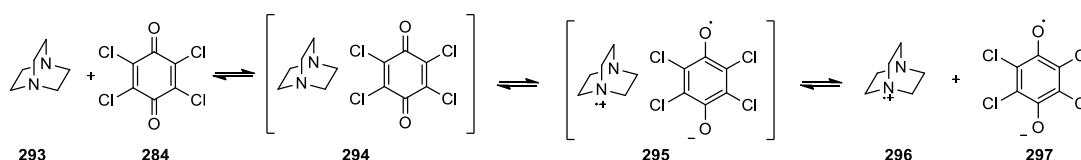
In 1971, Yamaoka *et al.*<sup>118</sup> suggested that the reaction of *n*-butylamine **289** with chloranil **284** gives the corresponding electron transfer complex **290**, which subsequently leads to the intermediate **291** before giving the substitution product **292** (Scheme 82).

#### Scheme 82



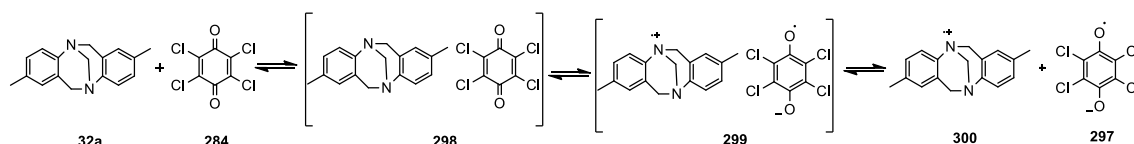
As early as in 1965, formation of stable radical cation of 1,4-diazabicyclo[2.2.2]octane (DABCO) **293** was reported.<sup>119</sup> It is stable due to the through-space interaction of nitrogen orbitals.<sup>120</sup> In 1977, the charge transfer (CT) complex **294** was reported in the reaction of DABCO with chloranil **284**.<sup>121</sup> Also, the CT complex was considered to be in equilibrium with the electron transfer (ET) complex and diradicals radical cation (**296**)-anion (**297**) pair (Scheme 83). The intensity of the esr signals were stronger in a more polar solvent such as THF compared to benzene.

**Scheme 83**



Tröger base and its derivatives are molecules with bridgehead nitrogens similar to DABCO. We have envisaged the preparation of molecular complex of Tröger base with acceptors. We have observed that mixing Tröger base **32a** with the electron acceptor chloranil **284** in solvents such as dichloromethane (DCM) and propylene carbonate (PC) leads to formation of paramagnetic intermediates **299** as detected by ESR spectroscopy with *g* value 2.00578 and 2.00605 (Scheme 84).

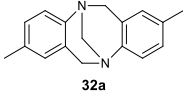
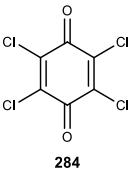
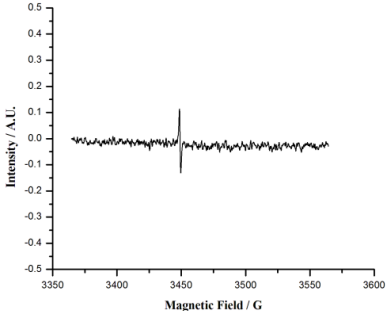
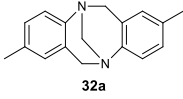
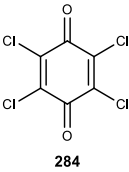
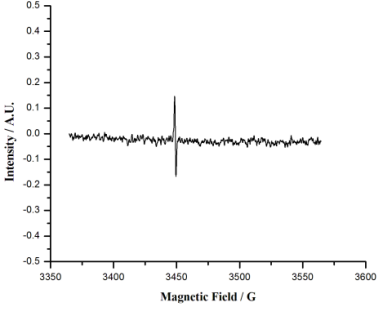
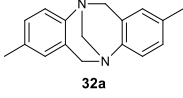
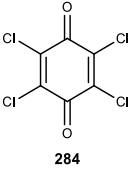
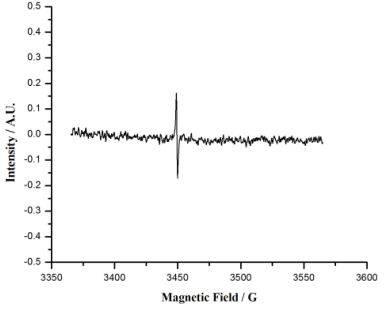
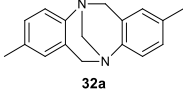
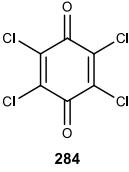
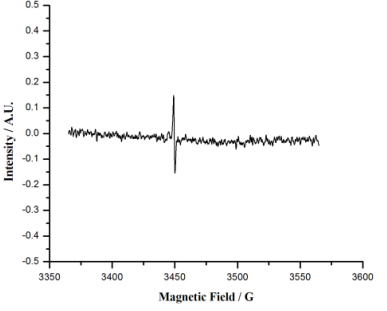
**Scheme 84**

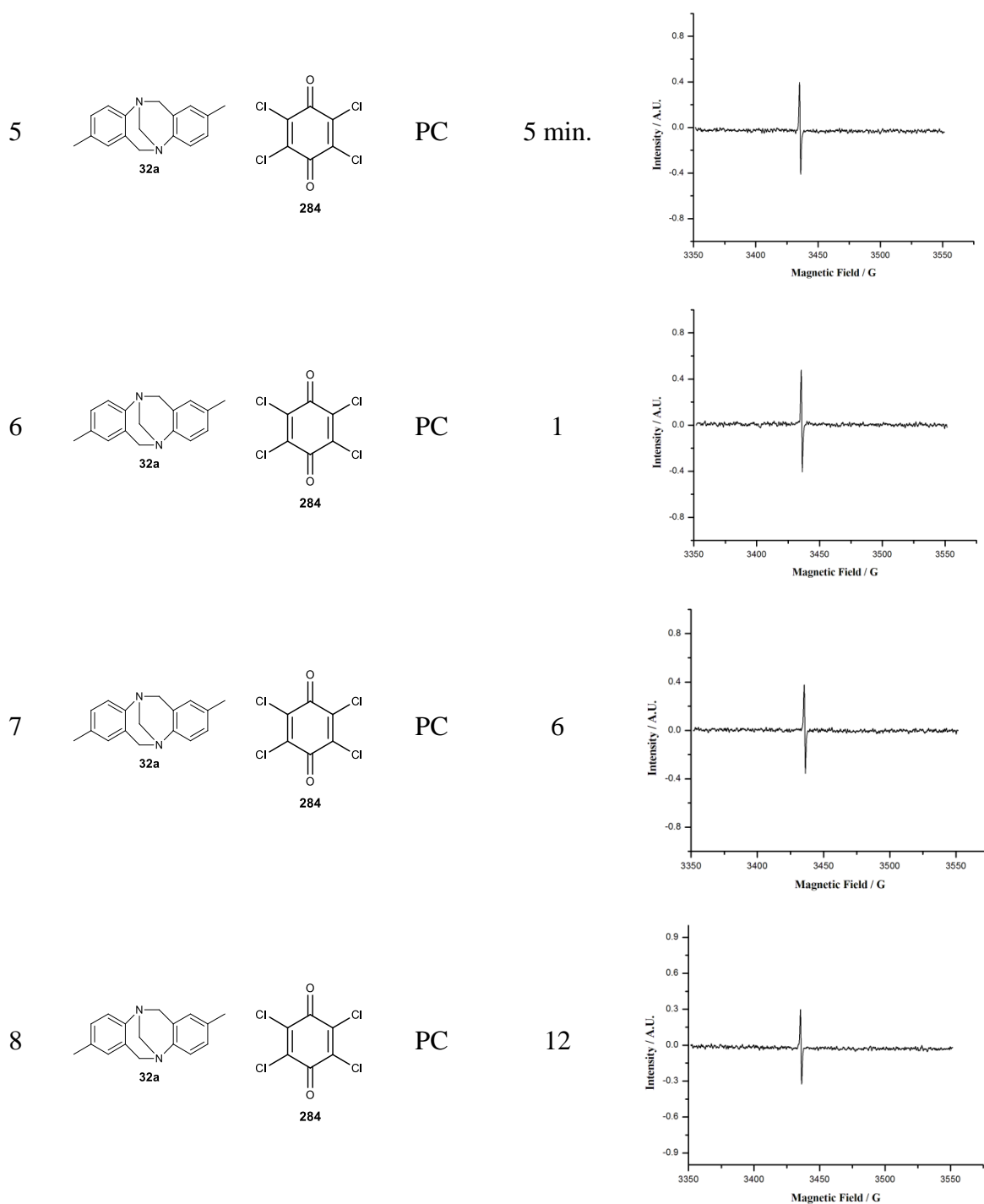


In general, the electron transfer complexes **299** prepared in this way are stable up to 24 h, but some decrease of intensity of esr signals was noticed with time (Table 32). We made attempts to crystallize the charge transfer complex using solvents such as CH<sub>2</sub>Cl<sub>2</sub>, PC,

dimethylformamide (DMF) and N-methyl-2-pyrrolidone (NMP), but crystals suitable for X-ray structural analysis could not be isolated. In the case of  $\text{CH}_2\text{Cl}_2$ , only chloranil crystals were isolated.

**Table 32.** ESR spectra of Tröger base with chloranil<sup>a</sup>

Entry	Donor	Acceptor	Solvent	Time (h)	ESR spectra
1			$\text{CH}_2\text{Cl}_2$	5 min.	
2			$\text{CH}_2\text{Cl}_2$	1	
3			$\text{CH}_2\text{Cl}_2$	6	
4			$\text{CH}_2\text{Cl}_2$	12	



<sup>a</sup>All the experiments were carried out in the ESR tube by mixing Tröger base **32a** (0.02 mmol) with chloranil **284** (0.02 mmol) in solvent (10 mg).

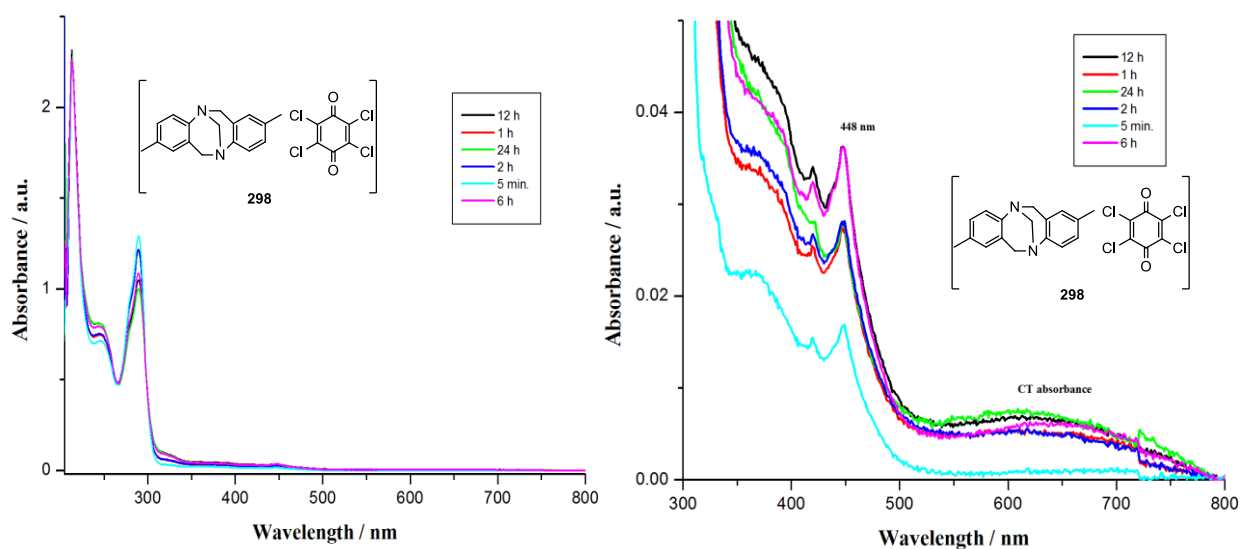
The electron transfer complex **299** showed a one line esr spectra. In this case, the hyperfine coupling was not observed.

In 1957, the line broadening of esr spectra of naphthalenide ion was observed by adding excess naphthalene.<sup>122</sup> The reported rate constants for electron transfer between naphthalene negative ion and naphthalene are in the range  $10^7$ - $10^9$  liter mole<sup>-1</sup>sec.<sup>-1</sup>

Such line broadening was also reported in the case of 2,3-dichloro-5,6-dicyano-1,4-benzoquinone (DDQ) radical anion with DDQ with fast exchange rate constant  $2.5 \times 10^9$  M<sup>-1</sup> S<sup>-1</sup> and activation energy of 1.6 kcal mol<sup>-1</sup> at 23 °C.<sup>113</sup>

Similar line-broadening of esr spectra observed for the TB-chloranil can be explained by considering the electron exchange phenomenon. It is obvious from Table 32 that the esr signal intensity is higher in PC solvent compare to CH<sub>2</sub>Cl<sub>2</sub>. Presumably, the ion pair dissociates to more extent in more polar PC solvent, leading to more intense esr signals.<sup>121</sup> Further, we have observed that the reaction of Tröger base with weak acceptors such as benzoquinone or naphthoquinone did not give electron transfer complex even in PC solvent.

Sersen *et al.*<sup>121</sup> reported that the reaction of *p*-chloranil with 1,4-diazabicyclo[2.2.2]octane gives 1:1 charge transfer complex. These authors confirmed the formation of the charge transfer complex by UV-Visible spectroscopy and assigned the absorption band of 450 nm of DABCO-chloranil system to chloranil anion radical. We have also examined the formation of charge transfer complex in the reaction of Tröger base with chloranil by UV-Visible spectroscopy. We mixed the 1:1 solution of Tröger base ( $10^{-4}$  M) and *p*-chloranil ( $10^{-4}$  M). The color change was not observed for this diluted solution. However, the characteristic absorbance band for chloranil anion radical was observed at 448 nm. The new absorbance band observed beyond 500 nm can be assigned to the absorption of the charge transfer (CT) complex **299**, because neither chloranil nor TB absorbance absorbed in this region. The UV-Visible spectra are shown in Figure 33.

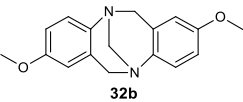
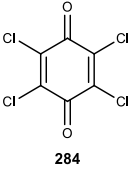
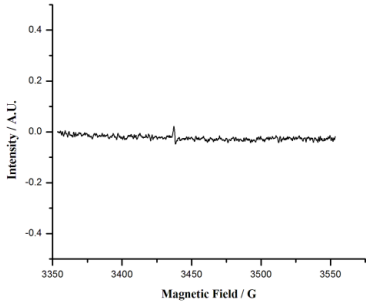
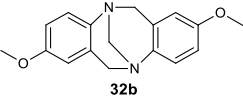
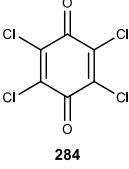
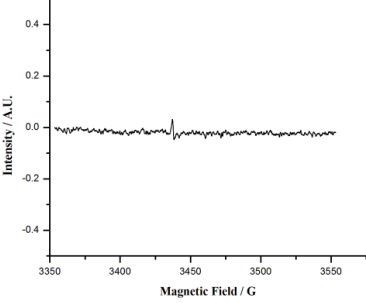
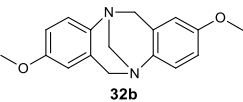
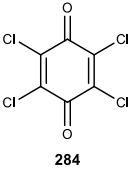
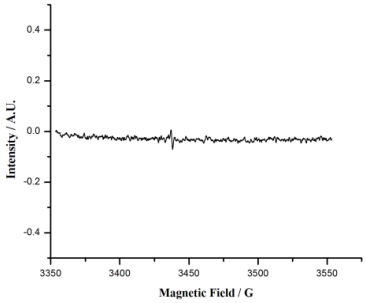
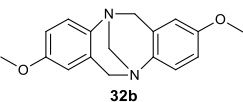
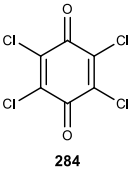
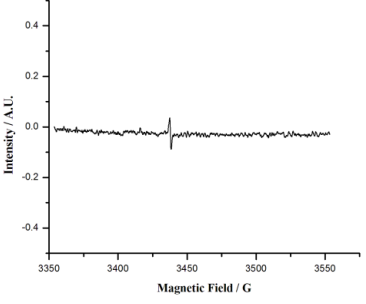


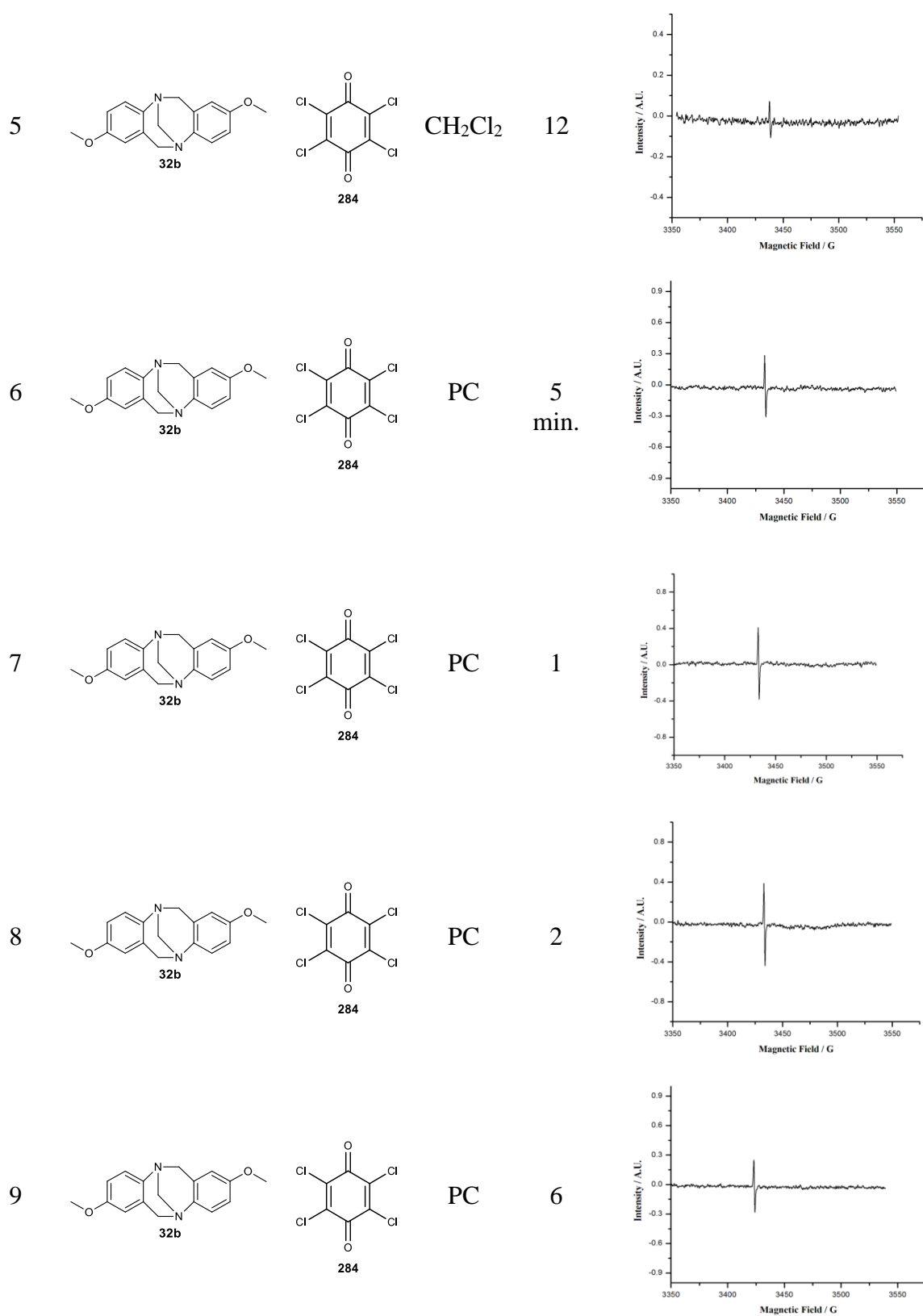
**Figure 33.** a) UV-vis spectra of a mixture of TB **32a** ( $1 \times 10^{-4}$  mol L $^{-1}$ ) and chloranil **284** ( $1 \times 10^{-4}$  mol L $^{-1}$ ) in PC at 25 °C. (b) Expanded UV-Visible spectra.

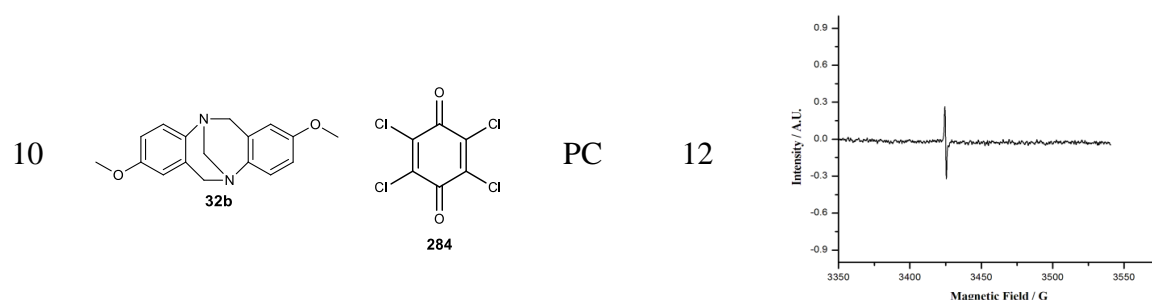
Previously, it was reported that the reaction of more nucleophilic methoxy Tröger base **32b** with dibenzoyl-L-tartaric acid resulted in the formation of salt while TB gives only hydrogen bonded aggregates.<sup>10</sup> We became interested to study the effect of substituents on the electron transfer (CT) complex formation. Therefore, we monitored the mixture of methoxy Tröger base **32b** with chloranil by esr spectroscopy in CH<sub>2</sub>Cl<sub>2</sub> and PC solvent. The results are presented in Table 33. Surprisingly, the paramagnetic intermediates formed from the reaction of methoxy Tröger base **32b** with chloranil gave relatively weak esr signals with g value 2.00585 and 2.00598.



**Table 33.** ESR spectra of methoxy Tröger base **32b** with chloranil<sup>a</sup>

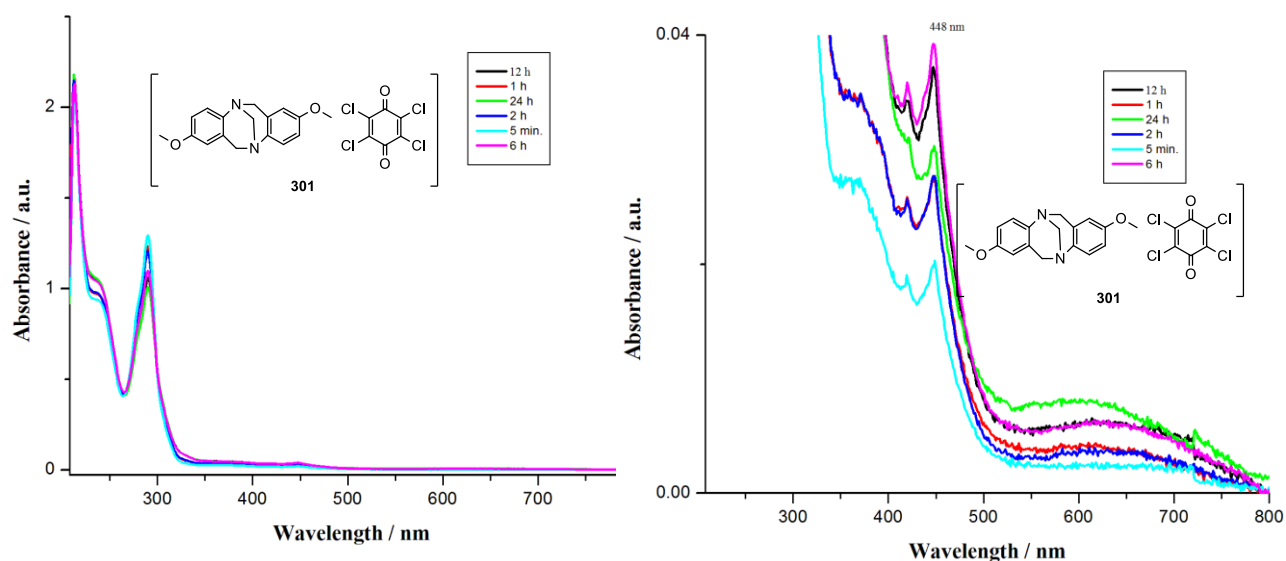
Entry	Donor	Acceptor	Solvent	Time	ESR spectra
				(h)	
1			CH <sub>2</sub> Cl <sub>2</sub>	5 min.	
2			CH <sub>2</sub> Cl <sub>2</sub>	1	
3			CH <sub>2</sub> Cl <sub>2</sub>	2	
4			CH <sub>2</sub> Cl <sub>2</sub>	6	





<sup>a</sup>All the experiments were carried out in the ESR tube by mixing methoxy Tröger base **32b** (0.02 mmol, 5.6 mg) with chloranil **284** (0.02 mmol, 4.9 mg) in solvent (10 mg).

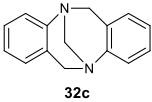
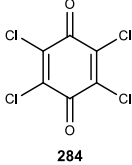
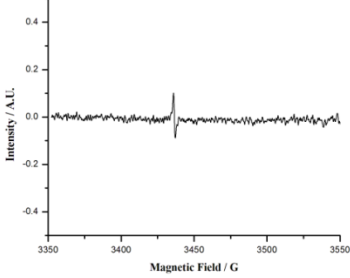
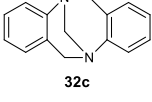
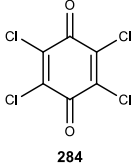
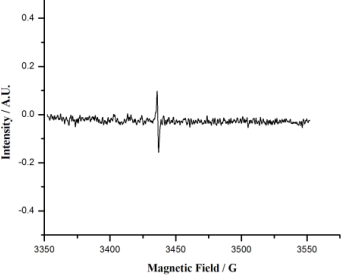
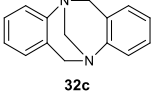
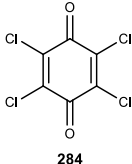
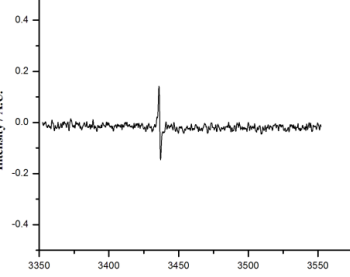
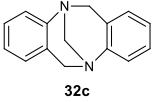
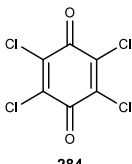
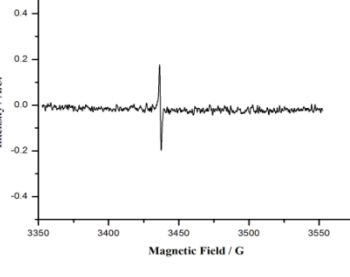
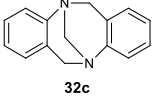
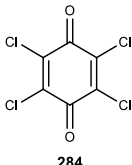
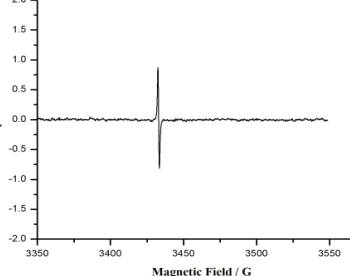
We recorded the UV-Vis spectra of 1:1 mixture of methoxy Tröger base ( $10^{-4}$  M) with chloranil ( $10^{-4}$  M) at different time intervals. The results are presented in Figure 34. The absorbance band at 448 nm was assigned to chloranil anion radical. The absorbance band observed beyond 500 nm can be assigned to charge transfer (CT) complexes **301** as in the case of Tröger base **32a**.

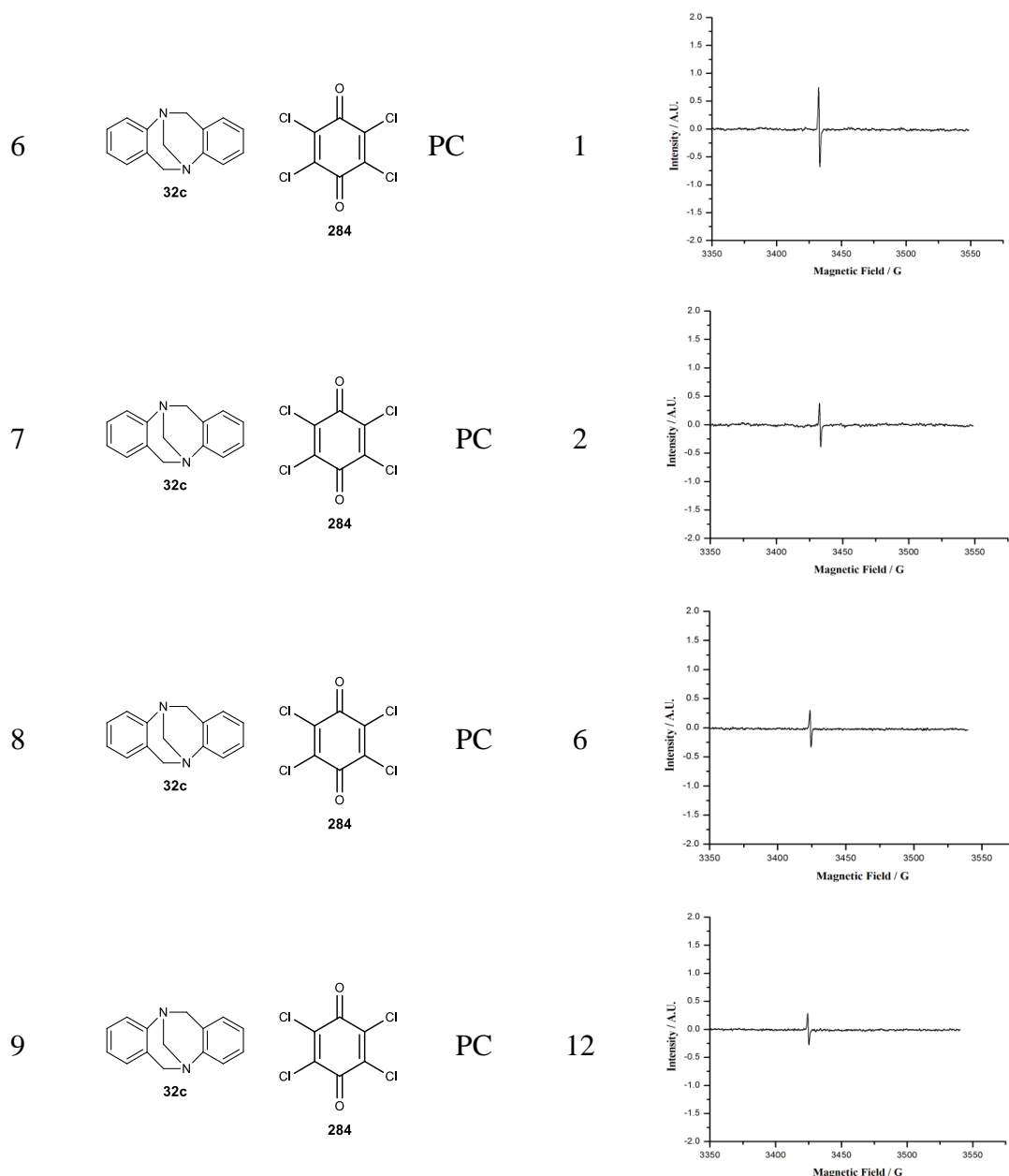


**Figure 34.** a) UV-vis spectra of a mixture of TB **32b** ( $1 \times 10^{-4}$  mol L<sup>-1</sup>) and chloranil **284** ( $1 \times 10^{-4}$  mol L<sup>-1</sup>) in PC at 25 °C. (b) Expanded UV-Visible spectra.

To understand further, we recorded the ESR spectra of 1:1 mixture of unsubstituted Tröger base **32c** and chloranil **284** in CH<sub>2</sub>Cl<sub>2</sub> and PC solvents. The results are presented in Table 34. In this case, we observed somewhat more intense esr signals compared to the methoxy Tröger base **32b** (g value 2.00591 and 2.00599).

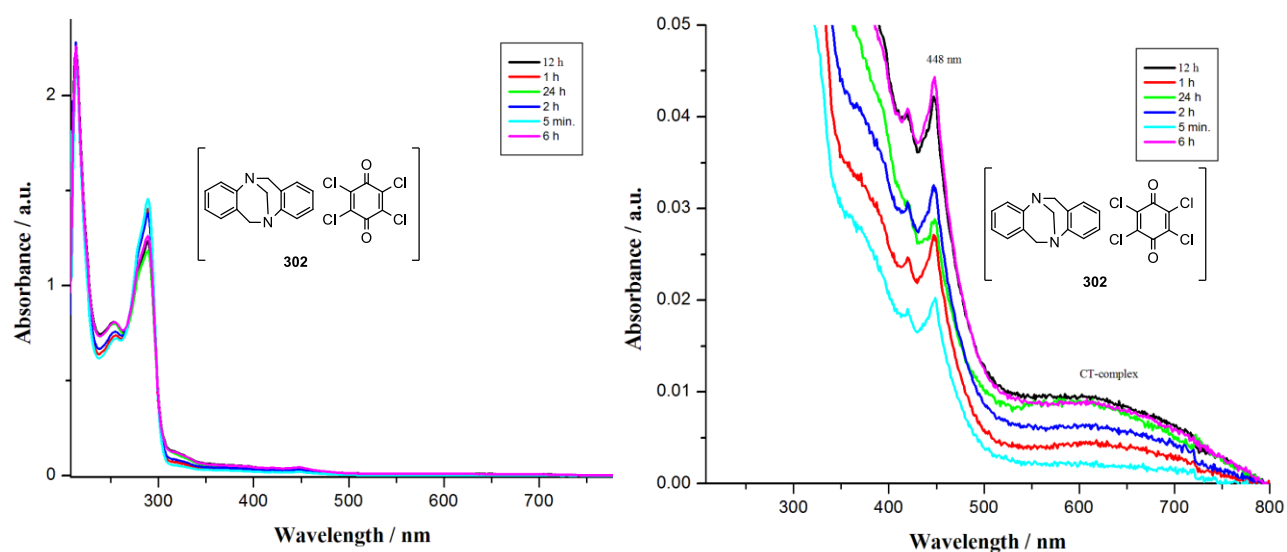
**Table 34.** ESR spectra of Tröger base **32c** with chloranil<sup>a</sup>

Entry	Donor	Acceptor	Solvent	Time	ESR spectra
(h)					
1			CH <sub>2</sub> Cl <sub>2</sub>	5 min.	
2			CH <sub>2</sub> Cl <sub>2</sub>	1	
3			CH <sub>2</sub> Cl <sub>2</sub>	2	
4			CH <sub>2</sub> Cl <sub>2</sub>	12	
5			PC	5 min.	



<sup>a</sup>All the experiments were carried out in the ESR tube by mixing Tröger base **32c** (0.02 mmol, 4.4 mg) with chloranil **284** (0.02 mmol, 4.9 mg) in solvent (10 mg).

Similarly, we recorded the UV-Vis spectra of 1:1 mixture of Tröger base **32c** ( $10^{-4}$  M) with chloranil **284** ( $10^{-4}$  M) at different time intervals. The results are presented in Figure 35. The absorbance band at 448 nm was assigned to chloranil anion radical. The absorbance band observed beyond 500 nm was assigned to charge transfer (CT) complexes **302** as in the case of Tröger base **32a**.

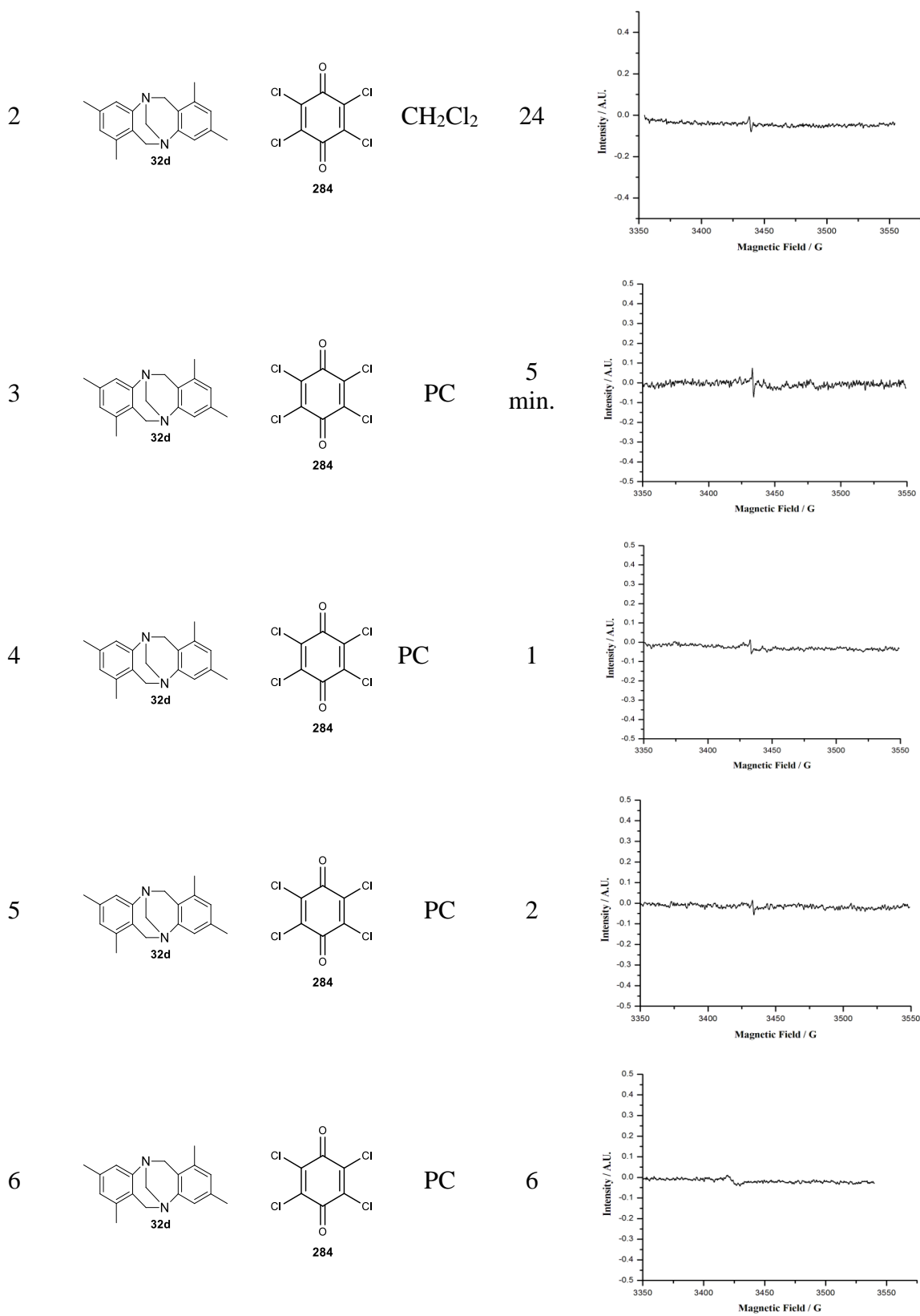


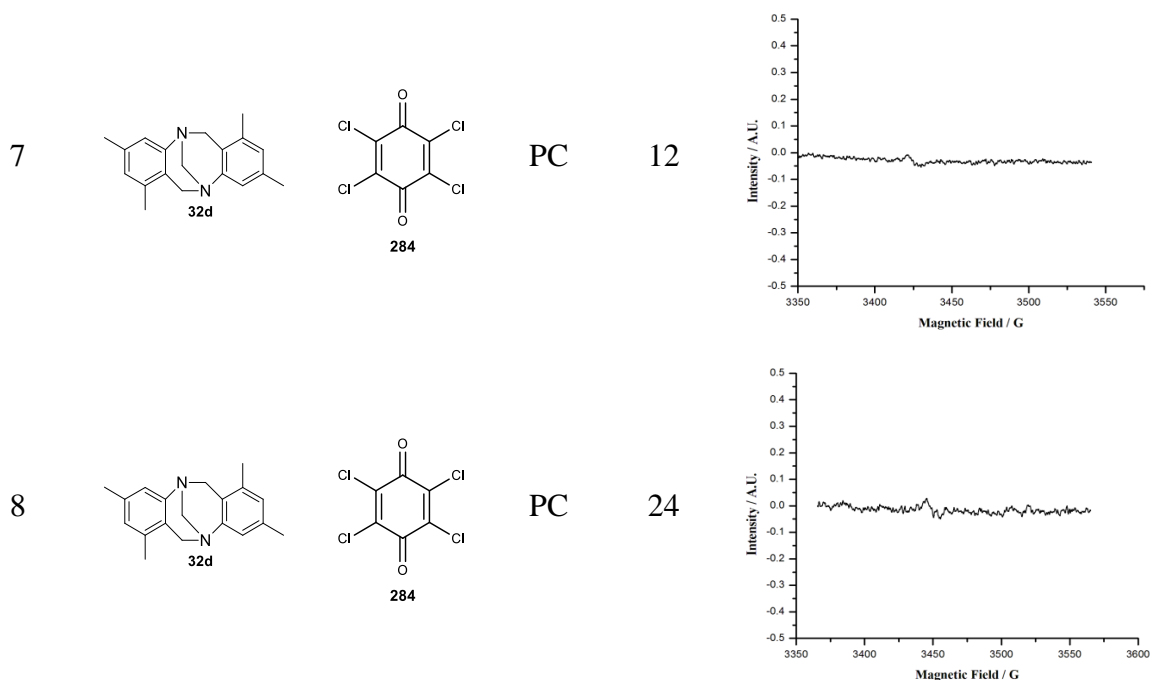
**Figure 35.** a) UV-vis spectra of a mixture of TB **32c** ( $1 \times 10^{-4}$  mol L $^{-1}$ ) and chloranil **284** ( $1 \times 10^{-4}$  mol L $^{-1}$ ) in PC at 25 °C. (b) Expanded UV-Visible spectra.

In the case of tetramethyl Tröger base derivative **32d**, the formation of paramagnetic intermediate was not observed up to 12 h in CH<sub>2</sub>Cl<sub>2</sub> solvent. But, after 24 h formation of paramagnetic intermediates were observed with *g* value 2.00588 (Table 35, Entry 2). In this case, only very weak esr signals were observed with *g* value 2.00595 in PC solvent compared to other TB derivatives (Table 35, Entry 3-8).

**Table 35.** ESR spectra of Tröger base **32d** with chloranil<sup>a</sup>

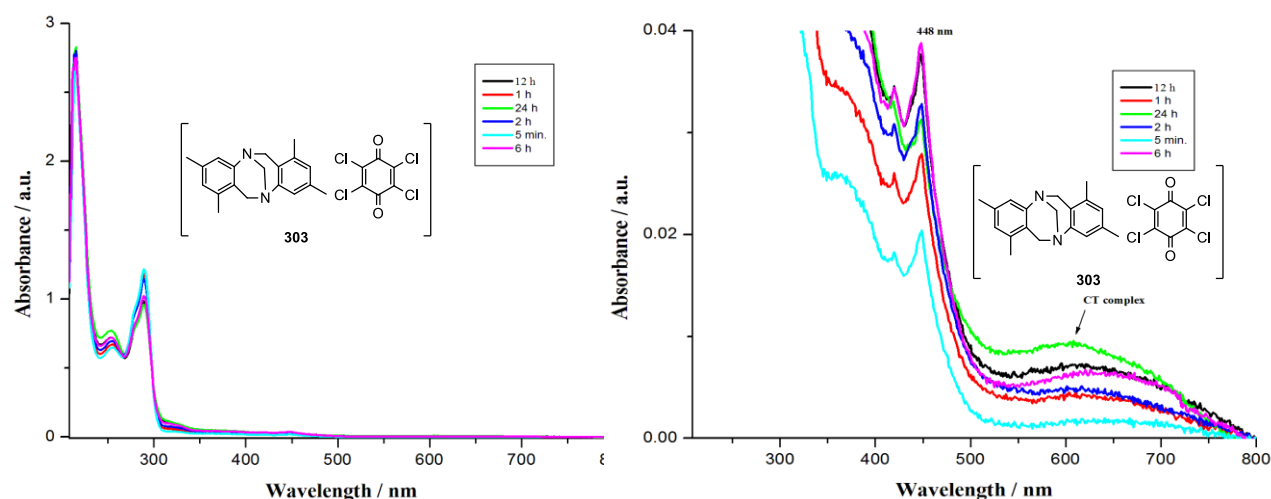
Entry	Donor	Acceptor	Solvent	Time	ESR spectra
(h)					
1			CH <sub>2</sub> Cl <sub>2</sub>	12	





<sup>a</sup>All the experiments were carried out in the ESR tube by mixing Tröger base **32d** (0.02 mmol, 5.5 mg) with chloranil **284** (0.02 mmol, 4.9 mg) in solvent (10 mg).

We have also recorded the UV-Vis spectra of 1:1 mixture of Tröger base **32d** ( $10^{-4}$  M) with chloranil **284** ( $10^{-4}$  M) at different time intervals. The results are presented in Figure 36. The absorbance bands correspond to chloranil anion radical and charge transfer (CT) complexes **303** (Figure 36).

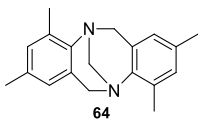
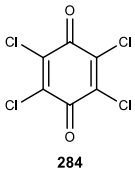
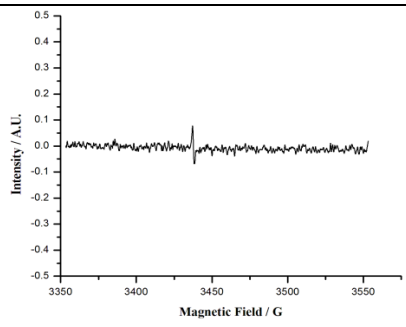
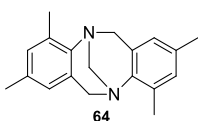
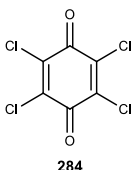
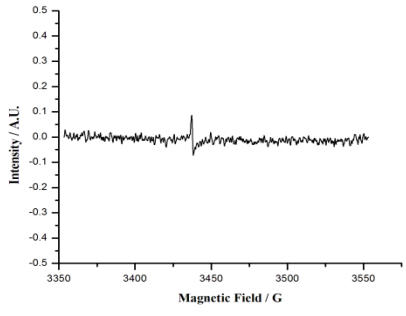
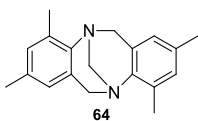
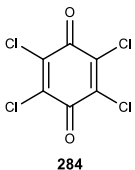
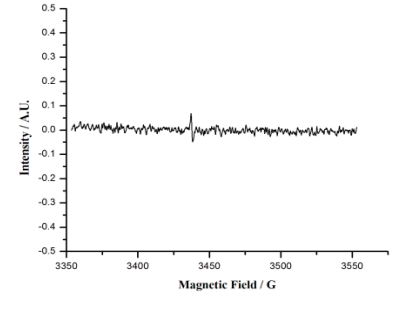


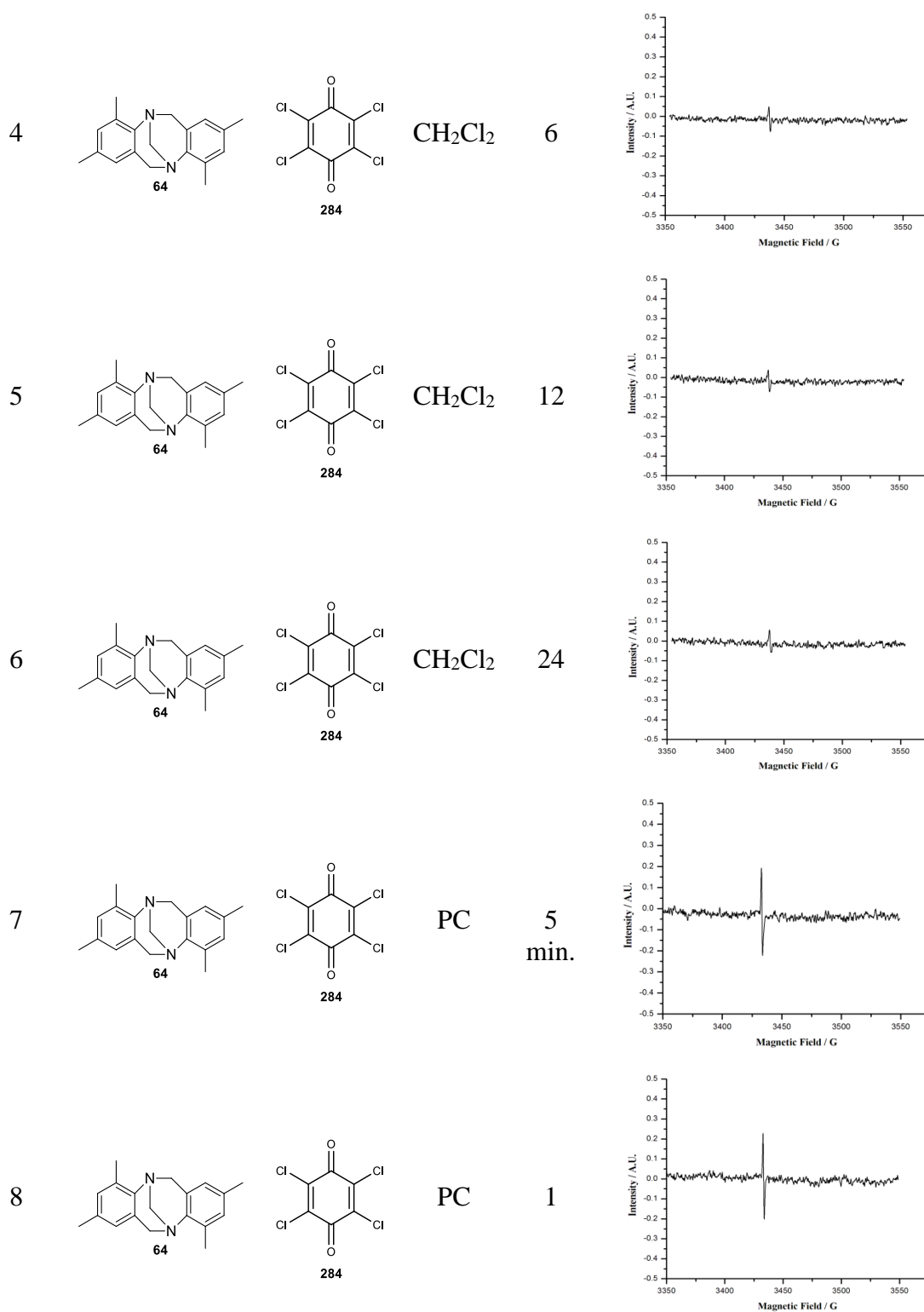
**Figure 36.** a) UV-vis spectra of a mixture of TB **32d** ( $1 \times 10^{-4}$  mol L<sup>-1</sup>) and chloranil **284** ( $1 \times 10^{-4}$  mol L<sup>-1</sup>) in PC at 25 °C. (b) Expanded UV-Visible spectra.

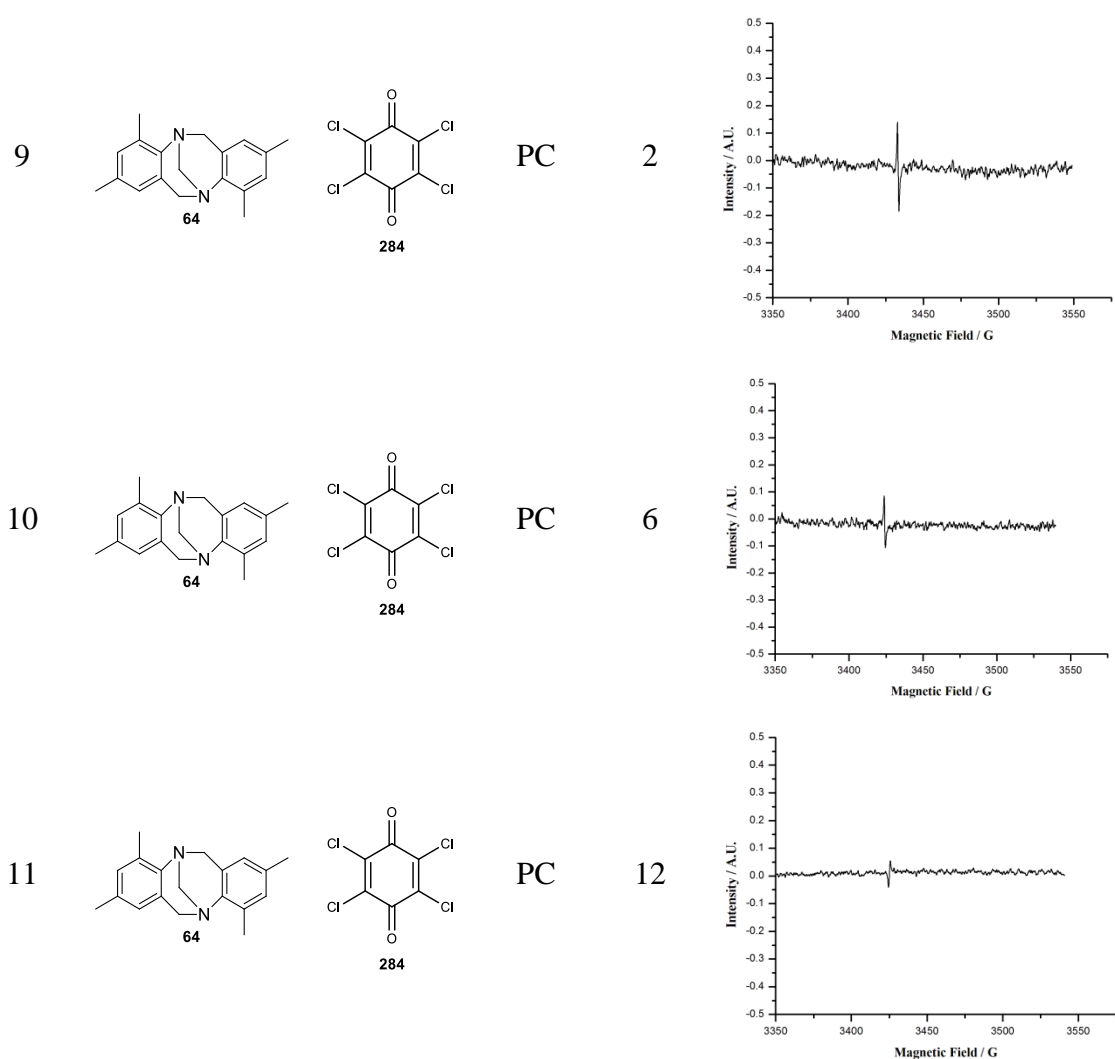


Tröger base **64** with tetramethyl groups gave similar results as observed in the case of TB **32a**. Also, in this case esr signals are somewhat intense compared with TB **32d**. Presumably, the methyl substitution in **32d** helps in stabilizes CT-complex formed. In the case of **64**, we observed esr signals in both  $\text{CH}_2\text{Cl}_2$  and PC solvents with  $g$  value 2.00587 and 2.00601 respectively (Table 36). The signals are somewhat weak compared to that observed for TB **32a** (Table 32). Presumably, the *ortho*-methyl substitution slows down the complex formation due to steric hindrance.

**Table 36.** ESR spectra of Tröger base **64** with chloranil<sup>a</sup>

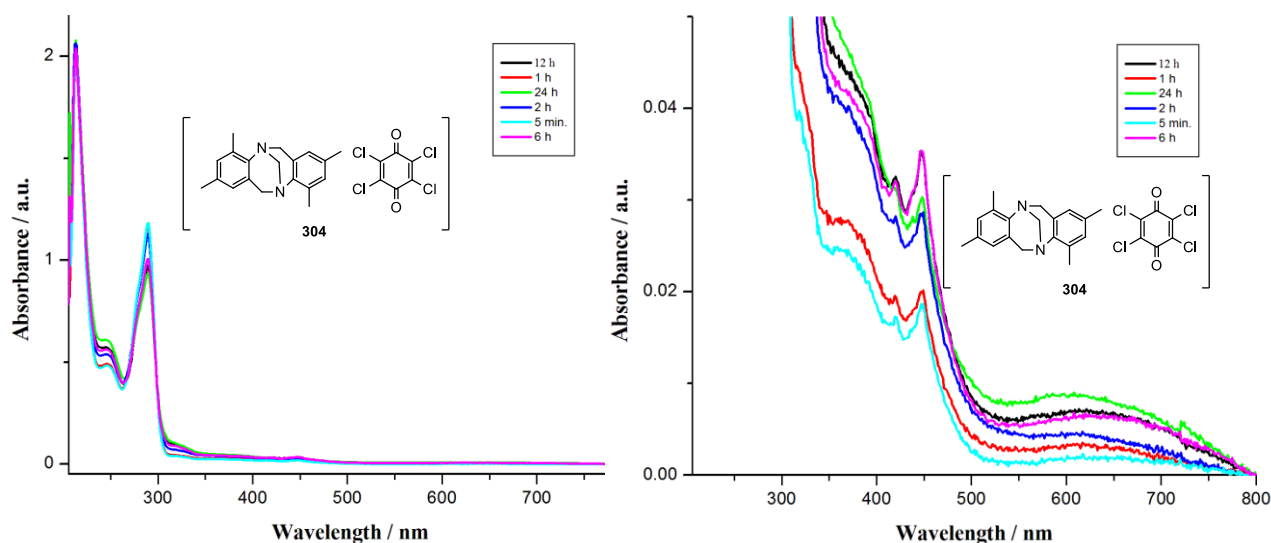
Entry	Donor	Acceptor	Solvent	Time	ESR spectra
(h)					
1			$\text{CH}_2\text{Cl}_2$	5 min.	
2			$\text{CH}_2\text{Cl}_2$	1	
3			$\text{CH}_2\text{Cl}_2$	2	





<sup>a</sup>All the experiments were carried out in the ESR tube by mixing Tröger base **64** (0.02 mmol, 5.5 mg) with chloranil **284** (0.02 mmol, 4.9 mg) in solvent (10 mg).

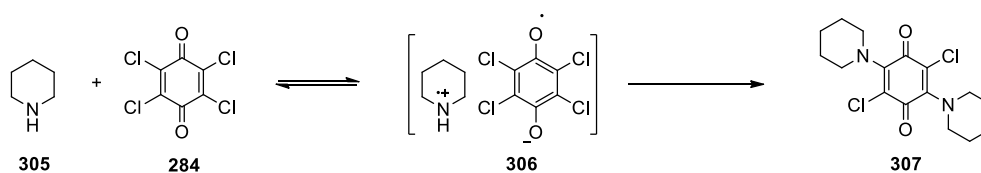
We have recorded the UV-Vis spectra of 1:1 mixture of Tröger base **64** ( $10^{-4}$  M) with chloranil **284** ( $10^{-4}$  M) at different time intervals. The results are presented in Figure 37. The absorbance band corresponds to chloranil anion radical and charge transfer (CT) complexes **304** were observed as observed in the other cases (Figure 37).



**Figure 37.** a) UV-vis spectra of a mixture of TB **64** ( $1 \times 10^{-4}$  mol L $^{-1}$ ) and chloranil **284** ( $1 \times 10^{-4}$  mol L $^{-1}$ ) in PC at 25 °C. (b) Expanded UV-Visible spectra.

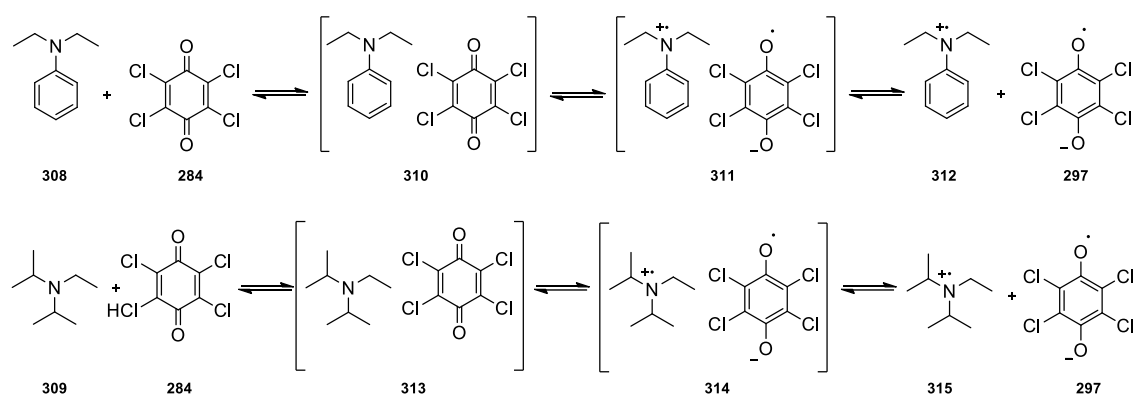
Previously, it was observed in this laboratory that the reaction of chloranil **284** with secondary amine **305** in DCM or PC solvent gives an esr signal. The intensity of signal decreases with time and disappears within 24 h and leads to the formation of aminoquinone **307** product (Scheme 85).<sup>123</sup>

#### Scheme 85



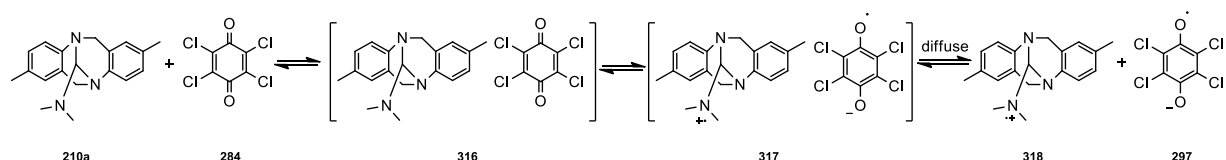
It was also observed in this laboratory that the tertiary amines **308** and **309** form charge transfer complexes with chloranil **284** in PC solvent. The reaction of amine **309** with chloranil gave very strong esr signals and intensity of esr signal decreased with time (Scheme 86).<sup>123</sup>

Scheme 86

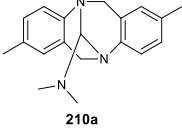
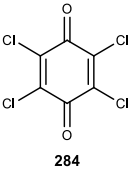
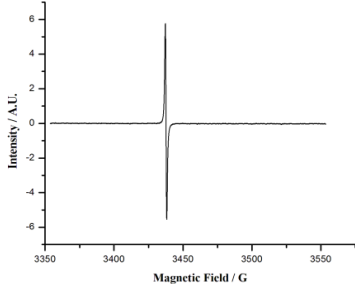
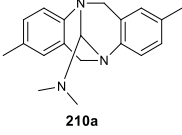
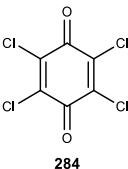
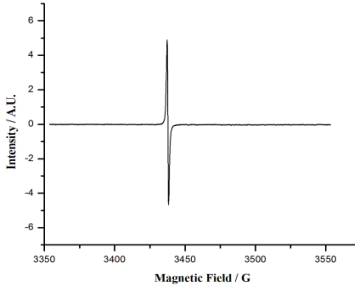
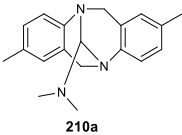
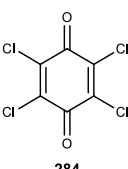
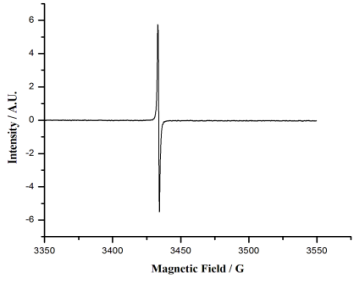
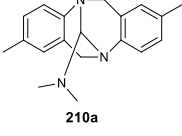
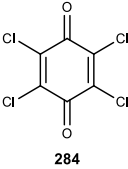
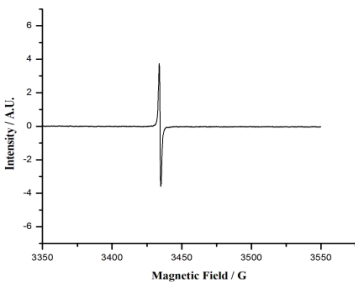
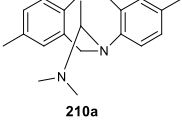
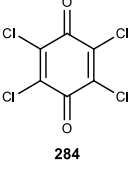
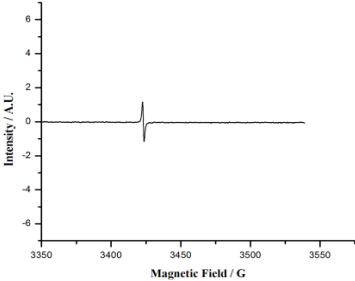


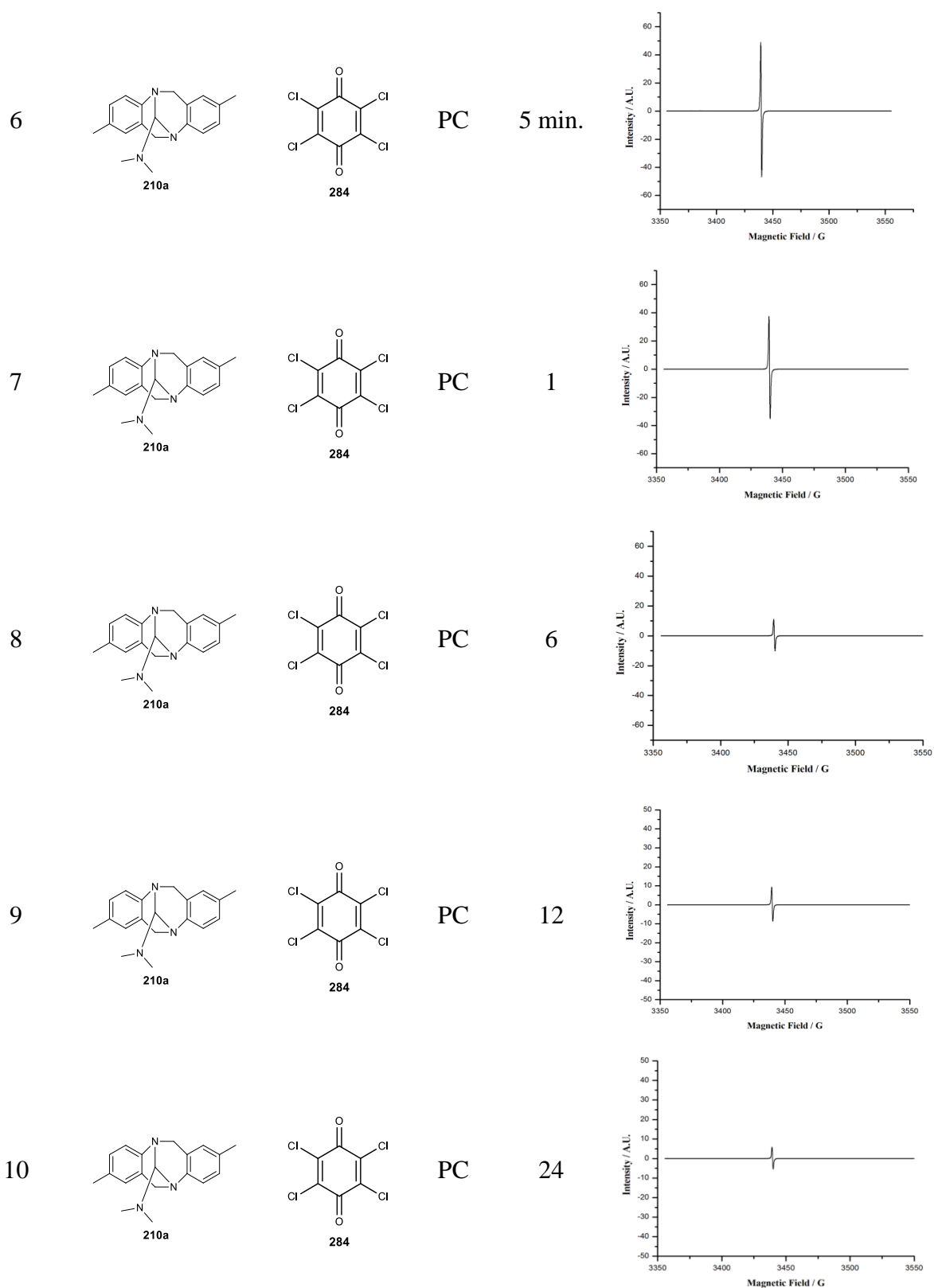
The Tröger base derivative **210a** has an alkylamine group in addition to bridgehead nitrogen atoms. It was of interest to us to examine whether the bridgehead nitrogen or the nitrogen of *N,N*-dimethyl group of 5,11-disubstituted derivative **210a** involves in the electron-transfer reaction. We recorded the esr spectra of 1:1 mixture of 5,11-substituted derivatives with chloranil in  $\text{CH}_2\text{Cl}_2$  and PC. The results are presented in the Table 37. In this case, we observed more intense esr signals (*g* value 2.00606 and 2.00600) compared to the parent Tröger base compound **32a**. This observation clearly suggests that derivative **210a** is a stronger donor (Scheme 87, Table 37). Again, decrease in intensity of esr signals were observed with time (Scheme 87).

Scheme 87

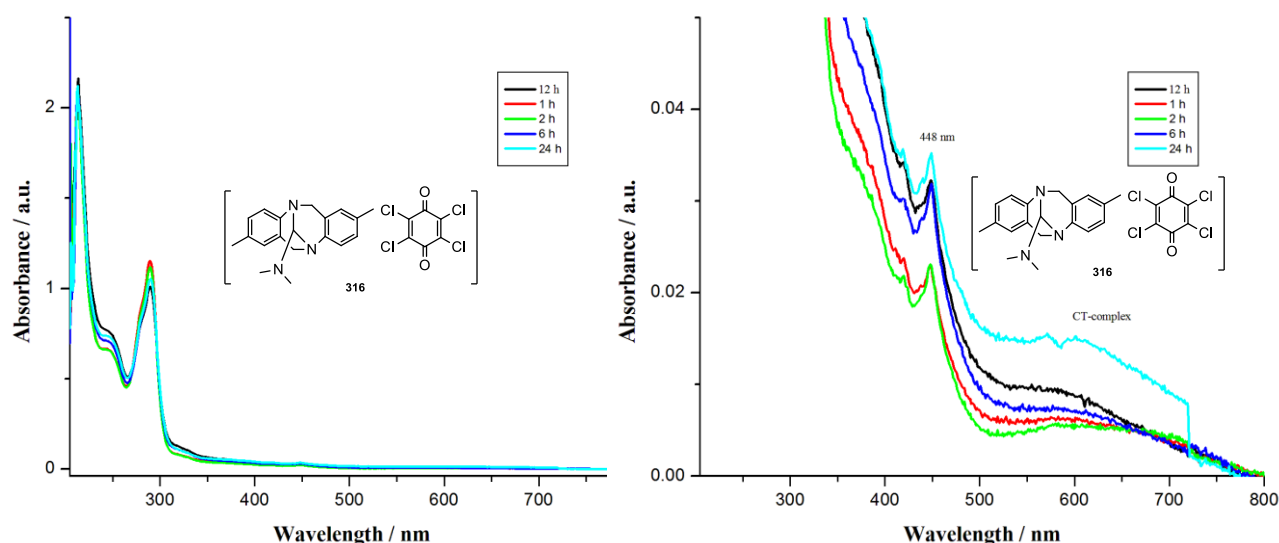


**Table 37.** ESR spectra of Tröger base **210a** with chloranil<sup>a</sup>

Entry	Donor	Acceptor	Solvent	Time	ESR spectra
				(h)	
1			CH <sub>2</sub> Cl <sub>2</sub>	5 min.	
2			CH <sub>2</sub> Cl <sub>2</sub>	1	
3			CH <sub>2</sub> Cl <sub>2</sub>	6	
4			CH <sub>2</sub> Cl <sub>2</sub>	12	
5			CH <sub>2</sub> Cl <sub>2</sub>	24	



<sup>a</sup>All the experiments were carried out in the ESR tube by mixing Tröger base **210a** (0.02 mmol, 5.8 mg) with chloranil **284** (0.02 mmol, 4.9 mg) in solvent (10 mg).

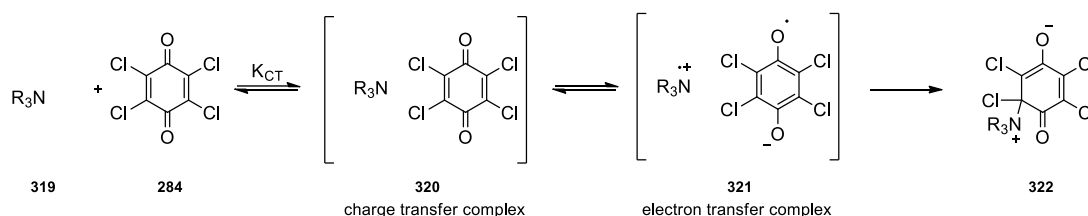


**Figure 38.** a) UV-vis spectra of a mixture of TB **210a** ( $1 \times 10^{-4}$  mol L $^{-1}$ ) and chloranil **284** ( $1 \times 10^{-4}$  mol L $^{-1}$ ) in PC at 25 °C. (b) Expanded UV-Visible spectra.

The UV-Vis study of 1:1 solution of Tröger base **210a** ( $10^{-4}$  M) with *p*-chloranil **284** ( $10^{-4}$  M) was also performed. The chloranil anion radical absorption was observed at 448 nm. The new absorbance band observed beyond 500 nm corresponds to charge transfer (CT) complex **316**. The UV-Visible spectra are shown in Figure 38.

The nature of the complex, paramagnetic species and the reason for the reduction of esr signal intensity with time are not clearly understood. One possibility is slow formation of a diamagnetic 1,4 addition product **322** (Scheme 88) as the reactivity of the tertiary amines and secondary amines is expected to be similar (See scheme 89).

### Scheme 88

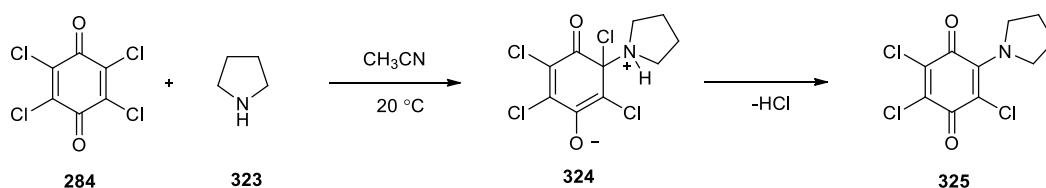


Very recently, Mayr and co-workers<sup>124,125</sup> reported that the reaction of secondary amine **323** with chloranil **284** gives the corresponding product **325** via the diamagnetic ionic



intermediate **324** (Scheme 89). It was also suggested that the reaction of amine with quinones is several orders of magnitude faster than that expected for single electron transfer (SET) process.<sup>124</sup> However, these authors did not report any esr spectrum of the intermediate formed.

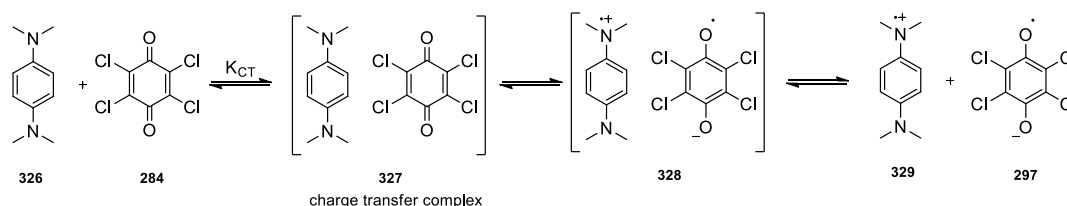
### Scheme 89



Although, Mayr and co-workers did not report reactions of tertiary amines with chloranil, these derivatives may also give addition products similar to that of secondary amines (Scheme 88). As discussed earlier, it was observed in this laboratory that mixing secondary amines with chloranil in different solvents gives intense esr signals which disappear in 24 h and the corresponding aminoquinone products are isolated.<sup>123</sup> Unfortunately, the ionic intermediates expected to be formed (Scheme 88) could not be isolated in pure form.

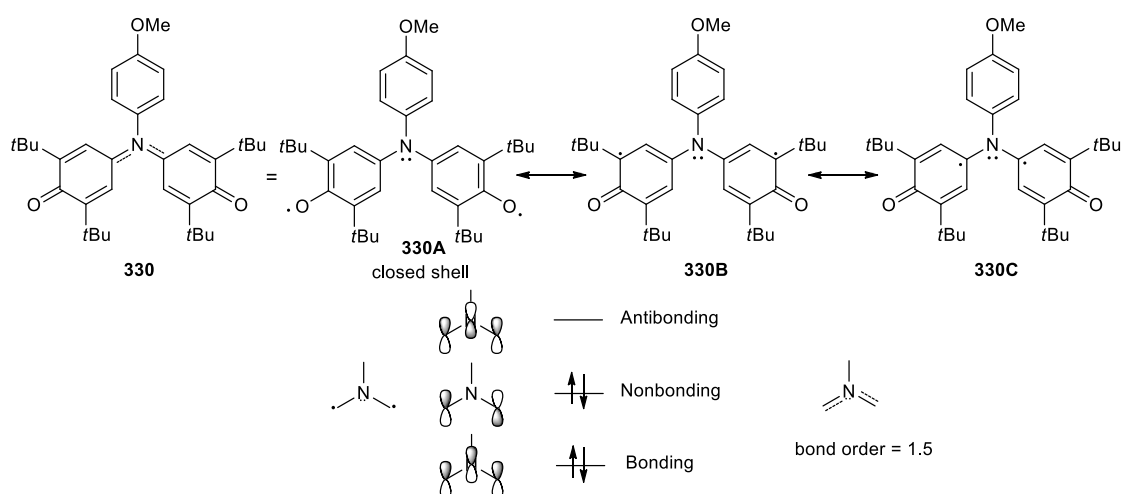
The charge-transfer complex **327** of *N,N,N',N'*-tetramethyl-*p*-phenylenediamine (TMPD) **326** with chloranil **284** was reported.<sup>126</sup> It was proposed that such complexes interchanged reversibly (Scheme 79).<sup>127</sup> The TMPD-chloranil system was also reported to give ionic diamagnetic complexes (Scheme 90).<sup>128</sup> However, the structure of such ionic diamagnetic complex was not reported in those early days.

### Scheme 90



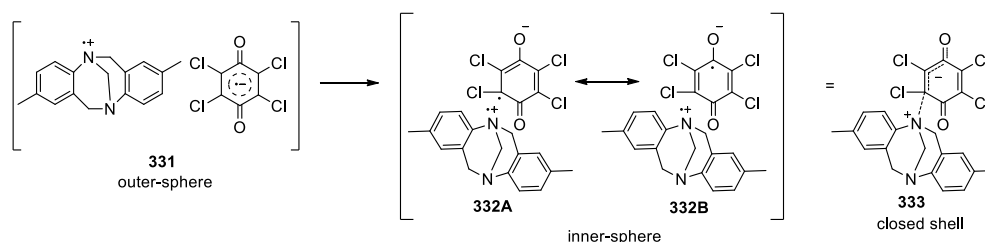
Very recently, Sakamaki *et al.*<sup>129</sup> reported that the C-N bond length of biradical **330A** is shorter (1.383 Å) than the usual C-N single bond (1.441 Å). The multiple-bond (1.5 bond order) character of the two C-N bonds was established by <sup>1</sup>H and <sup>13</sup>C signals of the *tert*-butyl groups. Huckel MO calculation for an isodistant azomethine ylide gave three MOs as shown in Scheme 91. The bonding orbital is doubly occupied, thus leading to a bond order of 1.5 (multiple-bond character) for the two C-N bonds. More interestingly, the orbital patterns of the HOMO and the LUMO of **330A**, calculated at RB3LYP/6-31G(d) level, clearly possess the nonbonding and antibonding character around the central nitrogen atom. The molecular design proposed here could provide novel closed-shell *p*-conjugated compounds with unusual bond character. The diradical system **330A** gave only a very weak esr signal.

Scheme 91



A possibility in the reaction of Tröger base with chloranil is formation of different types of electron transfer complexes like outer-sphere and inner-sphere complexes (Scheme 92). The decrease of esr signal intensity could be explained by considering the closed shell structure **333**.

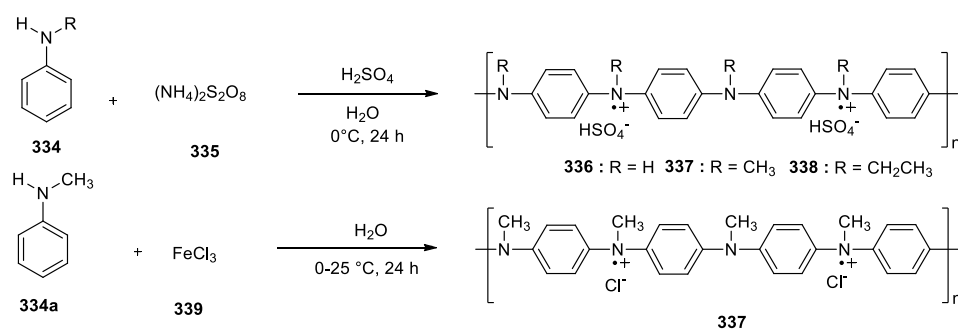
## Scheme 92



Unfortunately, such complexes could not be crystallized under the present reaction conditions. Although, the nature of the electron transfer complexes is not clearly understood, such complexes readily accessible as illustrated here. However, a difficulty is that the  $R_3N^{+\bullet}$  intermediate formed is still in the complexed form with the chloranil radical anion. Therefore, methods of preparation of such intermediates by other means like using metal ions like  $Cu^{2+}$  or  $Ce^{4+}$  or by anodic oxidation may be appropriate for further synthetic applications.<sup>130</sup> It may be of interest to note that the reaction of *N,N*-dialkylarylamine with metal salts ( $Ti^{4+}$  or  $Cu^{2+}$  or  $Ce^{4+}$ ) leads to the formation of benzidine derivatives *via* the formation of the corresponding radical cations.<sup>131</sup>

It is well known that oxidation of *N*-methylaniline **334** by anodic or oxidation by  $S_2O_8^{2-}$  or  $Fe^{3+}$  leads to polymerization (Scheme 93).<sup>132</sup>

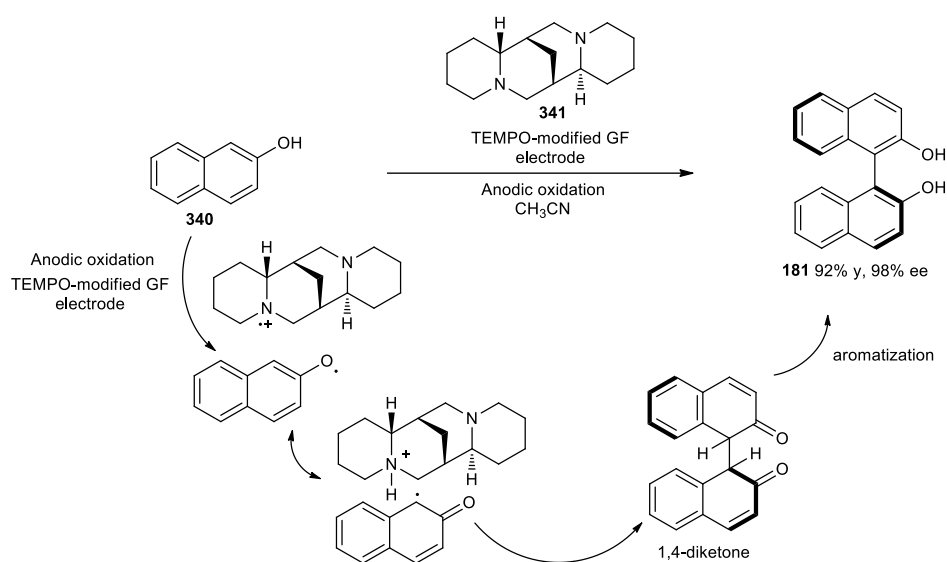
## Scheme 93



We have briefly studied the reactions of such systems. The results are discussed in Annexure-III. Similar oxidation of TB is expected to give the corresponding radical cation free of other organic species like chloranil radical anion.

It is of interest to note that the electrochemical oxidation of 2-naphthol on a TEMPO-modified graphite felt electrode in the presence of (-)-sparteine gave the bi-2-naphthol in 92% yield with 98% ee (Scheme 94).<sup>133</sup>

**Scheme 94**



Most probably, the reaction would involve the intermediacy of sparteine radical cation (Scheme 94). Such studies using chiral TB to investigate the reactivity of TB<sup>•+</sup> would give fruitful results.



## 2.9 Conclusions

---

A convenient resolution procedure was developed to access the enantiomers of tetramethyl Tröger base derivative in optically pure form using camphorsulfonic acid (CSA) as a resolving agent. The method was successfully employed for the resolution of dibromo-dimethyl substituted Tröger base derivatives to obtain enantiomerically pure samples with up to 95-99% ee. Whereas the *ortho*-methyl substituted Tröger base derivatives **64** and **65** gave 1:2 complexes with CSA, but *ortho*-bromo derivative **66** formed only a 1:1 complex. The (*S,S*)-**64** and (*S,S*)-**65** isomers are dextrorotatory, while the (*S,S*)-**66** isomer is levorotatory. The configurations at the stereogenic nitrogen centers of (+)-**64** and (+)-**65** were assigned as 5*S*,11*S* by single crystal analysis of the corresponding diastereomeric salts. The *ortho*-dibromo derivative **66** was readily functionalized to access new chiral amine systems containing chiral phenylethylamine moiety. The configuration of stereogenic nitrogen centers of (-)-**66** was determined as (*S,S*) by single crystal analysis of **200**.

A convenient method was also developed for the resolution of *ortho*-methoxy-substituted Tröger base derivative using dibenzoyl-L-tartaric acid as a resolving agent. The nitrogen centers were assigned as (*R,R*) for (+)-**204** from the X-ray diffraction analysis of the diastereomeric salt **206**.

The 5,11-substituted Tröger base derivatives were prepared by POCl<sub>3</sub> promoted one-pot reaction with amide. A method was also devised for the diastereoselective synthesis of Tröger base derivatives using (*S,S*)-*N,N*-bis( $\alpha$ -methylbenzyl)formamide as a carbonyl group partner. The configuration of newly formed nitrogen centers were assigned by crystal structure analysis of **216a** and **217a**. It was also observed that these chiral Tröger base derivatives undergo epimerization in solution as well as in solid state. The reaction of chiral

*ortho*-methyl derivative with DMF gave the corresponding 5,11-substituted product with retention of configuration. However, the chiral *para*-methyl derivative gave racemic mixture in the exchange reaction using DMF as amide partner.

The reaction of Tröger base with the benzyne intermediate formed using iodobenzene and *t*-BuOk as a base gave the bridge cleaved mono-N-arylated product in moderate to good yields.

Efforts were undertaken towards the hydroboration of prochiral olefins using chiral Tröger base borane complexes. It was found that the borane complexes of *para*-substituted derivatives hydroborate olefins to give alcohols with only up to 5% ee.

The reaction of Tröger base derivatives with chloranil gave the corresponding charge transfer complexes and paramagnetic intermediates. The 5,11-substituted derivative with alkyl amine group gave strong esr signals compared to parent compounds as in this case the electron donor is the alkyl amine moiety which is expected to be stronger base compared to bridgehead nitrogens that are aniline moieties.

### 3. Experimental Section

---

#### 3.1 General informations

Melting points were determined by superfit capillary point apparatus and reported melting points are uncorrected in this thesis. IR (KBr) and IR (neat) spectra were recorded on JASCO FT-IR spectrophotometer model-5300. The NMR spectra [ $^1\text{H}$  (400 MHz) and  $^{13}\text{C}$  (100 MHz)] were recorded on Bruker-Avance-400 spectrometers chloroform-d as solvent. Chemical shifts are expressed in  $\delta$  downfield with respect to the signal of internal standard tetramethylsilane ( $\delta = 0$  ppm). Coupling constants  $J$  are in Hz. Liquid chromatography (LC) and mass analysis (LC-MS) were performed using SHIMADZU-LCMS-2010A or HRMS by EI technique. HPLC analyses were performed on an SCL-10ATVP SHIMADZU instrument. Perkin-Elmer elemental analyzer-240C and Thermo finnigan analyzer Flash EA 1112 were used for the elemental analysis. Rudolph Analytical AUTOPOL-IV (readability  $\pm 0.001^\circ$ ) automatic polarimeter was used for checking optical rotations. The condition of the polarimeter was checked by measuring the optical rotation of a standard solution of (S)-(-)- $\alpha$ -methylbenzylamine  $[\alpha]_{\text{D}}^{25} = -29.6$  (c 0.74, EtOH) supplied by Aldrich.

Thin layer chromatography tests were carried out on pre-coated glass plates using silica gel-GF<sub>254</sub> containing 13% calcium sulfate as binder. The spots were visualized by UV light or exposure to iodine. Gravity column chromatography was used for the separation of compounds using silica gel (100-200 mesh) as stationary phase. All the glasswares were pre-dried at 100-120 °C in an air-oven for 4 h, assembled in hot condition and cooled under a



stream of dry nitrogen. Unless otherwise mentioned, all the operations and transfer of reagent were carried out using standard syringe-septum technique recommended for handling air sensitive reagents and organometallic compounds.

In all experiments, a round bottom flask of appropriate size with a side arm, a side septum, a magnetic stirring bar, a condenser and a connecting tube attached to a mercury bubbler was used. The outlet of the mercury bubbler was connected to the atmosphere by a long tube. All dry solvents and reagents used were distilled from appropriate drying agents. As a routine practice, all organic extracts were washed using saturated NaCl solution (brine) and dried over Na<sub>2</sub>SO<sub>4</sub> or K<sub>2</sub>CO<sub>3</sub> and concentrated on Heidolph-EL-rotary evaporator. All the yields reported are of isolated materials characterized by IR and NMR.

AlCl<sub>3</sub> and trifluoroacetic acid supplied by E-Merck (India) was used as received. 2,4-dimethylaniline, 2-bromo-4-methylaniline, 4-bromo-2-methylaniline, 4-bromo-2-methoxyaniline were purchased from commercial sources were used as received. Camphor sulfonic acid, dibenzoyl-L-tartaric acid (DBTA) and (S)- $\alpha$ -methylbenzylamine were purchased from Sigma Aldrich and used as received. Toluene and acetone purchased from E-Merck (India) was used as received for resolution experiments. 1.6 M *n*-BuLi purchased from commercial source was used as received. NaBH<sub>4</sub> was supplied by E-Merck (India) was used as received. Iodine was supplied by Spectrochem, India.

The (*S,S*)-*N,N*-bis( $\alpha$ -methylbenzyl)formamide was prepared following a reported procedure.<sup>134</sup> POCl<sub>3</sub>, DMF and DEF were supplied by commercial sources used as received. Dichloromethane was distilled using calcium hydride under nitrogen. The THF solvent

supplied by commercial sources, India were kept over sodium-benzophenone ketyl then freshly distilled before use. Toluene and diglyme were also kept over sodium-benzophenone ketyl, distilled and stored over sodium wire. Chiral 1,1-bi-2-naphthol was supplied by Gerchem Labs (P) Ltd. *t*-BuOK supplied by Hychem, India was used as received. DMF and DMSO were purchased from E-Merck, India and used as received in N-arylation reactions. CuBr was supplied by Sigma Aldrich.

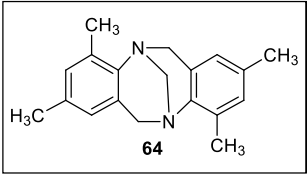
X-ray reflections were collected using Oxford CCD X-ray diffractometer (Yarnton, Oxford, UK) equipped with Mo-K $\alpha$  radiation ( $\lambda = 0.71073 \text{ \AA}$ ) and Cu- K $\alpha$  radiation ( $\lambda = 1.54184 \text{ \AA}$ ) sources. CrysAlisPro 171.33.55 software was for data reduction. Crystal structures were solved and refined using Olex2-1.0. Hydrogen atoms were experimentally located by the Fourier difference electron density method in all crystal structures. All O–H, and C–H were geometrically fixed by HFIX command in SHELX-TL programme of Bruker-AXS. Bruker SMART-APEX CCD diffractometer (Bruker-AXS, Germany, Karlsruhe) was used for the X-ray reflections. X-ray reflections were collected using Mo-K $\alpha$  X-radiation ( $\lambda = 0.71073 \text{ \AA}$ ) on the single crystal at 298K. Data reduction was performed using the Bruker SAINT software. Intensities for absorption were corrected by using SADABS and the Siemens detector absorption correction program (Bruker-AXS). All the crystal structures were solved and refined using SHELX-97 with anisotropic displacement for non-hydrogen atoms. Hydrogen atoms on oxygen experimentally located in difference electron density maps.

### 3.2 Synthesis of racemic Tröger base derivatives

#### 3.2.1 General procedure for the synthesis of tetramethylsubstituted Tröger base derivatives

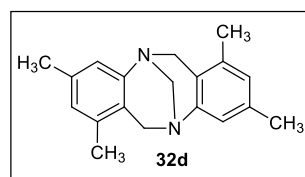
To a solution of substituted aniline (50 mmol) and paraformaldehyde (3.0 g, 100 mmol) in  $\text{CH}_2\text{Cl}_2$  (150 mL) was added  $\text{AlCl}_3$  (6.65 g, 50 mmol) under  $\text{N}_2$  atmosphere. The reaction mixture was allowed to stir for 12 h at 25 °C and the reaction was quenched with cold water. The reaction mixture was extracted using  $\text{CH}_2\text{Cl}_2$  and the combined organic extracts were successively washed with water, brine solution and dried over anhydrous  $\text{Na}_2\text{SO}_4$ . After removal of the solvent, the residue was subjected to chromatography on silica gel column using 2-5% ethyl acetate in hexane to elute the desired Tröger base derivatives.

#### 2,4,8,10-Tetramethyl-6H,12H-5,11-methanodibenzo[b,f][1,5]diazocine **64**

<b>Yield</b>	:	4.10 g (59%); White solid	
<b>mp</b>	:	110-112 °C (lit. <sup>135</sup> mp 114-115 °C)	
<b>IR (KBr)</b>	:	2947, 1430, 1215, 1031, 923 $\text{cm}^{-1}$	
<b><math>^1\text{H}</math> NMR</b>	:	(400 MHz, $\text{CDCl}_3$ ): $\delta$ 6.91 (s, 2H), 6.62 (s, 2H), 4.58 (d, $J = 16.0$ Hz, 2H), 4.36 (s, 2H), 3.98 (d, $J = 16.0$ Hz, 2H), 2.42 (s, 6H), 2.24 (s, 6H)	
<b><math>^{13}\text{C}</math> NMR</b>	:	(100 MHz, $\text{CDCl}_3$ ): $\delta$ 143.5, 133.1, 132.6, 129.8, 127.8, 124.8, 67.8, 55.1, 20.8, 17.0	

#### 1,3,7,9-Tetramethyl-6H,12H-5,11-methanodibenzo[b,f][1,5]diazocine **32d**

<b>Yield</b>	:	1.4 g (20%); White solid
<b>mp</b>	:	198-201 °C; (lit. <sup>36a</sup> mp 202-203 °C)
<b>IR (KBr)</b>	:	2914, 1710, 1439, 1263, 954 $\text{cm}^{-1}$



**<sup>1</sup>H NMR** : (400 MHz, CDCl<sub>3</sub>): δ 6.81 (s, 2H), 6.63 (s, 2H), 4.48 (d, *J* = 16.0 Hz, 2H), 4.22 (s, 2H), 3.99 (d, *J* = 16.0 Hz, 2H), 2.22 (s, 6H), 2.04 (s, 6H)

**<sup>13</sup>C NMR** : (100 MHz, CDCl<sub>3</sub>): δ 148.5, 136.4, 135.6, 126.6, 123.4, 66.2, 55.1, 20.9, 17.9

### 3.2.2 General procedure for the preparation of bromo-substituted and unsubstituted Tröger base derivatives

To a solution of substituted aniline (10 mmol) in trifluoroacetic acid (10 mL) was added paraformaldehyde (0.600 g, 20 mmol) under N<sub>2</sub> atmosphere at 0 °C. The reaction mixture was allowed to stir for 48 h at 25 °C and the reaction was quenched by aq. NaOH. The reaction mixture was extracted using CH<sub>2</sub>Cl<sub>2</sub> and the combined organic extracts were successively washed with water, brine solution and dried over anhydrous Na<sub>2</sub>SO<sub>4</sub>. After removal of the solvent, the residue was subjected to column chromatography on silica gel using ethyl acetate in hexane to elute the desired Tröger base derivatives.

#### 2,8-Dibromo-4,10-dimethyl-6H,12H-5,11-methanodibenzo[b,f][1,5]diazocine **65**

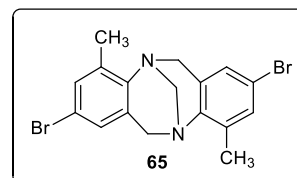
**Yield** : 2.0 g (98%); White solid

**mp** : 192-194 °C (lit.<sup>84</sup> mp 195.5-196.5 °C)

**IR (KBr)** : 2917, 1461, 1282, 923 cm<sup>-1</sup>

**<sup>1</sup>H NMR** : (400 MHz, CDCl<sub>3</sub>): δ 7.19 (s, 2H), 6.91 (s, 2H), 4.52 (d, *J* = 16.0 Hz, 2H), 4.32 (s, 2H), 3.90 (d, *J* = 16.0 Hz, 2H), 2.37 (s, 6H)

**<sup>13</sup>C NMR** : (100 MHz, CDCl<sub>3</sub>): δ 144.8, 135.3, 131.8, 129.9, 127.1, 116.8, 67.2, 54.6, 16.8



**4,10-Dibromo-2,8-dimethyl-6H,12H-5,11-methanodibenzo[b,f][1,5]diazocine 66**

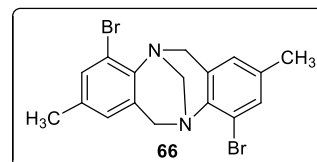
**Yield** : 1.98 g (97%); White solid

**mp** : 190-192 °C (lit.<sup>36a</sup> mp 188-189 °C)

**IR (KBr)** : 2946, 1427, 1230, 923 cm<sup>-1</sup>

**<sup>1</sup>H NMR** : (400 MHz, CDCl<sub>3</sub>): δ 7.27 (s, 2H), 6.74 (s, 2H), 4.54 (d, *J* = 16.0 Hz, 2H), 4.35 (s, 2H), 4.28 (d, *J* = 16.0 Hz, 2H), 2.21 (s, 6H)

**<sup>13</sup>C NMR** : (100 MHz, CDCl<sub>3</sub>): δ 142.0, 135.4, 131.9, 130.3, 126.7, 119.5, 67.8, 55.4, 20.5

**2,8-Dibromo-4,10-dimethoxy-6H,12H-5,11-methanodibenzo[b,f][1,5]diazocine 203**

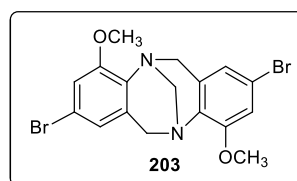
**Yield** : 1.4 g (64%); Yellow solid

**mp** : 229-231 °C (lit.<sup>85</sup> mp 233-234 °C)

**IR (KBr)** : 2967, 1567, 1468, 1248, 822 cm<sup>-1</sup>

**<sup>1</sup>H NMR** : (400 MHz, CDCl<sub>3</sub>): δ 6.82 (s, 2H), 6.70 (s, 2H), 4.47 (d, *J* = 20.0 Hz, 2H), 4.26 (s, 2H), 4.16 (d, *J* = 20.0 Hz, 2H), 3.89 (s, 6H)

**<sup>13</sup>C NMR** : (100 MHz, CDCl<sub>3</sub>): δ 153.5, 134.3, 130.8, 121.7, 117.2, 112.4, 67.6, 55.9, 53.8

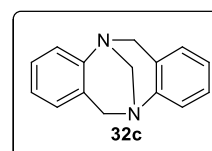
**6H,12H-5,11-methanodibenzo[b,f][1,5]diazocine 32c**

**Yield** : 0.832 g (75%); White solid

**mp** : 128-130 °C (lit.<sup>136</sup> mp 127-128 °C)

**IR (KBr)** : 2946, 1427, 1230, 923 cm<sup>-1</sup>

**<sup>1</sup>H NMR** : (400 MHz, CDCl<sub>3</sub>): δ 6.82-6.70 (m, 8H), 4.46 (d, *J* = 16.0 Hz, 2H), 4.24 (s, 2H), 4.14 (d, *J* = 16.0 Hz, 2H)



**<sup>13</sup>C NMR** : (100 MHz, CDCl<sub>3</sub>): δ 144.5, 134.3, 130.8, 121.7, 117.2, 112.4, 67.6, 55.9

### 3.2.3 Typical procedure for the synthesis of *ortho*-methoxy Tröger base derivatives

To a solution of Tröger base derivative (1 mmol, 0.440 g) in toluene:THF (30:1) was added 1.6 M *n*-BuLi (2.1 mmol, 1.4 mL) at -78 °C under N<sub>2</sub> atmosphere. The resulting mixture was allowed to stir for 10 min. followed by iodomethane was added at -78 °C. This mixture was allowed to stir for 1 h at -78 °C and quenched by ice cold water. The aqueous layer was extracted with ethyl acetate (2 x 15 mL) and the combined organic extracts were successively washed with water, brine and dried over anhydrous Na<sub>2</sub>SO<sub>4</sub>. After removal of the solvent, the residue was subjected to column chromatography on silica gel using ethyl acetate in hexane to elute the desired Tröger base derivative.

#### 2,8-Dimethyl-4,10-dimethoxy-6H,12H-5,11-methanodibenzo[b,f][1,5]diazocine **204**

**Yield** : 0.165 g (53%); Yellow solid

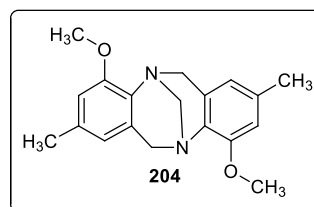
**mp** : 165-167 °C

**IR (KBr)** : 2936, 1578, 1482, 1315, 922 cm<sup>-1</sup>

**<sup>1</sup>H NMR** : (400 MHz, CDCl<sub>3</sub>): δ 6.52 (s, 2H), 6.37 (s, 2H), 4.49 (d, *J* = 16.0 Hz, 2H), 4.31 (s, 2H), 4.17 (d, *J* = 16.0 Hz, 2H), 3.90 (s, 6H), 2.23 (s, 6H)

**<sup>13</sup>C NMR** : (100 MHz, CDCl<sub>3</sub>): δ 152.6, 133.8, 132.9, 129.0, 119.1, 109.5, 68.0, 55.4, 54.3, 21.4

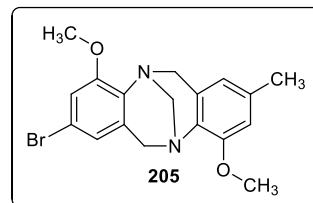
**HRMS (ESI)** *m/z* [M+H]<sup>+</sup> calcd for C<sub>19</sub>H<sub>22</sub>N<sub>2</sub>O<sub>2</sub>: 311.1760; found 311.1759



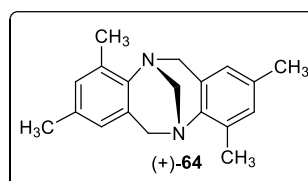
**2-Bromo-4,10-dimethoxy-8-methyl 6H,12H-5,11-methanodibenzo[b,f][1,5] diazocine 205****Yield** : 0.54 g (14%); Yellow solid**mp** : 137-140 °C**IR (KBr)** : 2921, 1570, 1473, 1134, 929 cm<sup>-1</sup>

**<sup>1</sup>H NMR** : (400 MHz, CDCl<sub>3</sub>): δ 6.81 (s, 1H), 6.71 (s, 1H), 6.53 (s, 2H), 6.37 (s, 2H), 4.48 (dd, *J* = 4.0 Hz, 2H), 4.28 (d, *J* = 4.0 Hz, 2H), 4.16 (m, 2H), 3.90 (s, 6H), 2.24 (s, 6H)

**<sup>13</sup>C NMR** : (100 MHz, CDCl<sub>3</sub>): δ 153.6, 152.6, 134.8, 134.2, 132.3, 131.2, 128.6, 121.8, 119.0, 116.9, 112.2, 109.7, 67.8, 55.8, 55.5, 54.2, 54.0, 21.4

**HRMS (ESI)** : *m/z* [M+H]<sup>+</sup> calcd for C<sub>18</sub>H<sub>19</sub>BrN<sub>2</sub>O<sub>2</sub>: 375.0709; found 375.0705**3.3 Resolution of tetrasubstituted Tröger base derivatives****3.3.1 Resolution of (±)-2,4,8,10-tetra-methyl-6H,12H-5,11-methanodibenzo[b,f][1,5] diazocine 64**

The (1*S*)-(+)-10-camphorsulfonic acid (2.32 g, 10.0 mmol) and *rac*-Tröger base **64** (1.39 g, 5.0 mmol) were taken in toluene (100 mL), and the contents were stirred at 25 °C for 6 h and filtered. The precipitate was suspended in a mixture of CH<sub>2</sub>Cl<sub>2</sub> and aq. Na<sub>2</sub>CO<sub>3</sub> (2 M) and stirred until dissolution occurred. The organic extracts were washed with brine, dried over anhydrous Na<sub>2</sub>SO<sub>4</sub>, and evaporated to obtain the (*S,S*)-**64** enantiomer in 99% ee. The filtrate was treated as outlined above with aq. Na<sub>2</sub>CO<sub>3</sub> to obtain the (*R,R*)-**64** enantiomer (80% ee, 49% yield).

**After decomposition****From precipitate**

**Yield** 0.630 g (45%)

$[\alpha]_{\text{D}}^{25}$  +28.6 (c 0.22, CHCl<sub>3</sub>)

#### From filtrate

**Yield** 0.684 g (49%)

$[\alpha]_{\text{D}}^{25}$  -22.6 (c 0.50, CHCl<sub>3</sub>)

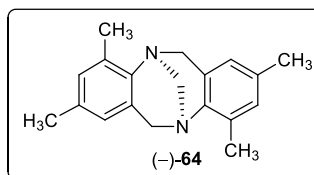
The samples were also analyzed by HPLC on Chiralcel-OJ-H column using hexane:i-PrOH/90:10; flow rate 0.5 mL/min.

### 3.3.2 Enrichment of enantiomeric purity of nonracemic (-)-**64** using (-)-camphorsulfonic acid

The nonracemic Troger base (*R,R*)-**64** (1.39 g, 5.0 mmol) and (1*R*)-(-)-10-camphorsulfonic acid (2.32 g, 10 mmol) were taken in toluene (40 mL), and the contents were stirred at 25 °C for 6 h and filtered. The precipitate was suspended in a mixture of CH<sub>2</sub>Cl<sub>2</sub> and aq. Na<sub>2</sub>CO<sub>3</sub> (2 M) and stirred until dissolution occurred. The organic extracts were washed with brine, dried over Na<sub>2</sub>SO<sub>4</sub>, and evaporated to dryness to obtain the (*R,R*)-**64** isomer (99% ee, 77% yield). The filtrate was concentrated, and the residue was treated as outlined above with aq. Na<sub>2</sub>CO<sub>3</sub> to obtain **64** enriched in the (*R,R*)-enantiomer (67% ee, 17% yield).

#### After decomposition

#### From precipitate





**Yield** 1.072 g (77%)

$[\alpha]_{\text{D}}^{25}$   $-28.8$  (c 0.50,  $\text{CHCl}_3$ )

**From filtrate**

**Yield** 0.237 g (17%)

$[\alpha]_{\text{D}}^{25}$   $-18.6$  (c 0.32,  $\text{CHCl}_3$ )

The samples were also analyzed by HPLC on Chiralcel-OJ-H column using hexane:i-PrOH/90:10; flow rate 0.5 mL/min.

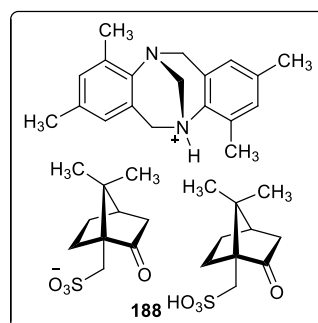
**188[(+)-CSA•(+)-64]**

**mp** : 128-131 °C (White solid)

**IR (KBr)** : 2958, 1738, 1482, 1415, 1155,  
1037, 857, 764  $\text{cm}^{-1}$

**$^1\text{H}$  NMR** : (400 MHz,  $\text{CDCl}_3$ ):  $\delta$  7.18 (brs, 3H), 6.98 (s, 2H), 6.69 (s, 2H), 4.99 (m, 4H), 4.12 (d,  $J = 16.4$  Hz, 2H), 3.41 (d,  $J = 14.8$  Hz, 2H), 2.97 (d,  $J = 14.8$  Hz, 2H), 2.48 (s, 6H), 2.44-2.35 (m, 3H), 2.22 (s, 6H), 2.09 (t,  $J = 4.4$  Hz, 2H), 2.03-2.00 (m, 2H), 1.95 (s, 1H), 1.91 (s, 1H), 1.85-1.78 (m, 2H), 1.43-1.37 (m, 2H), 1.06 (s, 6H), 0.87 (s, 6H)

**$^{13}\text{C}$  NMR** : (100 MHz,  $\text{CDCl}_3$ ):  $\delta$  217.8, 137.6, 135.3, 132.5, 131.8, 125.4, 124.1, 69.3, 58.5, 54.5, 48.3, 47.9, 42.8, 42.7, 26.9, 25.2, 20.8, 19.8, 19.7, 16.9



**HRMS (ESI) :**  $m/z$   $[M+Na]^+$  calcd for  $C_{39}H_{54}N_2S_4O_8$ : 765.3219; found 765.3221

### 3.3.3 Resolution of ( $\pm$ )-2,8-dibromo-4,10-dimethyl-6H,12H-5,11-methanodibenzo[b,f][1,5] diazocine **65**

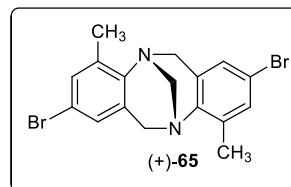
The (1*S*)-(+)-10-camphorsulfonic acid (2.32 g, 10.0 mmol) and *rac*-dibromo-Tröger base **65** (2.04 g, 5.0 mmol) were taken in toluene (100 mL), and the contents were stirred at 25 °C for 6 h and filtered. The precipitate was suspended in a mixture of  $CH_2Cl_2$  and aq.  $Na_2CO_3$  (2 M) and stirred until dissolution occurred. The organic extracts were washed with brine, dried over anhydrous  $Na_2SO_4$ , and evaporated to obtain the (*S,S*) enantiomer in 95% ee. The filtrate was treated as outlined above with aq.  $Na_2CO_3$  to obtain (–)-**65** enriched in the (*R,R*)-enantiomer (96% ee, 49% yield).

#### After decomposition

##### From precipitate

**Yield** 0.980 g (48%)

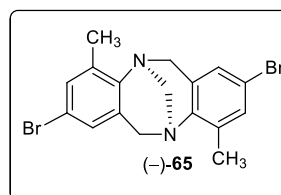
$[\alpha]_D^{25}$  +160.6 (c 0.60,  $CHCl_3$ )



##### From filtrate

**Yield** 1.007 g (49%)

$[\alpha]_D^{25}$  –159.0 (c 0.40,  $CHCl_3$ )



The samples were also analyzed by HPLC on Chiralcel-OJ-H column using hexane:i-PrOH/90:10; flow rate 0.5 mL/min.

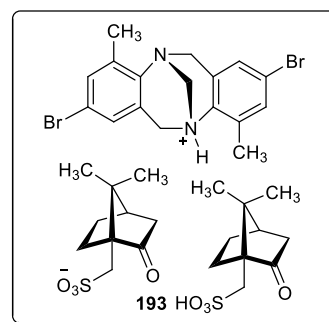
**193[(+)-CSA•(+)-65]****mp** : 148-150 °C (White solid)**IR (KBr)** : 2957, 1736, 1471, 1414, 1374, 1136, 857, 748 cm<sup>-1</sup>

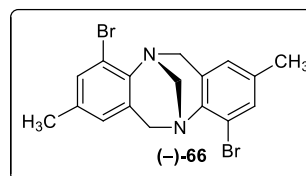
**<sup>1</sup>H NMR** : (400 MHz, CDCl<sub>3</sub>): δ 8.95 (brs, 3H), 7.33 (s, 1H), 7.09 (s, 1H), 5.09-5.05 (m, 4H), 4.14 (d, *J* = 20 Hz, 2H), 3.38 (d, *J* = 16 Hz, 2H), 2.95 (d, *J* = 16 Hz, 2H), 2.42-2.33 (m, 4H), 2.09-2.07 (m, 2H), 2.04-1.97 (m, 2H), 1.93 (s, 1H), 1.88 (s, 1H), 1.79-1.72 (m, 2H), 1.43-1.36 (m, 2H), 1.04 (s, 6H), 0.85 (s, 6H)

**<sup>13</sup>C NMR** : (100 MHz, CDCl<sub>3</sub>): δ 217.9, 136.7, 135.3, 133.9, 127.8, 126.3, 121.3, 68.9, 58.4, 54.0, 48.3, 48.1, 42.8, 42.6, 26.8, 25.3, 19.7, 19.6, 16.8

**HRMS (ESI)** : *m/z* [M+H]<sup>+</sup> calcd for C<sub>37</sub>H<sub>48</sub>Br<sub>2</sub>N<sub>2</sub>O<sub>8</sub>S<sub>2</sub>: 871.1298; found 871.1233**3.3.4 Resolution of (±)-4,10-dibromo-2,8-dimethyl-6H,12H-5,11-methanodibenzo[b,f][1,5] diazocine 66**

The (1*S*)-(+)-10-camphorsulfonic acid (1.16 g, 5.0 mmol) and *rac*-dibromo-Tröger base **66** (2.04 g, 5.0 mmol) were taken in toluene (15 mL), and the contents were stirred at 25 °C for 12 h and filtered. The precipitate was suspended in a mixture of CH<sub>2</sub>Cl<sub>2</sub> and aq. Na<sub>2</sub>CO<sub>3</sub> (2 M) and stirred until dissolution occurred. The organic extracts were washed with brine, dried over anhydrous Na<sub>2</sub>SO<sub>4</sub>, and evaporated to obtain the (*S,S*)-(-)-**66** enantiomer in 99% ee with 27% yield. The filtrate was treated as outlined above with aq. Na<sub>2</sub>CO<sub>3</sub> to obtain the (*R,R*)-(+)-**66** in 41% ee with 69% yield.



**After decomposition****From precipitate****Yield** 0.560 g (27%) $[\alpha]_{\text{D}}^{25}$  -180.6 (c 0.32, CHCl<sub>3</sub>)**From filtrate****Yield** 1.42 g (69%) $[\alpha]_{\text{D}}^{25}$  +72.0 (c 0.35, CHCl<sub>3</sub>)

The samples were also analyzed by HPLC on Chiralcel-OJ-H column using hexane:i-PrOH/90:10; flow rate 0.5 mL/min.

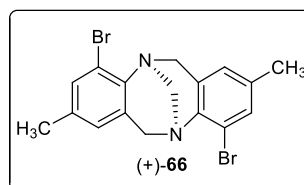
### 3.3.5 Enrichment of enantiomeric purity of nonracemic (+)-**66** using (-)-camphorsulfonic acid

The nonracemic Troger base (*R,R*)-**66** (2.04 g, 5.0 mmol) and (1*R*)-(-)-10-Camphorsulfonic acid (1.16 g, 5 mmol) were taken in toluene (15 mL), and the contents were stirred at 25 °C for 12 h and filtered. The precipitate was suspended in a mixture of CH<sub>2</sub>Cl<sub>2</sub> and aq. Na<sub>2</sub>CO<sub>3</sub> (2 M) and stirred until dissolution occurred. The organic extracts were washed with brine, dried over Na<sub>2</sub>SO<sub>4</sub>, and evaporated to dryness to obtain the (*R,R*)-**66** isomer (96% ee, 25% yield).

**After decomposition****From precipitate**

**Yield** 0.560 g (25%)

$[\alpha]_{\text{D}}^{25}$  +178.0 (c 0.77, CHCl<sub>3</sub>)



**From filtrate**

**Yield** 1.43 g (70%)

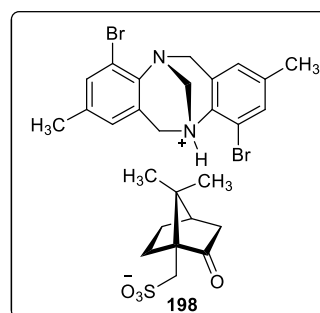
$[\alpha]_{\text{D}}^{25}$  +18.0 (c 0.35, CHCl<sub>3</sub>)

The samples were also analyzed by HPLC on Chiralcel-OJ-H column using hexane:i-PrOH/90:10; flow rate 0.5 mL/min.

**198[(+)-CSA•(-)-66]**

**mp** : 94-96 °C (White solid)

**IR (KBr)** : 2964, 1753, 1473, 1156, 1035, 854,  
789 cm<sup>-1</sup>



**<sup>1</sup>H NMR** : (400 MHz, CDCl<sub>3</sub>): δ 9.02 (brs, 2H), 7.36 (s, 2H), 6.85 (s, 2H), 5.01-4.95 (m, 4H), 4.42 (d, *J* = 16 Hz, 2H), 3.36 (d, *J* = 16 Hz, 1H), 2.88 (d, *J* = 16 Hz, 1H), 2.64-2.58 (m, 1H), 2.24 (s, 6H), 2.01-1.94 (m, 2H), 1.84 (d, *J* = 16 Hz, 1H), 1.75-1.68 (m, 1H), 1.07 (s, 3H), 0.82 (s, 3H)

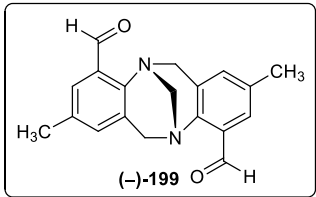
**<sup>13</sup>C NMR** : (100 MHz, CDCl<sub>3</sub>): δ 216.9, 139.3, 135.3, 133.6, 127.3, 127.1, 118.6, 69.6, 58.5, 54.7, 47.9, 47.5, 42.9, 42.7, 27.0, 24.8, 20.7, 19.9, 19.8

**HRMS (ESI)** : *m/z* [M+Na]<sup>+</sup> calcd for C<sub>27</sub>H<sub>32</sub>N<sub>2</sub>Br<sub>2</sub>O<sub>4</sub>S: 661.0347; found 661.0347

### 3.3.6 Typical procedure for the preparation of 2,8-dimethyl-6H,12H-5,11-methano-dibenzo[b,f][1,5]diazocine-4,10-dicarbaldehyde

To a solution of Tröger base derivative (–)-**66** (0.408 g, 1 mmol) in toluene:THF (30:1) was added 1.6 M *n*-BuLi (1.4 mL, 2.1 mmol) at 0 °C under N<sub>2</sub> atmosphere. The resulting mixture was allowed to stir for 10 min. followed by dimethyl formamide was added at 0 °C. This mixture was allowed to stir for 1 h at 0 °C and quenched by ice cold water. The aqueous layer was extracted with ethyl acetate (2 x 15 mL) and the combined organic extracts were successively washed with water, brine and dried over anhydrous Na<sub>2</sub>SO<sub>4</sub>. After removal of the solvent, the residue was subjected to chromatography on silica gel column using ethyl acetate in hexane to elute the desired Tröger base derivative.

#### 2,8-Dimethyl-6H,12H-5,11-methano-dibenzo[b,f][1,5]diazocine-4,10-dicarbaldehyde **199**

<b>Yield</b>	:	0.200 g (65%); Yellow solid	
<b>mp</b>	:	214-216 °C (lit. <sup>25</sup> mp 219-221 °C)	
<b>IR (KBr)</b>	:	2917, 1677, 1461, 1282, 923 cm <sup>-1</sup>	
<b><sup>1</sup>H NMR</b>	:	(400 MHz, CDCl <sub>3</sub> ): δ 10.51 (s, 2H), 7.52 (s, 2H), 6.95 (s, 2H), 4.84 (d, <i>J</i> = 16.0 Hz, 2H), 4.40 (s, 2H), 4.08 (d, <i>J</i> = 16.0 Hz, 2H), 2.26 (s, 6H)	
<b><sup>13</sup>C NMR</b>	:	(100 MHz, CDCl <sub>3</sub> ): δ 191.1, 148.0, 134.0, 133.5, 129.5, 129.0, 128.3, 66.6, 59.4, 20.6	
<b>[α]<sub>D</sub><sup>25</sup></b>	:	–923.7.0 (c 0.27, CHCl <sub>3</sub> ) {lit. <sup>25</sup> [α] <sub>D</sub> <sup>25</sup> = –874.6 (0.39, CHCl <sub>3</sub> )}	
<b>ee</b>	:	99% (Estimated by HPLC analysis on chiralcel OJ-H column, EtOH, flow rate 0.5 mL/min.	

### 3.3.7 General procedure for the preparation of 2,8-dimethyl-6H,12H-5,11-methano-dibenzo[b,f][1,5]diazocine-4,10-bis(methylene)bis(1-phenylethanamine)

To a solution of Tröger base derivative **199** (0.306 g, 1 mmol) in ethanol (15 mL) was added silica gel (0.5 g) and (*S*)- $\alpha$ -methylbenzylamine (0.242 g, 0.25 mL, 2 mmol). The resulting content was subjected to sonication at 65 °C for 0.5 h, followed by the mixture was filtered. To this filtrate NaBH<sub>4</sub> was added at 0 °C and allowed to stir for 3 h at 25 °C. After removal of the solvent, the residue was quenched by water and extracted using ethyl acetate. The ethyl acetate was removed by rotary evaporator and subjected to chromatography on silica gel using ethyl acetate in hexane to elute the desired Tröger base derivative.

#### 2,8-Dimethyl-6H,12H-5,11-methano-dibenzo[b,f][1,5]diazocine-4,10-bis(methylene)

##### bis(1-phenylethanamine) **200**

**Yield** : 0.470 g (91%); White solid

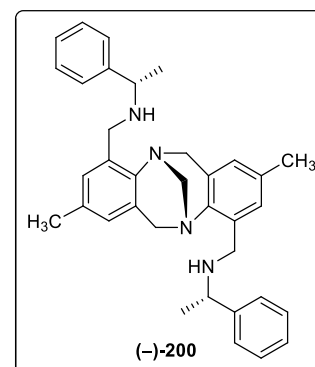
**mp** : 144-146 °C

**IR (KBr)** : 3304, 3030, 2964, 1468, 1221, 816 cm<sup>-1</sup>

**[ $\alpha$ ]<sub>D</sub><sup>25</sup>** : -139.2 (c 0.26, CHCl<sub>3</sub>)

**<sup>1</sup>H NMR** : (400 MHz, CDCl<sub>3</sub>):  $\delta$  7.44-7.39 (m, 8H), 7.31-7.29 (m, 2H), 6.92 (s, 2H), 6.60 (s, 2H), 4.44 (d, *J* = 16.0 Hz, 2H), 4.27 (s, 2H), 4.04 (d, *J* = 16.0 Hz, 2H), 3.97 (d, *J* = 12.0 Hz, 2H), 3.84 (q, *J* = 4.0 Hz, 2H), 3.57 (d, *J* = 12.0 Hz, 2H), 2.31(bris, 2H), 2.23 (s, 6H), 1.44 (d, *J* = 4.0 Hz, 6H)

**<sup>13</sup>C NMR** : (100 MHz, CDCl<sub>3</sub>):  $\delta$  145.9, 143.4, 134.7, 133.4, 129.0, 128.5, 128.1, 126.9, 126.8, 126.1, 67.2, 57.7, 55.9, 47.9, 24.5, 20.9



**HRMS (ESI) :**  $m/z$   $[M+H]^+$  calcd for  $C_{35}H_{40}N_4$ : 517.3332; found 517.3336

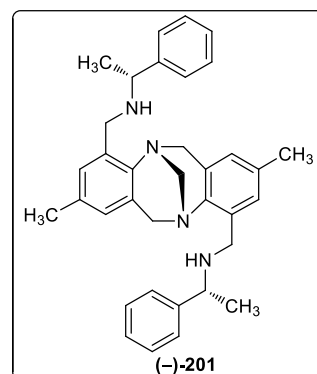
**2,8-Dimethyl-6H,12H-5,11-methano-dibenzo[b,f][1,5]diazocine-4,10-bis(methylene)bis(1-phenylethylamine) **201****

**Yield :** 0.450 g (87%)

**IR (Neat) :** 3304, 3030, 2964, 1468, 1221, 816  $cm^{-1}$

**$[\alpha]_D^{25}$  :**  $-49.7$  (c 0.34,  $CHCl_3$ )

**$^1H$  NMR :** (400 MHz,  $CDCl_3$ ):  $\delta$  7.46-7.44 (m, 4H),



7.41-7.37 (m, 4H) 7.31-7.26 (m, 2H), 7.03 (s, 2H), 6.58 (s, 2H), 4.37 (d,  $J = 16.0$  Hz, 2H), 4.17 (s, 2 H), 3.99 (s, 2H), 3.95-3.88 (m, 4H), 3.55 (d,  $J = 16.0$  Hz, 2H), 2.22 (s, 6H), 1.97 (brs, 2H), 1.44 (d,  $J = 4.0$  Hz, 6H)

**$^{13}C$  NMR :** (100 MHz,  $CDCl_3$ ):  $\delta$  145.9, 143.3, 134.8, 133.4, 128.7, 128.5, 127.9, 127.0, 126.8, 126.1, 67.3, 58.6, 55.9, 47.4, 24.6, 21.0

**HRMS (ESI) :**  $m/z$   $[M+H]^+$  calcd for  $C_{35}H_{40}N_4$ : 517.3332; found 517.3329

**3.3.8 Resolution of ( $\pm$ )-2,8-dimethyl-4,10-dimethoxy-6H,12H-5,11-methanodibenzo[b,f][1,5]diazocine **204****

The (–)-dibenzoyl-L-tartaric acid (1.43 g, 4.0 mmol) and *rac*-Tröger base **204** (0.620 g, 2.0 mmol) were taken in acetone (25 mL), and the contents were stirred at 25 °C for 12 h and filtered. The precipitate was suspended in a mixture of  $CH_2Cl_2$  and aq.  $Na_2CO_3$  (2 M) and stirred until dissolution occurred. The organic extracts were washed with brine, dried over anhydrous  $Na_2SO_4$ , and evaporated to obtain the (*R,R*)-(+)-**204** enantiomer in 99% ee and



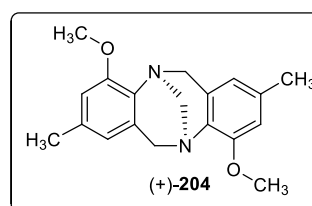
32% yield.  $[\alpha]_{\text{D}}^{25} = +98$  (c 0.25,  $\text{CHCl}_3$ ). The filtrate was treated as outlined above to obtain the (*S,S*)-(-)-**204** in 52% ee and 69% yield.

### After decomposition

#### From precipitate

**Yield** 0.200 g (32%)

$[\alpha]_{\text{D}}^{25} +98.0$  (c 0.25,  $\text{CHCl}_3$ )



#### From filtrate

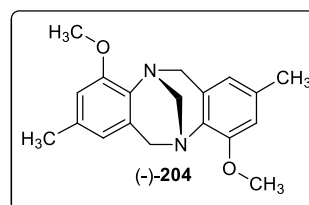
**Yield** 0.396 g (64%)

$[\alpha]_{\text{D}}^{25} -56.2$  (c 0.62,  $\text{CHCl}_3$ )

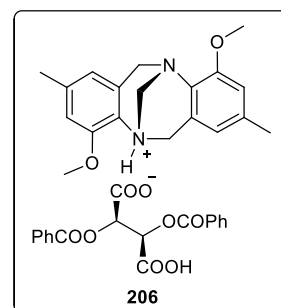
The samples were also analyzed by HPLC on Chiralcel-OJ-H column using EtOH; flow rate 0.5 mL/min.

### 3.3.9 Enrichment of enantiomeric purity of nonracemic (-)-**204** using (+)-DBTA.

The nonracemic Troger base (*S,S*)-**204** (0.620 g, 2.0 mmol) and (+)-DBTA (1.43 g, 4.0 mmol) were taken in acetone (25 mL), and the contents were stirred at 25 °C for 12 h and filtered. The precipitate was suspended in a mixture of  $\text{CH}_2\text{Cl}_2$  and aq.  $\text{Na}_2\text{CO}_3$  (2 M) and stirred until dissolution occurred. The organic extracts were washed with brine, dried over  $\text{Na}_2\text{SO}_4$ , and evaporated to dryness to obtain the (*S,S*)-(-)-**204** isomer (99% ee, 34% yield)

**After decomposition****From precipitate****Yield** 0.210 g (34%) $[\alpha]_{\text{D}}^{25}$  -102.3 (c 0.78, CHCl<sub>3</sub>)**From filtrate****Yield** 0.385 g (62%) $[\alpha]_{\text{D}}^{25}$  +19.0 (c 0.38, CHCl<sub>3</sub>)

The samples were also analyzed by HPLC on Chiralcel-OJ-H column using EtOH; flow rate 0.5 mL/min.

**206[(-)-DBTA•(+)-204]****mp** : 157-159 °C (White solid)**IR (KBr)** : 1721, 1491, 1265, 1109, 1070, 834 cm<sup>-1</sup>

**<sup>1</sup>H NMR** : (400 MHz, CDCl<sub>3</sub>): δ 8.04 (d, *J* = 8.0 Hz, 4H), 7.51-7.33 (m, 8H), 6.52 (s, 2H), 6.29 (s, 2H), 5.93 (s, 2H), 4.58 (d, *J* = 16 Hz, 2H), 4.10 (d, *J* = 16 Hz, 2H), 3.82 (s, 6H), 2.20 (s, 6H)

**<sup>13</sup>C NMR** : (100 MHz, CDCl<sub>3</sub>): δ 169.4, 165.4, 152.4, 136.6, 133.3, 130.1, 129.2, 128.3, 128.2, 127.2, 119.1, 110.6, 71.5, 67.6, 55.7, 53.5, 21.4

**HRMS (ESI) :**  $m/z$   $[M+H]^+$  calcd for  $C_{37}H_{36}N_2O_{10}$ : 669.2449; found 669.2449

### 3.4 Synthesis of 5,11-substituted Tröger base derivatives

#### 3.4.1 Typical procedure for diastereoselective synthesis of Tröger base derivative

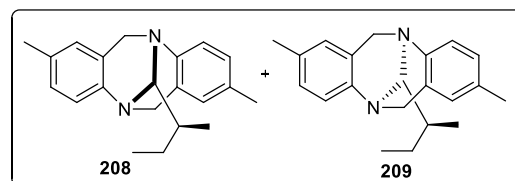
To a solution of *rac*-Tröger base **32a** (1.25 g, 5 mmol) and (*S*)-2-methyl butanal (0.439 g, 5 mmol) in 1,2-dichloroethane (15 mL) was added  $TiCl_4$  (1.9 g, 1.1 mL, 10 mmol) at 25 °C under  $N_2$  atmosphere. The reaction mixture was allowed to stir for 14 h at 83 °C. It was then cooled to 0 °C and quenched with 10% aq.  $K_2CO_3$  solution. The aqueous layer was extracted with  $CH_2Cl_2$  (2 x 15 mL) and the combined organic extracts were successively washed with water, brine and dried over anhydrous  $Na_2SO_4$ . After removal of the solvent, the residue was subjected to chromatography on silica gel column using 5% ethyl acetate in hexane to elute the desired Tröger base derivative.

#### 2,8-dimethyl-13-(2-butyl)-6H,12H-5,11-methanodibenzo[b,f][1,5]diazocine

The diastereomeric ratio was calculated on the basis of  $^1H$  NMR analysis of  $-CH_3$  proton of (*S*)-2-methyl-1-butyl moiety [For major 1.08 (d,  $J = 6.4$  Hz, 3H), and for minor 1.17 (d,  $J = 6.4$  Hz, 2H)]

**Yield** : 0.120 g (40%)

**IR (Neat)** : 2992, 2858, 1486, 838  $cm^{-1}$



**$^1H$  NMR** : (400 MHz,  $CDCl_3$ ):  $\delta$  7.08-6.99 (m, 7.2H), 6.76 (s, 1.5H), 6.73 (s, 2H), 4.68 (d,  $J = 4.0$  Hz, 0.7H), 4.64 (d,  $J = 4.4$  Hz, 1H), 4.52 (d,  $J = 6.4$  Hz, 0.7H), 4.48 (d,  $J = 6.4$  Hz, 1H), 4.23 (d,  $J = 3.6$  Hz, 1H), 4.19 (d,  $J = 3.6$  Hz, 0.8 H), 4.06 (s, 1H), 4.02 (s, 0.8H), 3.67 (m, 1.8H), 2.27 (s,

11H), 2.04–1.89(m, 1H), 1.89-1.83 (m, 0.7H), 1.68-1.62 (m, 1.7H),  
1.34-1.27 (m, 2H), 1.17 (d,  $J = 6.4$  Hz, 2H), 1.08 (d,  $J = 6.4$  Hz, 3H),  
1.00 (t,  $J = 7.2$  Hz, 3H), 0.92 (t,  $J = 7.2$  Hz, 2H)

**$^{13}\text{C}$  NMR** : (100 MHz,  $\text{CDCl}_3$ ):  $\delta$  148.5, 148.4, 143.6, 132.8, 132.6, 132.5, 128.3,  
128.2, 128.0, 127.9, 127.7, 127.1, 126.7, 125.8, 125.7, 125.0, 77.7,  
77.6, 60.9, 52.4, 52.1, 34.2, 33.7, 25.6, 25.2, 20.8, 20.7, 15.6, 15.2,  
11.1, 10.6

**LCMS** : (EI,  $m/z$ ): 303.25 ( $M+1$ )

**Analysis** : Anal. Calcd for  $\text{C}_{21}\text{H}_{26}\text{N}_2$ : C 82.31, H 8.55, N 9.14;

found: C 82.76, H 7.91, N 9.32

### 3.4.2 General procedure for the preparation of 5,11-substituted derivatives using $\text{POCl}_3$

To a solution of Tröger base derivative (2 mmol) and DMF (2.1 mmol, 0.153 g, 0.16 mL) in  $\text{CH}_2\text{Cl}_2$  (15 mL) was added  $\text{POCl}_3$  (0.535 g, 0.32 mL, 3.5 mmol) at 25 °C under  $\text{N}_2$  atmosphere. The reaction mixture was allowed to stir for 1 h at 25 °C. It was then cooled to 0 °C and quenched with 10% aq. NaOH solution. The aqueous layer was extracted with  $\text{CH}_2\text{Cl}_2$  (2 x 15 mL) and the combined organic extracts were successively washed with water, brine and dried over anhydrous  $\text{Na}_2\text{SO}_4$ . After removal of the solvent, the residue was subjected to chromatography on silica gel column using 5-10% ethyl acetate in hexane to elute the desired Tröger base derivative **210**.

**2,8-Dimethyl-13-(*N,N*-dimethylamino)-6H,12H-5,11-methanodibenzo[*b,f*][1,5]diazocine 210a**

**Yield** : 0.546 g (93%); White solid

**mp** : 102-104 °C

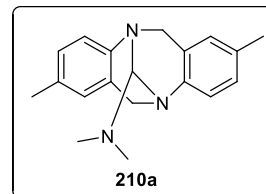
**IR (KBr)** : 2991, 1494, 1421, 1205, 835 cm<sup>-1</sup>

**<sup>1</sup>H NMR** : (400 MHz, CDCl<sub>3</sub>): δ 7.04-6.92 (m, 4H), 6.73 (s, 1H), 6.69 (s, 1H), 4.62 (d, *J* = 8.8 Hz, 1H), 4.58 (d, *J* = 8.8 Hz, 1H), 4.18 (d, *J* = 16.4 Hz, 1H), 3.85 (m, 2H), 2.42 (s, 6H), 2.23 (s, 3H), 2.20 (s, 3H)

**<sup>13</sup>C NMR** : (100 MHz, CDCl<sub>3</sub>): δ 146.4, 142.1, 133.2, 133.0, 128.2, 128.0, 127.8, 127.0, 126.9, 125.4, 125.2, 90.4, 59.5, 51.6, 41.6, 21.0, 20.9

**LCMS** : (EI, *m/z*): 294.25 (*M*+1)

**Analysis** : Calculated for C<sub>19</sub>H<sub>23</sub>N<sub>3</sub>: C, 77.78%; H, 7.90%; N, 14.32%;  
found: C, 77.65%, H, 7.93%, N, 14.21%



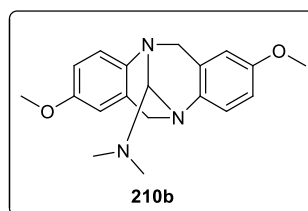
**2,8-Dimethoxy-13-(*N,N*-dimethylamino)-6H,12H-5,11-methanodibenzo[*b,f*][1,5]diazocine 210b**

**Yield** : 0.545 g (84%); White solid

**mp** : 111-113 °C

**IR (KBr)** : 2999, 1494, 1458, 1240, 835 cm<sup>-1</sup>

**<sup>1</sup>H NMR** : (400 MHz, CDCl<sub>3</sub>): δ 7.05 (d, *J* = 8.8 Hz, 1H), 6.99 (d, *J* = 8.8 Hz, 1H), 6.76-6.69 (m, 2H), 6.42 (d, *J* = 10.4 Hz, 2H), 4.61 (d, *J* = 9.6 Hz, 1H), 4.56 (d, *J* = 9.2 Hz, 1H), 4.14 (d, *J* = 16.8 Hz, 1H), 3.84-3.80 (m, 2H), 3.71 (s, 3H), 3.69 (s, 3H), 2.41 (s, 6H)



**<sup>13</sup>C NMR** : (100 MHz, CDCl<sub>3</sub>): δ 156.0, 155.8, 141.9, 137.7, 129.3, 129.1, 126.5, 126.3, 113.9, 113.7, 110.7, 110.4, 90.5, 59.6, 55.4, 55.3, 51.9, 41.5

**LCMS** : (EI, m/z): 326 (M+1)

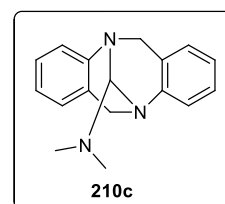
**Analysis** : Calculated for C<sub>19</sub>H<sub>23</sub>N<sub>3</sub>O<sub>2</sub>: C, 70.13%, H, 7.12%, N, 12.91%;  
found: C, 70.35%, H, 7.16%, N, 12.81%

**13-(*N,N*-dimethylamino)-6H,12H-5,11-methanodibenzo[*b,f*][1,5]diazocine 210c**

**Yield** : 0.464 g (88%); White solid

**mp** : 141-143 °C

**IR (KBr)** : 3063, 2945, 1481, 1448, 1275, 833 cm<sup>-1</sup>



**<sup>1</sup>H NMR** : (400 MHz, CDCl<sub>3</sub>): δ 7.17-7.07 (m, 4H), 6.97-6.86 (m, 4H), 4.68 (d, *J* = 9.2 Hz, 1H), 4.64 (d, *J* = 9.2 Hz, 1H), 4.25 (d, *J* = 16.4 Hz, 1H), 3.93 (d, *J* = 16.4 Hz, 1H), 3.88 (s, 1H), 2.43 (s, 6H)

**<sup>13</sup>C NMR** : (100 MHz, CDCl<sub>3</sub>): δ 149.0, 144.8, 128.7, 128.4, 127.2, 127.0, 126.6, 126.5, 125.7, 125.4, 123.8, 123.7, 90.1, 59.5, 51.6, 41.6

**LCMS** : (EI, m/z): 266.2 (M+1)

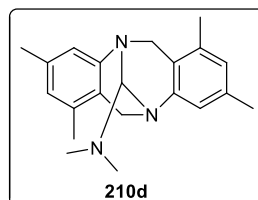
**Analysis** : Calculated for C<sub>17</sub>H<sub>19</sub>N<sub>3</sub>: C, 76.95%, H, 7.22%, N, 15.84%;  
found: C, 77.23%, H, 6.48%, N, 15.76%

**1,3,7,9-Tetramethyl-13-(*N,N*-dimethylamino)-6H,12H-5,11-methanodibenzo[*b,f*][1,5]diazocine 210d**

**Yield** : 0.551 g (86%); White solid

**mp** : 227-229 °C

**IR (KBr)** : 2995, 2914, 1435, 1280, 852 cm<sup>-1</sup>



- <sup>1</sup>H NMR** : (400 MHz, CDCl<sub>3</sub>): δ 6.83 (s, 1H), 6.77 (s, 1H), 6.64 (s, 1H), 6.62 (s, 1H), 4.46 (d, *J* = 16.4 Hz, 1H), 4.39 (d, *J* = 16.4 Hz, 1H), 4.15 (d, *J* = 16.4 Hz, 1H), 3.87 (d, *J* = 16.4 Hz, 1H), 3.79 (s, 1H), 2.41 (s, 6H), 2.26 (s, 3H), 2.24 (s, 3H), 2.07 (s, 6H)
- <sup>13</sup>C NMR** : (100 MHz, CDCl<sub>3</sub>): δ 149.3, 144.8, 136.5, 136.0, 135.0, 134.4, 126.4, 126.3, 124.0, 123.9, 123.8, 123.7, 89.8, 58.3, 50.3, 41.7, 21.1, 21.0, 18.1, 17.9
- LCMS** : (EI, *m/z*): 322.35 (*M*+1)
- Analysis** : Calculated for C<sub>21</sub>H<sub>27</sub>N<sub>3</sub>: C, 78.46%, H, 8.47%, N, 13.07%;  
found: C, 78.51%, H, 8.52%, N, 12.95%

**2,4,8,10-Tetramethyl-13-(*N,N*-dimethylamino)-6H,12H-5,11-methanodibenzo[*b,f*][1,5]diazocine 210e**

**Yield** : 0.418 g (65%); White solid

**mp** : 100-102 °C

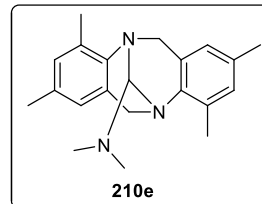
**IR (KBr)** : 2943, 1475, 1271, 815 cm<sup>-1</sup>

**<sup>1</sup>H NMR** : (400 MHz, CDCl<sub>3</sub>): δ 6.88 (s, 1H), 6.84 (s, 1H), 6.60 (s, 1H), 6.55 (s, 1H), 4.49 (d, *J* = 16.8 Hz, 1H), 4.43 (d, *J* = 16.8 Hz, 1H), 3.97 (d, *J* = 16.8 Hz, 1H), 3.84 (s, 1H), 3.63 (d, *J* = 16.8 Hz, 1H), 2.40 (s, 6H), 2.36 (s, 6H), 2.20 (s, 3H), 2.18 (s, 3H)

**<sup>13</sup>C NMR** : (100 MHz, CDCl<sub>3</sub>): δ 144.3, 139.8, 133.2, 132.9, 132.7, 129.6, 129.5, 128.3, 124.5, 124.4, 91.0, 56.0, 48.4, 41.6, 21.0, 20.9, 17.0, 16.9

**LCMS** : (EI, *m/z*): 322.35 (*M*+1)

**Analysis** : Calculated for C<sub>21</sub>H<sub>27</sub>N<sub>3</sub>: C, 78.46%, H, 8.47%, N, 13.07%.



found: C, 78.31%, H, 8.41%, N, 13.16%

**2, 8-Dimethyl-11,12-dihydro-6H-dibenzo[b,f] [1,5] diazocine-5-carbaldehyde 211**

**Yield** : 0.102 g (19%); White solid

**mp** : 159-162 °C

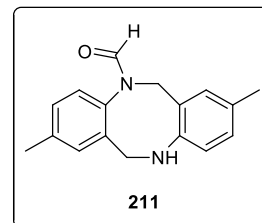
**IR (KBr)** : 3346, 2966, 2932, 2887, 1655, 1502 cm<sup>-1</sup>

**<sup>1</sup>H NMR** : (400 MHz, CDCl<sub>3</sub>): δ 8.42 (s, 1H), 7.07-7.02 (m, 3H), 6.94 (d, *J* = 7.6 Hz, 1H), 6.86 (d, *J* = 7.6 Hz, 1H), 6.52 (d, *J* = 8.0 Hz, 1H), 4.83 (s, 2H), 4.28 (s, 2H), 3.96 (brs, 1H), 2.32 (s, 3H), 2.22 (s, 3H)

**<sup>13</sup>C NMR** : (100 MHz, CDCl<sub>3</sub>): δ 162.7, 146.2, 138.5, 137.5, 134.7, 133.3, 130.9, 129.8, 129.5, 129.1, 125.4, 123.3, 119.3, 50.9, 50.2, 20.9, 20.4

**LCMS** : (EI, m/z): 267.20 (M+1)

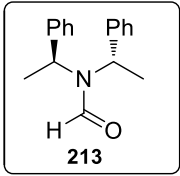
**Analysis** : Calculated for C<sub>17</sub>H<sub>18</sub>N<sub>2</sub>O: C, 76.66%, H, 6.81%, N, 10.52%, O, 6.01%; found: C, 76.51%, H, 6.75%, N, 10.45%



**3.4.3 Procedure for the preparation of chiral (*S,S*)-*N,N*-bis( $\alpha$ -methylbenzyl) formamide 213**

To a solution of (*S,S*)-*N,N*-bis( $\alpha$ -methylbenzylamine) (1.125 g, 5 mmol) in CH<sub>2</sub>Cl<sub>2</sub> was added acetic formic anhydride (0.880 g, 10 mmol) at 0 °C. The reaction mixture was allowed to stir for 2 h at 25 °C. It was then cooled to 0 °C and quenched with aq. NaHCO<sub>3</sub> solution. The aqueous layer was extracted with CH<sub>2</sub>Cl<sub>2</sub> (2 x 15 mL) and the combined organic extracts were successively washed with water, brine and dried over anhydrous Na<sub>2</sub>SO<sub>4</sub>. After removal of the solvent, the residue was subjected to chromatography on silica gel column using 7% ethyl acetate in hexane to elute the desired chiral amide derivative.



<b>Yield</b>	:	1.240 g (98%); White solid	
<b>mp</b>	:	79-81 °C (lit. <sup>134</sup> mp 82 °C)	
<b>IR (KBr)</b>	:	2975, 1644, 1245, 699 cm <sup>-1</sup>	
<b><sup>1</sup>H NMR</b>	:	(400 MHz, CDCl <sub>3</sub> ): δ 8.30 (s, 1H), 7.26-6.79 (m, 10H), 5.71 (q, <i>J</i> = 8.0 Hz, 1H), 4.49 (q, <i>J</i> = 8.0 Hz, 1H), 1.72-1.67 (m, 6H)	
<b><sup>13</sup>C NMR</b>	:	(100 MHz, CDCl <sub>3</sub> ): δ 162.6, 141.1, 139.9, 128.4, 128.3, 127.7, 127.4, 126.7, 52.9, 50.7, 22.4, 17.1	
<b>[α]<sub>D</sub><sup>25</sup></b>	:	-226 (c 0.30, CHCl <sub>3</sub> ) {lit. <sup>134</sup> [α] <sub>D</sub> <sup>25</sup> = -214.1 (1.02, CHCl <sub>3</sub> )}	

### 3.4.4 General procedure for the diastereoselective synthesis of Tröger base derivatives

To a solution of Tröger base derivatives (2 mmol) and (*S,S*)-*N,N*-bis( $\alpha$ -methylbenzyl)foramide (0.531 g, 2.1 mmol) in CH<sub>2</sub>Cl<sub>2</sub> (15 mL) was added POCl<sub>3</sub> (0.535 g, 0.32 mL, 3.5 mmol) at 25 °C under N<sub>2</sub> atmosphere. The reaction mixture was allowed to stir for 12 h at 25 °C. It was then cooled to 0 °C and quenched with 10% aq. NaOH solution. The aqueous layer was extracted with CH<sub>2</sub>Cl<sub>2</sub> (2 x 15 mL) and the combined organic extracts were successively washed with water, brine and dried over anhydrous Na<sub>2</sub>SO<sub>4</sub>. After removal of the solvent, the residue was subjected to chromatography on silica gel column using 3-10% ethyl acetate in hexane to elute the desired Tröger base derivative.

### 2,8-Dimethyl-13-bis(1-phenylethylamino)-6H,12H-5,11-methanodibenzo[b,f][1,5]

#### diazocine 214

The diastereomeric ratio was calculated on the basis of <sup>1</sup>H NMR analysis of -CH<sub>3</sub> proton of (*S,S*)-*N,N*-bis( $\alpha$ -methylbenzyl) moiety [For major 1.51 (d, *J* = 8.0 Hz, 6H), and for

minor 1.63 (d,  $J = 8.0$  Hz, 2H)]. Further, dr = 77:23 was estimated by chiral HPLC analysis on Chiral cell phenomenex cellulose-1 column, hexane/2-propanol = 99.5:0.5, flow rate 1 mL/min.

**Yield** : 0.712 g (75%); White solid

**mp** : 81-83 °C

**IR (KBr)** : 2924, 1493, 1450, 1209, 833  $\text{cm}^{-1}$

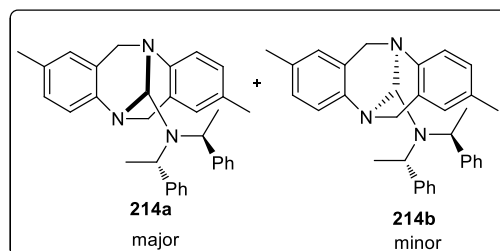
**$^1\text{H}$  NMR** : (400 MHz,  $\text{CDCl}_3$ ):  $\delta$  7.16-6.93 (m, 14H), 6.78-6.51 (m, 7H), 6.12 (d,  $J = 8.0$  Hz, 0.3H), 5.05 (d,  $J = 16.0$  Hz, 0.3H), 4.76 (m, 1H), 4.60 (m, 2.5H), 4.35 (d,  $J = 16.0$  Hz, 1H), 4.10-3.94 (m, 1.7H), 3.73 (d,  $J = 16.0$  Hz, 1H), 3.39 (d,  $J = 16.0$  Hz, 1H), 2.24-2.18 (m, 8H), 1.63 (d,  $J = 8.0$  Hz, 2H), 1.51 (d,  $J = 8.0$  Hz, 6H)

**$^{13}\text{C}$  NMR** : (100 MHz,  $\text{CDCl}_3$ ):  $\delta$  146.9, 146.7, 144.3, 142.7, 142.2, 133.1, 132.7, 129.2, 128.9, 128.0, 127.7, 127.6, 127.4, 127.2, 126.9, 126.5, 126.2, 125.8, 125.6, 125.4, 125.0, 83.5, 82.8, 59.9, 59.8, 52.5, 51.1, 51.0, 21.0, 20.9, 16.1

**$[\alpha]_{\text{D}}^{25}$**  : - 97.6 (c 0.38,  $\text{CHCl}_3$ )

**LCMS** : (EI, m/z): 474.35 (M+1)

**Analysis** : Calculated for  $\text{C}_{33}\text{H}_{35}\text{N}_3$ : C, 83.68%, H, 7.45%, N, 8.87%;



found: C, 83.49%, H, 7.51%, N, 8.95%

**2,8-Dimethoxy-13-bis(1-phenylethylamino)-6H,12H-5,11-methanodibenzo[b,f][1,5]diazocine 215**

The diastereomeric ratio was calculated on the basis of  $^1\text{H}$  NMR analysis of  $-\text{CH}_3$  proton of (*S,S*)-*N,N*-bis( $\alpha$ -methylbenzyl) moiety [For major 1.56 (d,  $J = 8.0$  Hz, 6H), and for minor 1.67 (d,  $J = 8.0$  Hz, 2H)]. Further, dr = 77:23 was estimated by chiral HPLC analysis on Chiral cell phenomenex cellulose-1 column, hexane/2-propanol = 99.5:0.5, flow rate 1 mL/min;

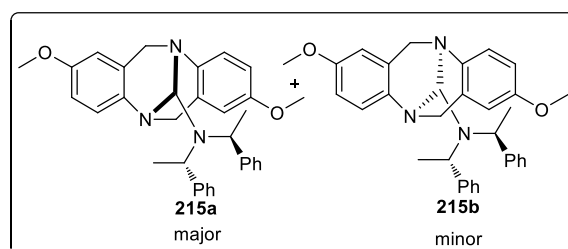
**Yield** : 0.665 g (66%)

**mp** : 90-92 °C

**IR (KBr)** : 2932, 1493, 1450, 1209, 835  $\text{cm}^{-1}$

**$^1\text{H}$  NMR** : (400 MHz,  $\text{CDCl}_3$ ):  $\delta$  7.21-7.06 (m, 11.5H), 6.82-6.75 (m, 6H), 6.48-6.44 (m, 1.6H), 6.35-6.34 (m, 1.3H), 6.18 (d,  $J = 8.0$  Hz, 0.4H), 5.30 (s, 1H), 5.09 (d,  $J = 16.0$  Hz, 0.4H), 4.83-4.78 (m, 1.3H), 4.66-4.62 (m, 2.8H), 4.46 (d,  $J = 16.0$  Hz, 1H), 4.14-3.96 (m, 1.7H), 3.75-3.73 (m, 8.5H), 3.38 (d,  $J = 16.0$  Hz, 1H), 1.67 (d,  $J = 8.0$  Hz, 2H), 1.56 (d,  $J = 8.0$  Hz, 6H)

**$^{13}\text{C}$  NMR** : (100 MHz,  $\text{CDCl}_3$ ):  $\delta$  155.9, 155.7, 155.1, 144.4, 142.4, 142.2, 138.3, 137.7, 130.5, 129.8, 129.7, 128.8, 128.4, 128.2, 127.9, 127.4, 126.7,



126.6, 126.5, 126.1, 125.8, 113.7, 113.3, 110.5, 110.4, 109.6, 83.7,  
83.0, 60.0, 55.4, 52.5, 51.3, 16.0, 15.8

$[\alpha]_{\text{D}}^{25}$  : - 92 (c 0.88,  $\text{CHCl}_3$ )

**LCMS** : (EI, m/z): 506.45 (M+1)

**Analysis** : Calculated for  $\text{C}_{33}\text{H}_{35}\text{N}_3\text{O}_2$ : C, 78.38%, H, 6.98%, N, 8.31%,  
O, 6.33%; found: C, 78.51%, H, 6.91%, N 8.25%

### 13-Bis(1-phenylethylamino)-6H,12H-5,11-methanodibenzo[b,f][1,5]diazocine **216**

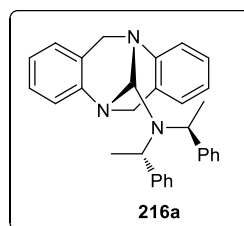
The diastereomeric ratio was calculated on the basis of  $^1\text{H}$  NMR analysis of  $-\text{CH}_3$  proton of (*S,S*)-*N,N*-bis( $\alpha$ -methylbenzyl) moiety [For major 1.57 (d,  $J = 7.2$  Hz, 6H), and for minor 1.69 (d,  $J = 7.2$  Hz, 2H)]. The diastereomeric mixture was crystallized from acetone to obtain compound **216a** in pure form.

**Yield** : 0.605 g (68%); White solid,

**mp** : 161-163  $^\circ\text{C}$ ;

**IR (KBr)** : 3024, 2928, 1496, 1449, 1212, 852  $\text{cm}^{-1}$

**$^1\text{H}$  NMR** : (400 MHz,  $\text{CDCl}_3$ ):  $\delta$  7.22-7.15 (m, 10H), 7.05-7.01 (m, 2H), 6.96-94 (m, 1H), 6.82-6.79 (m, 5H), 4.88 (s, 1H), 4.64 (d,  $J = 8.0$  Hz, 2H), 4.50 (d,  $J = 16.8$  Hz, 1H), 4.22 (d,  $J = 16.4$  Hz, 1H), 3.79 (d,  $J = 16.4$  Hz, 1H), 3.49 (d,  $J = 16.8$  Hz, 1H), 1.57 (d,  $J = 7.2$  Hz, 6H)



<b><math>^{13}\text{C}</math> NMR</b>	:	(100 MHz, $\text{CDCl}_3$ ): $\delta$ 149.6, 144.9, 144.3, 129.8, 129.2, 128.8, 127.5, 126.9, 126.8, 126.6, 126.3, 126.1, 125.8, 125.7, 123.7, 123.6, 82.6, 59.8, 52.6, 51.2, 15.9
<b><math>[\alpha]_{\text{D}}^{25}</math></b>	:	- 189.4 (c 0.32, $\text{CHCl}_3$ )
<b>LCMS</b>	:	(EI, m/z) 446.35 (M+1)
<b>Analysis</b>	:	Calculated for $\text{C}_{31}\text{H}_{31}\text{N}_3$ : C, 83.56%, H, 7.01%, N, 9.43%. found: C, 83.65%, H, 7.12%, N, 9.36%

**1,3,7,9-Tetramethyl-13-bis(1-phenylethylamino)-6H,12H-5,11-methanodibenzo[b,f][1,5]diazocine **217****

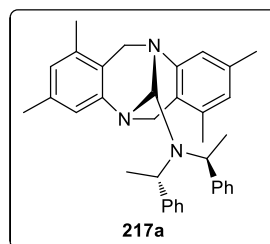
The diastereomeric ratio was calculated on the basis of  $^1\text{H}$  NMR analysis of  $-\text{CH}_3$  proton of (*S,S*)-*N,N*-bis( $\alpha$ -methylbenzyl) moiety [For major 1.57 (d,  $J = 7.2$  Hz, 6H), and for minor 1.69 (d,  $J = 7.2$  Hz, 4.4H)]. Further, dr = 60:40 was estimated by chiral HPLC analysis on Chiral cell phenomenex cellulose-1 column, hexane/2-propanol = 99.5:0.5, flow rate 0.6 mL/min; The diastereomeric mixture was crystallized from acetone to obtain compound **217a** in pure form.

**Yield** : 0.525 g (52%); White solid

**mp** : 221-223  $^{\circ}\text{C}$

**IR (KBr)** : 3026, 2926, 1494, 1448, 1211, 850  $\text{cm}^{-1}$

**$^1\text{H}$  NMR** : (400 MHz,  $\text{CDCl}_3$ ):  $\delta$  7.17-7.16 (m, 6H), 6.82-6.65 (m, 8H), 4.80 (s, 1H), 4.58 (d,  $J = 8.0$  Hz, 2H), 4.32 (d,  $J = 16.0$  Hz, 1H), 4.13 (d,  $J =$



16.0 Hz, 1H), 3.29 (q,  $J = 16.0$  Hz, 2H), 2.29 (s, 3H), 2.26 (s, 3H), 2.07 (s, 3H), 1.85 (s, 3H), 1.52 (d,  $J = 8.0$  Hz, 6H)

**$^{13}\text{C}$  NMR** : (100 MHz,  $\text{CDCl}_3$ ):  $\delta$  149.8, 144.6, 144.5, 136.2, 135.6, 134.9, 134.0, 128.8, 127.2, 126.0, 125.8, 125.1, 124.5, 123.8, 123.7, 81.8, 58.3, 52.3, 49.9, 21.0, 20.9, 17.9, 17.5, 15.4

$[\alpha]_{\text{D}}^{25}$  : - 264 (c 0.10,  $\text{CHCl}_3$ )

**LCMS** : (EI,  $m/z$ ): 502.45 ( $M+1$ )

**Analysis** : Calculated for  $\text{C}_{35}\text{H}_{39}\text{N}_3$ : C, 83.79%, H, 7.84%, N, 8.38%;

found: C, 83.65%, H, 7.78%, N, 8.26%

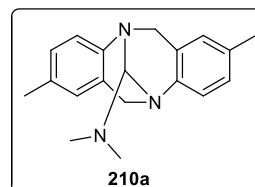
### 3.4.5 General procedure for the exchange of methylene bridge of chiral *para*-substituted Tröger base derivatives with formamides

To a stirred solution of chiral Tröger base derivative (2 mmol) and formamide (2.0 mmol) in  $\text{CH}_2\text{Cl}_2$  (15 mL) was added  $\text{POCl}_3$  (0.306 g, 0.18 mL, 2.0. mmol) at 25 °C under  $\text{N}_2$  atmosphere. The reaction mixture was allowed to stir for 1 h at 25 °C. It was then cooled to 0 °C and quenched with 10% aq. NaOH solution. The aqueous layer was extracted with  $\text{CH}_2\text{Cl}_2$  (2 x 15 mL) and the combined organic extracts were successively washed with water, brine and dried over anhydrous  $\text{Na}_2\text{SO}_4$ . After removal of the solvent, the residue was subjected to chromatography on silica gel column using ethyl acetate in hexane to elute the desired Tröger base derivative

**2,8-Dimethyl-13-(*N,N*-dimethylamino)-6H,12H-5,11-methano-dibenzo[b,f][1,5]diazocine 210a**

**Yield** : 0.412 g (70%); White solid.

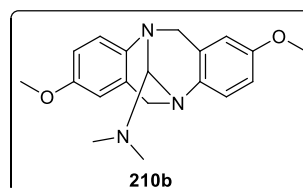
**mp** : 102-104 °C



**2,8-Dimethoxy-13-(*N,N*-dimethylamino)-6H,12H-5,11-methanodibenzo[b,f][1,5]diazocine 210b**

**Yield** : 0.444 g (68%); White solid

**mp** : 111-113 °C



**2,8-dimethyl-13-(*N,N*-diethylamino)-6H,12H-5,11-methanodibenzo[b,f][1,5]diazocine 210f**

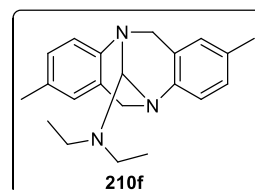
**Yield** : 0.402 g (63%); White solid

**IR (Neat)** : 2964, 2926, 1495, 1210, 832 cm<sup>-1</sup>

**<sup>1</sup>H NMR** : (400 MHz, CDCl<sub>3</sub>): δ 7.07-6.95 (m, 4H), 6.75 (s, 1H), 6.69 (s, 1H), 4.65 (q, *J* = 8.0 Hz, 2H), 4.40 (s, 1H), 4.20 (d, *J* = 16 Hz, 1H), 3.85 (d, *J* = 16 Hz, 1H), 3.06 (sex, *J* = 8.0 Hz, 2H), 2.79 (sex, *J* = 8.0 Hz, 2H), 2.25 (d, *J* = 8 Hz, 6H), 1.03 (t, *J* = 8.0 Hz, 6H)

**<sup>13</sup>C NMR** : (100 MHz, CDCl<sub>3</sub>): δ 146.8, 142.8, 133.2, 132.8, 128.8, 128.5, 128.1, 127.9, 127.1, 126.9, 125.6, 125.3, 85.8, 59.9, 51.7, 40.7, 21.1, 21.0, 11.1

**HRMS (ESI)** : *m/z* [M+H]<sup>+</sup> calcd for C<sub>21</sub>H<sub>27</sub>N<sub>3</sub>: 322.2284; found 322.2284.



**2,8-dimethoxy-13-(*N,N*-diethylamino)-6H,12H-5,11-methanodibenzo[*b,f*][1,5]diazocine 210g**

**Yield** : 0.428 g (61%); White solid

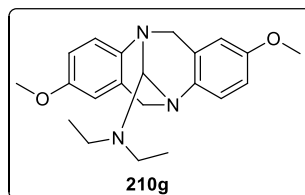
**mp** : 114-116 °C

**IR (KBr)** : 2958, 2827, 1495, 1320, 1243, 838 cm<sup>-1</sup>

**<sup>1</sup>H NMR** : (400 MHz, CDCl<sub>3</sub>): δ 7.06-7.00 (m, 2H), 6.75-6.68 (m, 2H), 6.44-6.39 (m, 2H), 4.59 (t, *J* = 16.0 Hz, 2H), 4.34 (s, 1H), 4.14 (d, *J* = 16.0 Hz, 1H), 3.77 (d, *J* = 16.0 Hz, 1H), 3.70 (d, *J* = 4 Hz, 6H), 3.00 (sex, *J* = 8.0 Hz, 2H), 2.74 (sex, *J* = 8.0 Hz, 2H), 0.98 (t, *J* = 8.0 Hz, 6H)

**<sup>13</sup>C NMR** : (100 MHz, CDCl<sub>3</sub>): δ 155.8, 155.5, 142.0, 138.1, 129.7, 129.3, 126.5, 126.2, 113.7, 113.4, 110.5, 110.4, 85.7, 59.8, 55.4, 55.2, 51.7, 40.4, 10.8

**HRMS (ESI)** : *m/z* [M+H]<sup>+</sup> calcd for C<sub>21</sub>H<sub>27</sub>N<sub>3</sub>O<sub>2</sub>: 354.2182; found 354.2183



### 3.4.6 General procedure for the exchange of methylene bridge of chiral *ortho*-substituted Tröger base derivatives with formamides

To a stirred solution of chiral *ortho*-substituted Tröger base derivative (2 mmol) and formamide (2.0 mmol) in CH<sub>2</sub>Cl<sub>2</sub> (15 mL) was added POCl<sub>3</sub> (0.245 g, 0.15 mL, 1.6. mmol) at 25 °C under N<sub>2</sub> atmosphere. The reaction mixture was allowed to stir for 30 min. at 25 °C. It was then cooled to 0 °C and quenched with 10% aq. NaOH solution. The aqueous layer was extracted with CH<sub>2</sub>Cl<sub>2</sub> (2 x 15 mL) and the combined organic extracts were successively washed with water, brine and dried over anhydrous Na<sub>2</sub>SO<sub>4</sub>. After removal of the solvent, the residue was subjected to chromatography on silica gel column using 3% ethyl acetate in hexane to elute the desired Tröger base derivative in 96% ee.



**2,4,8,10-Tetramethyl-13-(*N,N*-dimethylamino)-6H,12H-5,11-methanodibenzo[*b,f*][1,5]diazocine 210e**

**Yield** : 0.165 g (25%); White solid;

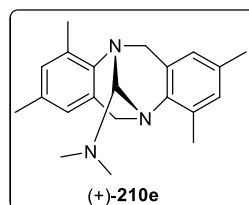
**mp** : 100-102 °C;

$[\alpha]_{\text{D}}^{25}$  : +33.6 (c 0.21, CHCl<sub>3</sub>).

**ee** : 96% (Estimated by HPLC analysis on chiralcel phenomenex

cellulose-1 column, hexane/2-propanol= 99.5:0.5, flow

rate 0.3 mL/min.



**2,4,8,10-Tetramethyl-13-(*N,N*-dimethylamino)-6H,12H-5,11-methanodibenzo[*b,f*][1,5]diazocine 210e**

**Yield** : 0.161 g (23%); White solid

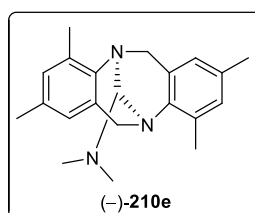
**mp** : 100-102 °C

$[\alpha]_{\text{D}}^{25}$  : -32.2 (c 0.28, CHCl<sub>3</sub>)

**ee** : 94% (Estimated by HPLC analysis on chiralcel phenomenex

cellulose-1 column, hexane/2-propanol= 99.5:0.5, flow

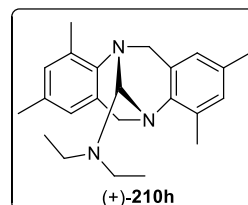
rate 0.3 mL/min



**2,4,8,10-Tetramethyl-13-(*N,N*-diethylamino)-6H,12H-5,11-methanodibenzo[*b,f*][1,5]diazocine 210h**

**Yield** : 0.168 g (22%)

**IR (neat)** : 2958, 1473, 1216, 1073, 854 cm<sup>-1</sup>



**<sup>1</sup>H NMR** : (400 MHz, CDCl<sub>3</sub>): δ 6.88 (s, 1H), 6.83 (s, 1H), 6.59 (s, 1H), 6.53 (s, 1H), 4.50 (d, *J* = 16.0 Hz, 1H), 4.43 (d, *J* = 16.0 Hz, 1H), 4.37 (s, 1H), 3.96 (d, *J* = 16.0 Hz, 1H), 3.59 (d, *J* = 16.0 Hz, 1H), 2.98 (sex, *J* = 8.0 Hz, 2H), 2.74 (sex, *J* = 8.0 Hz, 2H), 2.36 (s, 6H), 2.19 (d, *J* = 8.0 Hz, 6H), 0.98 (t, *J* = 8.0 Hz, 6H)

**<sup>13</sup>C NMR** : (100 MHz, CDCl<sub>3</sub>): δ 144.4, 140.3, 133.3, 132.8, 132.6, 132.3, 129.5, 129.3, 128.8, 128.6, 124.4, 124.3, 86.1, 56.2, 48.3, 40.6, 21.0, 20.8, 17.0, 16.9, 10.8

**HRMS (ESI)** *m/z* [M+H]<sup>+</sup> calcd for C<sub>23</sub>H<sub>31</sub>N<sub>3</sub>: 350.2597; found 350.2597

**[α]<sub>D</sub><sup>25</sup>** : +30.6 (c 0.21, CHCl<sub>3</sub>)

**ee** : 99% (Estimated by HPLC analysis on chiralcel phenomenex

cellulose-1 column, hexane/2-propanol= 99.9:0.1, flow

rate 0.8 mL/min.

**2,8-dibromo-4,10-dimethyl-13-(*N,N*-dimethylamino)-6H,12H-5,11-methanodibenzo  
[b,f][1,5] diazocine 210i**

**Yield** : 0.010 g (2%); White solid

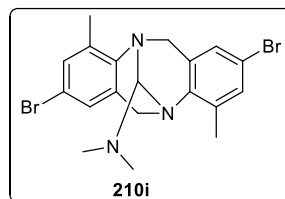
**mp** : 132-135 °C

**IR (KBr)** : 2942, 2805, 1578, 1468, 1210, 904, 843 cm<sup>-1</sup>

**<sup>1</sup>H NMR** : (400 MHz, CDCl<sub>3</sub>): δ 7.22 (s, 1H), 7.19 (s, 1H), 6.95 (s, 1H), 6.90 (s, 1H), 4.53-4.44 (m, 2H), 3.97 (d, *J* = 16.0 Hz, 1H), 3.84 (s, 1H), 3.63 (d, *J* = 16.0 Hz, 1H), 2.40 (s, 6H), 2.38 (s, 6H)

**<sup>13</sup>C NMR** : (100 MHz, CDCl<sub>3</sub>): δ 145.4, 141.2, 135.9, 135.4, 131.7, 131.5, 130.7, 130.4, 126.8, 126.7, 116.9, 116.7, 90.3, 55.4, 48.0, 41.3, 16.8, 16.6

**HRMS (ESI)** : *m/z* [M+H]<sup>+</sup> calcd for C<sub>19</sub>H<sub>21</sub>Br<sub>2</sub>N<sub>3</sub>: 450.0181; found 450.0186



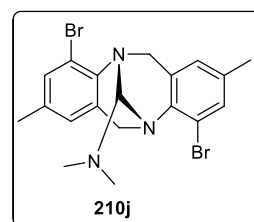
**4,10-dibromo-2,8-dimethyl-13-(*N,N*-dimethylamino)-6H,12H-5,11-methanodibenzo  
[b,f][1,5] diazocine 210j**

**Yield** : 0.052 g (5%); White solid

**mp** : 119-121 °C

**IR (KBr)** : 2942, 2810, 1457, 1353, 926 cm<sup>-1</sup>

**<sup>1</sup>H NMR** : (400 MHz, CDCl<sub>3</sub>): δ 7.28 (s, 1H), 7.24 (s, 1H), 6.75 (s, 1H), 6.70 (s, 1H), 4.49 (d, *J* = 16.0 Hz, 1H), 4.42 (d, *J* = 16.0 Hz, 1H), 4.26 (d, *J* = 16.0 Hz, 1H), 3.94 (d, *J* = 16.0 Hz, 1H), 3.86 (s, 1H), 2.41 (s, 6H), 2.22 (s, 3H), 2.19 (s, 3H)



**<sup>13</sup>C NMR** : (100 MHz, CDCl<sub>3</sub>): δ 142.8, 138.8, 135.2, 135.0, 131.8, 131.4, 131.3, 130.9, 126.3, 120.4, 120.1, 90.6, 56.2, 48.9, 41.3, 20.6, 20.5

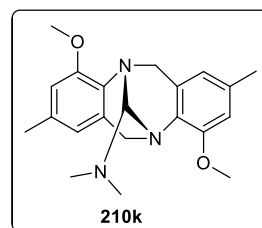
**HRMS (ESI)** : m/z [M+H]<sup>+</sup> calcd for C<sub>19</sub>H<sub>21</sub>Br<sub>2</sub>N<sub>3</sub>: 450.0181; found 450.0186

**ee** : 10% (Estimated by HPLC analysis on chiralcel phenomenex cellulose-1 column, hexane/2-propanol= 99.8:0.2, flow rate 1 mL/min.

**2,8-dimethyl-4,10-dimethoxy-13-(*N,N*-dimethylamino)-6H,12H-5,11-methanodibenzo [b,f][1,5] diazocine 210k**

**Yield** : 0.165 g (19%)

**IR (Neat)** : 2991, 1578, 1479, 1315, 936 cm<sup>-1</sup>



**<sup>1</sup>H NMR** : (400 MHz, CDCl<sub>3</sub>): δ 6.53-6.52 (m, 2H), 6.41 (s, 1H), 6.37 (s, 1H), 4.48 (d, *J* = 16 Hz, 1H), 4.42 (d, *J* = 16 Hz, 1H), 4.20 (d, *J* = 16 Hz, 1H), 3.91-3.87 (m, 8H), 2.44 (s, 6H), 2.23 (d, *J* = 8Hz, 6H)

**<sup>13</sup>C NMR** : (100 MHz, CDCl<sub>3</sub>): δ 153.1, 152.9, 134.1, 133.5, 133.2, 130.0, 129.4, 129.3, 119.1, 119.0, 110.3, 109.8, 90.9, 55.7, 55.6, 55.3, 47.5, 41.6, 21.4, 21.3

**HRMS (ESI)** : m/z [M+H]<sup>+</sup> calcd for C<sub>21</sub>H<sub>27</sub>N<sub>3</sub>O<sub>2</sub>: 354.2182; found 354.2181

**ee** : 10% (Estimated by HPLC analysis on chiralcel AD-H column, hexane/2-propanol= 99.5:0.5, flow rate 1 mL/min.

### 3.5 N-Arylation of Tröger base derivatives

#### 3.5.1 Typical procedure for the N-arylation of cyclic secondary diamine under copper catalyst

In a 10 mL reaction flask equipped with air condenser protected by a mercury trap, CuBr (0.014 g, 10 mol %), BINOL (0.057 g, 20 mol %), *t*-BuOK (0.336 g, 3 mmol) and toluene (5 mL) were placed under nitrogen. The contents were stirred for 30 min at 25 °C. To this, cyclic secondary diamine (0.238 g, 1 mmol) and 4-iodoanisole (0.702g, 3 mmol) were added and stirring was continued for 36 h at 120 °C. The reaction mixture was brought to 25 °C, diluted with ethyl acetate and water. The organic layer was separated and the aqueous layer was extracted with ethyl acetate (2 x 15 mL) and the combined organic extracts were successively washed with water, brine and dried over anhydrous Na<sub>2</sub>SO<sub>4</sub>. After removal of the solvent, the residue was subjected to chromatography on silica gel column using ethyl acetate in hexane to elute the desired N-arylated product.

#### 5-(4-methoxyphenyl)-2,8-dimethyl-5,6,11,12-tetrahydrodibenzo[b,f][1,5]diazocine 244a

**Yield** : (0.05 g) 15%

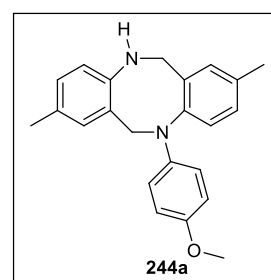
**mp** : 95-98 °C

**IR (KBr)** : 3386, 2920, 1501, 1276, 1243, 1161, 810 cm<sup>-1</sup>

**<sup>1</sup>H NMR** : (400 MHz, CDCl<sub>3</sub>): δ 7.29-7.06 (m, 4H), 6.86 (d, *J* = 8 Hz, 1H), 6.75

(s, 4H), 6.55 (d, *J* = 8Hz, 1H), 4.79 (s, 2H), 4.27 (s, 2H), 3.75 (s, 3H),

3.62 (brs, 1H), 2.37 (s, 3H), 2.29 (s, 3H)



**$^{13}\text{C}$  NMR** : (100 MHz,  $\text{CDCl}_3$ ):  $\delta$  151.9, 146.4, 144.4, 142.1, 136.0, 134.0, 132.7, 130.7, 129.0, 128.8, 128.6, 127.7, 125.4, 119.3, 116.5, 114.3, 55.6, 54.5, 51.4, 20.9, 20.5

**HRMS** :  $m/z$   $[\text{M}+\text{H}]^+$  calcd for  $\text{C}_{23}\text{H}_{24}\text{N}_2\text{O}$ : 345.1968; found 345.1968

### 3.5.2 Typical procedure for the $\text{Fe}_2\text{O}_3$ catalyzed N-arylation of cyclic secondary diamine

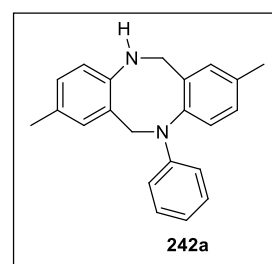
In a 10 mL reaction flask equipped with air condenser,  $\text{Fe}_2\text{O}_3$  (0.016 g, 10 mol %), *t*-BuOK (0.336 g, 3 mmol), cyclic secondary diamine (0.238 g, 1 mmol), iodobenzene (0.612 g, 3 mmol) and DMSO (2 mL) were placed in open atmosphere. The contents were allowed to stir for 24 h at 120 °C. The reaction mixture was brought to 25 °C, diluted with ethyl acetate and water. The organic layer was separated and the aqueous layer was extracted with ethyl acetate (2 x 15 mL) and the combined organic extracts were successively washed with water, brine and dried over anhydrous  $\text{Na}_2\text{SO}_4$ . After removal of the solvent, the residue was subjected to chromatography on silica gel column using ethyl acetate in hexane to elute the desired N-arylated product.

#### 2,8-dimethyl-5-phenyl-5,6,11,12-tetrahydrodibenzo[b,f][1,5]diazocine 242a

**Yield** : 0.210 g (67%)

**mp** : 155-159 °C

**IR (KBr)** : 3342, 2893, 2843, 1600, 1495, 1265, 827  $\text{cm}^{-1}$



**<sup>1</sup>H NMR** : (400 MHz, CDCl<sub>3</sub>): δ 7.21-7.14 (m, 6H), 6.93 (d, *J* = 8 Hz, 1H), 6.84-6.76 (m, 3H), 6.59 (d, *J* = 8 Hz, 1H), 4.85 (s, 2 H), 4.27 (s, 2H), 3.96 (brs, 1H), 2.45 (s, 3H), 2.37 (s, 3H)

**<sup>13</sup>C NMR** : (100 MHz, CDCl<sub>3</sub>): δ 147.7, 146.7, 143.4, 136.9, 135.1, 132.7, 130.5, 129.2, 128.8, 128.5, 128.3, 125.6, 119.7, 116.9, 114.0, 54.3, 51.3, 20.9, 20.4

**HRMS** : *m/z* [M+H]<sup>+</sup> calcd for C<sub>22</sub>H<sub>22</sub>N<sub>2</sub>: 315.1862; found 315.1858

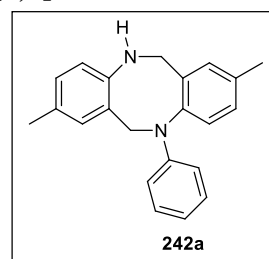
### 3.5.3 General procedure for the N-arylation of Tröger base derivatives

In a 10 mL reaction flask equipped with air condenser, *t*-BuOK (0.336 g, 3 mmol), Tröger base (0.250 g, 1 mmol), iodobenzene (0.612g, 3 mmol) and DMSO (2 mL) were placed in open atmosphere. The contents were allowed to stir for 24 h at 120 °C. The reaction mixture was brought to 25 °C, diluted with ethyl acetate and water. The organic layer was separated and the aqueous layer was extracted with ethyl acetate (2 x 15 mL) and the combined organic extracts were successively washed with water, brine and dried over anhydrous Na<sub>2</sub>SO<sub>4</sub>. After removal of the solvent, the residue was subjected to chromatography on silica gel column using ethyl acetate in hexane to elute the desired N-arylated product.

#### 2,8-dimethyl-5-phenyl-5,6,11,12-tetrahydrodibenzo[b,f][1,5]diazocine 242a

**Yield** : 0.204 g (65%)

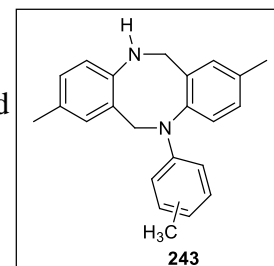
**mp** : 155-159 °C



**IR (KBr)** : 3342, 2893, 2843, 1600, 1495, 1265, 827  $\text{cm}^{-1}$

**2,8-dimethyl-5-(*p*-tolyl) and 5-(*m*-tolyl)-5,6,11,12-tetrahydrodibenzo[*b,f*][1,5]diazocine**  
**243**

**Yield** : 0.164 (50%) regeoisomeric ratio was calculated based on  $^1\text{H}$ -NMR analysis of  $\text{CH}_3$  protons 2.43 and 2.35.



All spectral details are for a mixture of regioisomers in 1:1 ratio.

**mp** : 105-109  $^{\circ}\text{C}$

**IR (KBr)** : 3369, 3008, 2909, 2860, 1600, 1501, 1265, 810  $\text{cm}^{-1}$

**$^1\text{H}$  NMR** : (400 MHz,  $\text{CDCl}_3$ ):  $\delta$  7.26-7.24 (m, 2H), 7.20-7.13 (m, 6H), 7.04 (d,  $J$  = 8 Hz, 2H), 6.92 (d,  $J$  = 8 Hz, 2H), 6.77 (d,  $J$  = 8 Hz, 2H), 6.67-6.59 (m, 4H), 4.85 (d,  $J$  = 2.8 Hz, 4H), 4.25 (d,  $J$  = 8 Hz, 4H), 2.44 (s, 6H), 2.37 (s, 6H), 2.32 (d,  $J$  = 8 Hz, 6H)

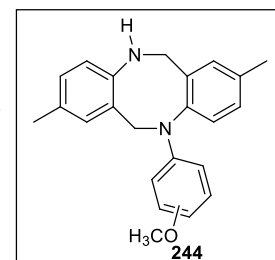
**$^{13}\text{C}$  NMR** : (100 MHz,  $\text{CDCl}_3$ ):  $\delta$  146.8, 145.7, 144.0, 143.7, 138.4, 137.1, 136.8, 135.3, 134.8, 132.9, 132.8, 130.7, 129.4, 129.3, 129.2, 129.0, 128.9, 128.8, 128.7, 128.6, 128.5, 128.4, 126.3, 126.0, 125.8, 119.9, 119.7, 118.2, 115.0, 114.6, 111.4, 54.6, 54.4, 51.6, 51.5, 21.9, 21.1, 21.0, 20.6, 20.4

**HRMS** :  $m/z$   $[\text{M}+\text{H}]^+$  calcd for  $\text{C}_{23}\text{H}_{24}\text{N}_2$ : 329.2018; found 329.2017



**5-(4-methoxyphenyl) and 5-(3-methoxyphenyl)-2,8-dimethyl-5,6,11,12-tetrahydrodibenzo[b,f][1,5]diazocine 244**

**Yield** : 0.200 g (60%) regeoisomeric ratio was calculated  
based on  $^1\text{H}$ -NMR analysis of  $\text{CH}_3$  protons



2.42-2.41 and 2.35-2.33. All spectral details are for a mixture of regioisomers in 1:1 ratio.

**mp** : 95-98 °C

**IR (KBr)** : 3386, 2920, 1501, 1276, 1243, 1161, 810  $\text{cm}^{-1}$

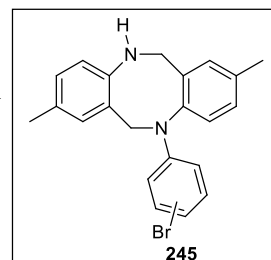
**$^1\text{H}$  NMR** : (400 MHz,  $\text{CDCl}_3$ ):  $\delta$  7.24 (d,  $J = 8$  Hz, 1H), 7.19-7.09 (m, 8H), 6.92-6.89 (m, 2H), 6.80 (s, 4H), 6.57 (t,  $J = 8$  Hz, 2H), 6.41-6.32 (m, 2H), 4.83 (d,  $J = 8$  Hz, 4H), 4.29 (s, 2H), 4.21 (s, 2H), 3.84 (brs, 1.5H), 3.78 (s, 6H), 2.41 (d,  $J = 4$  Hz, 6H), 2.34 (d,  $J = 8$  Hz, 6H)

**$^{13}\text{C}$  NMR** : (100 MHz,  $\text{CDCl}_3$ ):  $\delta$  160.3, 152.0, 149.3, 146.8, 146.4, 144.4, 143.4, 142.1, 137.1, 136.0, 135.5, 134.0, 132.8, 132.6, 130.7, 130.6, 129.5, 129.3, 129.0, 128.9, 128.8, 128.7, 128.6, 127.7, 126.0, 125.5, 120.0, 119.3, 116.4, 116.1, 114.8, 114.3, 107.1, 102.2, 100.4, 55.6, 55.0, 54.7, 54.5, 51.5, 51.4, 21.0, 20.9, 20.5

**HRMS** :  $m/z$   $[\text{M}+\text{H}]^+$  calcd for  $\text{C}_{23}\text{H}_{24}\text{N}_2\text{O}$ : 345.1968; found 345.1968

**5-(4-bromophenyl) and 5-(3-bromophenyl)-2,8-dimethyl-5,6,11,12-tetrahydrodibenzo[b,f][1,5]diazocine 245**

**Yield** : 0.175 (44%) regeoisomeric ratio was calculated  
based on  $^1\text{H}$ -NMR analysis of  $\text{CH}_3$  protons



2.37 and 2.29. All spectral details are for a mixture of regioisomers in 1:1 ratio.

**mp** : 120-124 °C

**IR (KBr)** : 3391, 2915, 2854, 1583, 1501, 1271, 805  $\text{cm}^{-1}$

**$^1\text{H}$  NMR** : (400 MHz,  $\text{CDCl}_3$ ):  $\delta$  7.15-7.04 (m, 10H), 6.95-6.77 (m, 5H), 6.63-6.47 (m, 5H), 4.74-4.73 (m, 4H), 4.20-4.18 (4H), 3.98 (brs, 1.5 H), 2.37 (s, 6H), 2.30 (s, 6H)

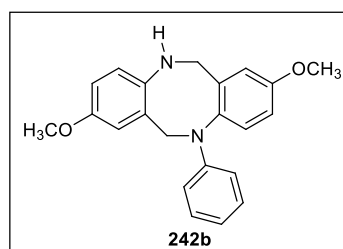
**$^{13}\text{C}$  NMR** : 143.1, 142.8, 137.2, 137.0, 136.8, 135.9, 135.5, 132.9, 132.8, 131.3, 130.8, 130.7, 129.9, 129.3, 129.2, 129.1, 129.0, 128.9, 128.3, 128.2, 125.1, 124.9, 122.9, 119.9, 119.8, 119.7, 117.0, 116.6, 116.0, 112.6, 109.1, 54.6, 54.3, 51.3, 21.1, 20.6

**HRMS** :  $m/z$   $[\text{M}+\text{H}]^+$  calcd for  $\text{C}_{22}\text{H}_{21}\text{N}_2\text{Br}$ : 393.0967; found 393.0966

**2,8-dimethoxy-5-phenyl-5,6,11,12-tetrahydrodibenzo[b,f][1,5]diazocine 242b**

**Yield** : 0.172 g (50%)

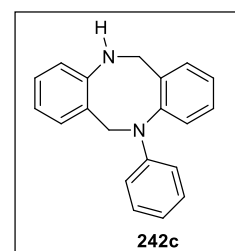
**mp** : 160-163 °C



- IR (KBr)** : 3364, 2997, 2926, 2827, 1589, 1490, 1249, 1205, 800  $\text{cm}^{-1}$ ,
- $^1\text{H}$  NMR** : (400 MHz,  $\text{CDCl}_3$ ):  $\delta$  7.18-7.16 (m, 3H), 6.91 (s, 1H), 6.85-6.81 (m, 2H), 6.70-6.66 (m, 5H), 4.75 (s, 2H), 4.13 (s, 2H), 3.84 (s, 3H), 3.80 (s, 3H)
- $^{13}\text{C}$  NMR** : (100 MHz,  $\text{CDCl}_3$ ):  $\delta$  157.6, 154.1, 148.2, 142.8, 139.6, 138.9, 130.2, 129.0, 128.8, 121.9, 117.9, 116.9, 114.9, 113.5, 113.5, 112.9, 55.6, 55.4, 54.9, 52.5
- HRMS** :  $m/z$   $[\text{M}+\text{H}]^+$  calcd for  $\text{C}_{22}\text{H}_{22}\text{N}_2\text{O}_2$ : 347.1760; found 347.1760.

**5-phenyl-5,6,11,12-tetrahydrodibenzo[b,f][1,5]diazocine 242c**

- Yield** : 0.168 g (59%)
- mp** : 134-137  $^\circ\text{C}$
- IR (KBr)** : 3397, 3057, 2865, 1589, 1495, 1435, 756  $\text{cm}^{-1}$
- $^1\text{H}$  NMR** : (400 MHz,  $\text{CDCl}_3$ ):  $\delta$  7.33-7.07 (m, 8H), 6.86-6.81 (m, 5H), 4.89 (s, 2H), 4.34 (s, 2H), 4.04 (brs, 1H)
- $^{13}\text{C}$  NMR** : (100 MHz,  $\text{CDCl}_3$ ):  $\delta$  148.8, 147.4, 146.1, 136.3, 132.5, 130.2, 128.7, 128.3, 128.2, 128.1, 125.2, 124.8, 119.8, 119.2, 117.6, 114.8, 54.0, 50.9
- HRMS** :  $m/z$   $[\text{M}+\text{H}]^+$  calcd for  $\text{C}_{20}\text{H}_{18}\text{N}_2$ : 287.1549; found 287.1552



**1,3,7,9-tetramethyl-5-phenyl-5,6,11,12-tetrahydrodibenzo[b,f][1,5]diazocine 242d**

**Yield** : 0.188 g (55%)

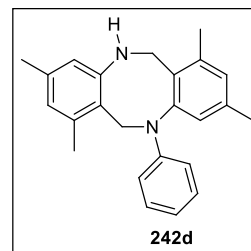
**mp** : 192-195 °C

**IR (KBr)** : 3375, 2964, 2909, 2860, 1589, 1490, 1342, 1216, 832, 745 cm<sup>-1</sup>

**<sup>1</sup>H NMR** : (400 MHz, CDCl<sub>3</sub>): δ 7.28-7.22 (m, 2H), 6.87-6.79 (m, 5H), 4.77 (s, 2H), 4.22 (s, 2H), 3.86 (brs, 1H), 2.31-2.28 (m, 6H), 2.23 (s, 3H), 2.15 (s, 3H)

**<sup>13</sup>C NMR** : (100 MHz, CDCl<sub>3</sub>): δ 149.3, 148.9, 145.1, 138.4, 137.6, 137.2, 136.8, 130.3, 129.1, 128.9, 127.4, 122.8, 119.4, 117.1, 117.0, 113.2, 50.23, 46.0, 21.1, 21.0, 19.4, 19.1

**HRMS** : m/z [M+H]<sup>+</sup> calcd for C<sub>24</sub>H<sub>25</sub>N<sub>2</sub>: 343.2175; found 343.2180

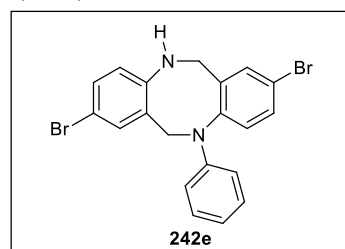
**2,8-dibromo-5-phenyl-5,6,11,12-tetrahydrodibenzo[b,f][1,5]diazocine 242e**

**Yield** : 0.104 g (24%)

**mp** : 198-202 °C

**IR (KBr)** : 3413, 3030, 2964, 1605, 1479, 1364, 1210, 871, 821, 745 cm<sup>-1</sup>

**<sup>1</sup>H NMR** : (400 MHz, CDCl<sub>3</sub>): δ 7.38-7.33 (m, 3H), 7.16-7.10 (m, 4H), 6.76-6.74 (m, 3H), 6.46 (d, *J* = 8 Hz, 1H), 4.79 (s, 2H), 4.27 (s, 2H), 3.99 (brs, 1H)



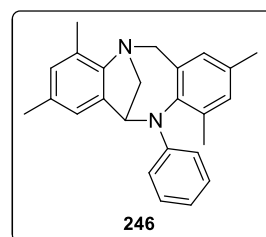
**$^{13}\text{C}$  NMR** : (100 MHz,  $\text{CDCl}_3$ ):  $\delta$  147.2, 146.5, 145.2, 137.4, 134.5, 132.9, 131.1, 130.9, 129.6, 129.2, 128.8, 126.2, 120.6, 118.7, 117.3, 115.8, 111.7, 53.1, 50.2

**HRMS** :  $m/z$   $[\text{M}+\text{H}]^+$  calcd for  $\text{C}_{20}\text{H}_{16}\text{N}_2\text{Br}_2$ : 442.9759; found 442.9744

**2,4,8,10-tetramethyl-11-phenyl-11,12-dihydro-6H-5,12-methanodibenzo[b,f][1,5]diazocine 246**

**Yield** : 0.125 g (35%)

**mp** : 135-138 °C



**IR (KBr)** : 2915, 2849, 1589, 1484, 1353, 1265, 1243, 849  $\text{cm}^{-1}$

**$^1\text{H}$  NMR** : (400 MHz,  $\text{CDCl}_3$ ):  $\delta$  7.19 (brs, 3H), 6.89 (s, 1H), 6.79-6.74 (m, 2H), 6.68 (s, 1H), 6.61 (s, 1H), 6.11 (brs, 1H), 5.29 (d,  $J = 4$  Hz, 1H), 4.33 (d,  $J = 16$  Hz, 1H), 4.18 (d,  $J = 12$  Hz, 1H), 3.67 (dd,  $J = 12$  Hz, 1H), 3.41 (d,  $J = 12$  Hz, 1H), 2.22 (s, 3H), 2.16 (d,  $J = 4$  Hz, 6H), 1.98 (s, 3H)

**$^{13}\text{C}$  NMR** : (100 MHz,  $\text{CDCl}_3$ ):  $\delta$  150.4, 146.7, 137.6, 137.5, 137.0, 136.5, 135.1, 134.2, 131.1, 130.3, 129.3, 128.2, 127.6, 121.9, 117.8, 65.5, 62.2, 59.4, 21.1, 20.7, 18.8, 16.9

**HRMS** :  $m/z$   $[\text{M}+\text{H}]^+$  calcd for  $\text{C}_{25}\text{H}_{26}\text{N}_2$ : 355.2175; found 355.2256

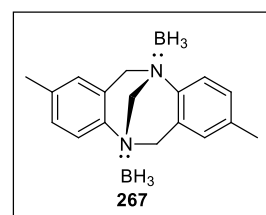
### 3.6 Hydroboration of olefins

#### 3.6.1 Preparation of Tröger base-borane complexes

To a two neck reaction flask containing  $\text{NaBH}_4$  in diglyme (5 mL) was added a solution of  $\text{I}_2$  in diglyme (15 mL) dropwise through addition funnel. The diborane gas generated in this way was bubbled through a side arm using bubbler into another reaction flask containing chiral Tröger base derivatives (5 mmol) in dry toluene (40 mL) at 0 °C. When the bubbling of the gas had ceased, the bubbler was removed and replaced by a glass stopper under nitrogen atmosphere. The concentration of this stock solution is approximately 0.12 M.

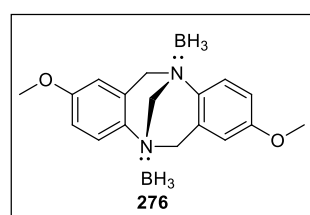
$^{11}\text{B}$  NMR (128.3 MHz, toluene,  $\delta$  ppm) -8.98

{ $\delta = 0$ ,  $\text{BF}_3\text{:Et}_2\text{O}$  (external reference)}



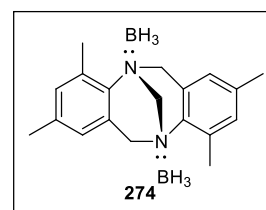
$^{11}\text{B}$  NMR (128.3 MHz, toluene,  $\delta$  ppm) -9.02

{ $\delta = 0$ ,  $\text{BF}_3\text{:Et}_2\text{O}$  (external reference)}



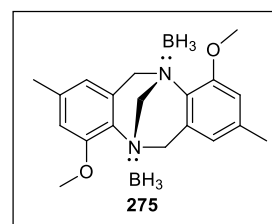
$^{11}\text{B}$  NMR (128.3 MHz, toluene,  $\delta$  ppm) -8.10

{ $\delta = 0$ ,  $\text{BF}_3\text{:Et}_2\text{O}$  (external reference)}



$^{11}\text{B}$  NMR (128.3 MHz, toluene,  $\delta$  ppm) -8.9

{ $\delta = 0$ ,  $\text{BF}_3\cdot\text{Et}_2\text{O}$  (external reference)}



### 3.6.2 Typical procedure for the estimation of the no. of coordinated 'N' atoms of the chiral Tröger base derivatives

To a reaction flask containing  $\text{PPh}_3$  (4 mmol, 1.048 g) was added borane complex stock solution (1 mmol, 8 mL) under  $\text{N}_2$  atmosphere at 25 °C. The reaction mixture was allowed to stir for 3 h at 25 °C. The solvent was evaporated and the residue was subjected to chromatography on silica gel column using hexane/ethyl acetate (96:4) as eluent to obtain triphenylphosphene-borane complex.

**Yield** : 44-47% (1.76-1.88 mmol)

$^{31}\text{P}$  NMR : (162 MHz, toluene,  $\delta$  ppm) 20.75 {  $\delta = 0$ ,  $\text{H}_3\text{PO}_4$  (external reference)}

### 3.6.3 General procedure for the hydroboration of olefins using chiral *ortho*-substituted Tröger base borane complexes

The reaction flask cooled under  $\text{N}_2$ , containing the corresponding borane complex (1 mmol, 8 mL in toluene), was added olefin (1 mmol) at 25 °C. This content was allowed to stir for 10 h at 25 °C. The reaction mixture was quenched with methanol (2 mL) and then oxidation was carried out for 4 h by adding 3 N NaOH (4 mL) and  $\text{H}_2\text{O}_2$  (30%, 4 mL). The organic layer was separated and the aqueous layer was extracted using ethyl acetate (2 x 10 mL). The combined organic layer was successively washed with water, brine and dried over

Na<sub>2</sub>SO<sub>4</sub>. The solvent was evaporated and the crude product was purified by chromatography on silica gel column using hexane/ethyl acetate (90:10) as eluent to isolate the product.

### 1,2-Diphenylethanol 264

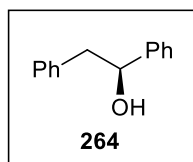
**Yield** : 79-98%

**mp** : 66-68 °C

**IR (KBr)** : 3315, 3024, 2920, 2854, 1030, 701 cm<sup>-1</sup>

**<sup>1</sup>H NMR** : (400 MHz, CDCl<sub>3</sub>): δ 7.32-7.22 (m, 10 H), 4.94-4.90 (m, 1H),  
3.00-3.09 (m, 2H), 2.14 (s, 1H)

**<sup>13</sup>C NMR** : (100 MHz, CDCl<sub>3</sub>): δ 143.8, 138.1, 129.5, 128.5, 128.4, 127.6,  
126.6, 125.9, 75.3, 46.1



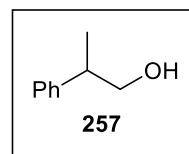
### 2-Phenylpropanol 257

**Yield** : 91-94%

**IR (neat)** : 3336, 3030, 2958, 1600, 1495, 1035, 756 cm<sup>-1</sup>

**<sup>1</sup>H NMR** : (400 MHz, CDCl<sub>3</sub>): δ 7.38-7.26 (m, 5H), 3.72 (d, *J* = 8.0 Hz, 2H),  
2.97 (d, *J* = 8.0 Hz, 1H), 1.48 (s, 1H), 1.31 (d, *J* = 8.0 Hz, 3H)

**<sup>13</sup>C NMR** : (100 MHz, CDCl<sub>3</sub>): δ 143.7, 128.7, 127.5, 126.7, 68.7, 42.5, 17.6



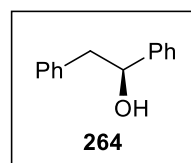


### 3.6.4 General procedure for the hydroboration of olefins using chiral *para*-substituted Tröger base borane complexes activated by iodine

The reaction flask cooled under N<sub>2</sub>, containing the corresponding borane complex (1 mmol, 8 mL in toluene), was added iodine (0.5 mmol, 0.125 g) in toluene (5 mL) at 0 °C. Then, olefin (1 mmol) was added at 0 °C. The resulting content was allowed to stir for 10 h at 25 °C. The reaction mixture was quenched with methanol (2 mL) and then oxidation was carried out for 4 h by adding 3 N NaOH (4 mL) and H<sub>2</sub>O<sub>2</sub> (30%, 4 mL). The organic layer was separated and the aqueous layer was extracted using ethyl acetate (2 x 10 mL). The combined organic layer was successively washed with water, brine and dried over Na<sub>2</sub>SO<sub>4</sub>. The solvent was evaporated and the crude product was purified by chromatography on silica gel column using hexane/ethyl acetate (90:10) as eluent to isolate the product.

#### 1,2-Diphenylethanol 264

**Yield** : 74-92%

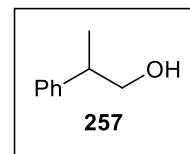


**IR (KBr)** : 3315, 3024, 2920, 2854, 1030, 701 cm<sup>-1</sup>

$[\alpha]_{\text{D}}^{25}$  : +3.6 (c, 0.5, EtOH), {lit.<sup>137</sup> for 100% ee,  $[\alpha]_{\text{D}}^{25} = +52.8$

(c, 1.40, EtOH(5% ee, confirmed by HPLC using chiral column, chiralcel OD-H, hexane/2-propanol= 90:10, flow rate: 0.5 mL/min.)

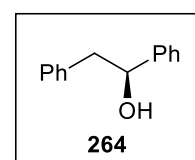
The spectral data of the corresponding products were showed 1:1 correspondence with the data obtained in the earlier experiments.

**2-Phenylpropanol 257****Yield** : 92%**IR (neat)** : 3336, 3030, 2958, 1600, 1495, 1035, 756 cm<sup>-1</sup>

The spectral data of the corresponding products were showed 1:1 correspondence with the data obtained in the earlier experiments.

**3.6.8 General procedure for the hydroboration of olefins using chiral Tröger base 32a borane complex activated by iodine in the presence of an additive.**

The reaction flask cooled under N<sub>2</sub>, containing the corresponding borane complex (1 mmol, 8 mL in toluene), was added iodine (0.5 mmol, 0.125 g) in toluene (5 mL). Then, olefin (1 mmol) and 1 mmol of additive were added immediately at 0 °C. The resulting content was allowed to stir for 12 h. The reaction mixture was quenched with methanol (2 mL) and then oxidation was carried out for 4 h by adding 3 N NaOH (4 mL) and H<sub>2</sub>O<sub>2</sub> (30%, 4 mL). The organic layer was separated and the aqueous layer was extracted using ethyl acetate (2 x 10 mL). The combined organic layer was successively washed with water, brine and dried over Na<sub>2</sub>SO<sub>4</sub>. The solvent was evaporated and the crude product was purified by chromatography on silica gel column using hexane/ethyl acetate (90:10) as eluent to isolate the product.

**1,2-Diphenylethanol 264****Yield** : 74-92%**IR (KBr)** : 3315, 3024, 2920, 2854, 1030, 701 cm<sup>-1</sup>

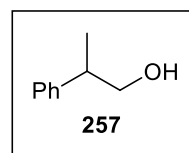
$[\alpha]_{\text{D}}^{25}$  : +3.2 (c, 0.72, EtOH), {lit.<sup>137</sup> for 100% ee,  $[\alpha]_{\text{D}}^{25} = +52.8$

(c, 1.40, EtOH(5% ee, confirmed by HPLC using chiral column,  
chiralcel OD-H, hexane/2-propanol= 90:10, flow rate: 0.5 mL/min.)

The spectral data of the corresponding products were showed 1:1 correspondence with the data obtained in the earlier experiments.

### 2-Phenylpropanol 257

**Yield** : 91%



**IR (neat)** : 3336, 3030, 2958, 1600, 1495, 1035, 756 cm<sup>-1</sup>

The spectral data of the corresponding products were showed 1:1 correspondence with the data obtained in the earlier experiments.

## References

---

1. Bushweller, C. H.; Wang, C. Y.; Reny, J.; Lourandos, M. Z. *J. Am. Chem. Soc.* **1977**, *99*, 3938.
2. a) Bushweller, C. H.; Anderson, W. G.; Stevenson, P. E.; Burkey, D. L.; Neil, J. W. *J. Am. Chem. Soc.* **1974**, *96*, 3892. b) Wash, P. L.; Renslo, A. R.; Rebek Jr., J. *Angew. Chem. Int. Ed.* **2001**, *40*, 1221.
3. Griffith, D. L.; Olson, B. L.; Roberts, J. D. *J. Am. Chem. Soc.* **1971**, *93*, 1648.
4. a) Brois, S. J. *J. Am. Chem. Soc.* **1968**, *90*, 506. b) Lehn, J. M.; Wagner, J. *Chem. Commun.* **1968**, 148. c) Felix, D.; Eschenmoser, A. *Angew. Chem.* **1968**, *7*, 224. d) Brois, S. J. *J. Am. Chem. Soc.* **1970**, *92*, 1079. e) Rauk, A.; Andose, J. D.; Frick, W. G.; Tang, R. J.; Mislow, K. J. *J. Am. Chem. Soc.* **1971**, *93*, 6507. f) Hall, J. H.; Bigard, W. S. *J. Org. Chem.* **1978**, *43*, 2785. g) Andose, J. D.; Lehn, J. M.; Mislow, K.; Wagner, J. *J. Am. Chem. Soc.* **1970**, *92*, 4050. h) Rudchenko, V. F.; Dyachenko, O. A.; Zolotoi, A. B.; Atovmyan, L. O.; Chervin, I. I.; Kostyanovsky, R. G. *Tetrahedron* **1982**, *38*, 961. i) Shustov, G. V.; Kadorkina, G. K.; Kostyanovsky, R. G.; Rauk, A. *J. Am. Chem. Soc.* **1988**, *110*, 1719. j) Trapp, O.; Sahraoui, L.; Hofstadt, W.; Konen, W. *Chirality* **2010**, *22*, 284.
5. a) Baechler, R. D.; Mislow, K. *J. Am. Chem. Soc.* **1970**, *92*, 3090. (b) Mislow, K.; Green, M. M.; Laur, P.; Melillo, J. T.; Simmons, T.; Ternay, A. L. *J. Am. Chem. Soc.* **1965**, *87*, 1958. (c) Valenzuela, F. A.; Green, T. K.; Dahl, D. B. *Anal. Chem.* **1998**, *70*, 3612.

6. Tröger, J. *J. Prakt. Chem.* **1887**, 36, 225.
7. a) Löb, Z. *Elektrochem.* **1898**, 4, 428. (b) Goecke, *ibid.* **1903**, 9, 470.
8. Eisner, A.; Wagner, E.C. *J. Am. Chem. Soc.* **1934**, 56, 1938.
9. Spielman, M. A. *J. Am. Chem. Soc.* **1935**, 57, 583.
10. a) Satishkumar, S.; Periasamy, M. *Tetrahedron: Asymmetry* **2006**, 17, 1116. b) Satishkumar, S.; Periasamy, M. *Tetrahedron: Asymmetry* **2009**, 20, 2257.
11. Satishkumar, S.; Periasamy, M. *Indian J. Chem.* **2008**, 47B, 1080.
12. Li, Z.; Xu, X.; Peng, Y.; Jiang, Z.; Ding, C.; Qian, X. *Synthesis* **2005**, 8, 1228.
13. a) Wilcox, C.S. *Tetrahedron Lett.* **1985**, 26, 5749. b) Adrian, J. C. Wilcox, C. S. *J. Am. Chem. Soc.* **1992**, 114, 1398. c) Miller, T.R.; Wagner, E.C. *J. Am. Chem. Soc.* **1941**, 63, 832. d) Häring, M. *Helv. Chim. Acta* **1963**, 46, 2970.
14. Hansson, A.; Jensen, J.; F. Wendt, O. F.; Warnmark, K. *Eur. J. Org. Chem.* **2003**, 3179.
15. Bag, B.G. Maitra, U. *Synth. Commun.* **1995**, 25, 1849.
16. a) Tatibouet, A.; Demeunynck, M.; Lhomme, J. *Synth. Commun.* **1996**, 26, 4375. b) Jensen, J.; Tejler, J.; Warnmark, K. *J. Org. Chem.* **2002**, 67, 6008. c) Faroughi, M.; Zhu, K.-X.; Jensen, P.; Craig, D. C.; Try, A. C. *Eur. J. Org. Chem.* **2009**, 4266. d) Bhuiyan, M. D. H.; Zhu, K.-X.; Jensen, P.; Try, A. C. *Eur. J. Org. Chem.* **2010**, 4662.
17. Bhuiyan, M. D. H.; Mahon, A. B.; Jensen, P.; Clegg, J. K.; Try, A. C. *Eur. J. Org. Chem.* **2009**, 687.
18. a) Meisenheimer, J.; Angermann, L.; Finn, O.; Vieweg, E. *Ber.Dtsch. Chem. Ges.* **1924**, 57, 1747. (b) Meisenheimer, J.; Theilacker, W. In: *Stereochemie*; Freudenberg, K., Ed.; Deuticke: Leipzig-Wien, **1933**, 1147. (c) Lambert, J. B. *Top. Stereochem.* **1971**, 6, 19.

19. Prelog, V.; Wieland, P. *Helv. Chim. Acta.* **1944**, 27, 1127.
20. Greenberg, A.; Molinaro, N.; Lang, M. *J. Org. Chem.* **1984**, 49, 1127.
21. Trapp, O.; Schurig, V. *J. Am. Chem. Soc.* **2000**, 122, 1424.
22. Revesz, A.; Schröder, D.; Rokob, T. A.; Havlik, M.; Dolensky, B. *Angew. Chem. Int. Ed.* **2011**, 50, 2401.
23. Trapp, O.; Trapp, G.; Kong, J.; Hahn, U.; Vogtle, F.; Schurig, V. *Chem. Eur. J.* **2002**, 8, 3629.
24. Lauber, A.; Zelenay, B.; Cvengros, J. *Chem. Commun.* **2014**, 50, 1195.
25. Ondrisek, P.; Schwenk, R.; Cvengros, J. *Chem. Commun.* **2014**, 50, 9168.
26. Hamada, Y.; Mukai, S. *Tetrahedron: Asymmetry* **1996**, 7, 2671.
27. Lenev, D. A.; Lyssenko, K. A.; Golovanov, D. G.; Buss, V.; Kostyanovsky, R. G. *Chem.–Eur. J.*, **2006**, 12, 6412.
28. Wilen, S. H.; Qi, J. Z.; Williard, P. G. *J. Org. Chem.* **1991**, 56, 485.
29. Valik, M.; Dolensky, B.; Herdtweck, E.; Kral, V. *Tetrahedron: Asymmetry* **2005**, 16, 1969.
30. Talas, E.; Margitfalvi, J.; Machytka, D.; Czugler, M. *Tetrahedron: Asymmetry* **1998**, 9, 4151.
31. Kostyanovsky, R. G.; Kostyanovsky, V. R.; Kadorkina, G. K.; Lyssenko, K. A. *Mendeleev Commun.* **2003**, 13, 111.
32. Tatibouet, A.; Demeunynck, M.; Andraud, C.; Collet, A.; Lhomme, J. *Chem. Commun.* **1999**, 161.
33. Jin, Z.; Guo, S. X.; Gu, X. P.; Qiu, L. L.; Wu, G. P.; Fang, J. X. *ARKIVOC* **2009**, 10, 25.
34. Rigol, S.; Beyer, L.; Hennig, L.; Sieler, J.; Giannis, A. *Org. Lett.* **2013**, 15, 1418.

35. a) Schunk, C.B.; Wezislá, B.; Urbahn, K.; Kiehne, U.; Daniels, J.; Schnakenburg, G.; Neese, F.; Lutzen, A. *ChemPlusChem* **2012**, *77*, 396. b) Shamshurin, D. V.; Zavarzin, I. V.; Yarovenko, V. N.; Chernoburova, E. I.; Krayushkin, M. M.; Volgin, Y. V.; Sharpovalova, E. N.; Nesterenko, P. N.; Shpigun, O. A. *Mendeleev Commun.* **2005**, *15*, 143. c) Okamoto, Y.; Nagamura, Y.; Fukumoto, T.; Hatada, K. *Polymer Journal* **1991**, *23*, 1197. d) Schurig, V.; Schmalzing, D.; Schleimer, M. *Angew. Chem. Int. Ed. Engl.* **1991**, *30*, 987. e) Okamoto, Y.; Sakamoto, H.; Hatada, K.; Irie, m. *Chem. Lett.* **1986**, 983. f) Mechref, Y.; Rassi, Z. E. *J. Chromatogr. A.* **1996**, *724*, 285. g) Krause, K.; Chankvetadze, B.; Okamoto, Y.; Blaschke, G. *Electrophoresis*, **1999**, *20*, 2772. h) Okamoto, Y.; Okamoto, I.; Yuki, H. *Chem. Lett.* **1981**, 835. i) Pedferri, M.; Zenoni, G.; Mazzotti, M.; Morbidelli, M. *Chem. Eng. Sci.* **1999**, *54*, 3735. j) Zenoni, G.; Pedferri, M.; Mazzotti, M.; Morbidelli, M. *J. Chromatogr. A.* **2000**, *888*, 73. k) Seidel-Morgenstern, A.; Guiochon, G. *J. Chromatogr.* **1993**, *631*, 37.
36. a) Didier, D.; Tylleman, B.; Lambert, N.; Velde, C. M. L. V.; Blockhuys, F.; Collas.; Sergeyev, S. *Tetrahedron* **2008**, *64*, 6252. (b). Schunk, C. B.; Wezislá, B.; Urbahn, K.; Kiehne, U.; Daniels, J.; Schnakenburg, G.; Neese, F.; Lutzen, A. *ChemPlusChem* **2012**, *77*, 396. (c). Didier, D.; Sergeyev, S. *ARKIVOC* **2009**, *14*, 124.
37. a) Metlesics, W.; Tavares, R.; Sternbach, L. H. *J. Org. Chem.* **1966**, *31*, 3356. b) Metlesics, W.; Resnick, T.; Silverman, G.; Tavares, R.; Sternbach, L. H. *J. Med. Chem.* **1966**, *9*, 633.
38. Maitra, U.; Bag, B. G. *J. Org. Chem.* **1992**, *57*, 6979.
39. Maitra, U.; Bag, B. G.; Powell, D. *J. Chem. Soc. Perkin Trans. I* **1995**, 2049.

40. Dolensky, B.; Elguero, J.; Kral, V.; Pardo, C.; Valik, M. *Adv. Heterocycl. Chem.* **2007**, 93, 1. b) Sergeyev, S. *Helv. Chim. Acta* **2009**, 92, 415. c) Runarsson, O. V.; Artacho, J.; Wärnmark, K. *Eur. J. Org. Chem.* **2012**, 7015.
41. Lemaire, V.; Cornil, J.; Didier, D.; Mujawase, A.; Sergeyev, S. *Helvetica Chimica Acta* **2007**, 90, 2087.
42. Didier, D.; Sergeyev, S. *Eur. J. Org. Chem.* 2007, 3905. b) Faroughi, M.; Jensen, P.; Try, A. C. *ARKIVOC*, **2009**, 2, 269.
43. a) Kiehne, U.; Lützen, A. *Synthesis* **2004**, 1695. b) Hof, F.; Schär, M.; Scofield, D. M.; Fischer, F.; Diederich, F.; Sergeyev, S. *Helv. Chim. Acta* **2005**, 88, 2333.
44. Jensen, J.; Wärnmark, K. *Synthesis* **2001**, 1873.
45. a) Jensen, J.; Strozyk, M.; Wärnmark, K. *Synthesis* **2002**, 18, 2761. b) Bew, S. P.; Legentil, L.; Scholier, V.; Sharma, S. V. *Chem. Commun.* **2007**, 389
46. Solano, C.; Svensson, D.; Olomi, Z.; Jensen, J.; Wendt, O. F.; Wärnmark, K. *Eur. J. Org. Chem.* **2005**, 3510.
47. a) Jensen, J.; Wärnmark, K. *Synthesis* **2001**, 12, 2761. b) Kiehne, U.; Bruhn, T.; Schnakenburg, G.; Frohlich, R.; Bringmann, G.; Lützen, A. *Chem. Eur. J.* **2008**, 14, 4246
48. . Didier, D.; Sergeyev, S. *Tetrahedron* **2007**, 63, 3864.
49. a) Weber, E.; Müller, U.; Worsch, D.; Vogtle, F.; Will, G.; Kirfel, A. *J. Chem. Soc. Chem. Commun.* **1985**, 1578.
50. Lenev, D. A.; Golovvanov, D. G.; Lyssenko, K. A.; Kostyanovsky, R. G. *Tetrahedron: Asymmetry* **2006**, 17, 2191.
51. a) Hamada, Y.; Mukai, S. *Tetrahedron: Asymmetry* **1996**, 7, 2671. b) Harmata, M.; Rayanil, K.-O.; Barnes, C. L. *Supramol. Chem.* **2006**, 18, 581.



52. Artacho, J.; Ascic, E.; Rantanen, T.; Karlsson, J.; Wallentin, C.-J.; Wang, R.; Wendt, O. F.; Harmata, M.; Snieckus, V.; Wärnmark, K. *Chem. Eur. J.* **2012**, *18*, 1038.
53. Artacho, J.; Ascic, E.; Rantanen, T.; Wallentin, C.-J.; Dawaigher, S.; Bergquist, K.-E.; Harmata, M.; Snieckus, V.; Wärnmark, K. *Org. Lett.* **2012**, *14*, 4706.
54. Copper, F. C.; Partridge, M. W. *J. Chem. Soc.* **1957**, 2888.
55. a) Johnson, R. A.; Gorman, R. R.; Wnuk, R. J.; Crittenden, N. J.; Aiken, J. W. *J. Med. Chem.* **1993**, *36*, 3202. b) Mahon, A. B.; Craig, D. C.; Try, A. C. *ARKIVOC* **2008**, *12*, 148.
56. Lee, K.Y.; Gowrisankar, S.; Kim, J. N. *Synlett* **2006**, *9*, 1389.
57. Lenev, D. A.; Chervin, I. I.; Lyssenko, K. A.; Kostyanovsky, R. G. *Tetrahedron Lett.* **2007**, *48*, 3363.
58. Mahon, A. B.; Craig, D. C.; Try, A. C. *Synthesis* **2009**, *5*, 636.
59. Faroughi, M.; Try, A. C.; Klepetko, J.; Turner, P. *Tetrahedron Lett.* **2007**, *48*, 6548.
60. Michon, C.; Sharma, A.; Bernardinelli, G.; Francotte, E.; Lacour, J. *Chem.commu*, **2010**, *46*, 2206.
61. Sharma, A.; Guenee, L.; Naubron, J.-V.; Lacour, J. *Angew. Chem. Int. Ed.* **2011**, *50*, 677.
62. Gao, X.; Hampton, C. S.; Harmata, M. *Eur. J. Org. Chem.* **2012**, 7053.
63. Paliwal, S.; Geib, S.; Wilcox, C. S. *J. Am. Chem. Soc.* **1994**, *116*, 4497.
64. Bhayana, B.; Ams, M. R. *J. Org. Chem.* **2011**, *76*, 3594.
65. Goldberg, Y.; Alper, H. *Tetrahedron Lett.* **1995**, *36*, 369.
66. Cuenu, F.; Abonia, R.; Bolanos, A.; Cabrera, A. *J. Organomet.Chem.* **2011**, *696*, 1834.
67. Pereira, R.; Cvengros, J. *Eur. J. Org. Chem.* **2013**, 4233.

68. a) Minder, B.; Schurch, M.; Mallat, T.; Baiker, A. *Catal. Lett.* **1995**, *31*, 143. b) Xu, F.; Tilleyer, R. D.; Tschaen, D. M.; Grabowski, E. J. J.; Reider, P. J. *Tetrahedron: Asymmetry* **1998**, *37*, 1651.
69. Harmata, M.; Kahraman, M. *Tetrahedron: Asymmetry* **2000**, *11*, 2875.
70. a) Shen, Y.-M.; Zhao, M.-X.; Xu, J.; Shi, Y. *Angew. Chem. Int. Ed.* **2006**, *45*, 8005.
71. Sturala, J.; Cibulka, R. *E. J. Org. Chem.* **2012**, 7066.
72. a) Pereira, R.; Cvengros, C. *J. Organomet.Chem.* **2013**, 729, 81. b) Cvengros, C.; Maennel, E.; Santschi, N. *Dalton Trans.*, **2012**, *41*, 7415.
73. France, S.; Guerin, D. J.; Miller, S. J. Lectka, T. *Chem. Rev.* **2003**, *103*, 2985.
74. a) Padmaja, M.; Periasamy, M. *Tetrahedron:Asymmetry* **2004**, *15*, 2437. (b). Periasamy, M.; Sreenivasaperumal, M.; Padmaja, M.; Rao, V. D. *ARKIVOC* **2004**, *8*, 4. (c). Vairaprakash, P.; Periasamy, M. *J. Org. Chem.* **2006**, *71*, 3636. (d) Periasamy, M.; Edukondalu, A.; Reddy, P. O. *J. Org. Chem.* **2015**, *80*, 3651.
75. (a) Periasamy, M.; Kumar, N. S.; Sivakumar, S.; Rao, V. D.; Ramanathan, C. R.; Venkatraman, L. *J. Org. Chem.* **2001**, *66*, 3828. (b) Periasamy, M.; Sivakumar, S.; Reddy, M. N.; Padmaja, M. *Org. Lett.* **2004**, *6*, 265. (c) Periasamy, M.; Reddy, M. N.; Anwar, S. *Tetrahedron:Asymmetry* **2004**, *15*, 1809. (d) Periasamy, M.; Sivakumar, S.; Reddy, M. N. *Synthesis* **2003**, *13*, 965. (e) Periasamy, M.; Ramanathan, C. R.; Sampath Kumar, N. *Tetrahedron:Asymmetry* **1999**, *10*, 2307.
76. Ramanathan, C. R.; Periasamy, M. *Tetrahedron:Asymmetry* **1998**, *9*, 2651.
77. Periasamy, M.; Rao, V. D.; Perumal, M. S. *Tetrahedron:Asymmetry* **2001**, *12*, 1887.
78. a) Periasamy, M.; Venkatraman, L.; Sivakumar, S.; Sampath Kumar, N.; Ramanathan, C. R. *J. Org. Chem.* **1999**, *64*, 7643. (b) Periasamy, M.; Ramanathan, C. R. Bhanu Prasad, A. S; Bhaskar Kanth, J. V. *Enantiomer* **1998**, *3*, 3. (c) Periasamy, M.;

- Venkatraman, L.; Thomas, K. R. J. *J. Org. Chem.* **1997**, 62, 4302. (d) Venkatraman, L.; Periasamy, M. *Tetrahedron:Asymmetry* **1996**, 7, 2471. (e) Periasamy, M. Bhanu Prasad, A. S.; Bhaskar Kanth, J. V.; Kishan Reddy, Ch. *Tetrahedron:Asymmetry* **1995**, 6, 341.
79. Jameson, D. L.; Field, T.; Schmidt, M. R.; DeStefano, A. K.; Stiteler, C. J.; Venditto, V. J.; Krovic, B.; Hoffman, C. M.; Ondisco, M. T.; Belowich, M. E. *J. Org. Chem.* **2013**, 78, 11590.
80. Lenev, D.; Lyssenko, K. A.; Golovanov, D. G.; Malyshev, O. R.; Levkin, P. A.; Kostyanovsky, R. G. *Tetrahedron Lett.* **2006**, 47, 319.
81. Satishkumar, S. Ph.D. Thesis **2009**, University of Hyderabad.
82. Vairaprakash, P.; Periasamy, M. *J. Chem Sci.* **2008**, 120, 175.
83. Kiehne, U.; Bruhn, T.; Schnakenburg, G.; Frohlich, R.; Bringmann, G.; Lutzen, A. *Chem. Eur. J.* **2008**, 14, 4246.
84. a) Jensen, J.; Warnmark, K. *Synthesis* **2001**, 12, 1873.
85. Malik, Q. M.; Ijaz, S.; Craig, D. C.; Try, A. C. *Tetrahedron* **2011**, 67, 5798.
86. a) Malik, Q. M.; Mahon, A. B.; Craig, D. C.; Try, A. C. *Tetraheron* **2011**, 67, 8509.  
b) Reddy, M. B.; Manjula, A.; Rao, B. V.; Sridhar, B. *Eur. J. Org. Chem.* **2012** 312.
87. Pujari, S. A.; Guenee, L.; Lacour, J. *Org. Lett.* **2013**, 15, 3930.
88. (a) Fischer, C.; Koenig, B. *Beilstein J. Org. Chem.* **2011**, 7, 59. (b) Hong, Y.; Senanayake, C. H.; Xiang, T.; Vandenbossche, C. P.; Tanoury, G. J.; Bakale, R. P.; Wald, S. A. *Tetrahedron Lett.* **1998**, 39, 3121. (c) *CRC Handbook of Pesticides*; Milne, G. W. A., Ed.; CRC Press: Boca Raton, **1994**. (d) Shiota, Y. *J. Mater. Chem.* **2000**, 10, 1.

89. a) Monnier, F.; Taillefer, M. *Angew. Chem., Int. Ed.* **2009**, *48*, 6954. (b) Kunz, K.; Scholz, U.; Ganzer, D. *Synlett* **2003**, 2428. (c) Ley, S. V.; Thomas, A. W. *Angew. Chem., Int. Ed.* **2003**, *42*, 5400.
90. a) Hartwig, J. F. *Acc. Chem. Res.* **2008**, *41*, 1534. b) Wolfe, J. P.; Wagaw, S.; Marcoux, J.-F.; Buchwald, S. L. *Acc. Chem. Res.* **1998**, *31*, 805.
91. a) Chan, D. M. T.; Monaco, K. L.; Wang, R. P.; Winter, M. P. *Tetrahedron Lett.* **1998**, *39*, 2933. b) Evans, D. A.; Katz, J. L.; West, T. R. *Tetrahedron Lett.* **1998**, *39*, 2937. (c) Qiao, J. X.; Lam, P. Y. S. *Synthesis* **2011**, 829.
92. a) Kuhl, N.; Hopkinson, M. N.; Wencel-Delord, J.; Glorius, F. *Angew. Chem., Int. Ed.* **2012**, *51*, 10236. b) Cho, S. H.; Kim, J. Y.; Kwak, J.; Chang, S. *Chem. Soc. Rev.* **2011**, *40*, 5068. c) Zhang, M.; Zhang, A. *Synthesis* **2012**, 1. d) Barker, T. J.; Jarvo, E. R. *Synthesis* **2011**, 3954. e) Ou, L.; Shao, J.; Zhang, G.; Yu, Y. *Tetrahedron Lett.* **2011**, *52*, 1430. f) Xiao, Q.; Tian, L.; Tan, R.; Xia, Y.; Qiu, D.; Zhang, Y.; Wang, J. *Org. Lett.* **2012**, *14*, 4230. g) Zhu, C.; Li, G.; Ess, D. H.; Falck, J. R.; Kurti, L. *J. Am. Chem. Soc.* **2012**, *134*, 18253. h) Mlynarski, S. N.; Karns, A. S.; Morken, J. P. *J. Am. Chem. Soc.* **2012**, *134*, 16449. i) Coeffard, V.; Moreau, X.; Thomassigny, C.; Greck, C. *Angew. Chem., Int. Ed.* **2013**, *52*, 5684.
93. Ramirez, C. L.; Pegoraro, C.; Trupp, L.; Bruttomesso, A.; Amorebieta, V.; Vera, D. M. V.; Parise, A. R. *Phys. Chem. Chem. Phys.* **2011**, *13*, 20076.
94. Neogi, I.; Jhulki, S.; Ghosh, A.; Chow, T. J.; Moorthy, J. N. *ACS Appl. Mater. Interfaces.* **2015**, *7*, 3298.
95. Sathyanarayana, A.; Prabusankar, G. *New J. Chem.* **2014**, *38*, 3613.
96. Kanth, J. V. B.; Periasamy, M. *J. Org. Chem.* **1993**, *58*, 3156.
97. Periasamy, M.; Vairaprakash, P.; Dalai, M. *Organometallics*, **2008**, *27*, 1963.

98. Alakonda, L.; Periasamy, M. *Synthesis*, **2012**, *44*, 1063.
99. Alakonda, L.; Periasamy, M. *J. Organomet. Chem.* **2009**, *694*, 3859.
100. a) Shi, L.; Wang, M.; Fan, C. A.; Zhang, F. M.; Tu, Y. Q. *Org. Lett.* **2003**, *5*, 3515.  
(b) Bajracharya, G. B.; Daugulis, O. *Org. Lett.* **2008**, *10*, 4625.
101. a) Brown, H. C.; Chandrasekharan, J. *J. Am. Chem. Soc.* **1984**, *106*, 1863. b) Pasto, D. J.; Lepeska, B.; Cheng, T –C. *J. Am. Chem. Soc.* **1972**, *94*, 6083. (c) Pasto, D. J.; Cumbo, C. C.; Balasubramanian, P. *J. Am. Chem. Soc.* **1966**, *88*, 2187. (d) Kalbalka, G. W.; Wadgaonkar, P. P.; Shoup, T. M. *Organometallics* **1990**, *9*, 1316. (e) Dewar, M. J.S.; Mckee, M. L. *Inorg. Chem.* **1978**, *17*, 1075. (f) Streitwieser, A.; Verbit, L.; Bittman, K. *J. Org. Chem.* **1967**, *32*, 1530. (g) Rickborn, B.; Wood, S. E. *J. Org. Chem.* **1983**, *48*, 555.
102. Narayana, C.; Periasamy, M. *Chem. Commun.* **1987**, 1857.
103. Julia, M. C.; Vedejs, E. *J. Am. Chem. Soc.* **2005**, *127*, 5766.
104. Anwar, S. Ph.D. Thesis **2008**, University of Hyderabad. b). Selva Ganesan, S. Ph. D. Thesis, **2009**, School of chemistry, University of Hyderabad.
105. a) Periasamy, M.; Muthukumaragopal, G. P.; Sanjeevakumar, N. *Tetrahedron Lett.* **2007**, *48*, 6966. b) Anwar, S.; Periasamy, M. *Tetrahedron: Asymmetry* **2006**, *17*, 3244. c) Kanth, J. V. B.; Periasamy, M. *J. Chem. Soc. Chem. Commun.*, **1990**, 1145.  
d) Reddy, Ch. K.; Periasamy, M. *Tetrahedron Lett.* **1989**, *30*, 5663. e) Reddy, Ch. K.; Periasamy, M. *Tetrahedron* **1992**, *48*, 8329. f) Reddy, Ch. K.; Periasamy, M. *Tetrahedron Lett.* **1990**, *31*, 1919. g) Reddy, Ch. K.; Kanth, J. V. B.; Periasamy, M. *Synth. Commun.* **1994**, *243*, 313.
106. Vries, T. S. D.; Prokofjevs, A.; Vedejs, E. *Chem. Rev.* **2012**, *112*, 4246.

107. a) Mulliken, R. S. *J. Am. Chem. Soc.* **1952**, 74, 811. b) McConnell, Ham, Platt, *J. Chem. Phys.* **1953**, 21, 66.
108. Bijl, D.; Kainer, H.; Innes, A. C. R. *J. Chem. Phys.* **1959**, 30, 765.
109. a) Taube, H.; Myers, H. J.; Rich, R. L. *J. Am. Chem. Soc.* **1953**, 75, 4118. b) Taube, H. *Science* **1984**, 226, 1028.
110. a) Marcus, R. A. *J. Chem. Phys.* **1956**, 24, 966. b) Marcus, R. A. *Angew. Chem. Int. ed.* **1993**, 32, 1111.
111. a) Marcus, R. A. *Discuss. Faraday Soc.* **1960**, 29, 21. b) Marcus, R. A. *J. Phys. Chem.* **1963**, 67, 853. c) Marcus, R. A. *J. Chem. Phys.* **1965**, 43, 679. d) Marcus, R. A. *Rev. Mod. Phys.* **1993**, 65, 599. e) Marcus, R. A. Sutin, N. *Biochim. Biophys. Acta.* **1983**, 8, 391.
112. a) Rosokha, S. V.; Kochi, J. K. *New J. Chem.* **2002**, 26, 851. b) Rosokha, S. V. Dibro, S. M.; Rosokha, t. Y.; Kochi, J. K. *photochem. Photobiol. Sci.* **2006**, 5, 914.
113. Rosokha, S. V.; Kochi, J. K. *Acc. Chem. Res.* **2008**, 41, 641.
114. a) Rathore, R.; Lindeman, S. V.; Kochi, J. K. *J. Am. Chem. Soc.* **1997**, 119, 9393. b) Bondi, A. *J. Phys. Chem.* **1964**, 68, 441.
115. a) Fukuzumi, S.; Wong, C. L.; Kochi, J. K.; *J. Am. Chem. Soc.* **1980**, 102, 2928. b) Kochi, J. K. *Pure Appl. Chem.* **1990**, 52, 571. c) Kochi, J. K. *Angew. Chem. Int. Ed. Engl.* **1988**, 27, 1227. d) Sun, D. L.; Rosokha, S. V.; Lindeman, S. V.; Kochi, J. K. *J. Am. Chem. Soc.* **2003**, 125, 15950.
116. a) Rosokha, S. V.; Kochi, J. K. *J. Am. Chem. Soc.* **2007**, 129, 3683. b) Sun, D.; Rosokha, S. V.; Kochi, J. K. *J. Phys. Chem. B.* **2007**, 111, 6655.
117. Nogami, T.; Yoshihara, K.; Hosoya, H.; Nagakura, S. *J. Phys. Chem.* **1969**, 73, 2670.
118. Yamaoka, T.; Nagakura, S. *Bull. Chem. Soc. Japan* **1971**, 44, 2971.

119. a) Mckinney, T. M.; Geske, D. H. *J. Am. Chem. Soc.* **1965**, 87, 3013.
120. a) Nelsen, S. F.; Ippoliti, J. T. *J. Am. Chem. Soc.* **1986**, 108, 4879. b) Zwier, J. M.; Brouwer, A. M.; Keszthelyi, T.; Balakrishnan, G.; Offersgaard, J. F.; Wilbrandt, R.; Barbosa, F.; Buser, U.; Amaudrut, J.; Gescheidt, G.; Nelsen, S. F.; Little, C. D. *J. Am. Chem. Soc.* **2002**, 124, 159. c) Zheng, Z. R.; Evans, D. H.; Nelsen, S. F. *J. Org. Chem.* **2000**, 65, 1793.
121. Sersen, F.; Koscal, S.; Banacky, P.; Krasnec, L. *Collection Czechoslov. Chem. Commun.* **1977**, 42, 2173.
122. Ward, R. L.; Weissman, S. I. *J. Am. Chem. Soc.* **1957**, 79, 2086.
123. Periasamy, M.; Shanmugaraja, M.; Ramusagar, M. *unpublished results*.
124. Guo, X.; Mayr, H. *J. Am. Chem. Soc.* **2014**, 136, 11499.
125. Guo, X.; Mayr, H. *J. Am. Chem. Soc.* **2013**, 135, 12377.
126. a) Nagakura, S. *Mol. Cryst. Liq. Cryst.* **1985**, 126, 9. b) Nogami, T.; Yamaoka, T.; Yoshihara, K.; Nagakura, S. *Bull. Chem. Soc. Japan.* **1971**, 44, 380. c) Sato, Y.; Kinoshita, M.; Sano, M.; Akamatu, H. *Bull. Chem. Soc. Japan.* **1970**, 43, 2370 d) Foster, R.; Thomson, J. *Trans. Faraday. Soc.* **1962**, 58, 860.
127. a) Lu, J. M.; Rosokha, S. V.; Lindeman, S. V.; Neretin, I. S.; Kochi, J. K. *J. Am. Chem. Soc.* **2005**, 127, 1797. b) Lu, J. M.; Rosokha, S. V.; Lindeman, S. V.; Neretin, I. S.; Kochi, J. K. *J. Am. Chem. Soc.* **2006**, 128, 16708.
128. Soos, Z.G.; Keller, H. J.; Ludolf, K.; Queckborner, J.; Wehe, D. *J. Chem. Phys.* **1981**, 74, 5287.
129. Sakamaki, D.; Yano, S.; Kobashi, T.; Seki, S.; Kurahashi, T.; Matsubara, S.; Ito, A.; Tanaka, K. *Angew. Chem. Int. Ed.* **2015**, 54, 8267.

130. a) Mastracchio, A.; Warkentin, A. A.; Walji, A. M.; MacMillan, D. W. C. *Proc. Nat. Acad. Sci. USA*, **2010**, *107*, 20648. b) Beeson, T. B.; Mastracchio, A.; Hong, J. B.; Ashton, K.; MacMillan, D. W. C. *SCIENCE* **2007**, *316*, 27.
131. a) Periasamy, M.; Jayakumar, K. N.; Bharathi, P. *J. Org. Chem.* **2000**, *65*, 3548. b) Xi, C.-J.; Jiang, Y.-F.; Yang, X.-H. *Tetrahedron Lett.* **2005**, *46*, 3909. c) Jiang, Y.-F.; Xi, C.-J.; Yang, X.-H. *Synlett* **2005**, 1381. d) Yang, X.-H.; Xi, C.-J.; Jiang, Y.-F. *Synth. Commun.* **2006**, *36*, 2413. e) Kirchgessner, M.; Sreenath, K.; Gopidas, K. R. *J. Org. Chem.* **2006**, *71*, 9849. f) Sreenath, K.; Suneesh, C. V.; Kumar, V. K. R.; Gopidas, K. R. *J. Org. Chem.* **2008**, *73*, 3245.
132. a) Willstatter, R.; Dorogi, S. *Ber.* **1909**, *42*, 4118. b) Mohilner, D. M.; Adams, R. N. Argersinger, W. J. *J. Am. Chem. Soc.* **1962**, *84*, 3618. c) Davied, S.; Nicolau, Y. F.; Melis, F.; Revillon, A. *Synth Met.* **1995**, *69* 125. d) MacDiarmid, A. G.; Chiang, J. C.; Richter, A. F.; Epstein, A. J. *Synth. Met.* **1987**, *18*, 285.
133. Osa, T.; Kashiwagi, Y.; Yanagisawa, Y.; Bobbitt, J. M. *J. Chem. Soc. Chem. Commun.* **1994**, 2535.
134. Iseki, K.; Kuroki, Y.; Kobayashi, Y. *Tetrahedron: Asymmetry* **1998**, *9*, 2889.
135. Sucholeiki, I.; Lynch, V.; Phan, L.; Wilcox, C. S. *J. Org. Chem.* **1988**, *53*, 98.
136. Li, Z.; Xu, X.; Peng, Y.; Jiang, Z.; Ding, C.; Qian, X. *Synthesis* **2005**, 1228.
137. Gerrard, W.; Kenyon, J. *J. Chem. Soc.* **1928**, 2564.

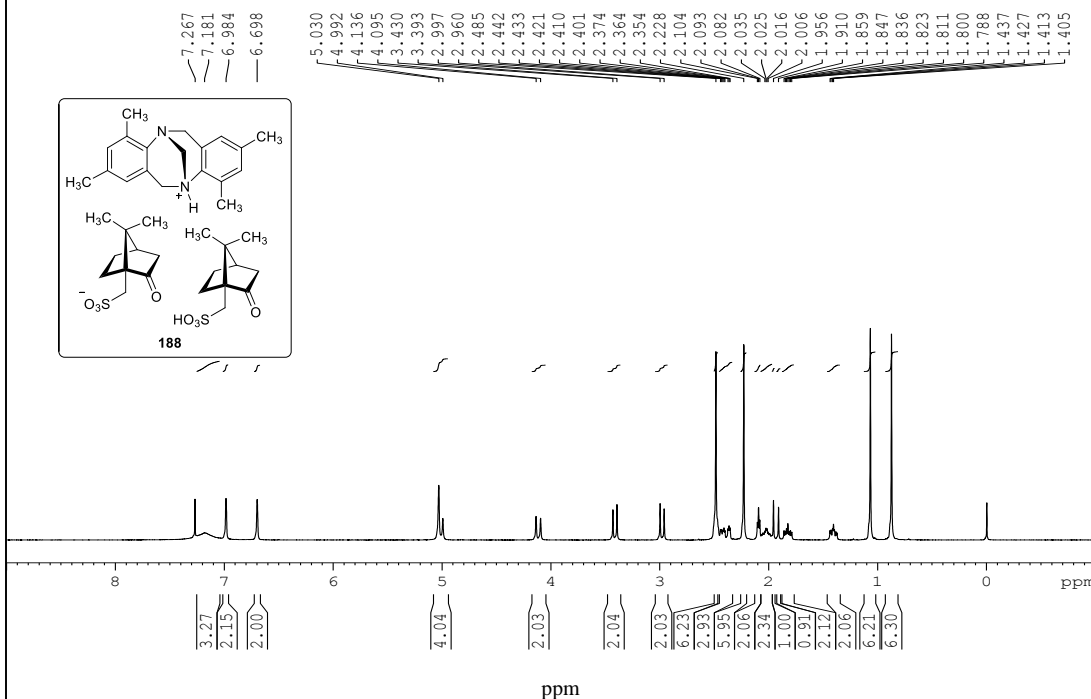
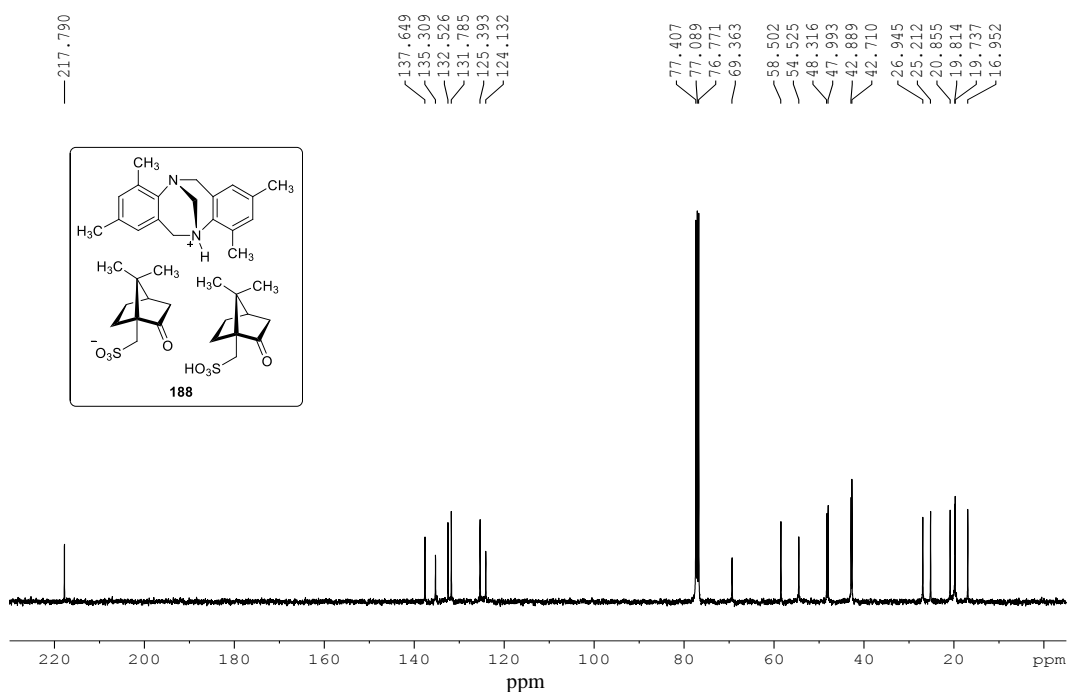


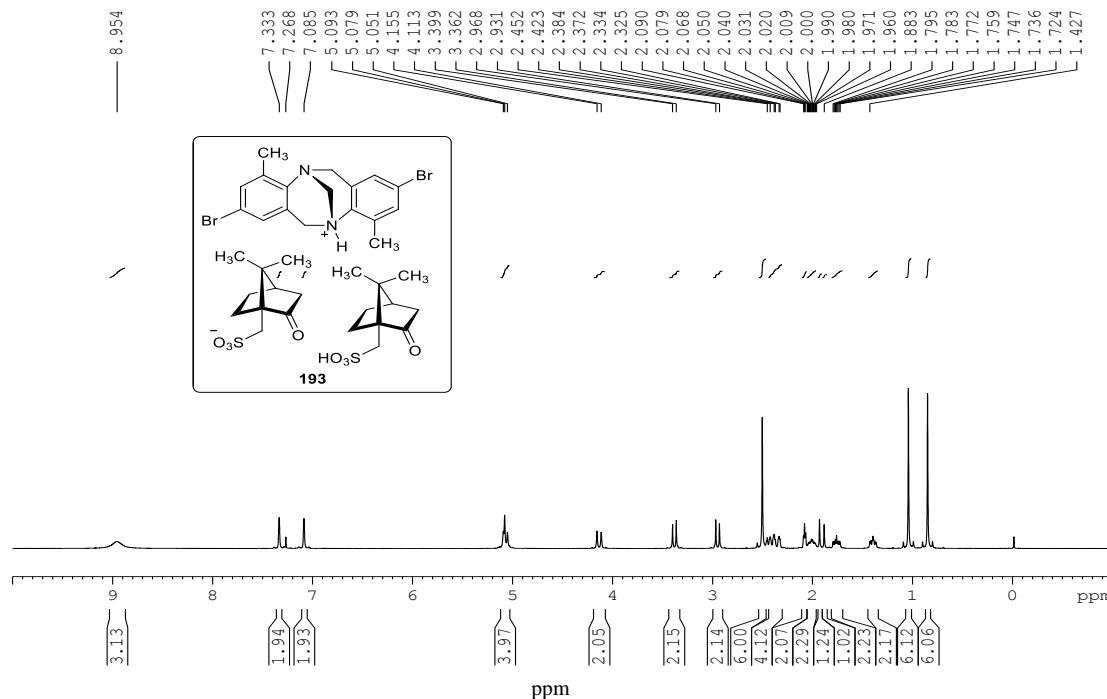
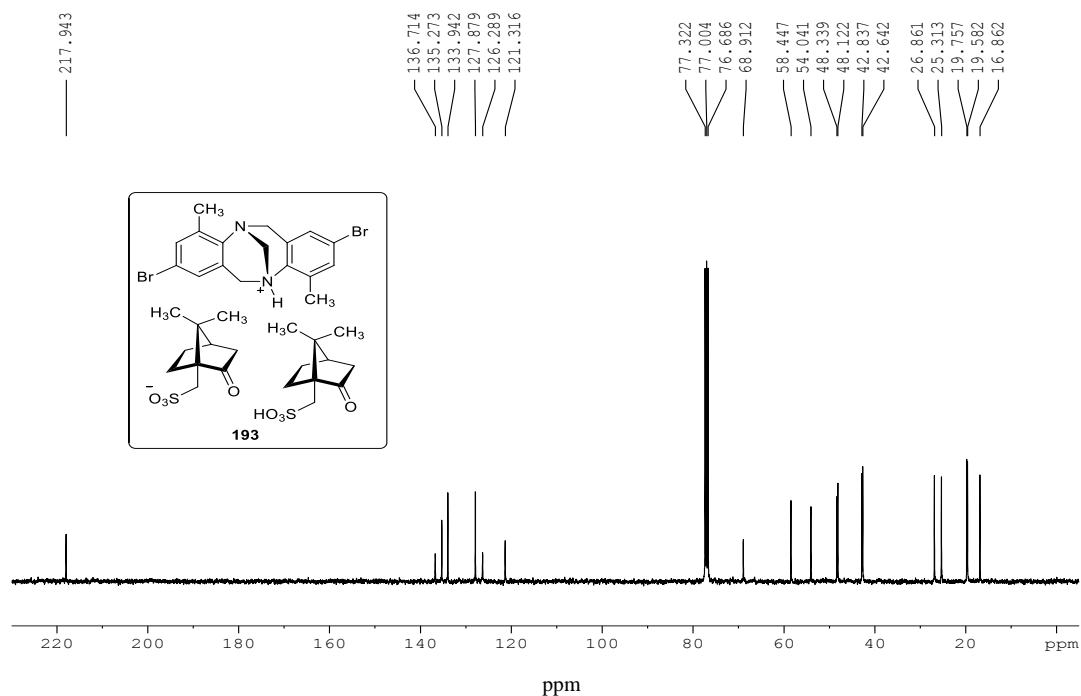
---

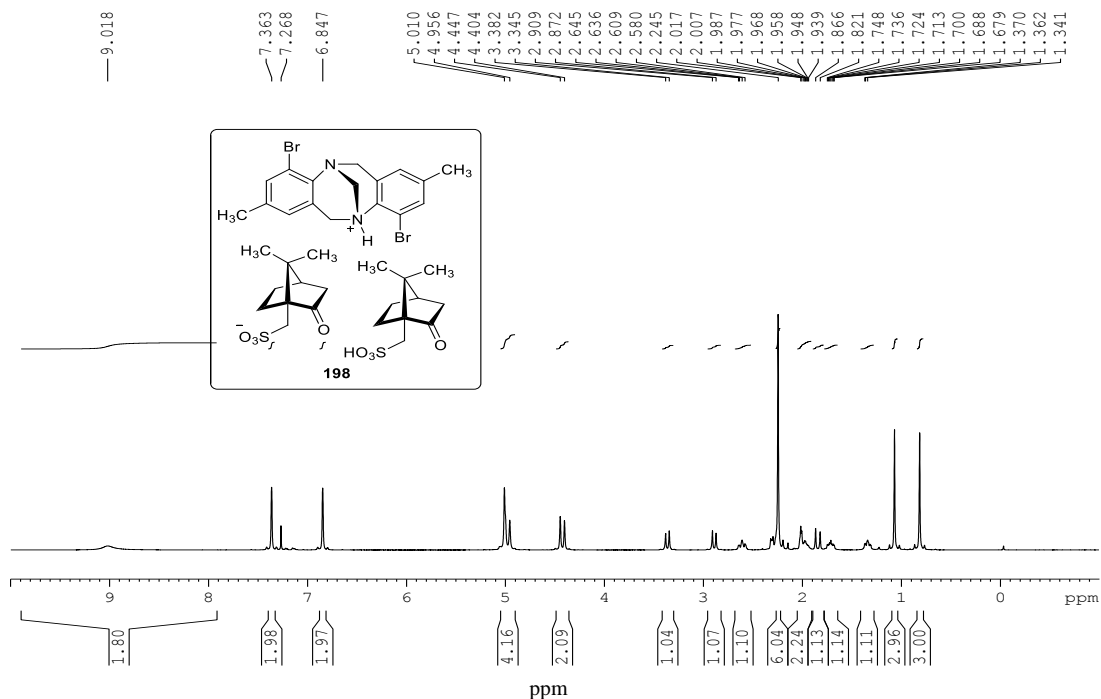
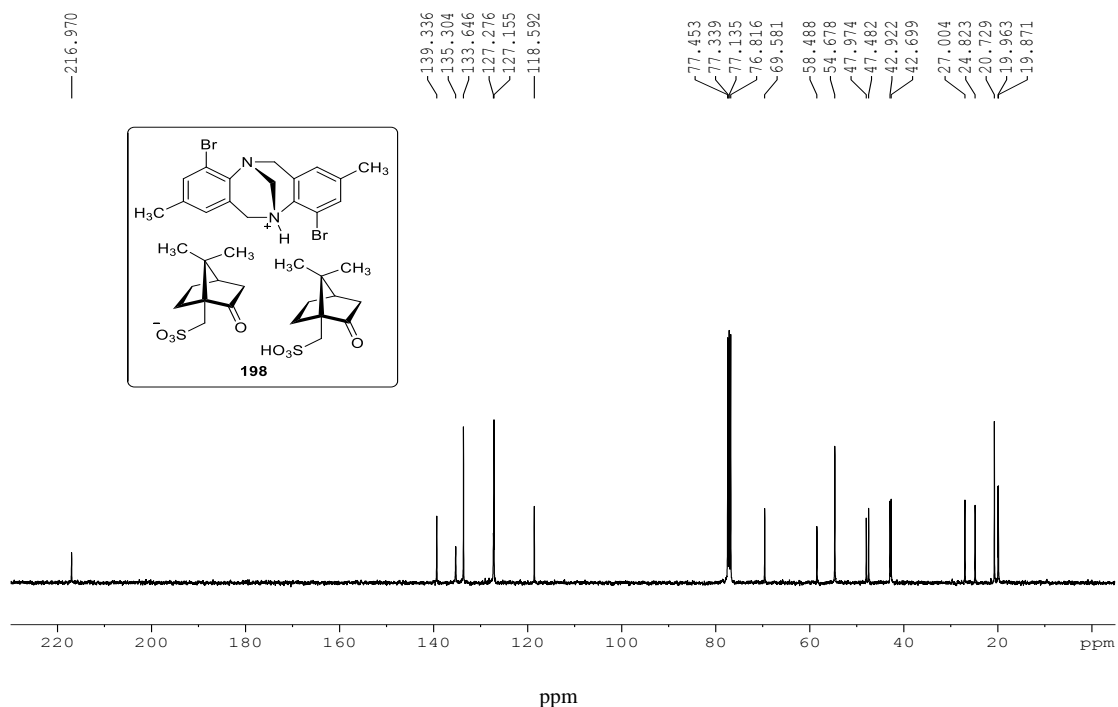
*Appendix I*

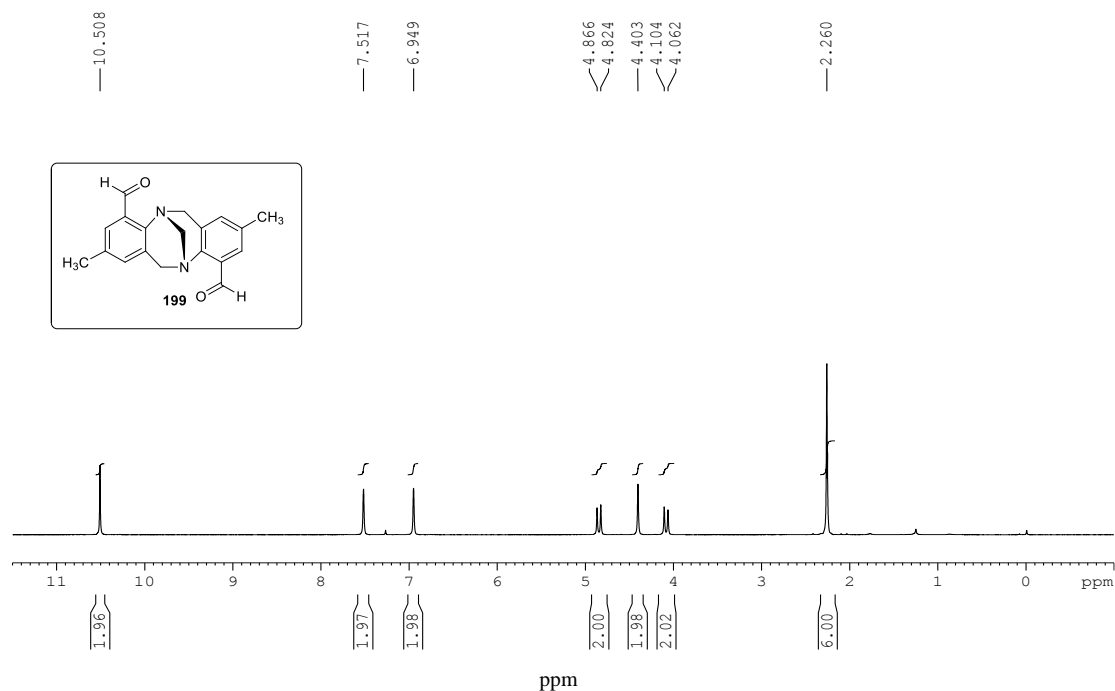
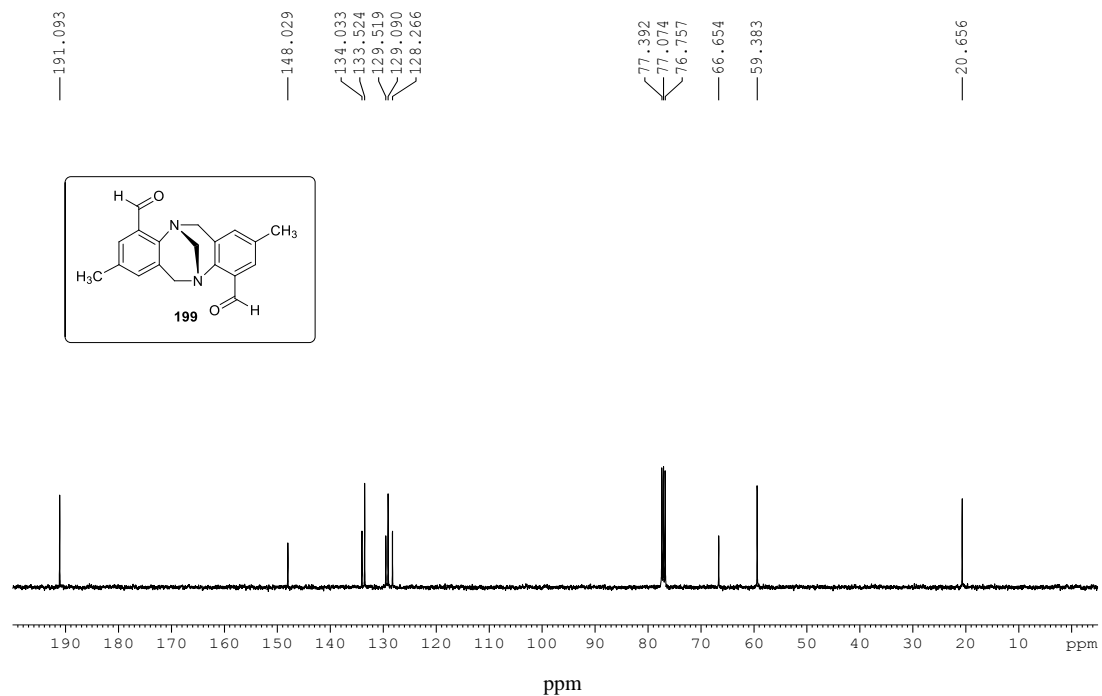
*(Representative Spectra)*

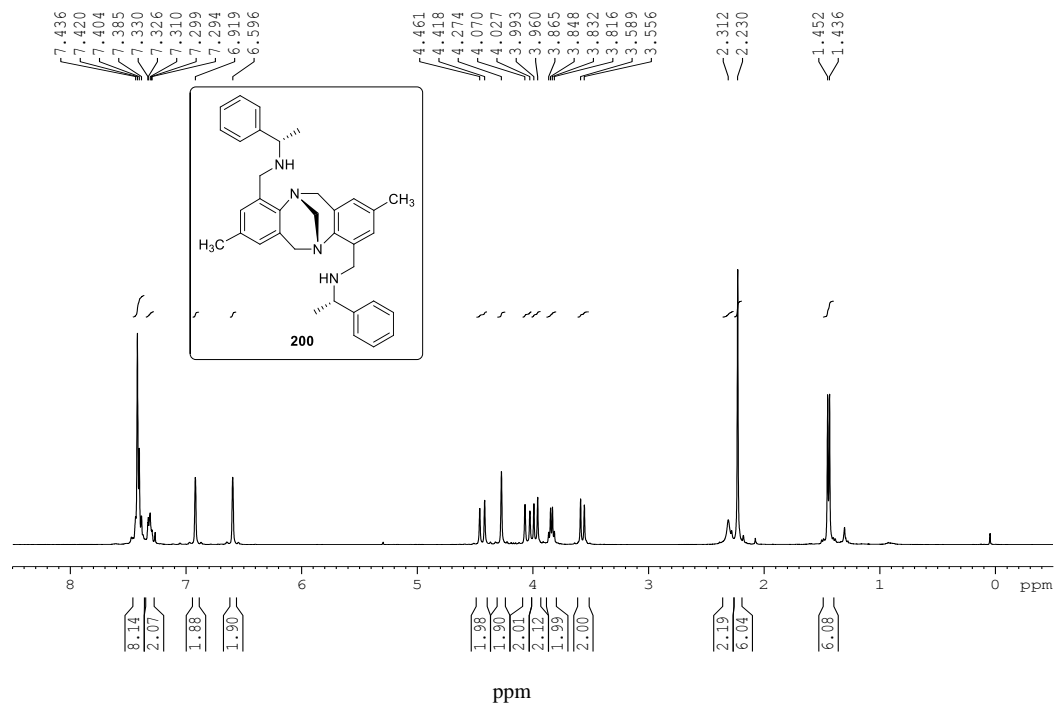
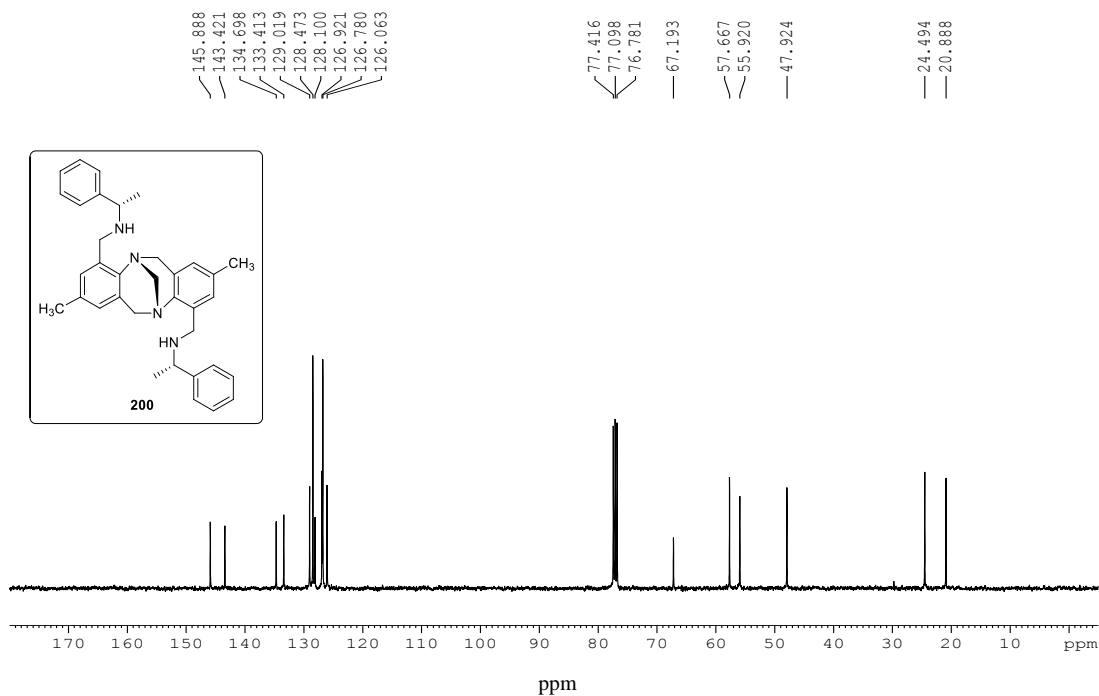
---

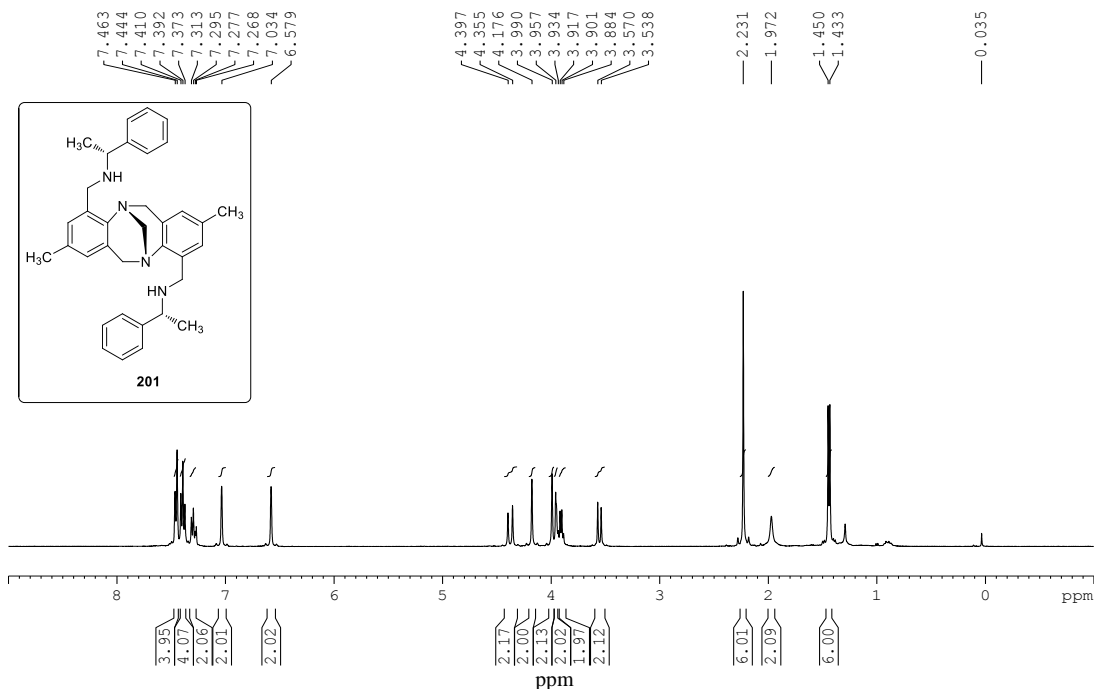
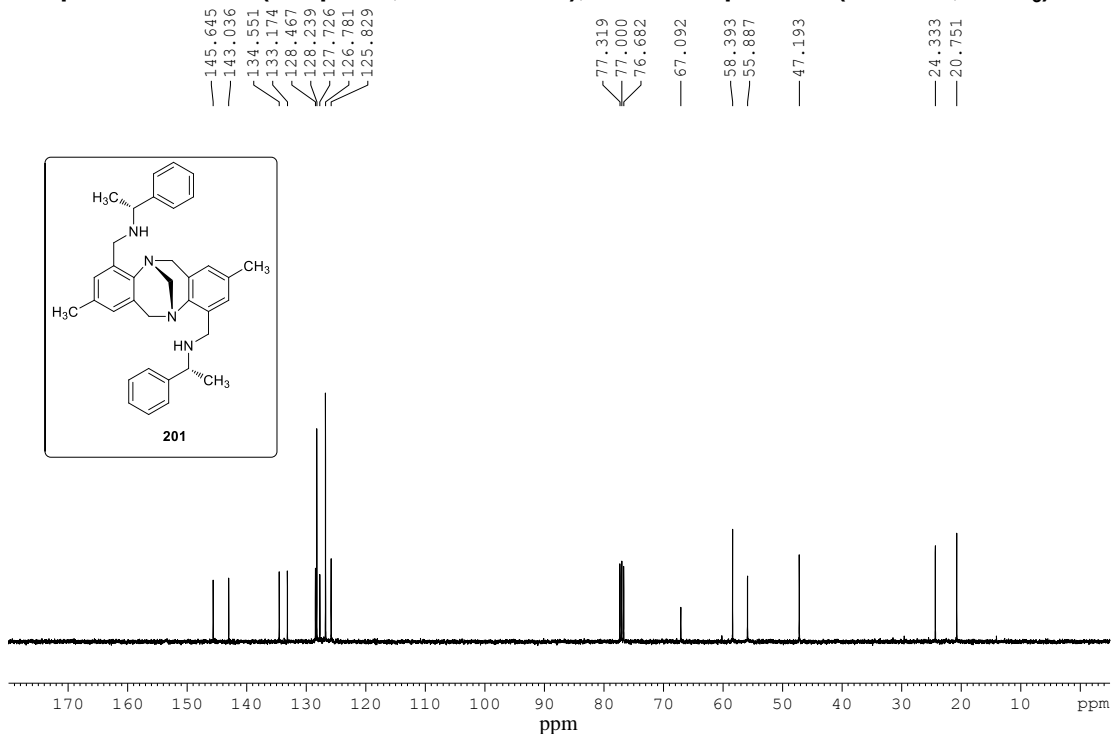
**Spectrum No. 1 (Chapter 3, Section 3.3.2),  $^1\text{H}$  NMR Spectrum (400 MHz,  $\text{CDCl}_3$ )****Spectrum No. 2 (Chapter 3, Section 3.3.2),  $^{13}\text{C}$  NMR Spectrum (100 MHz,  $\text{CDCl}_3$ )**

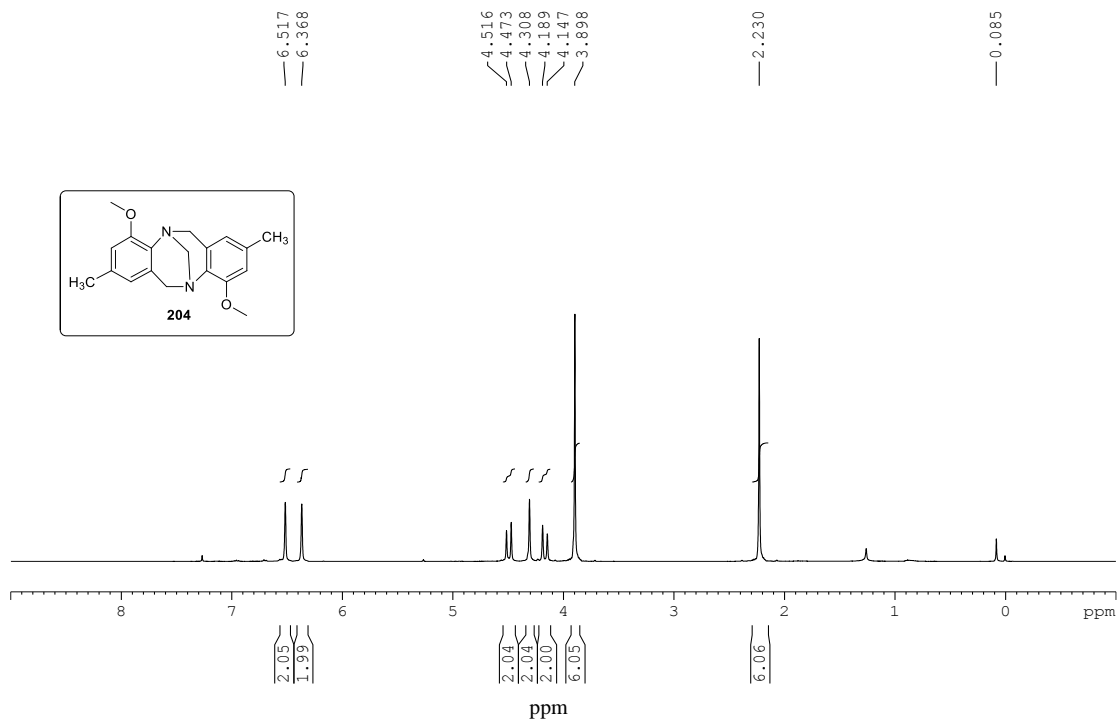
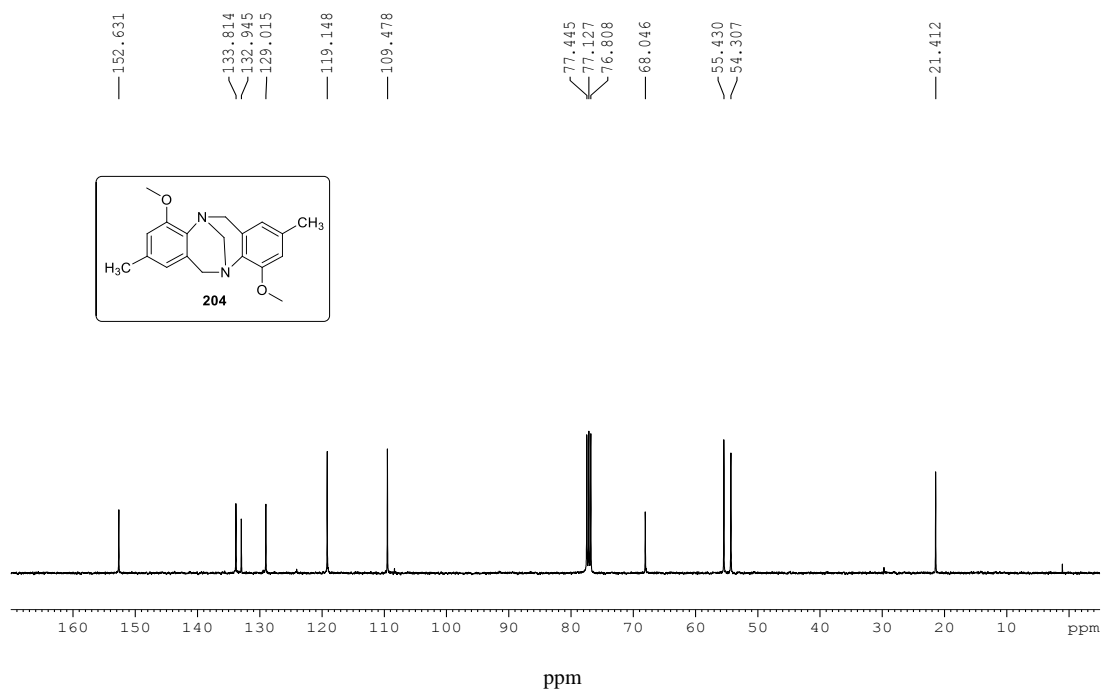
**Spectrum No. 3 (Chapter 3, Section 3.3.3),  $^1\text{H}$  NMR Spectrum (400 MHz,  $\text{CDCl}_3$ )**

**Spectrum No. 4 (Chapter 3, Section 3.3.3),  $^{13}\text{C}$  NMR Spectrum (100 MHz,  $\text{CDCl}_3$ )**


**Spectrum No. 5 (Chapter 3, Section 3.3.5),  $^1\text{H}$  NMR Spectrum (400 MHz,  $\text{CDCl}_3$ )**

**Spectrum No. 6 (Chapter 3, Section 3.3.5),  $^{13}\text{C}$  NMR Spectrum (100 MHz,  $\text{CDCl}_3$ )**


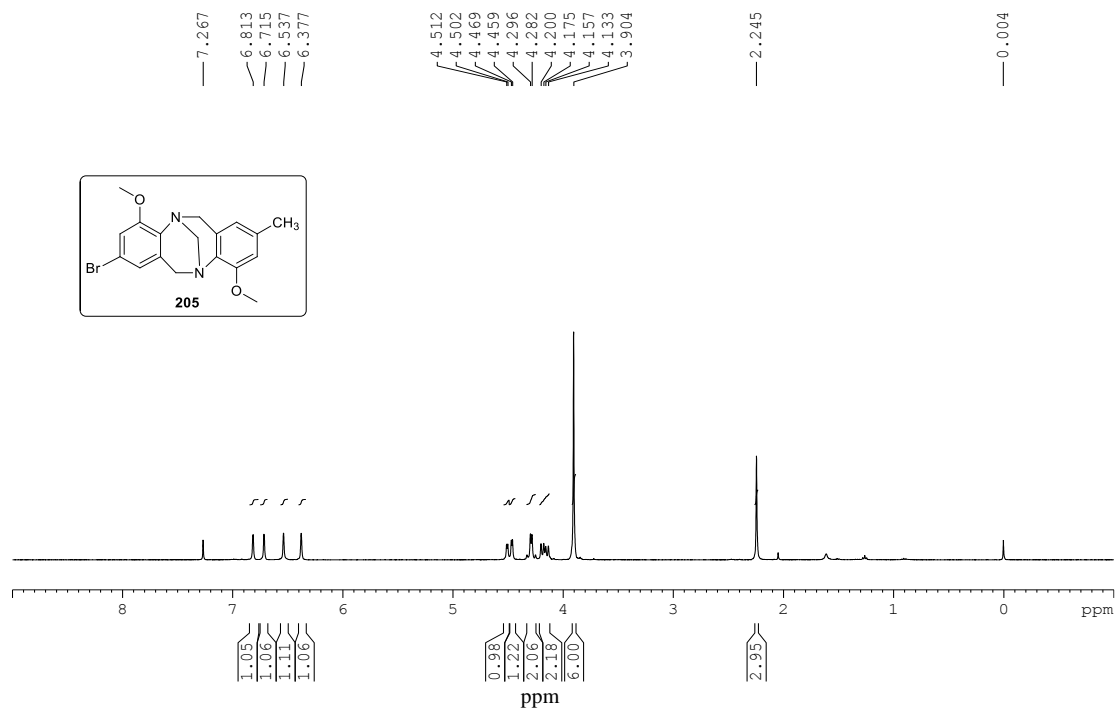
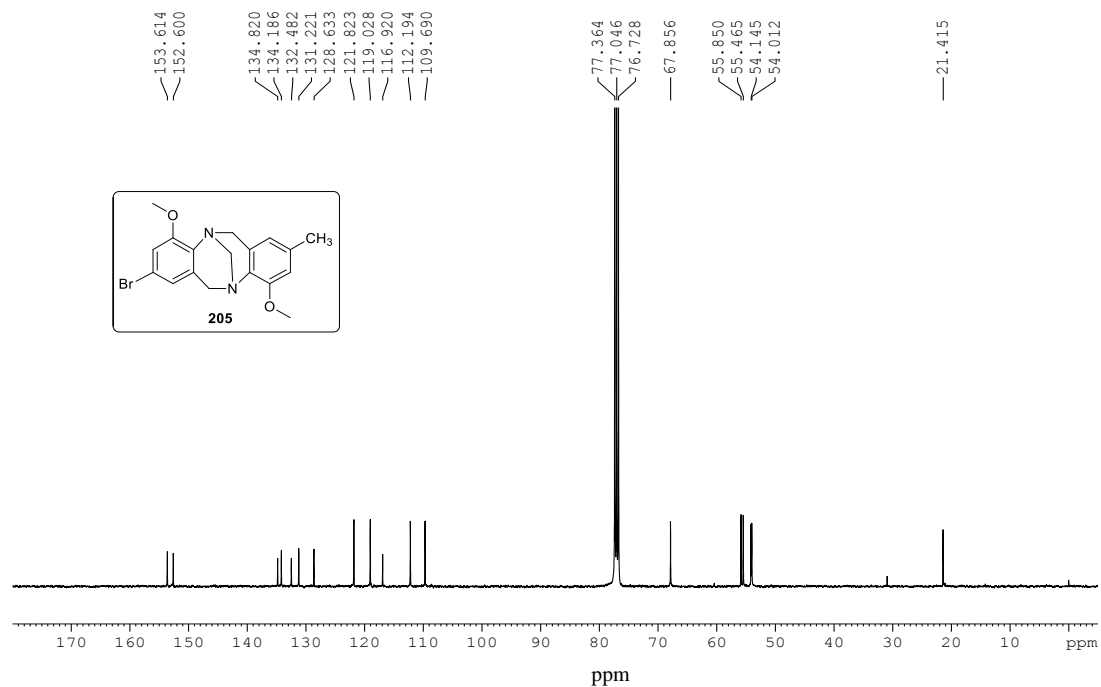
**Spectrum No. 7 (Chapter 3, Section 3.3.6),  $^1\text{H}$  NMR Spectrum (400 MHz,  $\text{CDCl}_3$ )****Spectrum No. 8 (Chapter 3, Section 3.3.6),  $^{13}\text{C}$  NMR Spectrum (100 MHz,  $\text{CDCl}_3$ )**

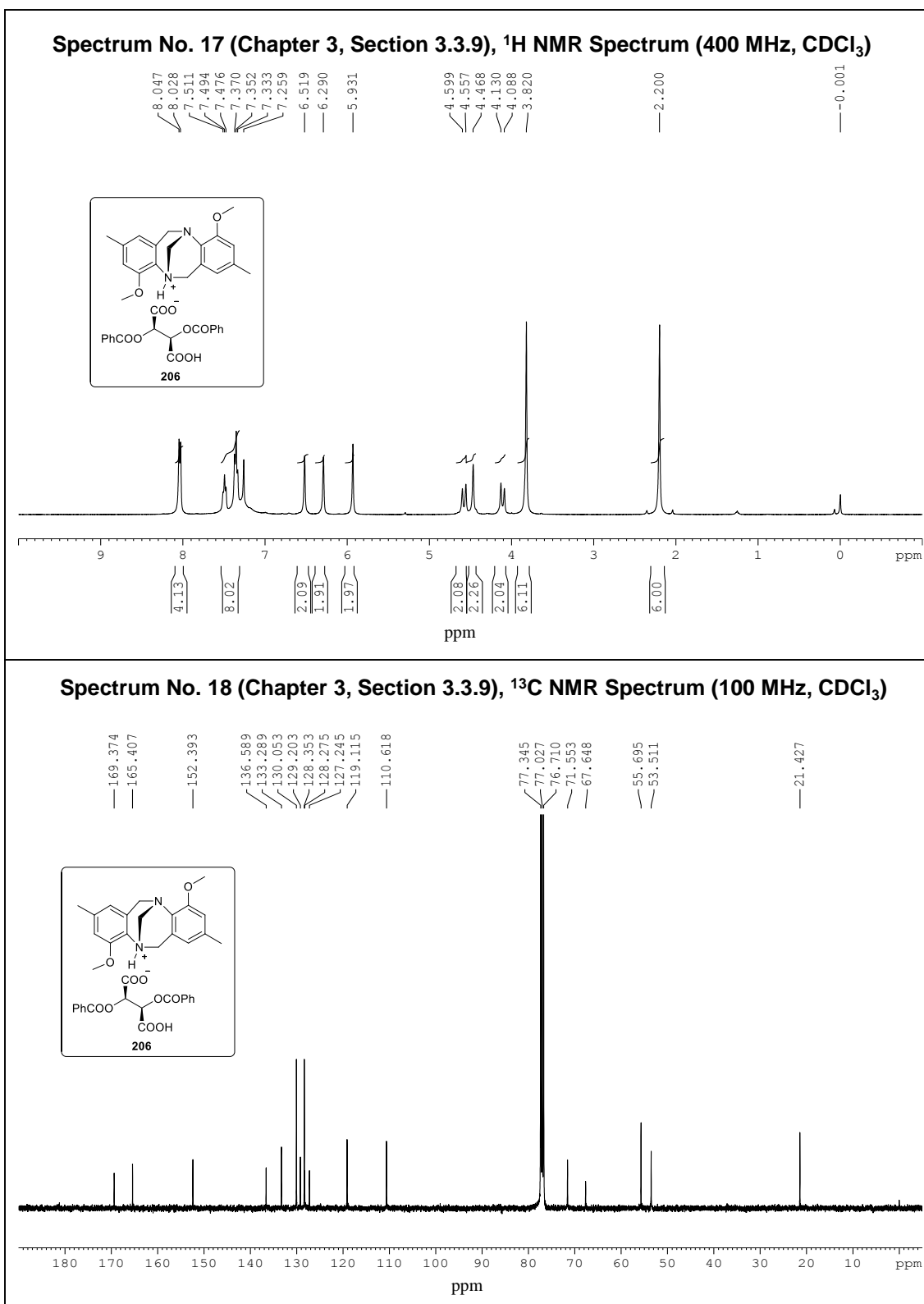
**Spectrum No. 9 (Chapter 3, Section 3.3.7),  $^1\text{H}$  NMR Spectrum (400 MHz,  $\text{CDCl}_3$ )****Spectrum No. 10 (Chapter 3, Section 3.3.7),  $^{13}\text{C}$  NMR Spectrum (100 MHz,  $\text{CDCl}_3$ )**

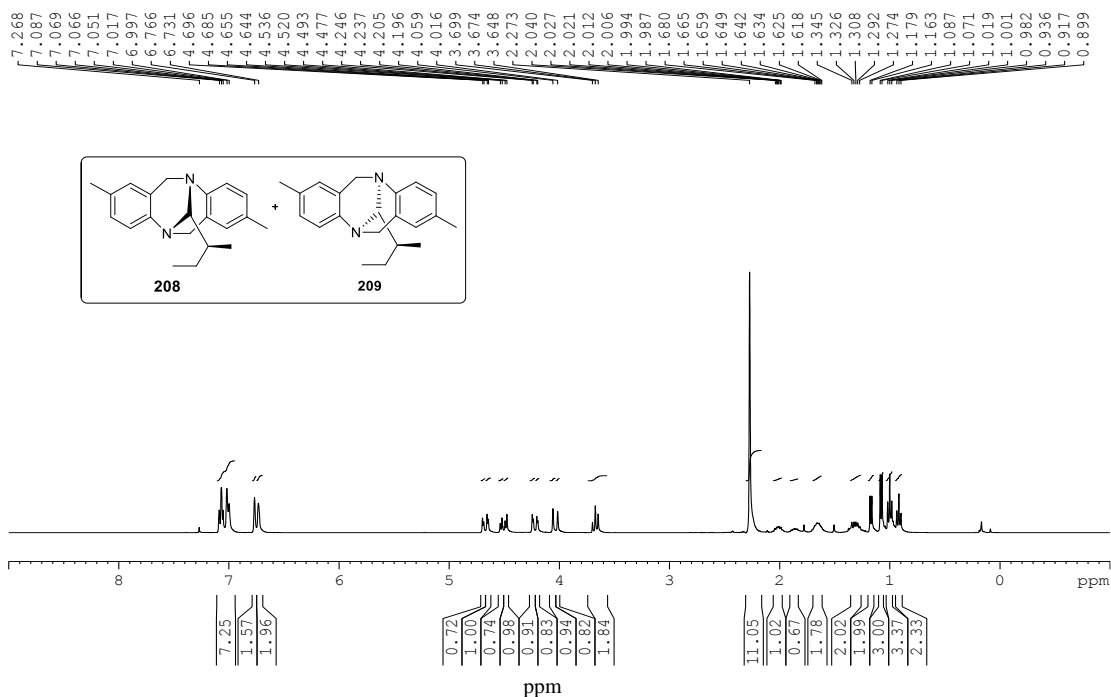
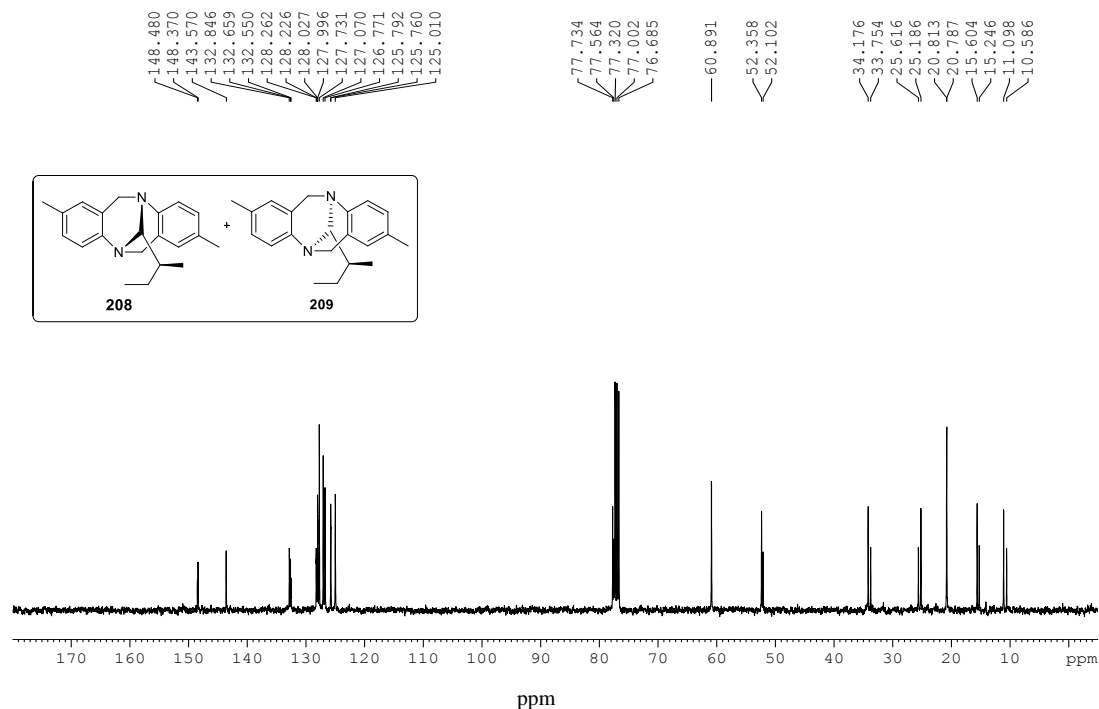
**Spectrum No. 11 (Chapter 3, Section 3.3.7),  $^1\text{H}$  NMR Spectrum (400 MHz,  $\text{CDCl}_3$ )****Spectrum No. 12 (Chapter 3, Section 3.3.7),  $^{13}\text{C}$  NMR Spectrum (100 MHz,  $\text{CDCl}_3$ )**

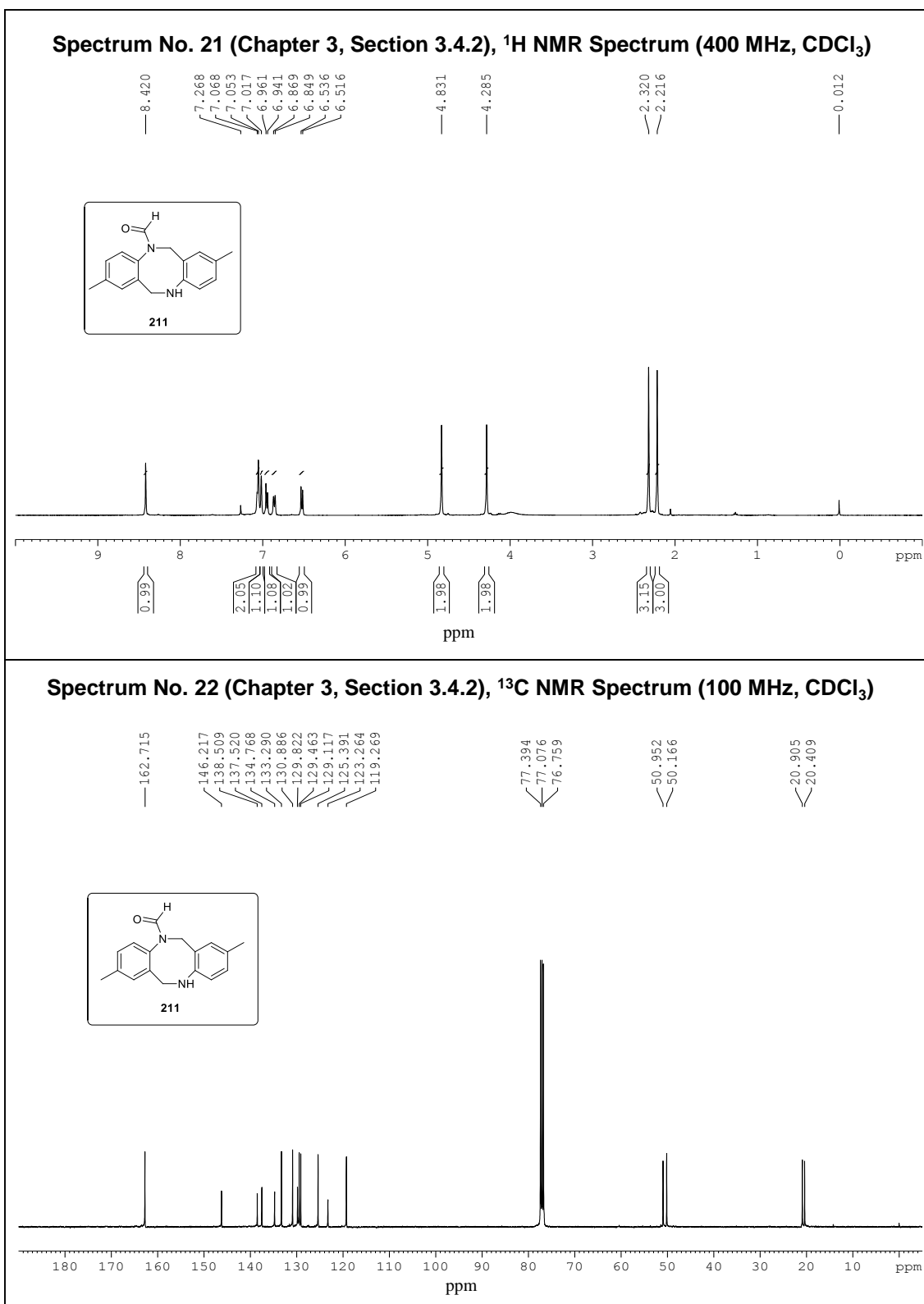
**Spectrum No. 13 (Chapter 3, Section 3.2.3),  $^1\text{H}$  NMR Spectrum (400 MHz,  $\text{CDCl}_3$ )****Spectrum No. 14 (Chapter 3, Section 3.2.3),  $^{13}\text{C}$  NMR Spectrum (100 MHz,  $\text{CDCl}_3$ )**

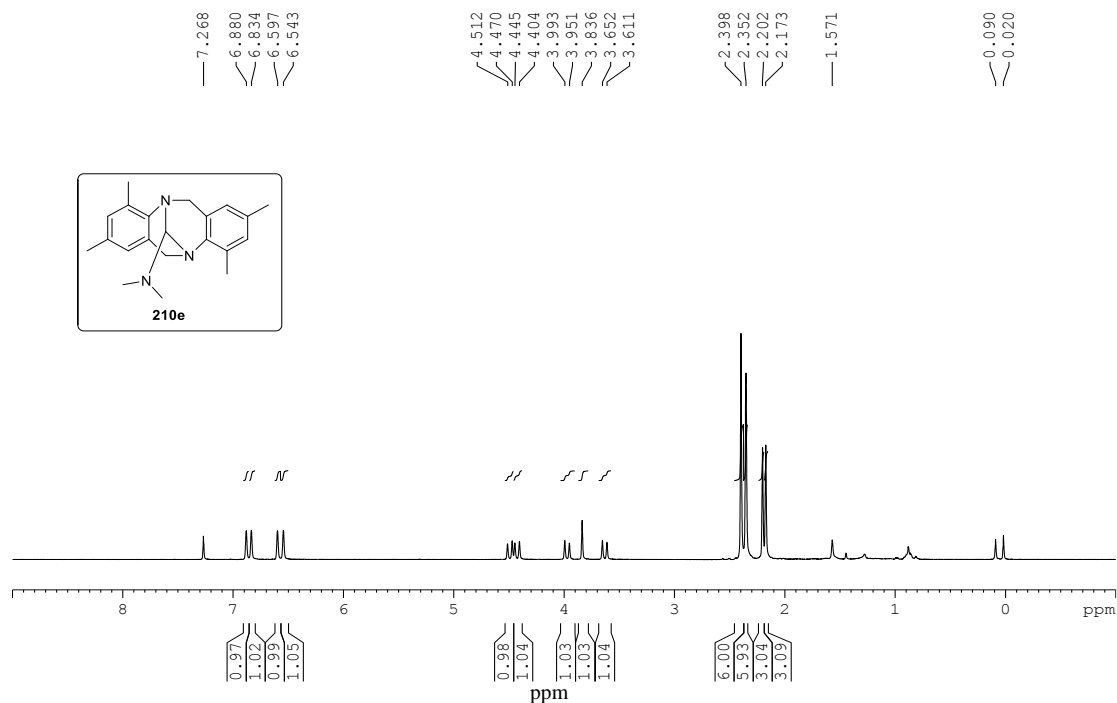
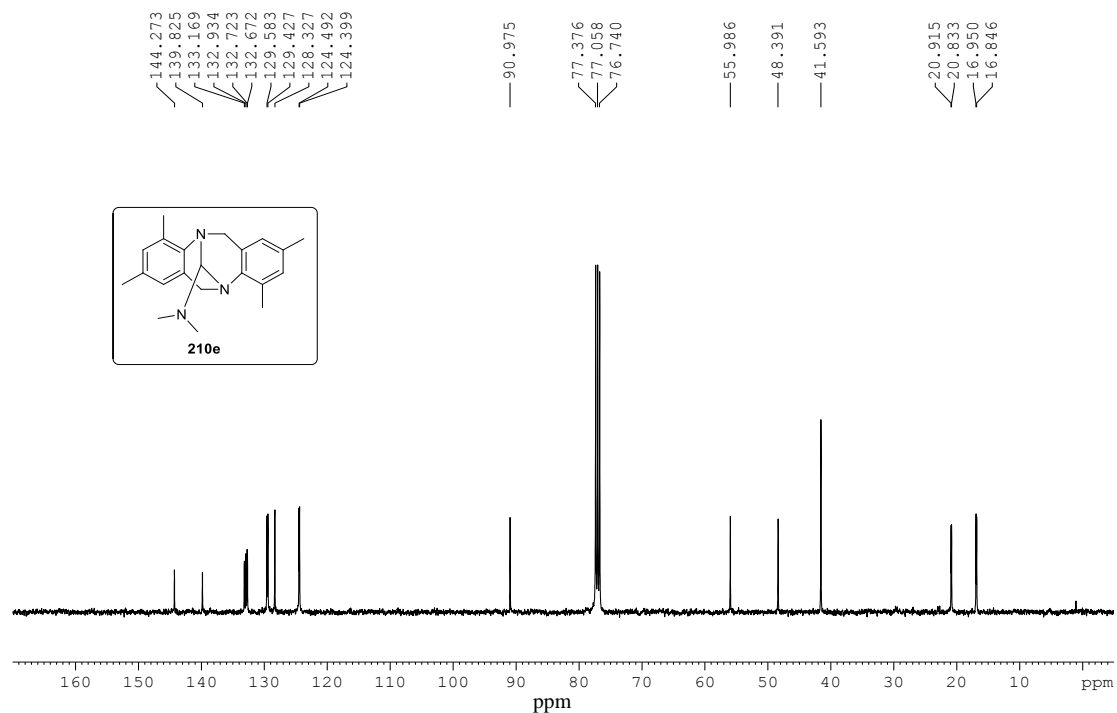


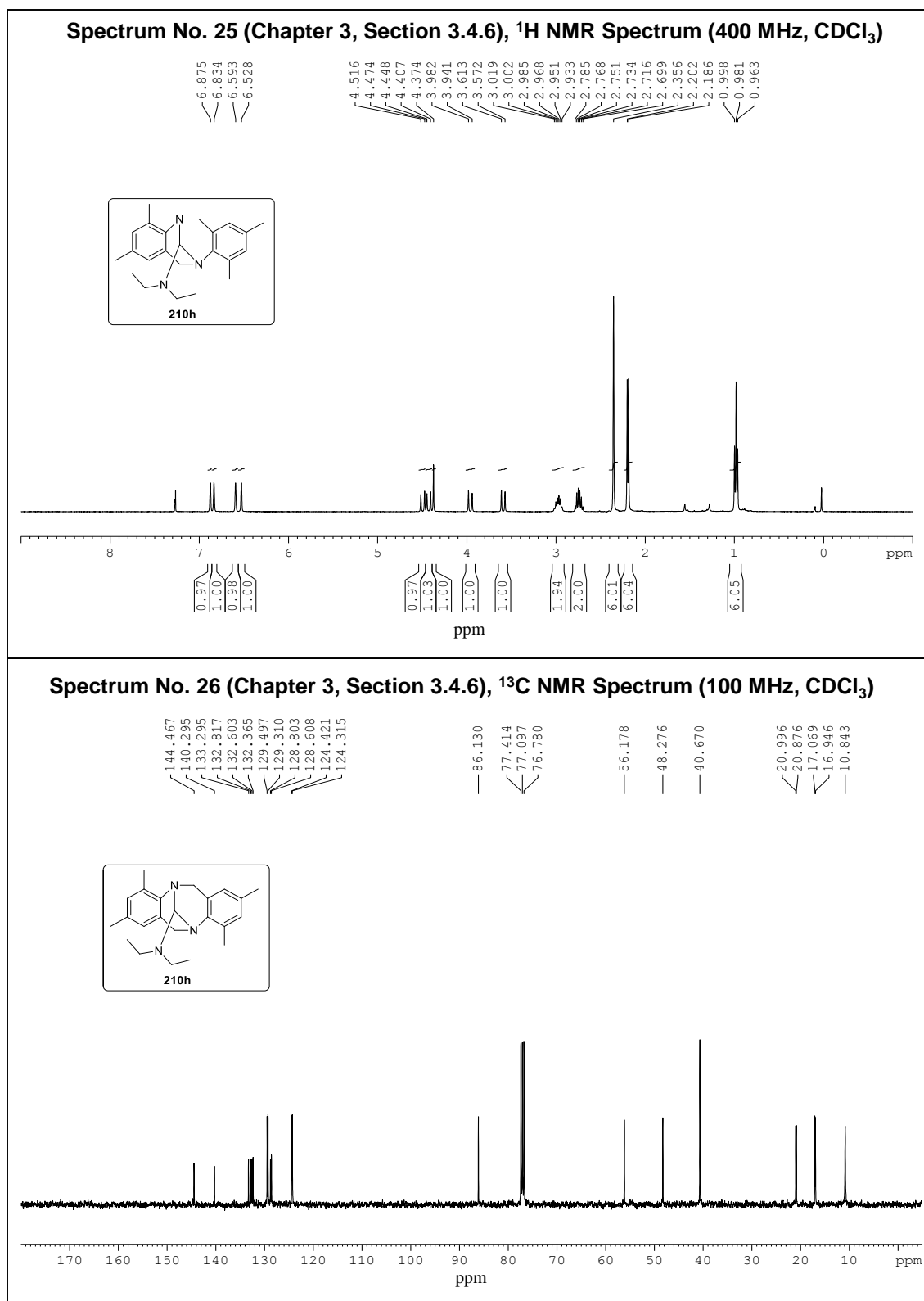
**Spectrum No. 15 (Chapter 3, Section 3.2.3),  $^1\text{H}$  NMR Spectrum (400 MHz,  $\text{CDCl}_3$ )****Spectrum No. 16 (Chapter 3, Section 3.2.3),  $^{13}\text{C}$  NMR Spectrum (100 MHz,  $\text{CDCl}_3$ )**

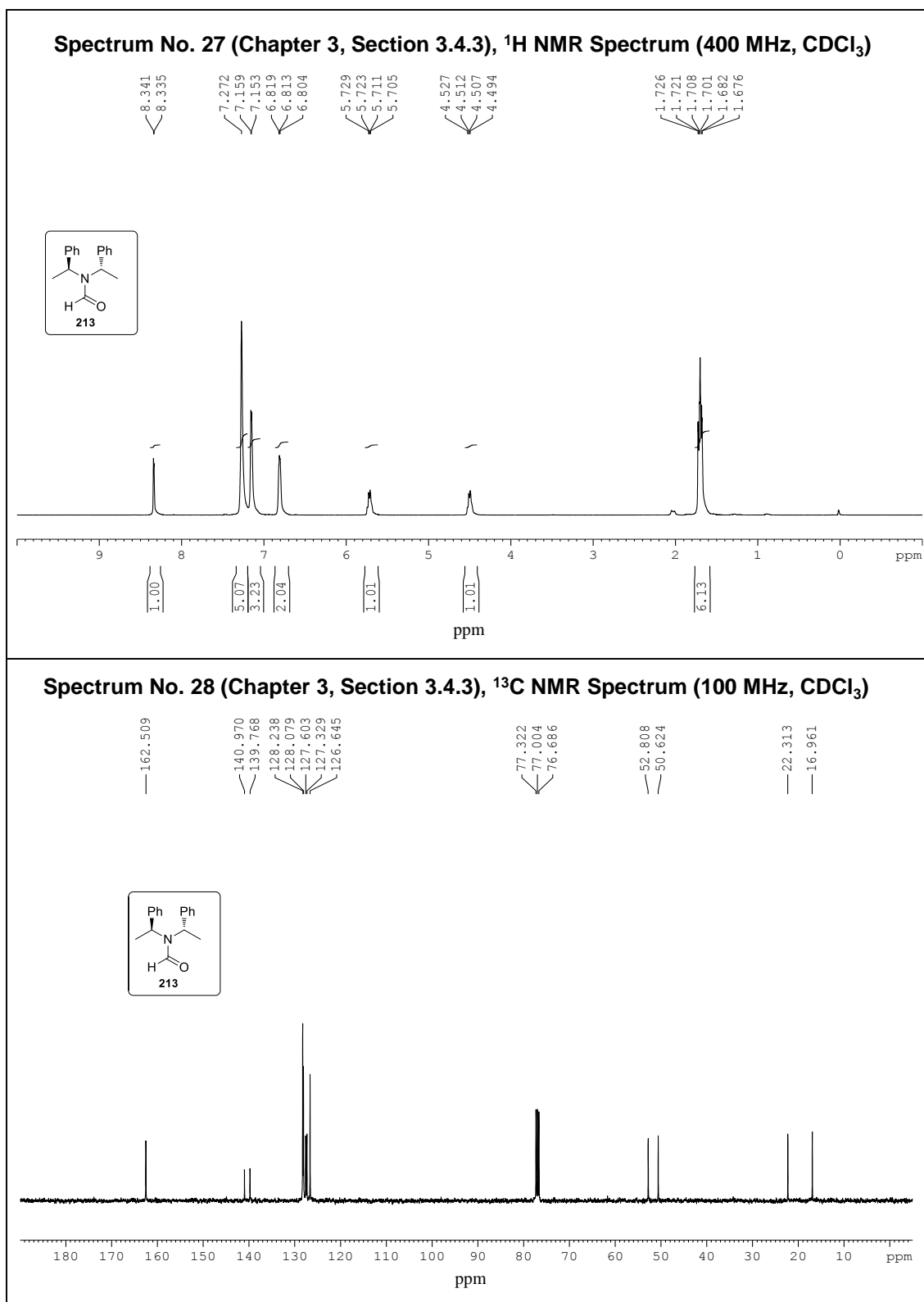


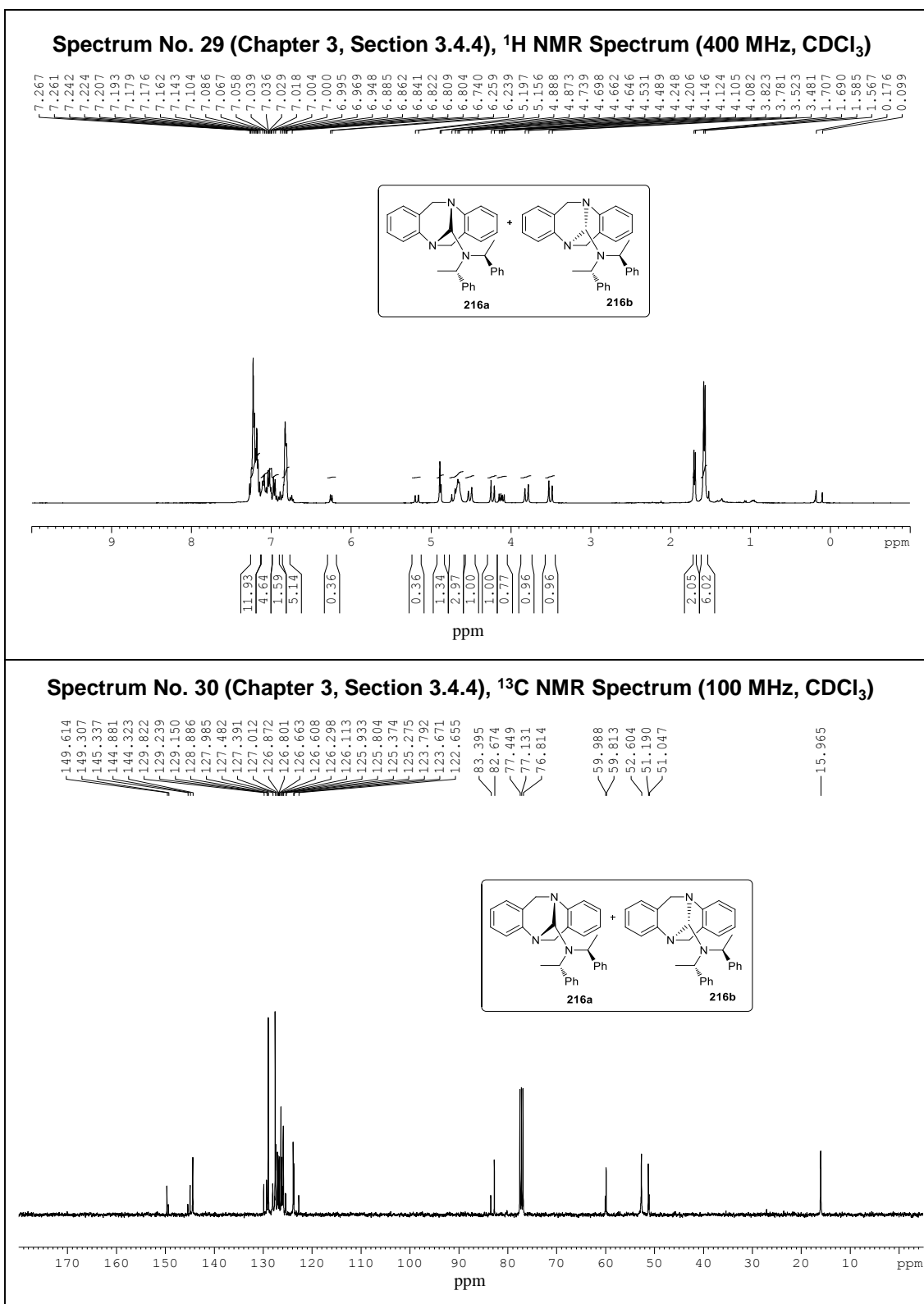
**Spectrum No. 19 (Chapter 3, Section 3.4.1),  $^1\text{H}$  NMR Spectrum (400 MHz,  $\text{CDCl}_3$ )****Spectrum No. 20 (Chapter 3, Section 3.4.1),  $^{13}\text{C}$  NMR Spectrum (100 MHz,  $\text{CDCl}_3$ )**



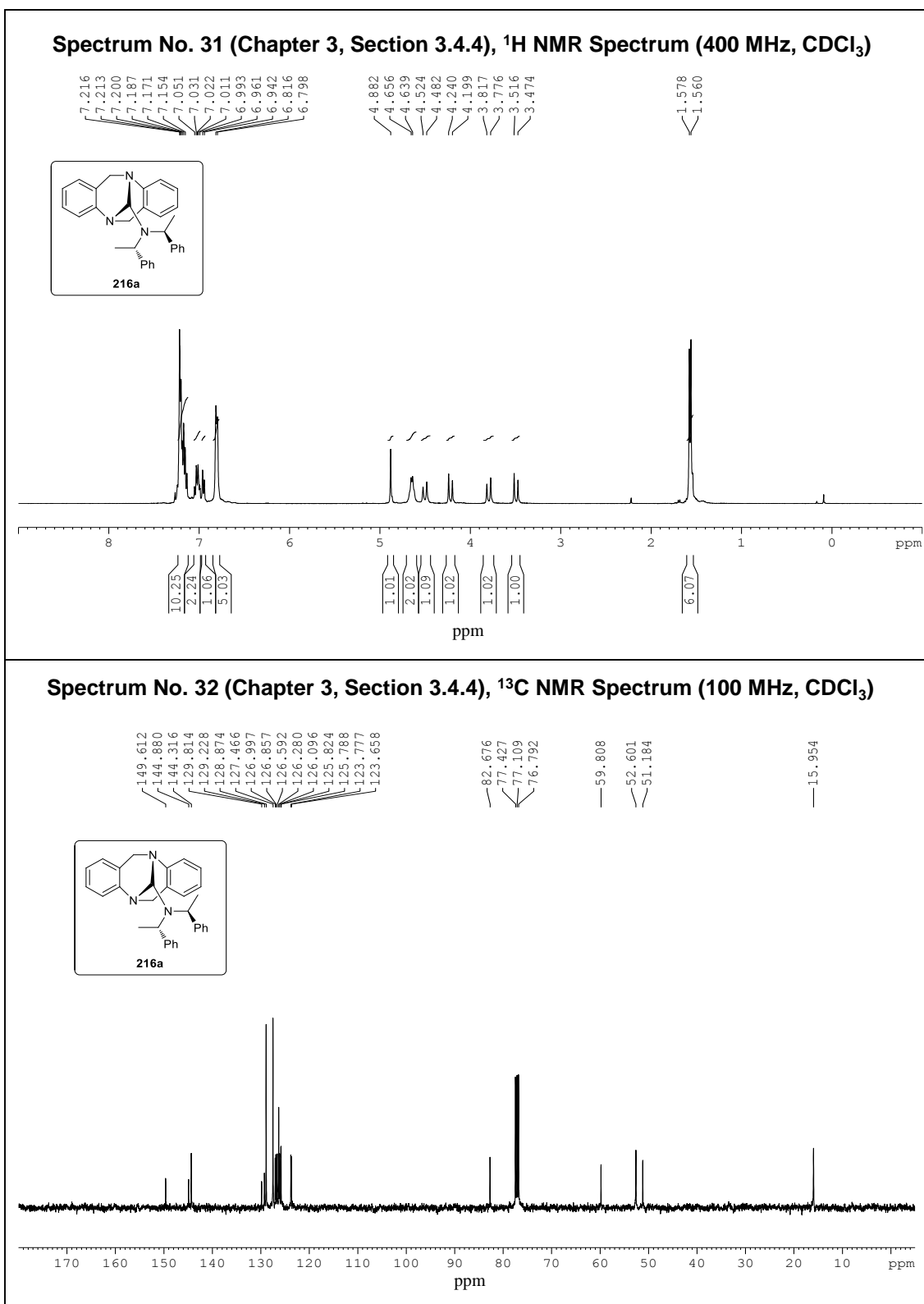
**Spectrum No. 23 (Chapter 3, Section 3.4.2),  $^1\text{H}$ NMR Spectrum (400 MHz,  $\text{CDCl}_3$ )****Spectrum No. 24 (Chapter 3, Section 3.4.2),  $^{13}\text{C}$  NMR Spectrum (100 MHz,  $\text{CDCl}_3$ )**

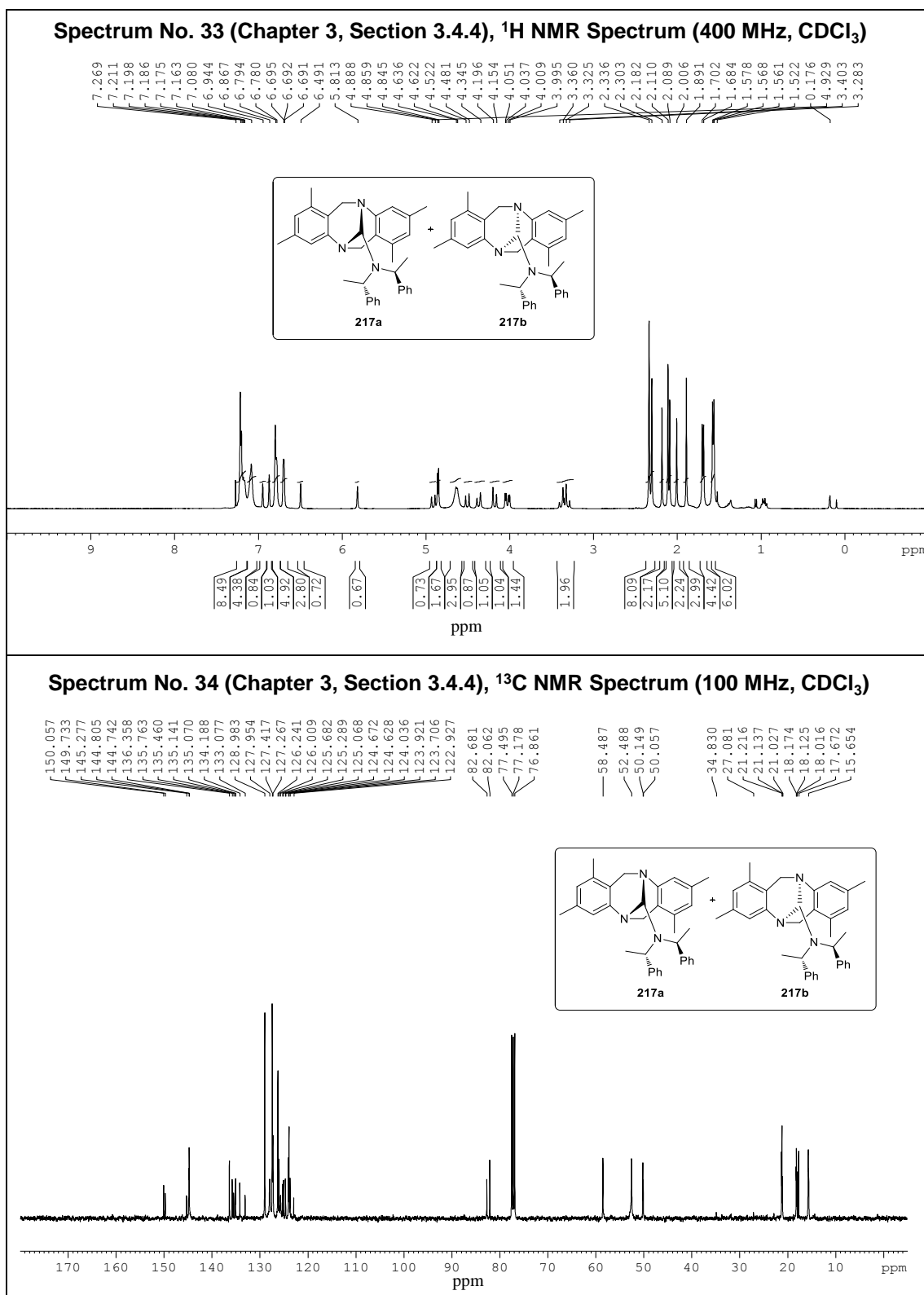


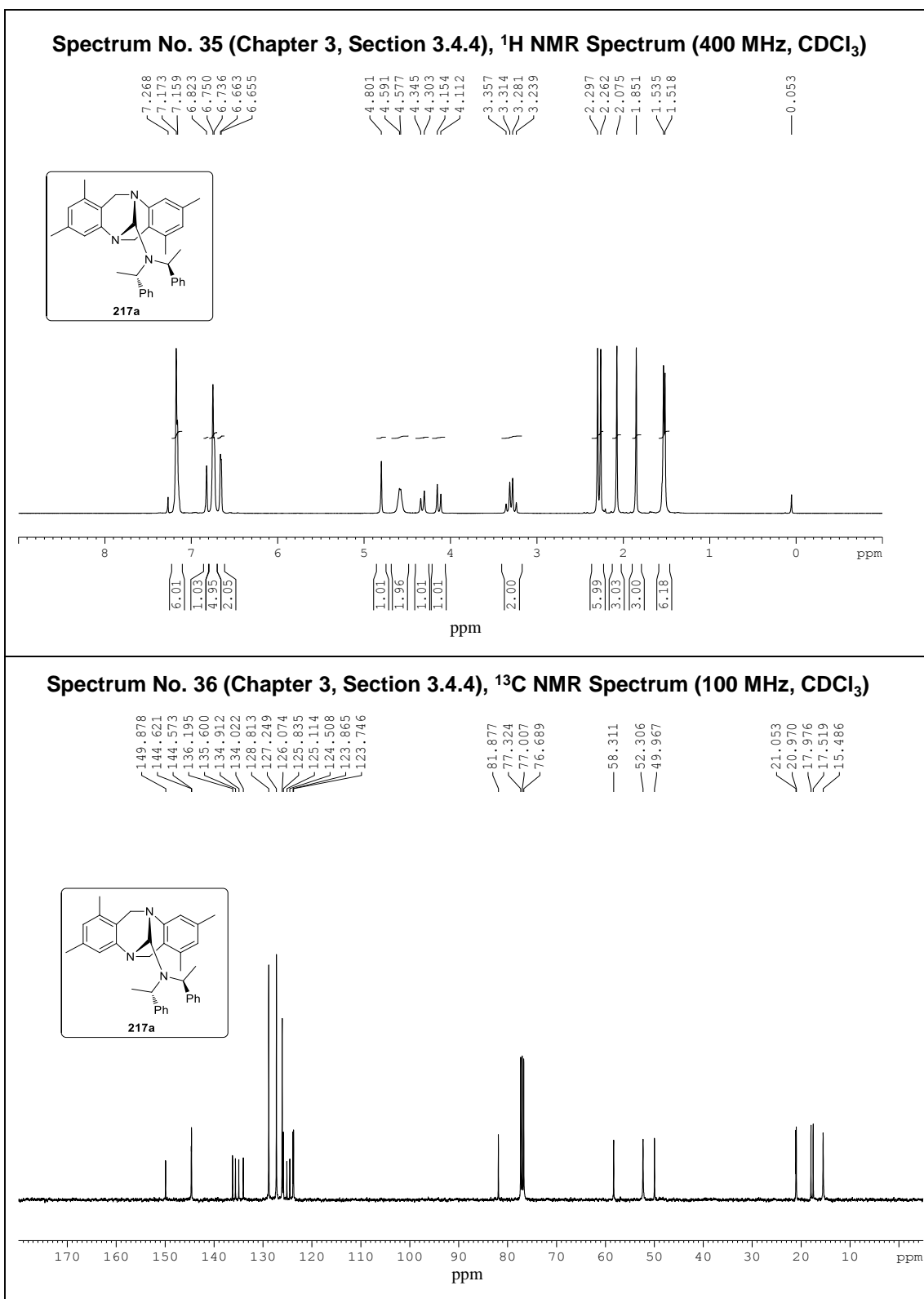


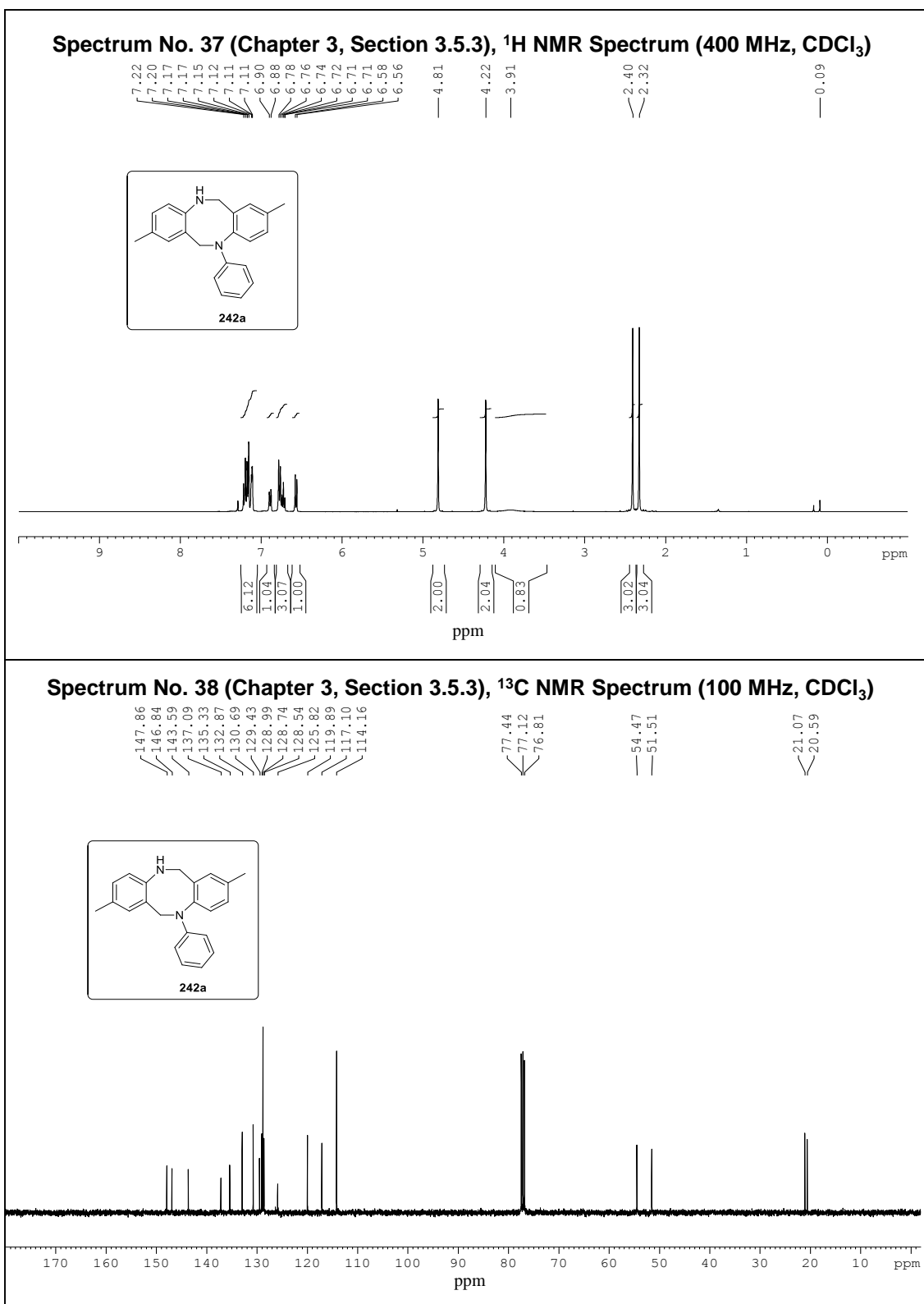


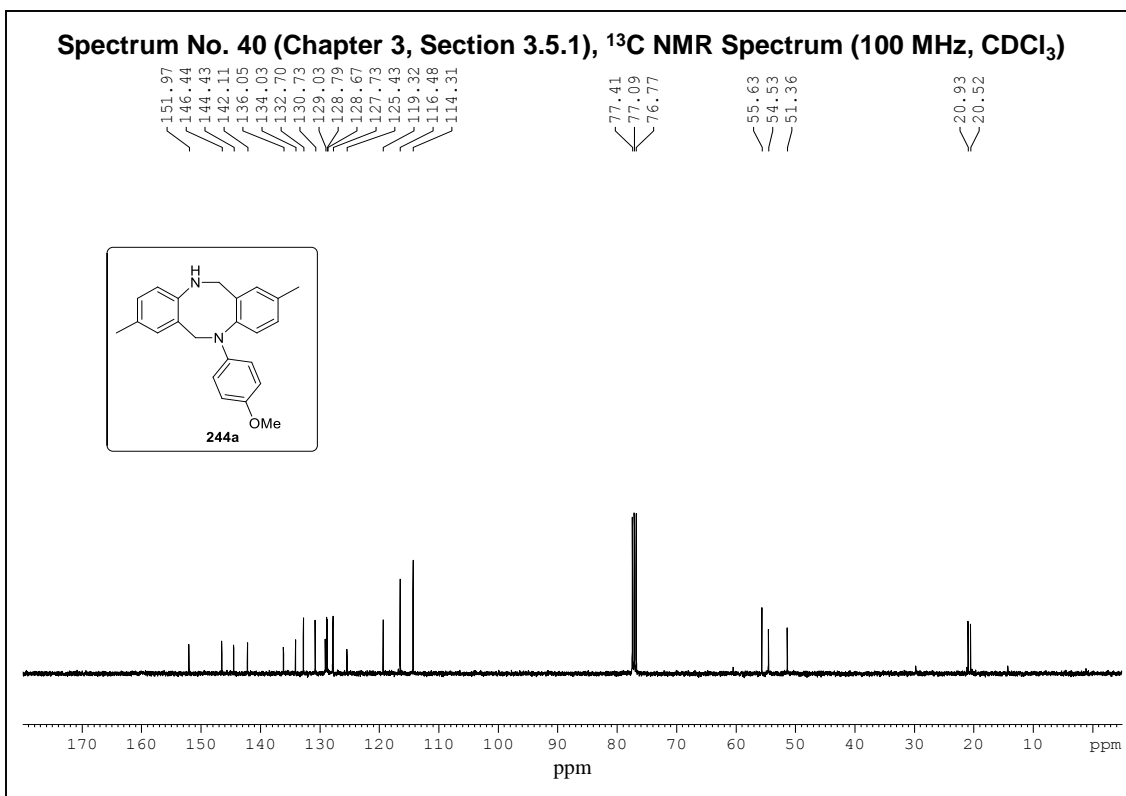
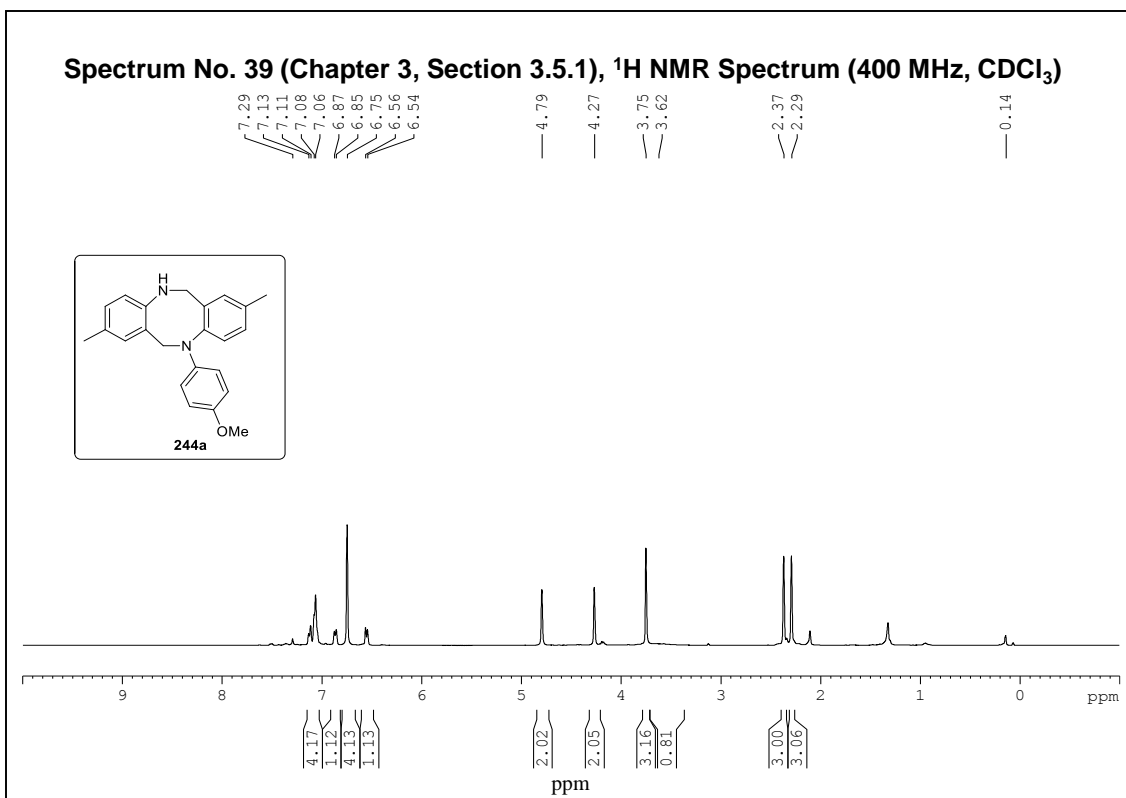


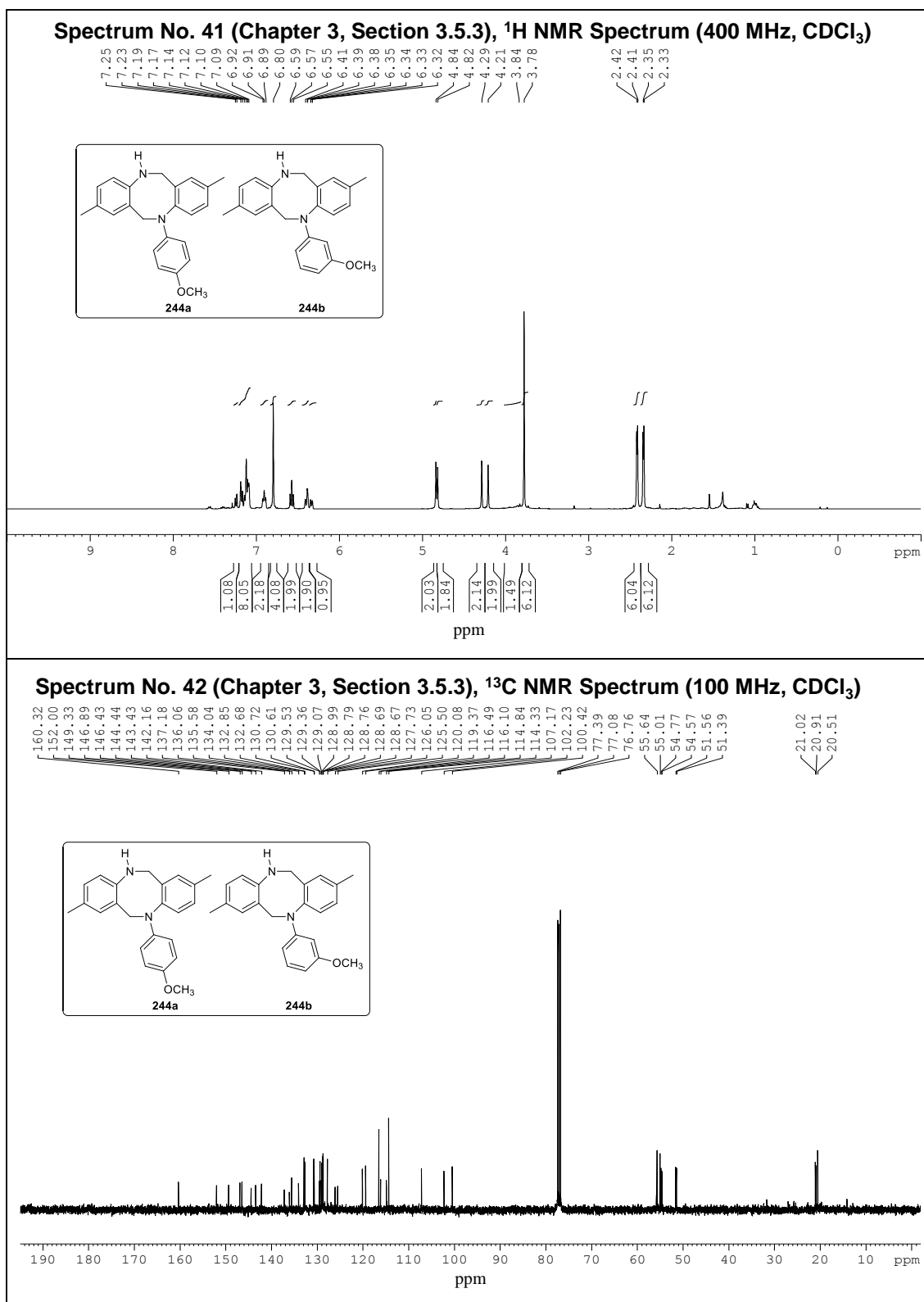


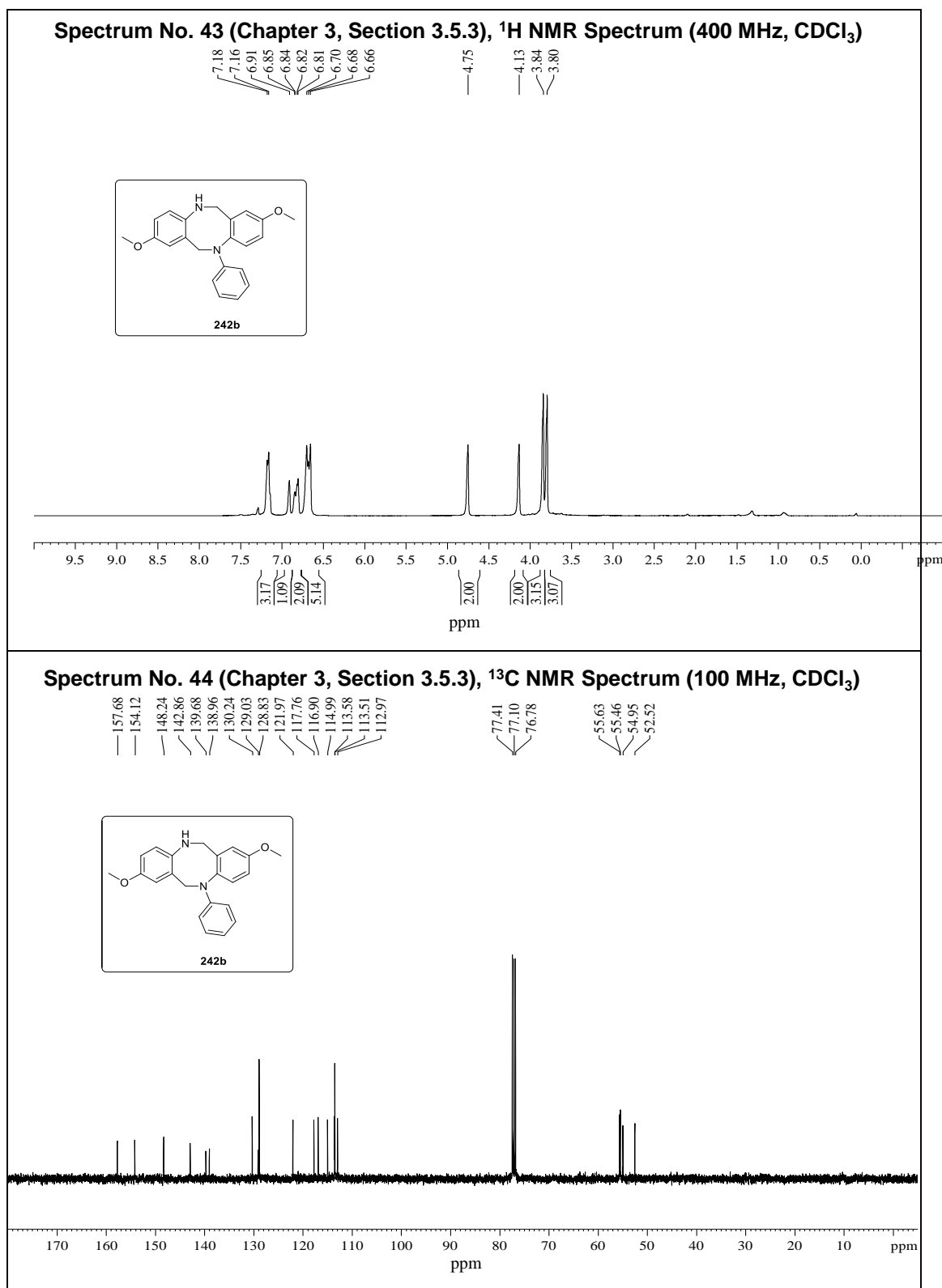


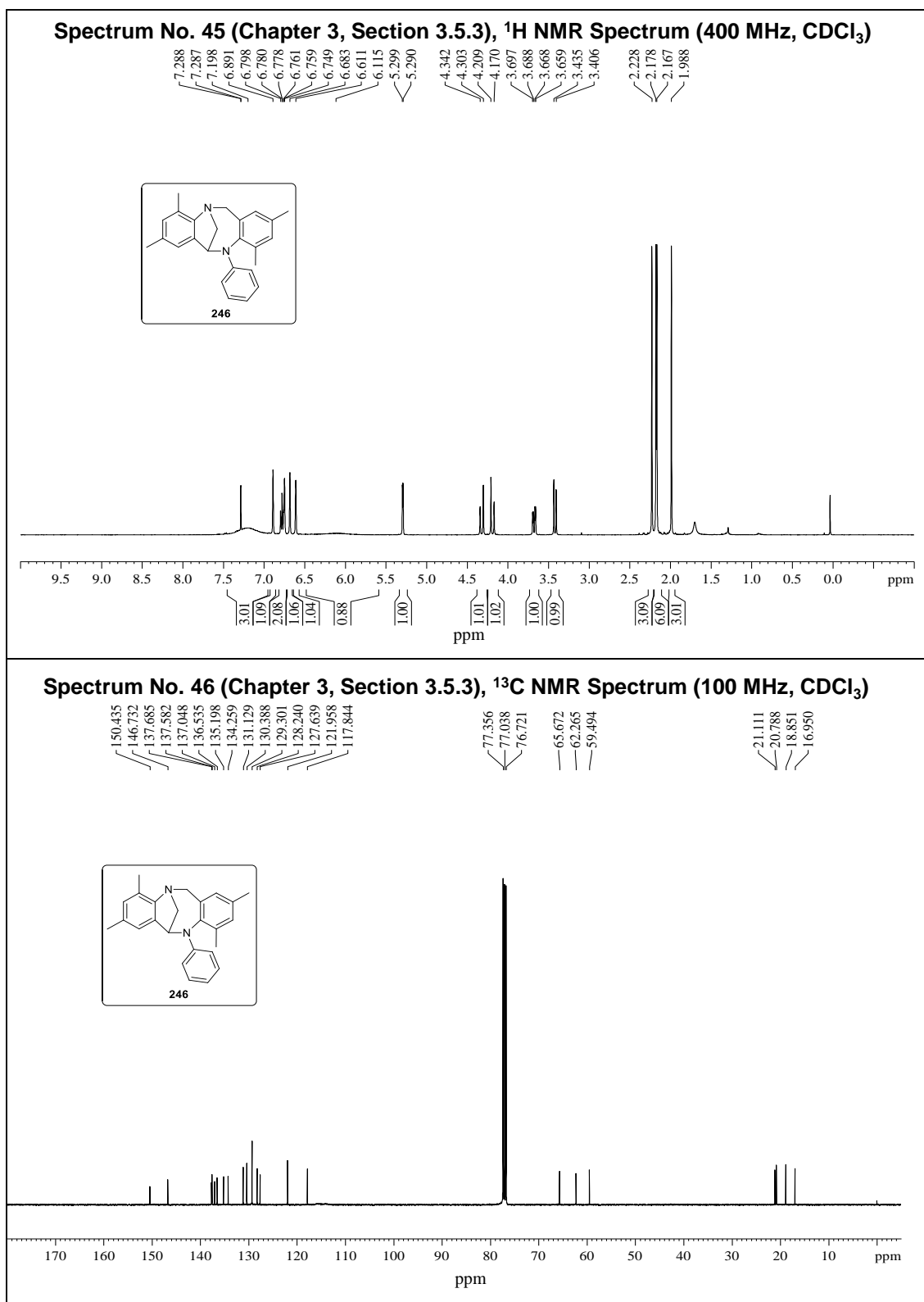




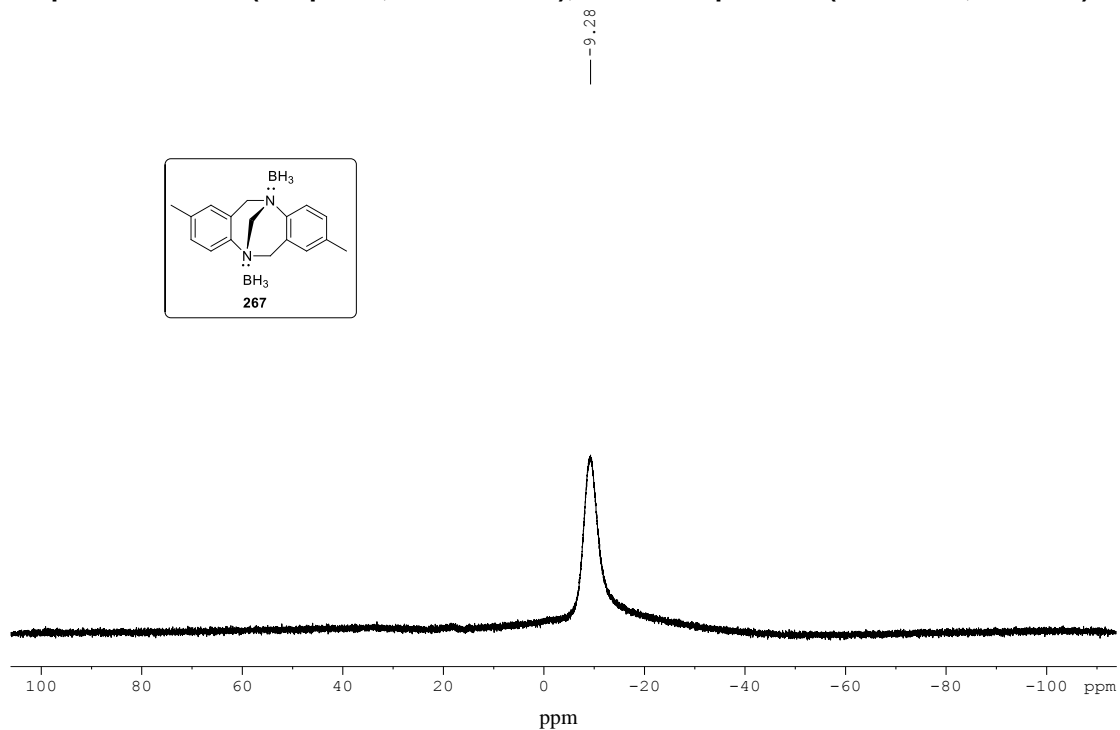
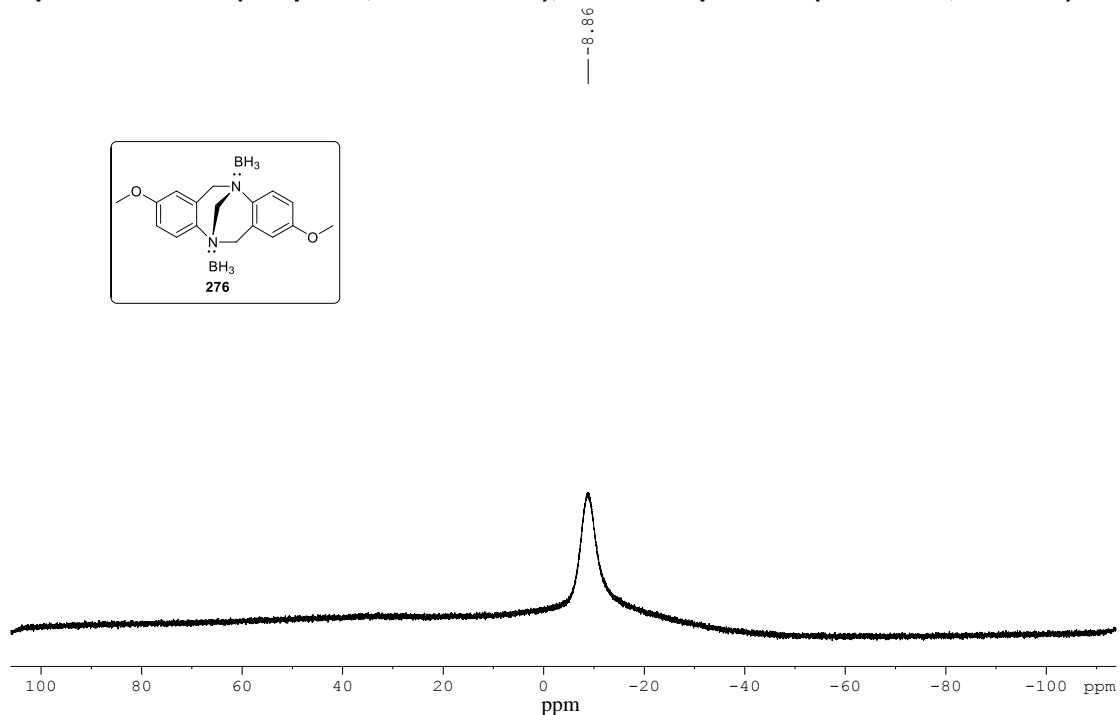


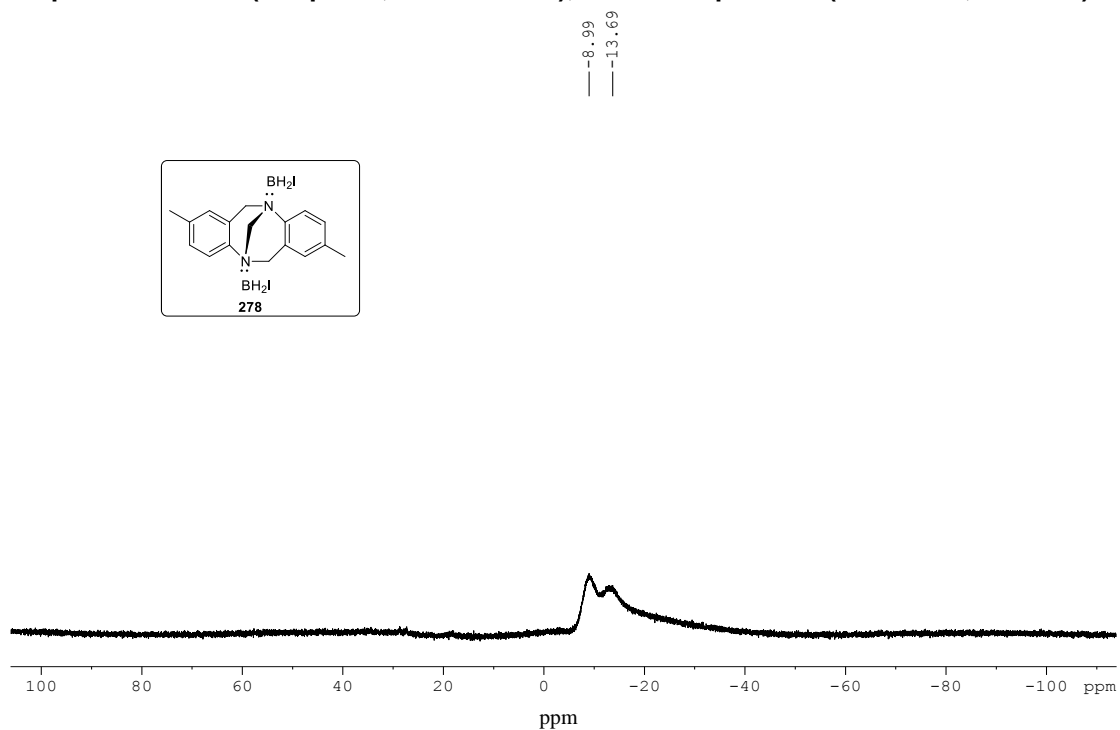
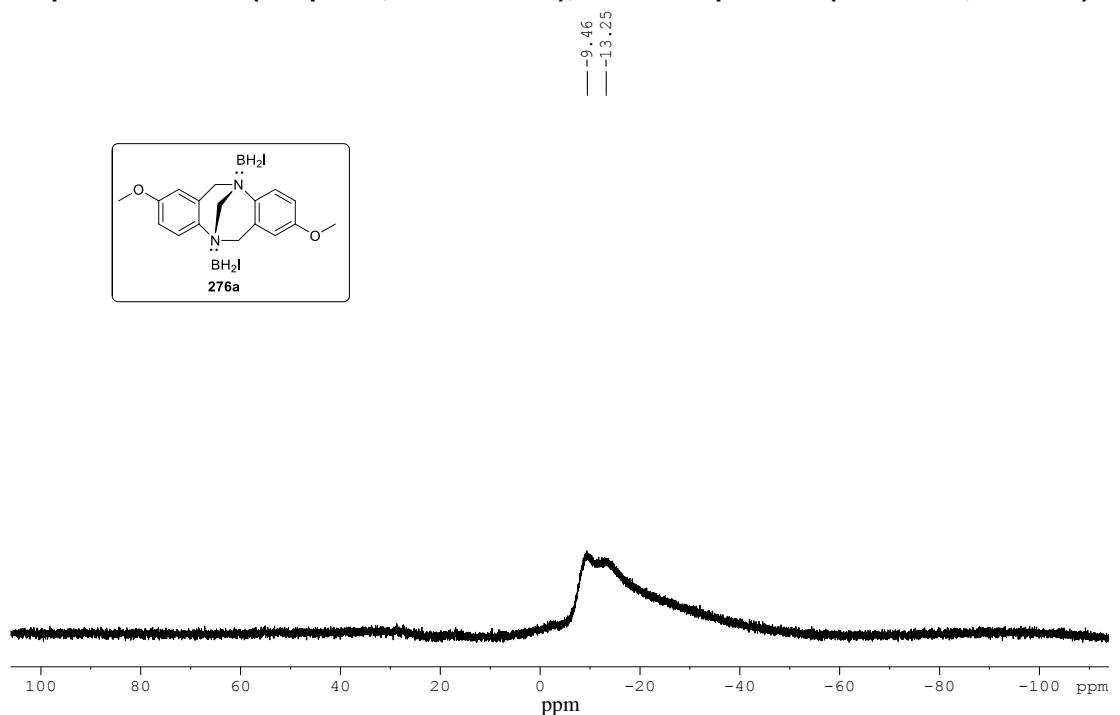


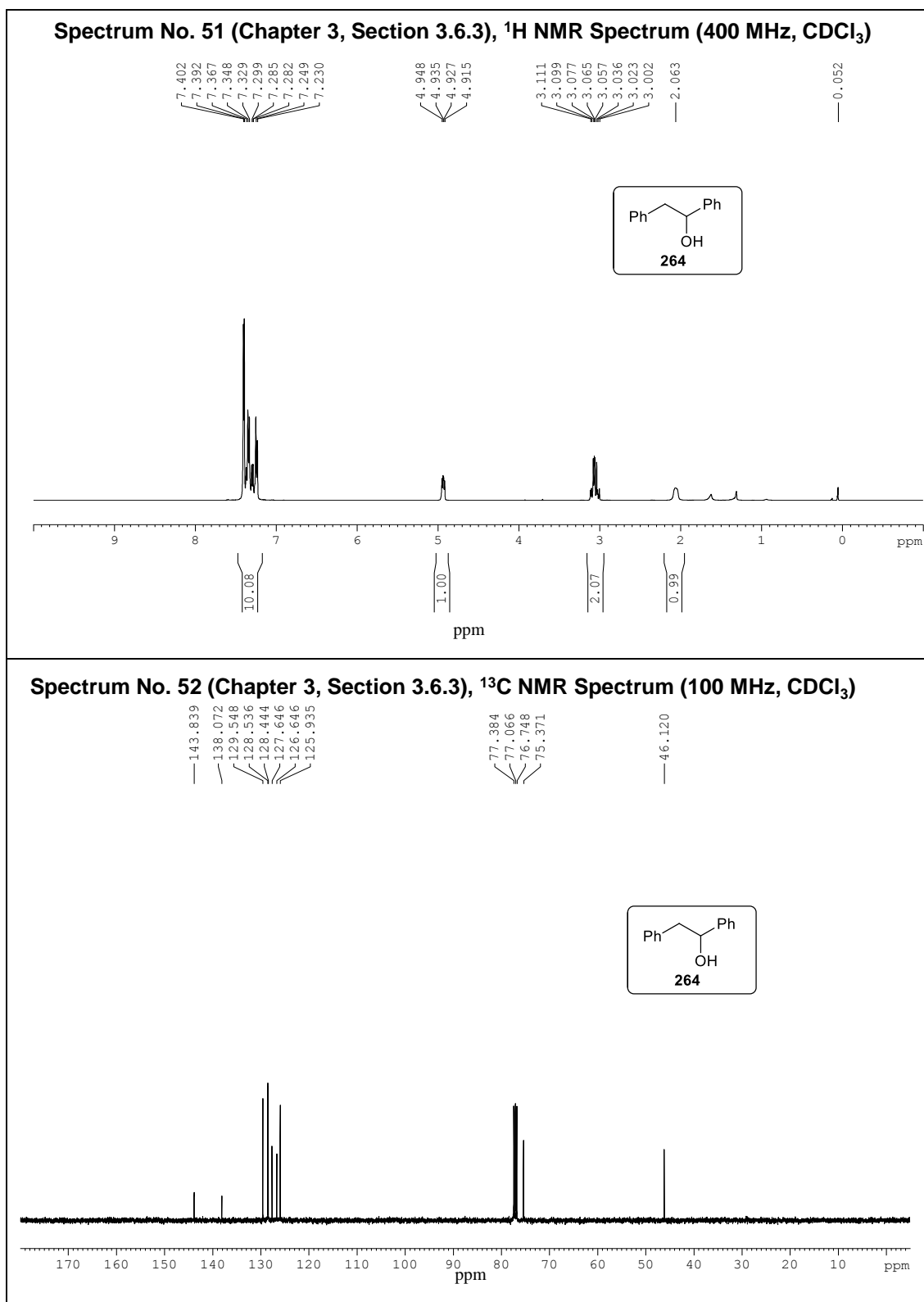


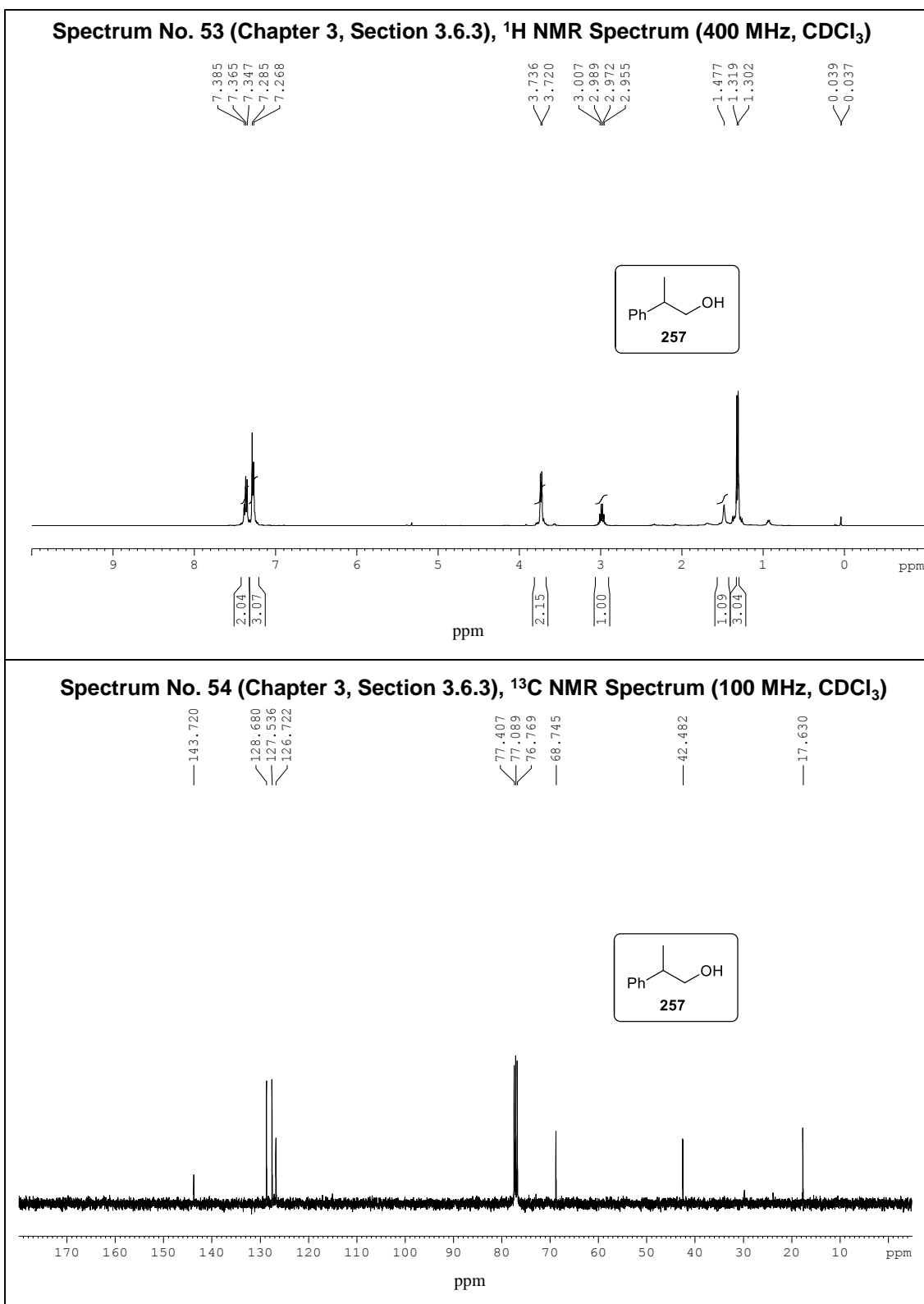




**Spectrum No. 47 (Chapter 3, Section 3.6.1),  $^{11}\text{B}$  NMR Spectrum (128.3 MHz, Toluene)****Spectrum No. 48 (Chapter 3, Section 3.6.1),  $^{11}\text{B}$  NMR Spectrum (128.3 MHz, Toluene)**

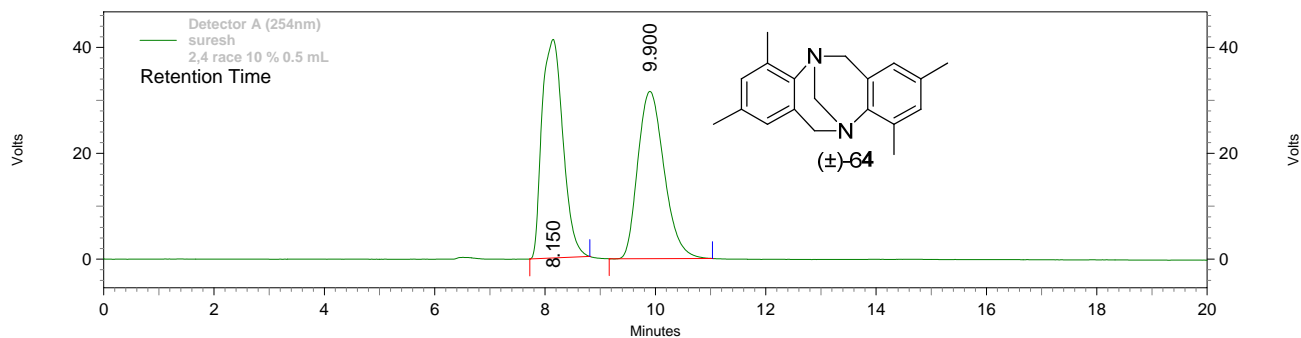
**Spectrum No. 49 (Chapter 3, Section 3.6.4),  $^{11}\text{B}$  NMR Spectrum (128.3 MHz, Toluene)****Spectrum No. 50 (Chapter 3, Section 3.6.4),  $^{11}\text{B}$  NMR Spectrum (128.3 MHz, Toluene)**







**HPLC Profile of (±)-64:** chiral column Chiralcel OJ-H, hexanes:i-PrOH/90:10; flow rate 0.5 mL/min

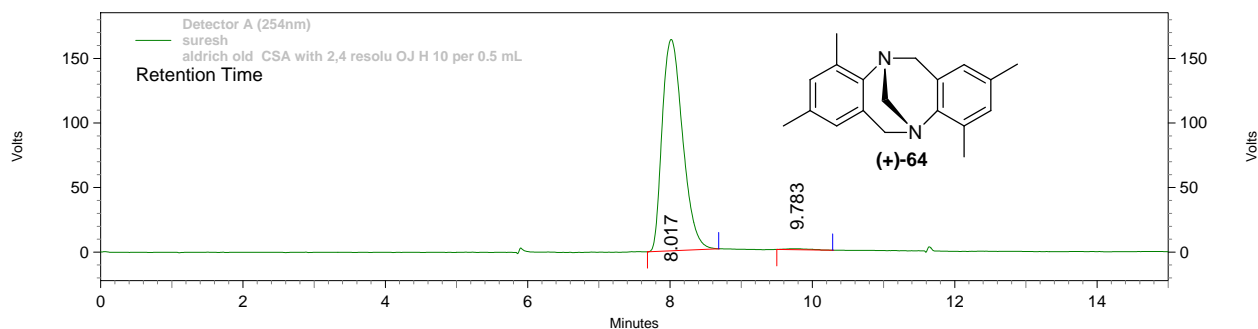


**Detector A (254nm)**

Pk #	Retention Time	Area	Area %	Height	Height %
1	8.150	1088652	51.033	41271	56.637
2	9.900	1044571	48.967	31598	43.363

Total		2133223	100.000	72869	100.000
-------	--	---------	---------	-------	---------

**HPLC Profile of (+)-64:** chiral column Chiralcel OJ-H, hexanes:i-PrOH/90:10; flow rate 0.5 mL/min

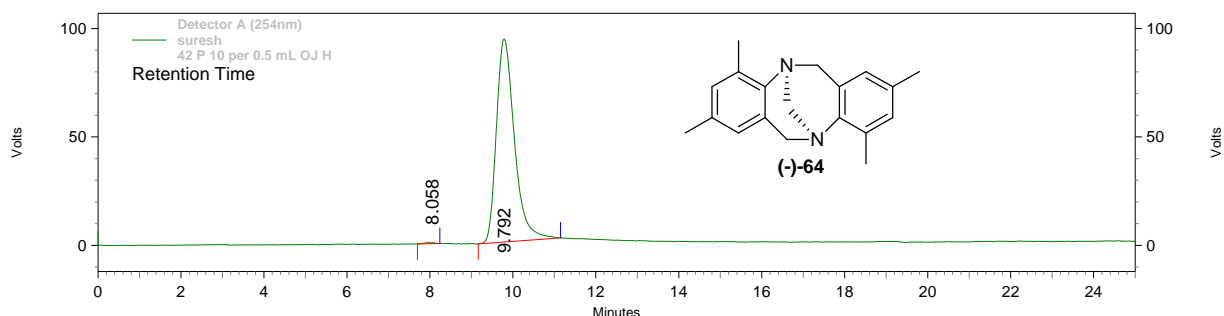


**Detector A (254nm)**

Pk #	Retention Time	Area	Area %	Height	Height %
1	8.017	3266195	99.426	163738	99.534
2	9.783	18849	0.574	767	0.466

Total		3285044	100.000	164505	100.000
-------	--	---------	---------	--------	---------

**HPLC Profile of (–)-64:** chiral column Chiralcel OJ-H, hexanes:i-PrOH/90:10; flow rate 0.5 mL/min

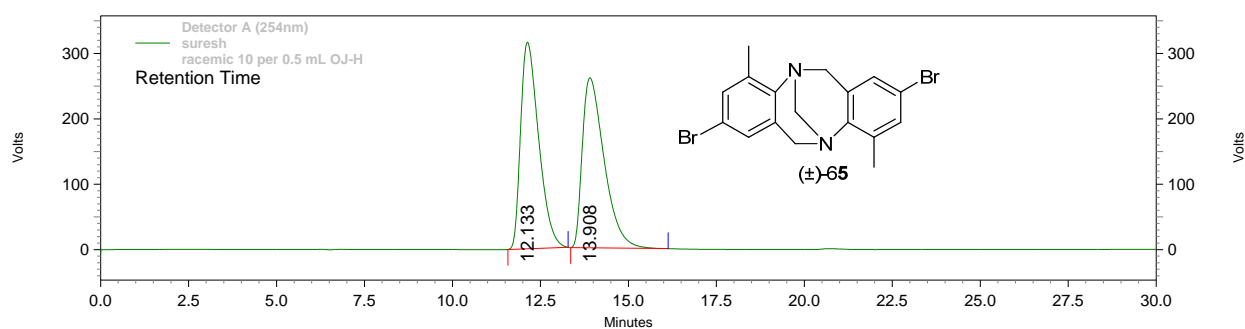


**Detector A (254nm)**

Pk #	Retention Time	Area	Area %	Height	Height %
1	8.058	7502	0.265	460	0.489
2	9.792	2825169	99.735	93561	99.511

Total		2832671	100.000	94021	100.000
-------	--	---------	---------	-------	---------

**HPLC Profile of (±)-65:** chiral column Chiralcel OJ-H, hexanes:i-PrOH/90:10; flow rate 0.5 mL/min

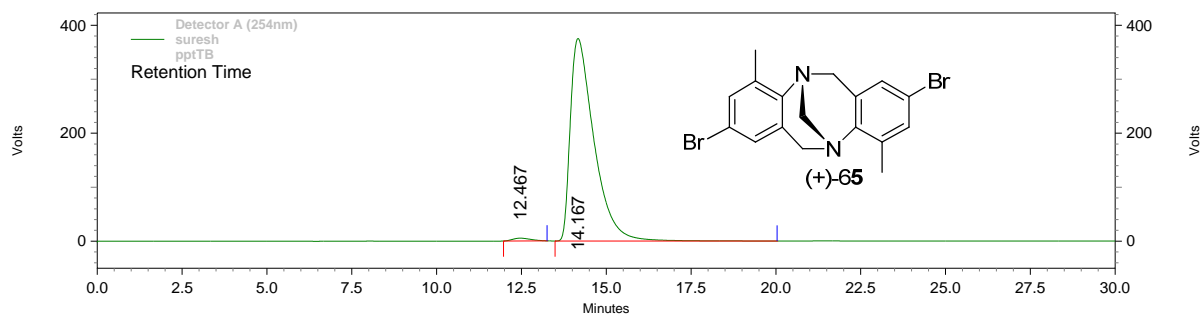


**Detector A (254nm)**

Pk #	Retention Time	Area	Area %	Height	Height %
1	12.133	11261776	50.125	315948	54.858
2	13.908	11205716	49.875	259993	45.142

Total		22467492	100.000	575941	100.000
-------	--	----------	---------	--------	---------

**HPLC Profile of (+)-65:** chiral column Chiralcel OJ-H, hexanes:i-PrOH/90:10; flow rate 0.5 mL/min

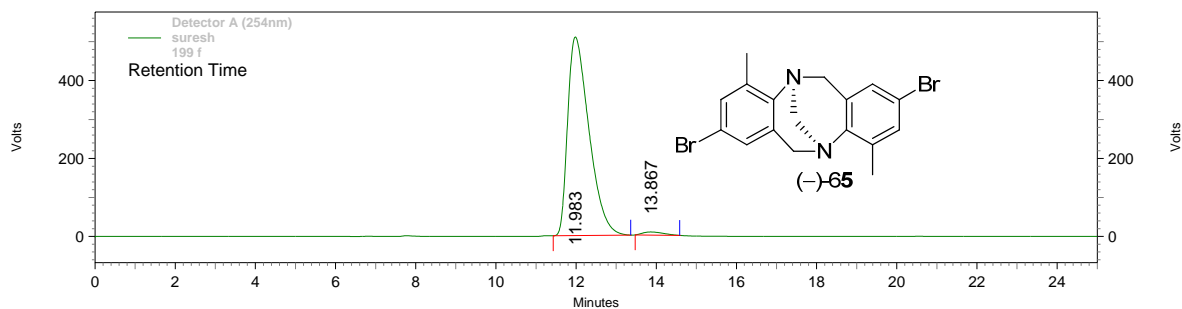


**Detector A (254nm)**

Pk #	Retention Time	Area	Area %	Height	Height %
1	12.467	191014	1.037	5175	1.360
2	14.167	18235747	98.963	375320	98.640

Total		18426761	100.000	380495	100.000
-------	--	----------	---------	--------	---------

**HPLC Profile of (–)-65:** chiral column Chiralcel OJ-H, hexanes:i-PrOH/90:10; flow rate 0.5 mL/min



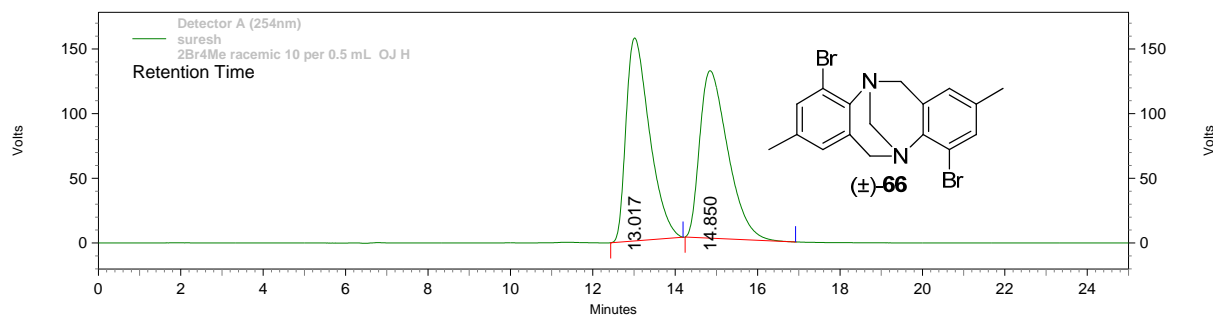
**Detector A (254nm)**

Pk #	Retention Time	Area	Area %	Height	Height %
1	11.983	18841935	98.505	509802	98.461
2	13.867	286002	1.495	7970	1.539

Total		19127937	100.000	517772	100.000
-------	--	----------	---------	--------	---------



**HPLC Profile of (±)-66:** chiral column Chiralcel OJ-H, hexanes:i-PrOH/90:10; flow rate 0.5 mL/min

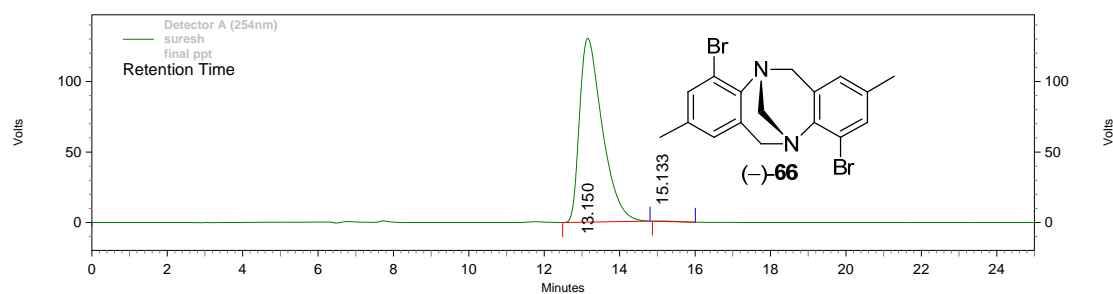


**Detector A (254nm)**

Pk #	Retention Time	Area	Area %	Height	Height %
1	13.017	6219603	50.368	156993	54.808
2	14.850	6128745	49.632	129450	45.192

Total		12348348	100.000	286443	100.000
-------	--	----------	---------	--------	---------

**HPLC Profile of (–)-66:** chiral column Chiralcel OJ-H, hexanes:i-PrOH/90:10; flow rate 0.5 mL/min

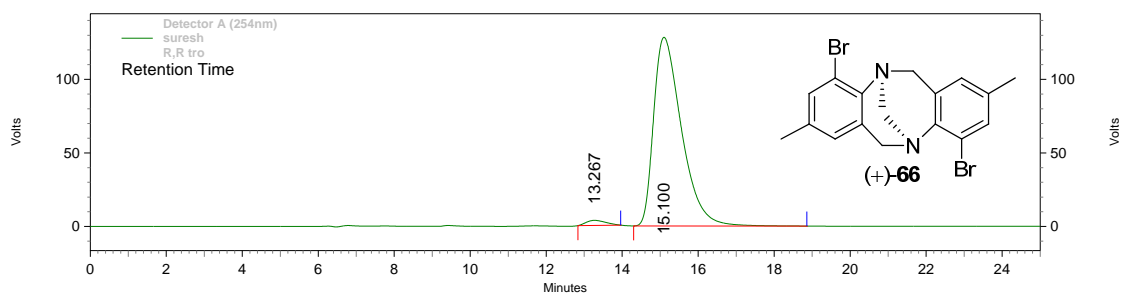


**Detector A (254nm)**

Pk #	Retention Time	Area	Area %	Height	Height %
1	13.150	5454207	99.824	130247	99.816
2	15.133	9622	0.176	240	0.184

Total		5463829	100.000	130487	100.000
-------	--	---------	---------	--------	---------

**HPLC Profile of (+)-66:** chiral column Chiralcel OJ-H, hexanes:i-PrOH/90:10; flow rate 0.5 mL/min

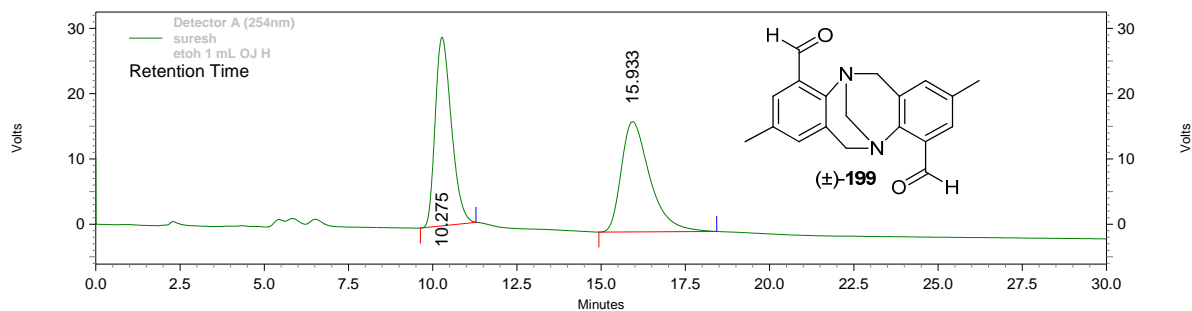


**Detector A (254nm)**

Pk #	Retention Time	Area	Area %	Height	Height %
1	13.267	123159	1.849	3442	2.614
2	15.100	6538133	98.151	128240	97.386

Total		6661292	100.000	131682	100.000
-------	--	---------	---------	--------	---------

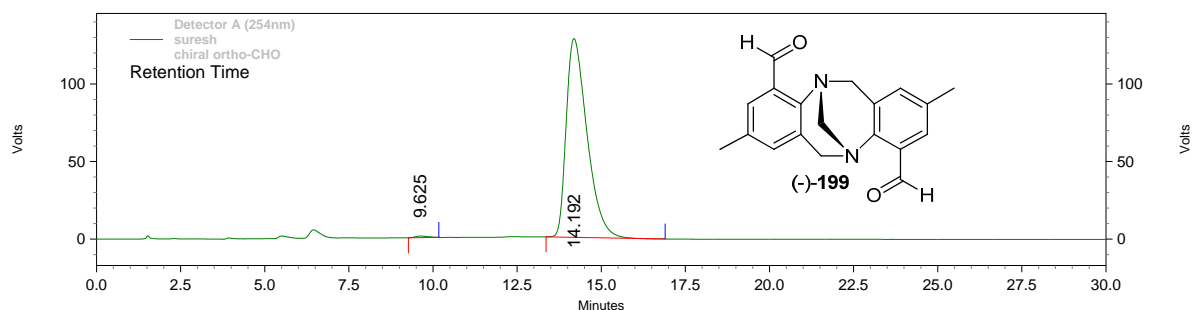
**HPLC Profile of (±)-199:** chiral column Chiralcel OJ-H, EtOH; flow rate 1.0 mL/min



**Detector A (254nm)**

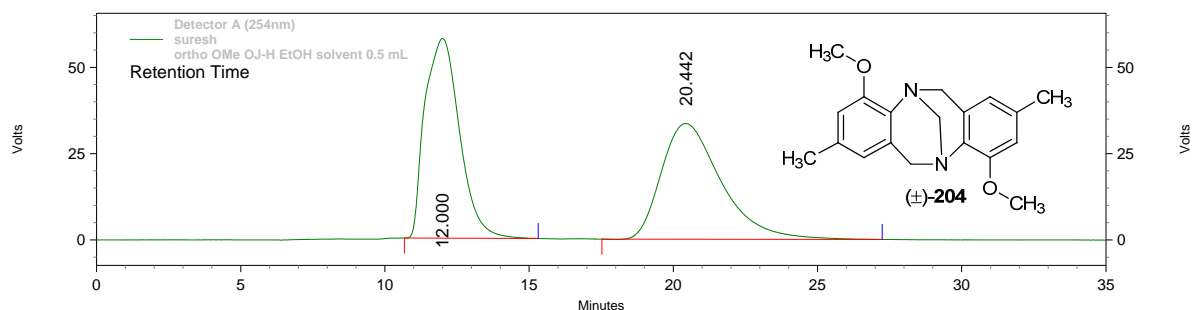
Pk #	Retention Time	Area	Area %	Height	Height %
1	10.275	966477	49.280	28889	63.116
2	15.933	994716	50.720	16882	36.884

Total		1961193	100.000	45771	100.000
-------	--	---------	---------	-------	---------

**HPLC Profile of (-)-199:** chiral column Chiralcel OJ-H, EtOH; flow rate 0.5 mL/min

**Detector A (254nm)**

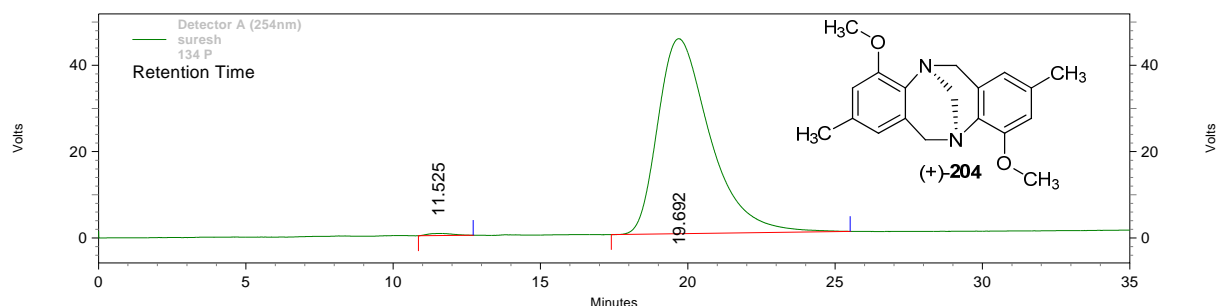
Pk #	Retention Time	Area	Area %	Height	Height %
1	9.625	26027	0.470	1019	0.789
2	14.192	5514625	99.530	128090	99.211

Total		5540652	100.000	129109	100.000
-------	--	---------	---------	--------	---------

**HPLC Profile of (±)-204:** chiral column Chiralcel OJ-H, EtOH; flow rate 0.5 mL/min

**Detector A (254nm)**

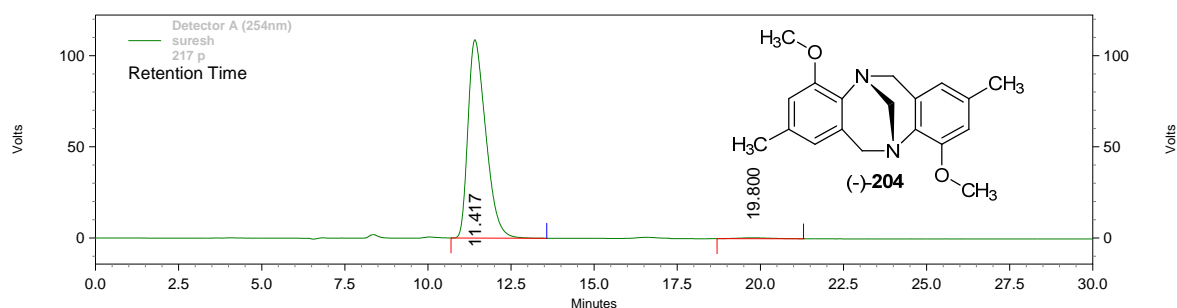
Pk #	Retention Time	Area	Area %	Height	Height %
1	12.000	4828779	50.003	57869	63.297
2	20.442	4828171	49.997	33555	36.703

Total		9656950	100.000	91424	100.000
-------	--	---------	---------	-------	---------

**HPLC Profile of (+)-204:** chiral column Chiralcel OJ-H, EtOH; flow rate 0.5 mL/min**Detector A (254nm)**

Pk #	Retention Time	Area	Area %	Height	Height %
1	11.525	28894	0.517	485	1.062
2	19.692	5557610	99.483	45165	98.938

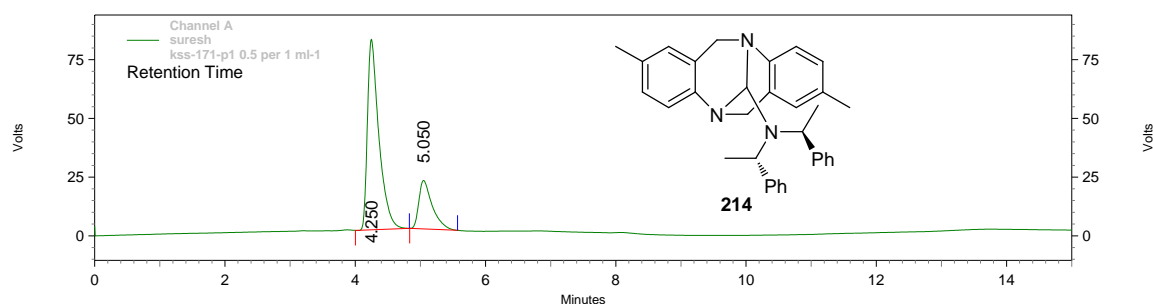
Total		5586504	100.000	45650	100.000
-------	--	---------	---------	-------	---------

**HPLC Profile of (-)-204:** chiral column Chiralcel OJ-H, EtOH; flow rate 0.5 mL/min**Detector A (254nm)**

Pk #	Retention Time	Area	Area %	Height	Height %
1	11.417	4060149	99.160	108718	99.548
2	19.800	34399	0.840	494	0.452

Total		4094548	100.000	109212	100.000
-------	--	---------	---------	--------	---------

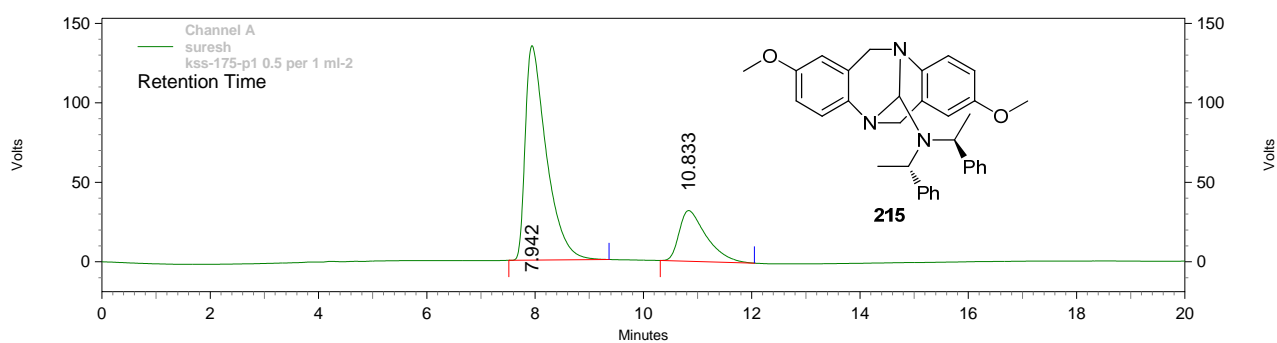
**HPLC Profile of 214:** chiral column Chiral cell phenomenex cellulose-1, hexanes:i-PrOH/99.5:0.5; flow rate 1.0 mL/min



**Detector A (254nm)**

Pk #	Retention Time	Area	Area %	Height	Height %
1	4.250	991832	77.074	81032	79.699
2	5.050	295018	22.926	20641	20.301
Total		1286850	100.000	101673	100.000

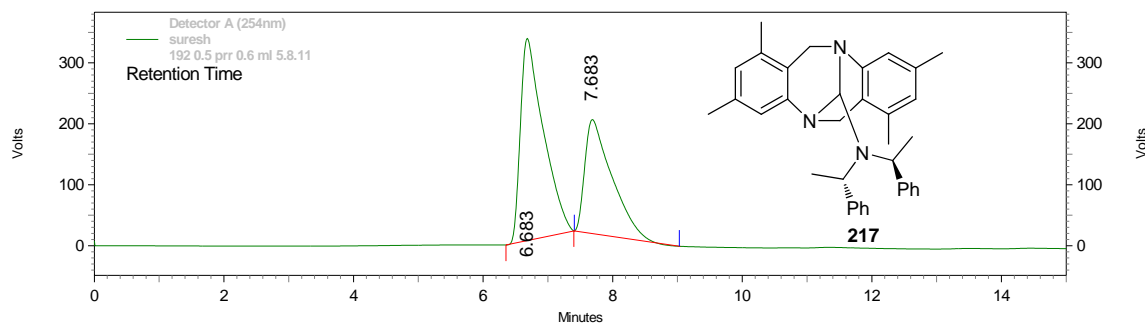
**HPLC Profile of 215:** chiral column Chiral cell phenomenex cellulose-1, hexanes:i-PrOH/99.5:0.5; flow rate 1.0 mL/min



**Detector A (254nm)**

Pk #	Retention Time	Area	Area %	Height	Height %
1	7.942	3655141	76.709	134944	80.893
2	10.833	1109806	23.291	31873	19.107
Total		4764947	100.000	166817	100.000

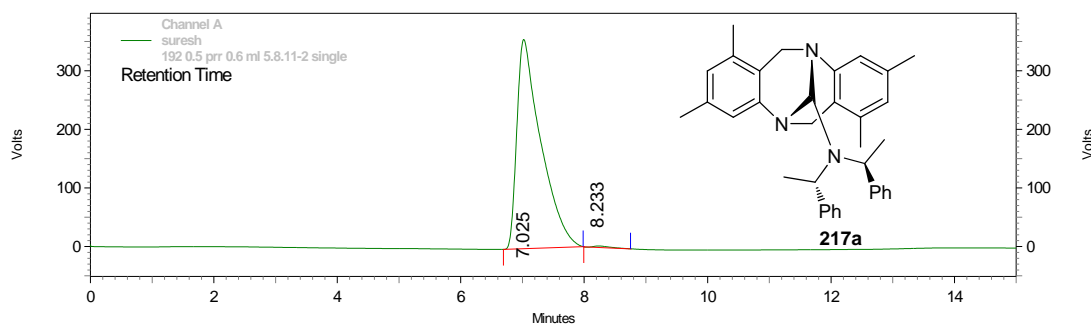
**HPLC Profile of 217:** chiral column, Chiral cell phenomenex cellulose-1, hexanes:i-PrOH/99.5:0.5; flow rate 0.6 mL/min



#### Detector A (254nm)

Pk #	Retention Time	Area	Area %	Height	Height %
1	6.683	8150753	59.879	331414	63.951
2	7.683	5461242	40.121	186821	36.049
Total		13611995	100.000	518235	100.000

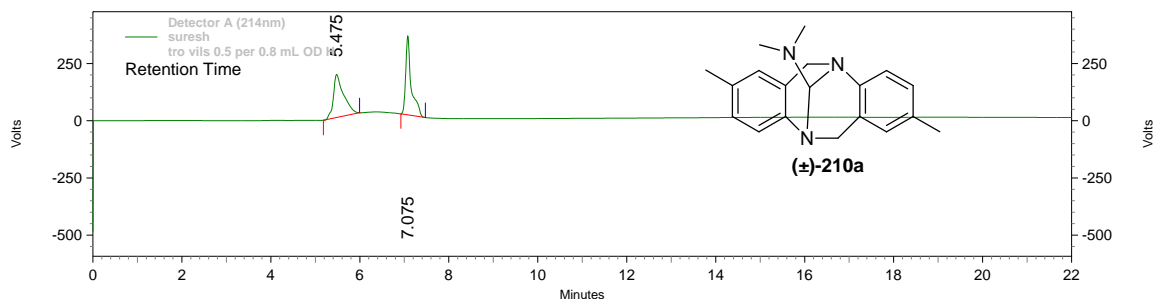
**HPLC Profile of 217a:** chiral column, Chiral cell phenomenex cellulose-1, hexanes:i-PrOH/99.5:0.5; flow rate 0.6 mL/min



#### Detector A (254nm)

Pk #	Retention Time	Area	Area %	Height	Height %
1	7.025	9649699	99.542	357014	99.312
2	8.233	44447	0.458	2473	0.688
Total		9694146	100.000	359487	100.000

**HPLC Profile of (±)-210a:** chiral column Chiral cell OD-H, hexanes:i-PrOH/99.5:0.5; flow rate 0.8 mL/min

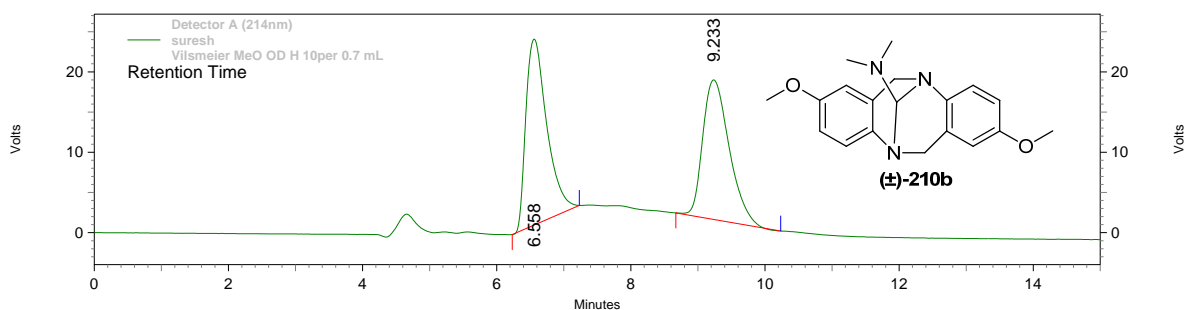


#### Detector A (214nm)

Pk #	Retention Time	Area	Area %	Height	Height %
1	5.475	3005344	50.070	188510	35.387
2	7.075	2996998	49.930	344193	64.613

Total		6002342	100.000	532703	100.000
-------	--	---------	---------	--------	---------

**HPLC Profile of (±)-210b:** chiral column Chiral cell OD-H, hexanes:i-PrOH/90:10; flow rate 0.7 mL/min

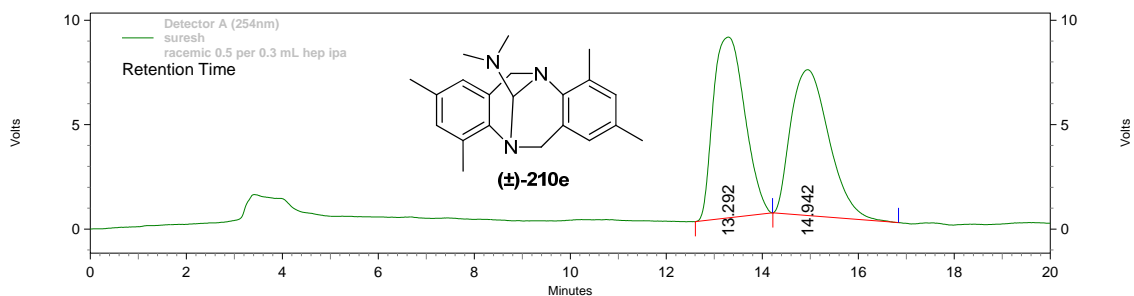


#### Detector A (214nm)

Pk #	Retention Time	Area	Area %	Height	Height %
1	6.558	501812	51.329	23127	57.133
2	9.233	475821	48.671	17352	42.867

Total		977633	100.000	40479	100.000
-------	--	--------	---------	-------	---------

**HPLC Profile of (±)-210e:** chiral column Chiral cell phenomenex cellulose-1, hexanes:i-PrOH/99.5:0.5; flow rate 0.3 mL/min

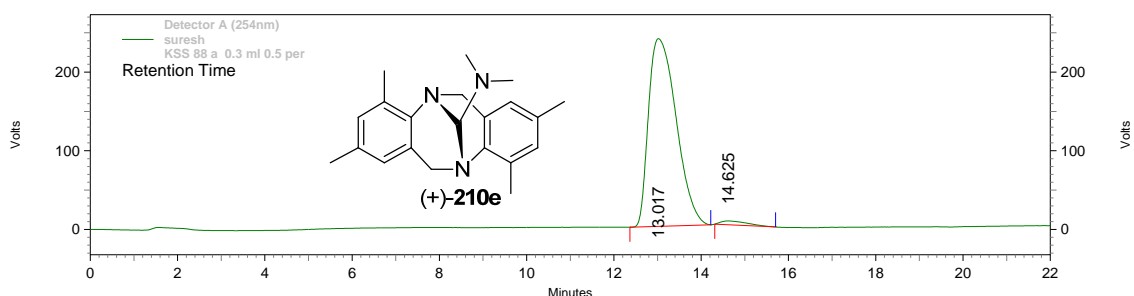


**Detector A (254nm)**

Pk #	Retention Time	Area	Area %	Height	Height %
1	13.292	395629	50.663	8658	55.358
2	14.942	385273	49.337	6982	44.642

Total		780902	100.000	15640	100.000
-------	--	--------	---------	-------	---------

**HPLC Profile of (+)-210e:** chiral column Chiral cell phenomenex cellulose-1, hexanes:i-PrOH/99.5:0.5; flow rate 0.3 mL/min



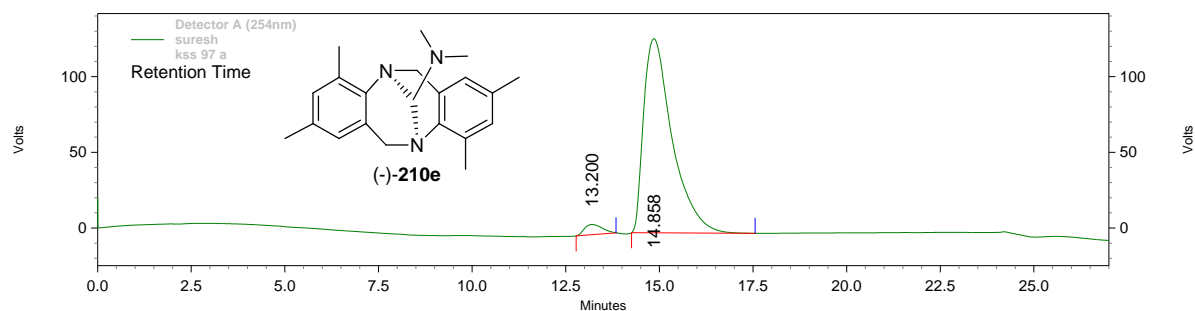
**Detector A (254nm)**

Pk #	Retention Time	Area	Area %	Height	Height %
1	13.017	10514135	98.021	238563	97.966
2	14.625	212297	1.979	4952	2.034

Total		10726432	100.000	243515	100.000
-------	--	----------	---------	--------	---------



**HPLC Profile of (–)-210e:** chiral column Chiral cell phenomenex cellulose-1, hexanes:i-PrOH/99.5:0.5; flow rate 0.3 mL/min

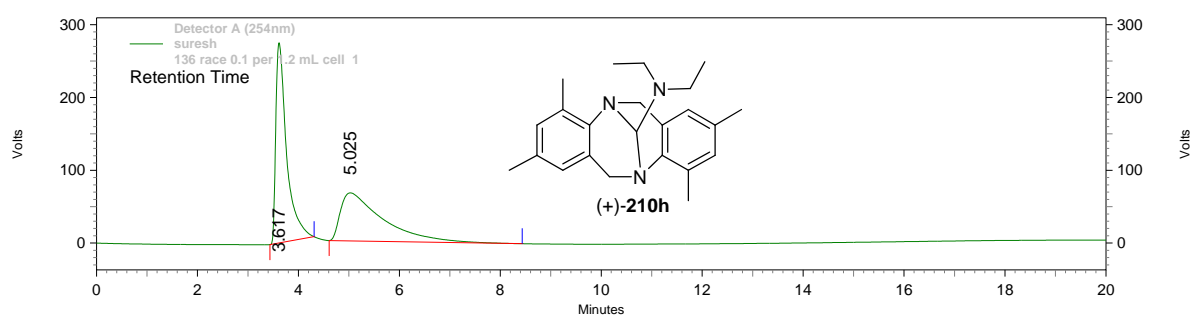


**Detector A (254nm)**

Pk #	Retention Time	Area	Area %	Height	Height %
1	13.200	222250	3.167	6677	4.952
2	14.858	6795584	96.833	128165	95.048

Total		7017834	100.000	134842	100.000
-------	--	---------	---------	--------	---------

**HPLC Profile of (±)-210h:** chiral column Chiral cell phenomenex cellulose-1, hexanes:i-PrOH/99.9:0.1; flow rate 1.2 mL/min

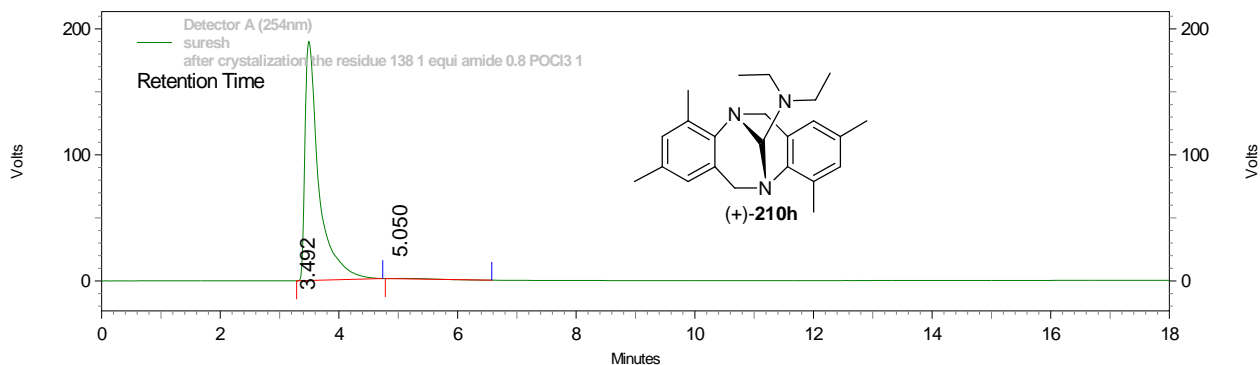


**Detector A (254nm)**

Pk #	Retention Time	Area	Area %	Height	Height %
1	3.617	4086581	51.506	274704	80.629
2	5.025	3847551	48.494	65998	19.371

Total		7934132	100.000	340702	100.000
-------	--	---------	---------	--------	---------

**HPLC Profile of (+)-210h:** chiral column Chiral cell phenomenex cellulose-1, hexanes:i-PrOH/99.9:0.1; flow rate 1.2 mL/min

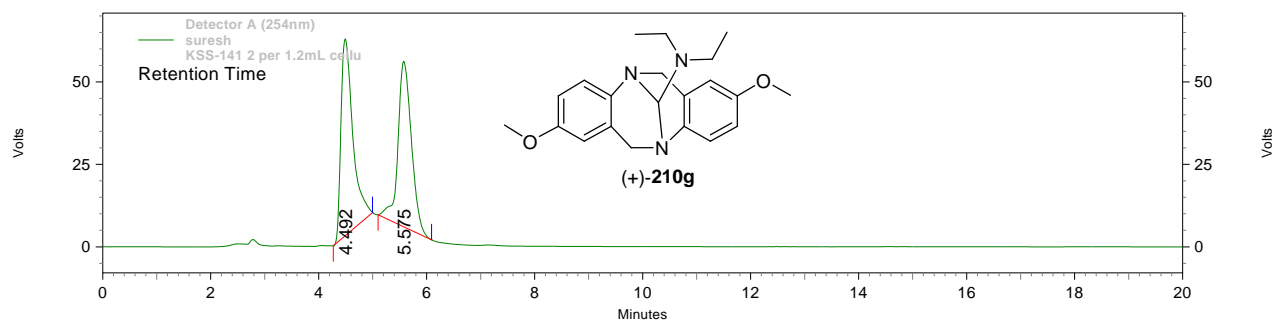


#### Detector A (254nm)

Pk #	Retention Time	Area	Area %	Height	Height %
1	3.492	3082453	99.635	189631	99.845
2	5.050	11286	0.365	294	0.155

Total		3093739	100.000	189925	100.000
-------	--	---------	---------	--------	---------

**HPLC Profile of (+)-210g:** chiral column Chiral cell phenomenex cellulose-1, hexanes:i-PrOH/98:2; flow rate 1.2 mL/min

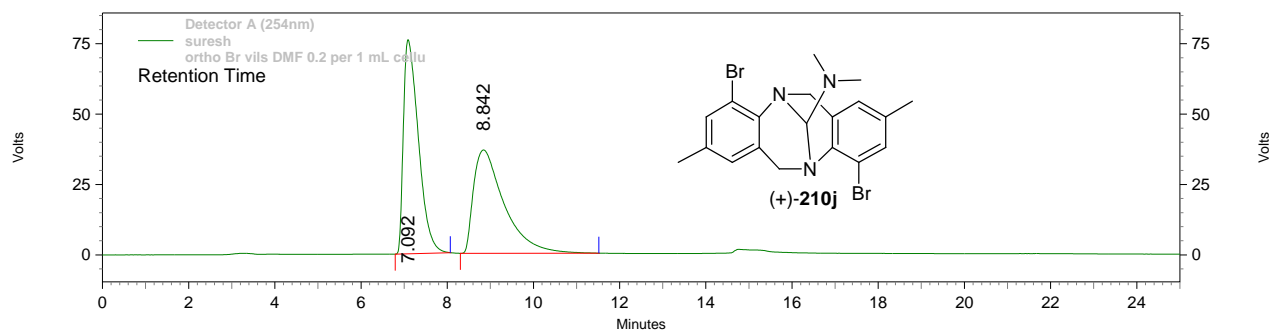


#### Detector A (254nm)

Pk #	Retention Time	Area	Area %	Height	Height %
1	4.492	910303	51.042	59596	54.313
2	5.575	873144	48.958	50131	45.687

Total		1783447	100.000	109727	100.000
-------	--	---------	---------	--------	---------

**HPLC Profile of (±)-210j:** chiral column Chiral cell phenomenex cellulose-1, hexanes:i-PrOH/99.8:0.2; flow rate 1.0 mL/min

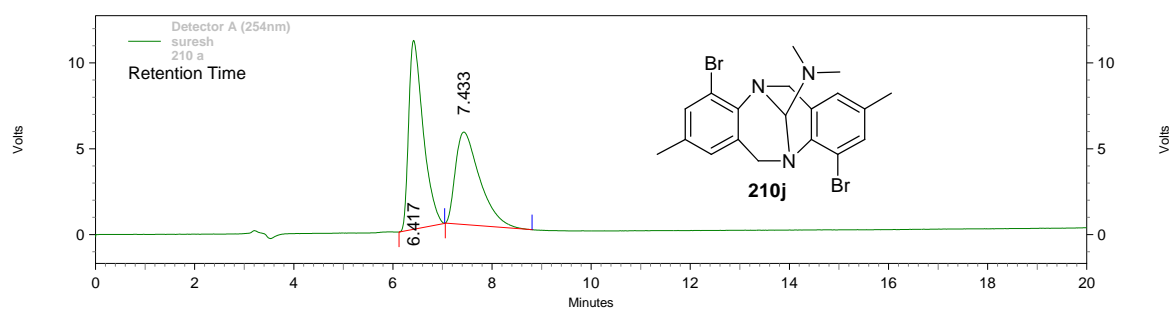


**Detector A (254nm)**

Pk #	Retention Time	Area	Area %	Height	Height %
1	7.092	1837338	50.287	76026	67.434
2	8.842	1816368	49.713	36715	32.566

Total		3653706	100.000	112741	100.000
-------	--	---------	---------	--------	---------

**HPLC Profile of 210j:** chiral column Chiral cell phenomenex cellulose-1, hexanes:i-PrOH/99.8:0.2; flow rate 1.0 mL/min

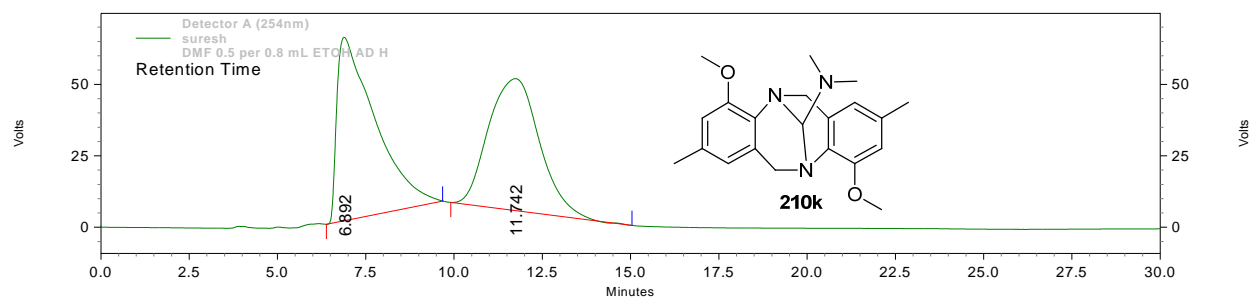


**Detector A (254nm)**

Pk #	Retention Time	Area	Area %	Height	Height %
1	6.417	223873	54.918	11003	67.120
2	7.433	183775	45.082	5390	32.880

Total		407648	100.000	16393	100.000
-------	--	--------	---------	-------	---------

**HPLC Profile of 210k:** chiral column Chiralcel AD-H, hexanes:i-PrOH/99.5:0.5; flow rate 0.8 mL/min

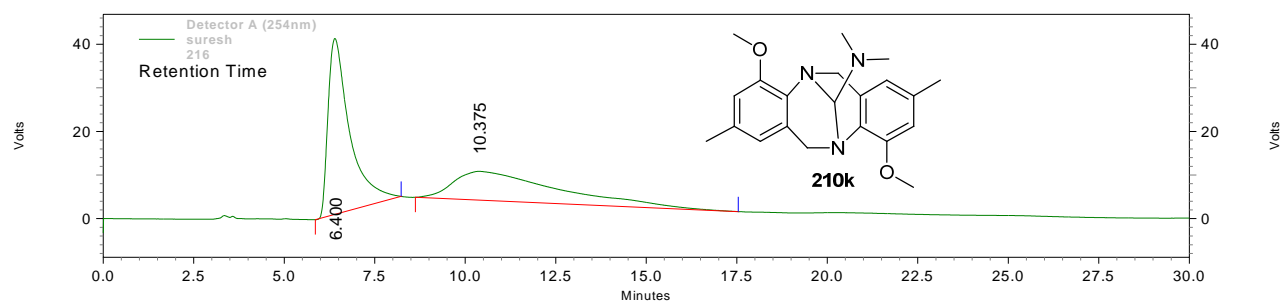


**Detector A (254nm)**

Pk #	Retention Time	Area	Area %	Height	Height %
1	6.892	4819146	50.908	64144	58.149
2	11.742	4647204	49.092	46165	41.851

Total		9466350	100.000	110309	100.000
-------	--	---------	---------	--------	---------

**HPLC Profile of 210k:** chiral column Chiralcel AD-H hexanes:i-PrOH/99.5:0.5; flow rate 0.8 mL/min



**Detector A (254nm)**

Pk #	Retention Time	Area	Area %	Height	Height %
1	6.400	1677063	55.170	40317	85.922
2	10.375	1362728	44.830	6606	14.078

Total		3039791	100.000	46923	100.000
-------	--	---------	---------	-------	---------

---

## *Appendix II*

*(X-Ray Crystallographic Data)*

---

**Table 1.** Atomic coordinates ( $\times 10^4$ ) and equivalent isotropic displacement parameters ( $\text{\AA}^2 \times 10^3$ ) for **188**.  $U(\text{eq})$  is defined as one third of the trace of the orthogonalized  $U_{ij}$  tensor.

atom	x	y	z	$U(\text{eq})$
S(3)	4265(1)	4654(1)	6648(1)	48(1)
S(2)	5150(1)	993(1)	4837(1)	44(1)
S(1)	513(1)	6830(1)	1848(1)	44(1)
S(4)	1207(1)	1477(1)	10100(1)	51(1)
O(7)	3715(4)	338(3)	4678(1)	55(1)
O(15)	538(4)	1182(3)	9592(2)	64(1)
O(12)	4905(4)	4095(3)	7170(1)	59(1)
O(2)	769(5)	7305(4)	1216(1)	66(1)
N(4)	1649(4)	8870(3)	5514(1)	35(1)
N(3)	-1162(4)	9207(3)	5941(1)	41(1)
O(1)	1948(4)	6095(3)	2010(1)	53(1)
O(11)	5499(4)	4503(4)	6099(2)	69(1)
N(5)	3981(4)	5099(3)	1154(1)	35(1)
O(14)	-186(4)	2219(3)	6365(1)	57(1)
N(11)	6813(4)	5637(3)	753(1)	40(1)
O(13)	3833(5)	5970(3)	6607(2)	71(1)
O(9)	4877(5)	1108(3)	5466(1)	69(1)
O(17)	1633(5)	2787(3)	10121(2)	77(1)
O(4)	379(5)	10541(3)	2698(2)	66(1)
O(16)	0(5)	1024(4)	10655(2)	76(1)
O(8)	6721(5)	436(4)	4655(2)	76(1)
O(18)	5674(4)	-1116(3)	10383(1)	58(1)
C(34)	1174(4)	7583(3)	5387(1)	34(1)
O(10)	6552(5)	2304(4)	6108(2)	77(1)
C(17)	4414(4)	3733(3)	1296(1)	32(1)
C(36)	-678(4)	8930(3)	6522(2)	36(1)
C(12)	7446(5)	4386(4)	1000(2)	43(1)
C(33)	-483(4)	7205(4)	5489(2)	39(1)
C(15)	6404(4)	5674(3)	167(2)	36(1)
O(6)	5201(5)	5174(3)	3983(2)	67(1)
C(62)	1237(4)	3260(3)	7055(2)	35(1)
C(30)	2425(5)	6796(3)	5161(2)	39(1)
C(53)	7511(5)	2786(4)	3596(2)	51(1)
C(72)	4211(4)	275(3)	9694(2)	36(1)
C(3)	3614(5)	1574(4)	1663(2)	42(1)
C(61)	2522(5)	3720(4)	6534(2)	44(1)
C(31)	2352(4)	8837(4)	6092(2)	38(1)
C(57)	5384(5)	4367(3)	3656(2)	43(1)
C(14)	4751(4)	5592(3)	66(2)	34(1)

C(42)	-40(5)	8200(3)	2852(2)	36(1)
C(35)	980(4)	8785(3)	6603(2)	34(1)
C(16)	6080(4)	3403(4)	1211(1)	38(1)
O(3)	-1054(4)	6166(4)	2027(2)	72(1)
C(6)	3339(4)	5391(3)	563(2)	36(1)
C(58)	4748(5)	2375(3)	3359(2)	43(1)
C(27)	-902(5)	6003(4)	5355(2)	45(1)
C(29)	1922(5)	5606(4)	5037(2)	44(1)
C(8)	5586(5)	5840(4)	-988(2)	41(1)
C(10)	7670(5)	5822(4)	-316(2)	42(1)
C(48)	860(5)	7368(3)	3329(2)	42(1)
C(13)	5462(5)	5986(4)	1153(2)	42(1)
C(80)	4180(6)	2305(5)	8896(2)	63(1)
C(66)	-1633(5)	2479(4)	7330(2)	49(1)
C(68)	235(5)	4205(4)	7430(2)	43(1)
C(32)	169(5)	9781(4)	5527(2)	42(1)
C(23)	256(5)	8554(3)	7658(2)	41(1)
C(2)	5255(5)	1189(4)	1585(2)	44(1)
C(24)	-1390(5)	8669(4)	7575(2)	43(1)
C(19)	1348(5)	3188(4)	1629(2)	50(1)
C(4)	3155(4)	2841(3)	1521(1)	37(1)
C(78)	5194(5)	1388(4)	9283(2)	43(1)
C(9)	7226(5)	5899(4)	-876(2)	42(1)
C(40)	4226(5)	7169(4)	5046(2)	51(1)
C(7)	4365(5)	5686(3)	-512(2)	39(1)
C(65)	-891(5)	3121(4)	7797(2)	48(1)
C(26)	-1819(5)	8091(4)	5715(2)	45(1)
C(28)	266(6)	5193(4)	5127(2)	46(1)
C(38)	-3724(5)	8991(5)	6949(2)	60(1)
C(51)	5108(5)	2615(3)	4487(2)	44(1)
C(52)	5650(5)	2937(3)	3826(2)	36(1)
C(46)	-1955(6)	7725(5)	3759(2)	58(1)
C(74)	5639(5)	-514(3)	9899(2)	42(1)
C(63)	1790(5)	2219(4)	7533(2)	50(1)
C(25)	-1919(5)	8859(4)	7013(2)	41(1)
C(22)	1447(5)	8607(3)	7167(2)	38(1)
C(67)	-203(5)	2599(3)	6840(2)	43(1)
C(71)	2968(5)	494(4)	10223(2)	44(1)
C(56)	5404(6)	4602(4)	2989(2)	52(1)
C(45)	-150(6)	7956(4)	3847(2)	49(1)
C(41)	511(5)	8251(3)	2198(2)	44(1)
C(1)	6470(5)	2119(4)	1356(2)	44(1)
C(47)	-1889(5)	7917(4)	3075(2)	52(1)
C(73)	3535(5)	-535(4)	9248(2)	50(1)

C(79)	6227(6)	2197(4)	9617(2)	58(1)
C(54)	7553(6)	2976(5)	2919(2)	60(1)
C(43)	211(5)	9545(3)	3031(2)	42(1)
C(64)	366(6)	2163(5)	8047(2)	60(1)
C(37)	780(6)	8376(5)	8273(2)	56(1)
C(44)	182(6)	9394(4)	3694(2)	50(1)
C(76)	6232(5)	450(4)	8919(2)	50(1)
C(49)	569(7)	5921(4)	3379(2)	61(1)
C(20)	5169(6)	5931(5)	-1615(2)	58(1)
C(55)	5732(6)	3255(4)	2833(2)	49(1)
C(69)	1247(6)	4893(5)	7820(2)	64(1)
C(75)	4902(6)	-353(5)	8711(2)	65(1)
C(77)	7022(5)	-419(4)	9392(2)	51(1)
C(60)	5050(7)	949(4)	3300(2)	62(1)
C(70)	-697(6)	5211(4)	7061(2)	59(1)
C(50)	2720(6)	7637(5)	3254(2)	60(1)
C(39)	-191(8)	3891(5)	4976(2)	70(1)
C(59)	2868(6)	2598(5)	3435(2)	62(1)
C(18)	5681(7)	-210(4)	1749(2)	64(1)
C(21)	9481(5)	5909(5)	-217(2)	61(1)
O(5)	8933(5)	8838(4)	629(2)	90(1)

**Table 2.** Atomic coordinates ( $\times 10^4$ ) and equivalent isotropic displacement parameters ( $\text{\AA}^2 \times 10^3$ ) for **193**.  $U(\text{eq})$  is defined as one third of the trace of the orthogonalized  $U_{ij}$  tensor.

atom	x	y	z	U(eq)
C(28)	3451(5)	4886(4)	-190(2)	12(1)
C(29)	3338(5)	6995(4)	728(2)	12(1)
C(36)	5291(5)	5269(4)	-297(2)	17(1)
C(32)	2152(5)	5705(4)	33(2)	10(1)
C(47)	6151(5)	776(4)	9136(2)	12(1)
C(49)	6348(5)	2555(4)	8302(2)	11(1)
C(48)	6652(5)	1102(4)	8476(2)	8(1)
C(54)	5737(6)	487(4)	8023(2)	13(1)
O(12)	6158(4)	3366(3)	8634(1)	18(1)
C(53)	8567(5)	962(4)	8232(2)	16(1)
C(50)	6315(6)	2753(4)	7645(2)	15(1)
C(52)	8561(6)	1140(5)	7558(2)	20(1)
C(51)	6685(6)	1388(4)	7490(2)	16(1)
C(56)	3821(6)	675(4)	8116(2)	20(1)
C(55)	6103(6)	-962(4)	7972(2)	19(1)
Br(1)	6263(1)	4018(1)	2942(1)	20(1)
Br(3)	1811(1)	6555(1)	3032(1)	19(1)
Br(2)	6889(1)	-2451(1)	6462(1)	18(1)



Br(4)	653(1)	1649(1)	-413(1)	18(1)
S(3)	5323(1)	2836(1)	1264(1)	14(1)
S(2)	2183(1)	9655(1)	4790(1)	19(1)
C(59)	6695(6)	7624(5)	4556(2)	16(1)
C(8)	6721(5)	3959(4)	3725(2)	12(1)
O(16)	823(4)	278(3)	1056(1)	18(1)
C(7)	5426(5)	3809(4)	4183(2)	12(1)
C(21)	1165(5)	6740(4)	2270(2)	12(1)
O(14)	6598(4)	2604(3)	736(1)	19(1)
C(34)	1940(5)	6959(4)	1231(2)	10(1)
N(1)	2648(4)	7019(3)	150(2)	12(1)
O(15)	5942(4)	2374(3)	1803(1)	18(1)
C(10)	8795(5)	3984(4)	4390(2)	14(1)
O(6)	2618(4)	10985(3)	4834(2)	27(1)
C(72)	1386(6)	419(5)	2726(2)	21(1)
O(8)	6722(4)	7009(3)	5037(2)	21(1)
O(5)	941(4)	9160(3)	5330(2)	26(1)
O(13)	4846(4)	4185(3)	1187(2)	22(1)
C(75)	2258(6)	3178(5)	2429(2)	21(1)
N(11)	7852(4)	3821(3)	5448(2)	11(1)
C(68)	2267(5)	1420(4)	1713(2)	12(1)
C(76)	303(5)	3409(4)	1677(2)	17(1)
C(14)	5799(5)	3731(4)	4757(2)	12(1)
N(2)	-207(4)	7366(3)	577(2)	11(1)
C(71)	88(5)	1352(5)	2462(2)	17(1)
C(20)	2409(5)	6777(4)	1795(2)	12(1)
C(22)	-531(6)	6826(4)	2200(2)	14(1)
N(5)	4951(4)	3247(3)	5841(2)	11(1)
O(7)	1553(4)	9415(3)	4262(2)	24(1)
C(16)	7121(5)	1540(4)	5893(2)	12(1)
C(2)	6294(6)	-677(4)	6250(2)	12(1)
C(6)	4344(5)	3535(4)	5243(2)	11(1)
C(19)	10615(5)	4064(5)	4490(2)	17(1)
C(26)	1261(5)	3305(4)	-218(2)	11(1)
C(64)	6218(6)	9553(5)	3949(2)	18(1)
C(57)	3983(5)	8662(5)	4902(2)	16(1)
C(31)	479(6)	5323(4)	134(2)	13(1)
C(69)	791(5)	704(4)	1524(2)	16(1)
C(3)	4600(6)	-352(4)	6343(2)	15(1)
C(18)	2297(5)	1262(4)	6295(2)	17(1)
C(58)	5226(5)	8419(4)	4363(2)	13(1)
C(30)	1151(5)	7935(4)	160(2)	14(1)
C(15)	7461(5)	3849(4)	4859(2)	12(1)
C(23)	-1009(5)	6997(4)	1641(2)	12(1)

C(67)	3571(5)	1831(4)	1179(2)	13(1)
C(9)	8389(5)	4033(4)	3824(2)	14(1)
C(12)	8503(5)	2563(4)	5688(2)	14(1)
C(60)	8077(6)	7743(5)	4042(2)	19(1)
C(17)	5410(5)	1865(4)	5980(2)	11(1)
C(33)	247(5)	7083(4)	1157(2)	12(1)
C(24)	-914(5)	6233(5)	352(2)	16(1)
C(70)	-655(5)	637(4)	2014(2)	16(1)
C(61)	7269(6)	8613(5)	3578(2)	19(1)
C(65)	7263(6)	10397(5)	4268(2)	22(1)
C(63)	4534(5)	7585(5)	3932(2)	17(1)
C(27)	2942(6)	3670(4)	-315(2)	14(1)
C(73)	2836(5)	404(5)	2204(2)	17(1)
C(13)	6434(5)	4163(4)	5844(2)	13(1)
C(74)	1242(5)	2420(4)	2067(2)	13(1)
C(4)	4132(5)	935(4)	6196(2)	13(1)
C(1)	7552(5)	229(4)	6034(2)	13(1)
C(66)	5151(6)	10455(5)	3568(2)	24(1)
C(35)	-2862(5)	7098(5)	1577(2)	19(1)
C(62)	5918(6)	7768(5)	3383(2)	23(1)
C(25)	12(5)	4100(4)	7(2)	12(1)
S(1)	1398(1)	4977(1)	6527(1)	13(1)
O(4)	1446(4)	8728(3)	7371(1)	17(1)
O(1)	1704(4)	5450(3)	5893(1)	18(1)
O(3)	-240(4)	4352(3)	6710(2)	23(1)
O(2)	2820(4)	4162(3)	6684(1)	18(1)
C(39)	1268(5)	7718(4)	7700(2)	13(1)
C(37)	1488(6)	6414(4)	6869(2)	14(1)
C(40)	1277(6)	7544(4)	8367(2)	16(1)
C(46)	3778(6)	5728(5)	7897(2)	19(1)
C(43)	-942(5)	6086(5)	7775(2)	16(1)
C(38)	973(5)	6359(4)	7527(2)	11(1)
C(45)	1524(6)	4015(4)	8045(2)	18(1)
C(42)	-962(5)	5887(5)	8452(2)	16(1)
C(41)	908(6)	6085(5)	8524(2)	16(1)
C(44)	1871(5)	5496(4)	7993(2)	14(1)
S(4)	6263(1)	-849(1)	9490(1)	12(1)
O(9)	7901(4)	-1376(3)	9309(2)	23(1)
O(11)	5976(4)	-720(3)	10122(1)	18(1)
O(10)	4839(4)	-1576(3)	9336(1)	18(1)
O(17)	7556(4)	347(3)	830(2)	19(1)
O(18)	9991(5)	6950(3)	5232(2)	24(1)

---

**Table 3.** Atomic coordinates (  $\times 10^4$ ) and equivalent isotropic displacement parameters ( $\text{\AA}^2 \times 10^3$ ) for **66**. U(eq) is defined as one third of the trace of the orthogonalized  $U^{ij}$  tensor.

atom	x	y	z	U(eq)
Br(1)	4393(1)	5630(1)	5373(1)	58(1)
Br(2)	-156(1)	11363(1)	9697(1)	63(1)
C(5)	1902(6)	7445(6)	6420(3)	34(1)
C(13)	3992(7)	9174(6)	8389(4)	40(1)
C(4)	2296(5)	5949(6)	6011(3)	37(1)
C(8)	2370(6)	9892(6)	8459(4)	37(1)
N(2)	3049(5)	8743(6)	6382(3)	39(1)
C(1)	-822(6)	6320(7)	6860(4)	38(1)
C(11)	4695(9)	9317(8)	10375(4)	54(1)
N(1)	1228(5)	10264(5)	7515(3)	38(1)
C(6)	272(6)	7601(6)	6854(3)	34(1)
C(15)	2164(6)	10245(7)	6511(4)	42(1)
C(9)	1973(6)	10283(6)	9527(4)	42(1)
C(12)	5135(8)	8934(8)	9333(5)	49(1)
C(16)	-1573(8)	3423(7)	6566(5)	55(1)
C(2)	-403(6)	4832(6)	6502(4)	40(1)
C(14)	4528(6)	8675(8)	7274(4)	43(1)
C(3)	1209(7)	4690(7)	6052(4)	44(1)
C(7)	-220(6)	9177(6)	7317(4)	39(1)
C(10)	3084(8)	9984(7)	10453(4)	52(1)
C(17)	5964(12)	9051(14)	11390(5)	83(3)

**Table 4.** Atomic coordinates (  $\times 10^4$ ) and equivalent isotropic displacement parameters ( $\text{\AA}^2 \times 10^3$ ) for **200**. U(eq) is defined as one third of the trace of the orthogonalized  $U^{ij}$  tensor.

atom	x	y	z	U(eq)
N(1)	-4750(1)	-7169(5)	-7617(1)	52(1)
N(2)	-4845(1)	-2288(4)	-9199(1)	48(1)
C(6)	-3868(1)	-5450(5)	-8184(1)	46(1)
C(4)	-3937(1)	-4572(5)	-9645(2)	43(1)
C(5)	-4219(1)	-4130(4)	-9013(2)	43(1)
C(3)	-3300(1)	-6250(5)	-9426(2)	49(1)
C(2)	-2937(1)	-7560(5)	-8602(2)	50(1)
C(9)	-4163(1)	-5218(6)	-7486(2)	51(1)
C(1)	-3235(1)	-7144(6)	-7997(2)	51(1)
C(10)	-5005(1)	-7259(6)	-6911(2)	51(1)
C(12)	-4302(1)	-7373(6)	-5924(2)	50(1)
C(18)	-2270(2)	-9459(8)	-8386(2)	67(1)

C(16)	-3089(2)	-9379(7)	-4738(2)	72(1)
C(17)	-3721(2)	-9264(7)	-5636(2)	65(1)
C(15)	-3035(2)	-7588(8)	-4110(2)	70(1)
C(13)	-4220(2)	-5562(7)	-5290(2)	61(1)
C(14)	-3591(2)	-5688(8)	-4388(2)	73(1)
C(11)	-5605(2)	-9395(7)	-7128(2)	66(1)
C(7)	-5642(1)	-3379(5)	-9408(2)	50(1)
C(8)	-5000	-761(7)	-10000	54(1)

**Table 5.** Atomic coordinates ( $\times 10^4$ ) and equivalent isotropic displacement parameters ( $\text{\AA}^2 \times 10^3$ ) for **206**.  $U(\text{eq})$  is defined as one third of the trace of the orthogonalized  $U_{ij}$  tensor.

atom	x	y	z	U(eq)
C(13)	5789(2)	9437(2)	6829(6)	60(1)
O(7)	7621(1)	-321(1)	9815(4)	58(1)
O(6)	7898(1)	937(1)	9048(4)	56(1)
N(5)	5317(1)	9044(2)	6688(5)	58(1)
O(1)	6836(1)	138(2)	6745(4)	73(1)
C(15)	5999(2)	8166(2)	6672(6)	57(1)
C(4)	4542(2)	8820(2)	4721(6)	57(1)
O(10)	7219(1)	8800(2)	4509(5)	81(1)
O(9)	4265(1)	8620(2)	6118(4)	73(1)
N(11)	6236(2)	9231(2)	5603(4)	57(1)
C(16)	5106(2)	9020(2)	4986(5)	50(1)
O(2)	7682(2)	487(2)	5963(4)	75(1)
O(4)	7596(2)	125(2)	12907(4)	78(1)
C(10)	6890(2)	8356(2)	5283(6)	64(1)
C(30)	7282(2)	411(2)	6968(6)	58(1)
C(1)	5189(2)	9228(2)	1996(6)	61(1)
C(17)	5425(2)	9202(2)	3616(6)	53(1)
C(2)	4631(2)	9067(2)	1730(6)	64(1)
C(12)	6029(2)	9385(2)	3847(6)	58(1)
C(3)	4317(2)	8849(2)	3107(6)	62(1)
C(14)	6369(2)	8564(2)	5851(6)	59(1)
O(3)	6998(2)	898(2)	12281(4)	83(1)
C(29)	7344(2)	688(2)	8789(5)	51(1)
C(32)	7271(2)	435(2)	11913(6)	59(1)
O(5)	7604(2)	1850(2)	7914(5)	88(1)
C(6)	5453(2)	8412(2)	7367(6)	67(1)
C(28)	7983(2)	1533(2)	8472(6)	64(1)
O(8)	6931(2)	-1027(2)	10072(6)	100(1)
C(31)	7245(2)	188(2)	10103(5)	55(1)
C(19)	3701(2)	8385(3)	5903(7)	79(2)

C(9)	7025(2)	7725(3)	5507(6)	79(2)
C(8)	6653(3)	7320(3)	6314(7)	82(2)
C(33)	7418(2)	-909(2)	9806(6)	66(1)
C(27)	8568(2)	1730(3)	8622(7)	77(2)
C(22)	8703(2)	2347(3)	8286(7)	86(2)
C(34)	7849(3)	-1366(2)	9357(7)	75(1)
C(21)	7783(2)	8625(3)	4104(8)	100(2)
C(35)	7734(3)	-2001(2)	9318(8)	101(2)
C(7)	6142(2)	7546(2)	6839(6)	75(1)
C(18)	4355(2)	9109(3)	39(6)	94(2)
C(39)	8381(3)	-1189(3)	8940(12)	132(3)
C(23)	9248(3)	2551(4)	8366(10)	112(2)
C(36)	8130(4)	-2441(3)	8908(10)	121(3)
C(26)	8992(2)	1324(3)	9173(14)	146(4)
C(24)	9657(4)	2151(5)	8845(16)	173(5)
C(38)	8788(3)	-1628(4)	8475(16)	179(5)
C(37)	8654(4)	-2259(4)	8533(14)	153(4)
C(20)	6798(3)	6622(3)	6495(9)	120(3)
C(25)	9541(3)	1519(4)	9351(17)	186(5)

**Table 6.** Atomic coordinates ( $\times 10^4$ ) and equivalent isotropic displacement parameters ( $\text{\AA}^2 \times 10^3$ ) for **211**. U(eq) is defined as one third of the trace of the orthogonalized  $U_{ij}$  tensor.

atom	x	y	z	U(eq)
N(2)	10854(4)	5704(3)	2595(2)	49(1)
C(5)	7476(5)	7134(3)	2738(3)	51(1)
C(7)	8069(4)	4956(3)	2670(3)	44(1)
C(12)	9647(4)	5079(3)	3063(3)	43(1)
C(8)	6956(5)	4341(3)	3131(3)	52(1)
C(11)	10036(5)	4551(3)	3897(3)	53(1)
C(1)	9626(5)	7869(3)	3707(3)	57(1)
C(2)	8529(6)	8389(4)	4280(4)	68(1)
C(14)	9177(5)	7236(3)	2945(3)	48(1)
N(1)	6895(5)	6546(3)	1967(3)	63(1)
C(9)	7341(5)	3819(3)	3971(3)	53(1)
C(4)	6362(5)	7658(4)	3317(4)	70(2)
C(10)	8902(6)	3939(3)	4340(3)	56(1)
C(3)	6859(6)	8266(4)	4059(4)	70(1)
C(13)	10507(5)	6766(4)	2346(3)	56(1)
C(6)	7588(5)	5525(4)	1776(3)	60(1)
C(16)	6105(6)	3103(4)	4436(4)	84(2)
O(1)	13418(3)	5783(3)	1933(3)	84(1)
C(17)	12329(5)	5322(4)	2344(3)	61(1)
C(15)	9095(8)	9077(5)	5075(4)	101(2)

**Table 7.** Atomic coordinates ( $\times 10^4$ ) and equivalent isotropic displacement parameters ( $\text{\AA}^2 \times 10^3$ ) for **210d**.  $U(\text{eq})$  is defined as one third of the trace of the orthogonalized  $U_{ij}$  tensor.

atom	x	y	z	U(eq)
N(1)	3107(1)	2337(2)	1775(1)	35(1)
N(2)	4177(1)	820(2)	1582(1)	34(1)
N(3)	3212(1)	-27(2)	2071(1)	40(1)
C(11)	2519(1)	2065(2)	1210(1)	33(1)
C(10)	2722(2)	1112(2)	842(1)	34(1)
C(5)	4661(1)	2009(2)	1496(1)	33(1)
C(6)	4427(2)	3363(2)	1595(1)	35(1)
C(9)	3572(2)	304(2)	1038(1)	38(1)
C(12)	1725(2)	2744(3)	1048(1)	40(1)
C(8)	3693(1)	1178(2)	1981(1)	34(1)
C(4)	5388(2)	1778(3)	1314(1)	39(1)
C(1)	4939(2)	4467(3)	1515(1)	42(1)
C(3)	5892(2)	2860(3)	1229(1)	43(1)
C(15)	2119(2)	863(3)	306(1)	42(1)
C(7)	3640(2)	3592(3)	1802(1)	40(1)
C(13)	1111(2)	2488(3)	519(1)	47(1)
C(2)	5660(2)	4203(3)	1334(1)	48(1)
C(14)	1320(2)	1557(3)	154(1)	49(1)
C(019)	2647(2)	297(4)	2420(1)	54(1)
C(16)	2317(2)	-123(3)	-118(1)	61(1)
C(20)	3798(2)	-1158(3)	2333(1)	59(1)
C(18)	6691(2)	2601(4)	1048(1)	60(1)
C(19)	4717(2)	5947(3)	1617(2)	66(1)
C(17)	219(2)	3147(4)	362(2)	76(1)

**Table 8.** Atomic coordinates ( $\times 10^4$ ) and equivalent isotropic displacement parameters ( $\text{\AA}^2 \times 10^3$ ) for **216a**.  $U(\text{eq})$  is defined as one third of the trace of the orthogonalized  $U_{ij}$  tensor.

atom	x	y	z	U(eq)
N(1)	8721(1)	1000(2)	7534(1)	34(1)
N(2)	6703(1)	1879(2)	6769(1)	35(1)
C(3)	7487(2)	973(2)	7640(2)	32(1)
N(4)	7420(1)	1534(2)	8710(1)	34(1)
C(5)	6188(2)	1584(2)	8881(2)	38(1)
C(6)	8165(2)	-553(2)	10106(2)	36(1)
C(7)	9212(2)	2556(2)	7706(2)	39(1)
C(8)	8565(2)	2272(3)	10570(2)	48(1)

C(9)	5711(2)	3228(3)	8764(2)	53(1)
C(10)	8350(2)	3758(2)	7129(2)	39(1)
C(11)	7572(2)	-2257(3)	11388(2)	49(1)
C(12)	8365(2)	1032(2)	9686(2)	36(1)
C(13)	7714(2)	366(2)	5592(2)	40(1)
C(14)	6545(2)	993(3)	5740(2)	43(1)
C(15)	8742(2)	419(2)	6461(2)	39(1)
C(16)	7793(2)	-798(3)	11069(2)	42(1)
C(17)	6363(2)	4501(3)	6160(2)	53(1)
C(18)	7153(2)	3389(2)	6680(2)	36(1)
C(19)	8717(2)	5240(3)	7032(2)	51(1)
C(20)	5285(2)	419(3)	8231(2)	41(1)
C(21)	7718(2)	-3493(3)	10761(2)	57(1)
C(22)	7790(2)	-290(3)	4598(2)	56(1)
C(23)	8339(2)	-1820(3)	9500(2)	45(1)
C(24)	6744(3)	5975(3)	6073(2)	67(1)
C(25)	3552(2)	-227(4)	6760(2)	65(1)
C(26)	5289(2)	-1060(3)	8609(2)	56(1)
C(27)	9820(2)	-116(3)	6311(2)	54(1)
C(28)	4402(2)	810(3)	7291(2)	50(1)
C(29)	8851(3)	-822(4)	4456(2)	72(1)
C(30)	8107(2)	-3273(3)	9816(2)	57(1)
C(31)	4449(3)	-2116(3)	8070(3)	74(1)
C(32)	7924(3)	6345(3)	6504(2)	67(1)
C(33)	9875(3)	-736(4)	5314(2)	73(1)
C(34)	3573(3)	-1690(4)	7149(3)	75(1)

**Table 9.** Atomic coordinates ( $\times 10^4$ ) and equivalent isotropic displacement parameters ( $\text{\AA}^2 \times 10^3$ ) for **217a**.  $U(\text{eq})$  is defined as one third of the trace of the orthogonalized  $U_{ij}$  tensor.

atom	x	y	z	$U(\text{eq})$
N(2)	4615(4)	-604(2)	1466(2)	36(1)
N(3)	3323(4)	436(2)	2105(2)	35(1)
N(1)	2036(4)	-700(2)	1511(2)	35(1)
C(1)	3339(5)	-475(3)	1868(2)	37(1)
C(2)	1798(4)	1781(3)	2219(2)	36(1)
C(3)	4657(5)	-1517(3)	1227(2)	37(1)
C(4)	5741(5)	1147(3)	2235(2)	38(1)
C(5)	3452(5)	-2056(3)	1224(2)	38(1)
C(6)	1957(5)	-201(3)	926(2)	40(1)
C(7)	4492(5)	684(3)	2569(2)	38(1)
C(8)	5947(6)	-1851(3)	1001(2)	46(1)
C(9)	2015(5)	-1679(3)	1441(2)	44(1)

C(10)	1898(5)	757(3)	2309(2)	43(1)
C(11)	5678(5)	2048(3)	2110(3)	50(1)
C(12)	3548(6)	-2952(3)	1019(2)	45(1)
C(13)	3154(6)	180(3)	641(2)	41(1)
C(14)	4606(5)	50(3)	935(2)	40(1)
C(15)	609(6)	-59(4)	674(3)	54(2)
C(16)	6054(6)	-2725(3)	764(2)	45(1)
C(17)	1412(6)	423(4)	2967(3)	59(2)
C(18)	4847(6)	-3255(3)	785(2)	49(1)
C(19)	2016(5)	2114(4)	1612(3)	51(1)
C(20)	1427(6)	2375(3)	2691(3)	51(1)
C(21)	8101(5)	1158(5)	1774(3)	73(2)
C(22)	1587(9)	853(4)	-135(3)	77(2)
C(23)	6987(5)	709(4)	2061(3)	53(1)
C(24)	2954(7)	708(4)	102(3)	62(2)
C(25)	7451(6)	-3074(4)	498(3)	67(2)
C(26)	7997(6)	2064(5)	1654(3)	69(2)
C(27)	1892(6)	3009(4)	1481(3)	63(2)
C(28)	6773(6)	2507(4)	1813(3)	62(2)
C(29)	1305(7)	3277(4)	2562(3)	68(2)
C(30)	1534(6)	3599(4)	1957(4)	68(2)
C(31)	2254(7)	-3555(4)	1027(3)	68(2)
C(32)	393(8)	486(4)	150(3)	67(2)
C(33)	4248(9)	1141(6)	-218(4)	106(3)
C(34)	-1101(9)	701(6)	-93(4)	105(3)
C(35)	4966(6)	-88(3)	3004(2)	52(1)

**Table 10.** Atomic coordinates ( $\times 10^4$ ) and equivalent isotropic displacement parameters ( $\text{\AA}^2 \times 10^3$ ) for **210h**.  $U(\text{eq})$  is defined as one third of the trace of the orthogonalized  $U^{\text{ij}}$  tensor.

atom	x	y	z	U(eq)
N(2)	8162(1)	2780(2)	1851(1)	49(1)
N(1)	7119(1)	2599(2)	573(1)	51(1)
C(3)	7539(1)	1811(2)	2196(1)	46(1)
C(4)	8508(1)	861(2)	828(1)	51(1)
C(5)	7212(1)	388(2)	3321(1)	58(1)
C(6)	7810(1)	1328(2)	2993(1)	52(1)
C(7)	6088(1)	472(2)	2119(1)	54(1)
C(8)	7333(1)	427(2)	-365(1)	52(1)
N(3)	7137(1)	5025(2)	1358(1)	59(1)
C(10)	6671(1)	1395(2)	1760(1)	47(1)
C(11)	7658(1)	1283(2)	348(1)	49(1)



C(12)	9025(1)	-403(2)	588(1)	56(1)
C(13)	6363(1)	1954(2)	911(1)	53(1)
C(14)	7694(1)	3707(2)	1152(1)	52(1)
C(15)	7864(1)	-842(2)	-569(1)	58(1)
C(16)	8711(1)	-1286(2)	-105(1)	58(1)
C(17)	6346(1)	-60(2)	2898(1)	59(1)
C(18)	8862(1)	1747(2)	1605(1)	55(1)
C(19)	8722(1)	1875(3)	3492(1)	68(1)
C(20)	6428(1)	877(3)	-901(1)	66(1)
C(21)	7536(2)	5920(3)	2091(1)	71(1)
C(22)	9251(2)	-2718(3)	-331(1)	77(1)
C(23)	6819(2)	6147(3)	678(1)	78(1)
C(24)	5930(2)	6942(3)	672(2)	95(1)
C(25)	5708(2)	-1089(3)	3268(2)	88(1)
C(26)	8459(2)	6759(4)	2129(2)	108(1)

**Table 11.** Atomic coordinates ( $\times 10^4$ ) and equivalent isotropic displacement parameters ( $\text{\AA}^2 \times 10^3$ ) for **242a**. U(eq) is defined as one third of the trace of the orthogonalized  $U_{ij}$  tensor.

atom	x	y	z	U(eq)
N(1)	4399(2)	2966(1)	4896(3)	50(1)
N(2)	5636(2)	4474(1)	4856(4)	53(1)
C(6)	6159(2)	4138(2)	6713(4)	48(1)
C(4)	6258(2)	3350(2)	9493(4)	53(1)
C(17)	4643(2)	2192(2)	4885(4)	47(1)
C(13)	4292(2)	3832(2)	2191(4)	49(1)
C(5)	5728(2)	3627(2)	7618(4)	47(1)
C(7)	4690(2)	3428(2)	6692(4)	50(1)
C(18)	5116(2)	1787(2)	6623(5)	56(1)
C(8)	3843(2)	3335(2)	3076(4)	49(1)
C(22)	4423(2)	1787(2)	3105(5)	57(1)
C(19)	5334(3)	1013(2)	6569(6)	68(1)
C(12)	3753(2)	4167(2)	384(4)	58(1)
C(3)	7194(2)	3561(2)	10511(5)	59(1)
C(2)	7596(2)	4070(2)	9571(5)	62(1)
C(20)	5088(3)	616(2)	4811(6)	72(1)
C(14)	5335(2)	3962(2)	3105(4)	52(1)
C(1)	7091(2)	4353(2)	7714(5)	60(1)
C(9)	2892(2)	3187(2)	2206(5)	60(1)
C(11)	2798(3)	4006(2)	-536(5)	63(1)
C(15)	7742(3)	3258(3)	12546(6)	86(1)

C(21)	4638(3)	1008(2)	3100(6)	67(1)
C(10)	2378(2)	3517(2)	396(5)	65(1)
C(16)	2248(3)	4354(3)	-2528(6)	97(2)

**Table 12.** Atomic coordinates ( $\times 10^4$ ) and equivalent isotropic displacement parameters ( $\text{\AA}^2 \times 10^3$ ) for **246**. U(eq) is defined as one third of the trace of the orthogonalized  $U_{ij}$  tensor.

atom	x	y	z	U(eq)
N(2)	2346(1)	3127(1)	8068(1)	39(1)
N(4)	6692(1)	2374(1)	2362(1)	42(1)
N(1)	1369(2)	3245(1)	9740(1)	44(1)
N(3)	3925(2)	1440(2)	1363(2)	53(1)
C(20)	3339(2)	2784(2)	8192(1)	36(1)
C(12)	1404(2)	4378(2)	8630(2)	37(1)
C(1)	990(2)	5027(2)	8014(2)	40(1)
C(13)	739(2)	3833(2)	9093(1)	38(1)
C(15)	480(2)	1781(2)	7905(2)	40(1)
C(45)	7360(2)	1833(2)	2017(2)	39(1)
C(43)	5488(2)	1490(2)	3213(2)	42(1)
C(44)	6551(2)	2233(2)	3312(2)	39(1)
C(14)	1146(2)	2313(2)	7430(2)	38(1)
C(4)	-397(2)	3877(2)	8903(2)	44(1)
C(25)	3155(2)	1696(2)	7687(2)	49(1)
C(21)	4536(2)	3502(2)	8796(2)	47(1)
C(10)	2541(2)	4090(2)	8932(2)	39(1)
C(3)	-790(2)	4544(2)	8284(2)	47(1)
C(2)	-120(2)	5131(2)	7850(2)	45(1)
C(42)	4136(2)	2534(2)	1968(2)	49(1)
C(23)	5292(2)	2082(2)	8359(2)	47(1)
C(34)	7497(2)	2873(2)	4342(2)	44(1)
C(41)	5195(2)	3288(2)	2096(2)	46(1)
C(9)	667(2)	2031(2)	6291(2)	45(1)
C(6)	-652(2)	968(2)	7223(2)	46(1)
C(22)	5494(2)	3150(2)	8880(2)	51(1)
C(35)	5766(2)	2668(2)	1549(2)	46(1)
C(11)	2643(2)	3795(2)	9965(2)	46(1)
C(31)	5423(2)	1394(2)	4165(2)	49(1)
C(32)	6362(2)	1978(2)	5192(2)	50(1)
C(46)	7337(2)	1747(2)	994(2)	52(1)
C(8)	-443(2)	1183(2)	5656(2)	53(1)
C(7)	-1121(2)	639(2)	6098(2)	50(1)
C(50)	8097(2)	1373(2)	2694(2)	50(1)

C(5)	915(2)	2059(2)	9133(2)	48(1)
C(30)	4386(2)	819(2)	2122(2)	53(1)
C(26)	5577(2)	4379(2)	2674(2)	54(1)
C(33)	7398(2)	2715(2)	5264(2)	51(1)
C(24)	4120(2)	1362(2)	7772(2)	53(1)
C(40)	8608(2)	3740(2)	4469(2)	63(1)
C(47)	8028(2)	1230(2)	685(2)	60(1)
C(36)	4647(2)	1655(2)	760(2)	57(1)
C(17)	-1150(2)	3240(2)	9346(2)	62(1)
C(49)	8792(2)	880(2)	2376(2)	58(1)
C(48)	8761(2)	798(2)	1369(2)	61(1)
C(18)	1333(2)	2642(2)	5766(2)	63(1)
C(29)	3426(2)	2844(2)	2422(2)	60(1)
C(27)	4890(2)	4727(2)	3146(2)	62(1)
C(16)	-576(2)	5891(2)	7240(2)	66(1)
C(28)	3840(2)	3952(2)	3005(2)	67(1)
C(39)	6271(3)	1833(2)	6210(2)	74(1)
C(19)	-2336(2)	-258(2)	5379(2)	75(1)
C(38)	2273(3)	2024(3)	2281(3)	92(1)
C(37)	5290(3)	5917(2)	3796(3)	94(1)

---

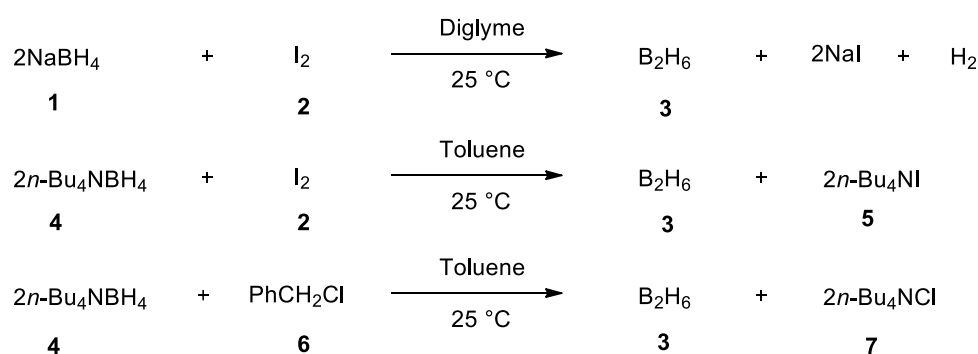
**Synthesis and application of poly(N-methylaniline)**

---

## III. 1 Introduction

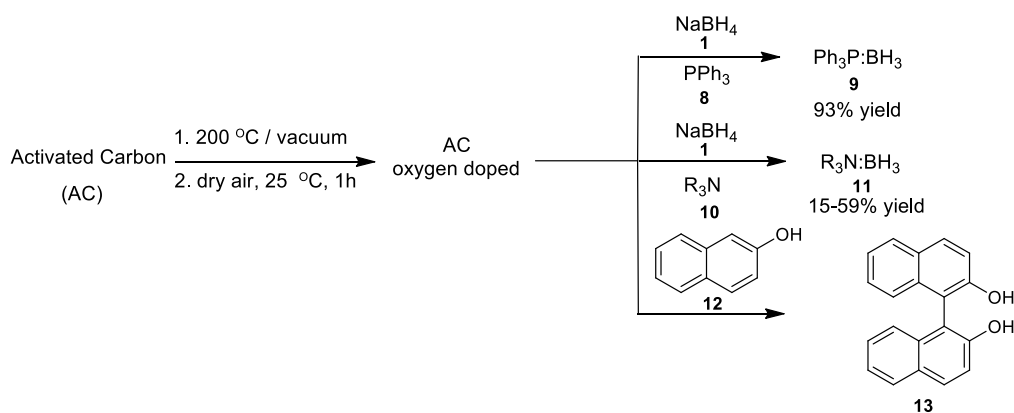
There has been continued interest on the development of boron chemistry in this laboratory. Previously, the  $\text{NaBH}_4/\text{I}_2$ ,  $n\text{-Bu}_4\text{NBH}_4/\text{I}_2$  and  $n\text{-Bu}_4\text{NBH}_4/\text{PhCH}_2\text{Cl}$  reagent systems were developed for the generation of diborane gas (Chart 1).<sup>1-13</sup> Thus, the generated gas was complexed with Lewis bases such as THF,  $\text{S}(\text{CH}_3)_2$  and  $\text{N}(\text{Et}_2)\text{Ph}$  for further applications.

**Chart 1**



Recently, new synthetic methods were developed based on the carbon materials and borohydride reagent system for the preparation of Lewis base borane complexes and oxidative coupling of 2-naphthol to bi-2-naphthol (Scheme 1).<sup>14</sup>

**Scheme 1**

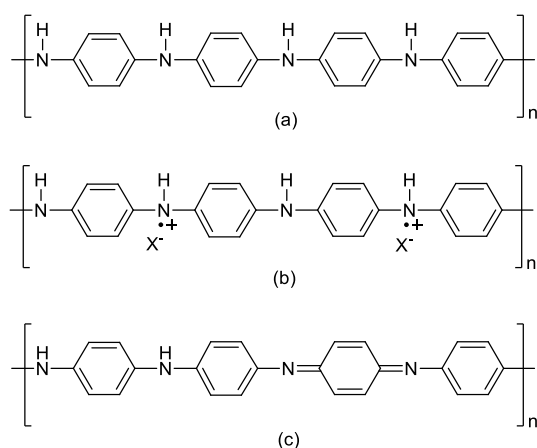


We have briefly investigated the use of polyaniline derivatives for such applications.

## III. 2 Results and Discussion

### III. 2.1 Synthesis of polyaniline derivatives

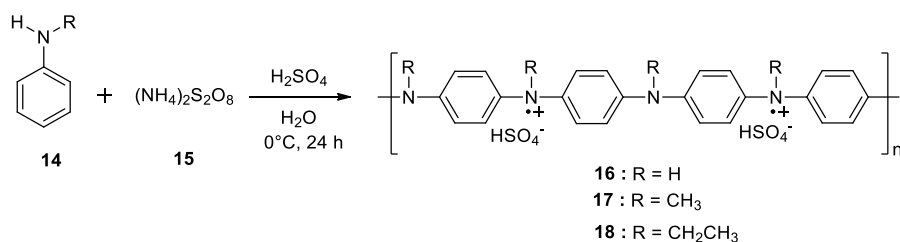
Over the last several decades, polyaniline has attracted continued research efforts due to its ease of preparation, environmental stability, conductivity and optical properties.<sup>15</sup> The existence of this polymer in various oxidation states such as completely reduced leucoemeraldine base (LEB), completely oxidized pernigraniline base (PNB) and partially oxidized emeraldine base (EB) prompted us to synthesize derivatives of polyaniline for application in oxidation-reduction reactions (Figure 1).<sup>16</sup>



**Figure 1**(a) leucoemeraldine base (b) emeraldine base (c) pernigraniline base

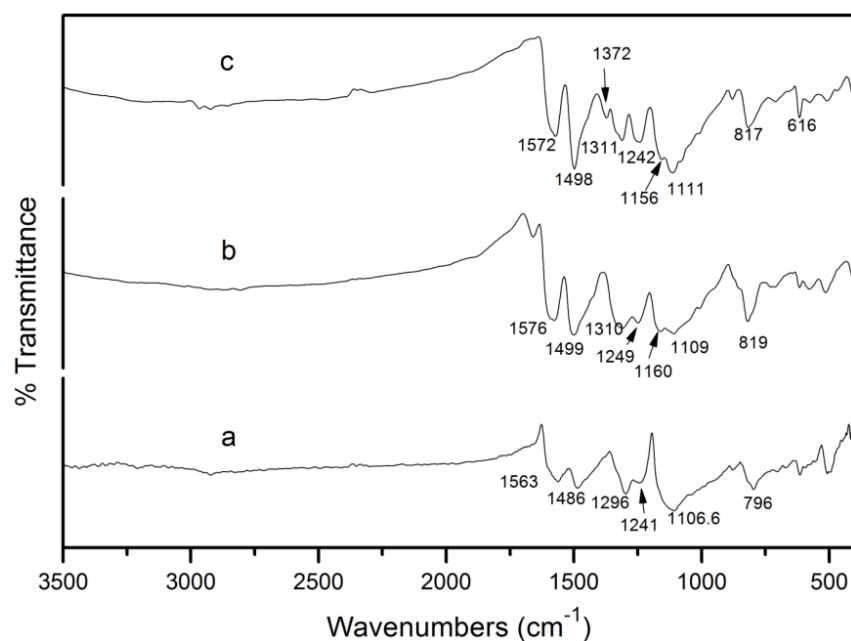
Generally, polyaniline derivatives are prepared from the corresponding monomer by either electrochemical polymerization or oxidative chemical polymerization.<sup>17</sup> We have decided to synthesis by oxidative chemical polymerization using  $(NH_4)_2S_2O_8$  as an oxidant (Scheme 2).<sup>17</sup>

Scheme 2

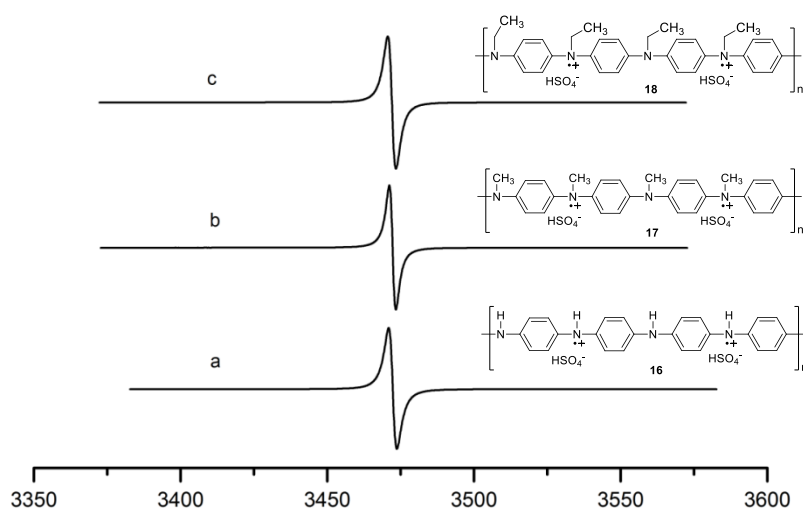


Accordingly, we have carried out the polymerization of 0.5 M aniline in 0.25 M solution of H<sub>2</sub>SO<sub>4</sub> using 0.5 M solution of (NH<sub>4</sub>)<sub>2</sub>S<sub>2</sub>O<sub>8</sub> for 24 h at 0 °C (Scheme 1). Thus, polyaniline (PANI) obtained in this way shows characteristic IR absorption at 1563 and 1486 cm<sup>-1</sup> that were attributed to the quinoid and benzenoid rings respectively. The absorption at 1296 and 1241 cm<sup>-1</sup> are assigned to  $\pi$ -electron delocalization and C-N<sup>+</sup> stretching. Further, absorption at 1106 and 796 cm<sup>-1</sup> are assigned to -NH<sup>+</sup>= and C-H out of plane deformation of 1,4-disubstituted benzene rings, have also been observed.<sup>18</sup> Similarly, poly(*N*-methylaniline) (PNMA) and poly(*N*-ethylaniline) (PNEA) have also been synthesized using 0.5 M solution of (NH<sub>4</sub>)<sub>2</sub>S<sub>2</sub>O<sub>8</sub> as oxidant for 24 h at 0-25 °C. The FT-IR spectra of PANI, PNMA and PNEA are presented in Figure 2.

The IR spectrum of PNMA also shows characteristic absorption for quinoid and benzenoid rings at 1576 and 1499 cm<sup>-1</sup> respectively. The FT-IR spectrum of PNMA has very close resemblance to that of the polyaniline. Poly(*N*-ethylaniline) showed better resolved peaks at 1311 and 1242 cm<sup>-1</sup>, which are assigned to  $\pi$ -electron delocalization and C-N<sup>+</sup> stretching in the case of polyaniline. We have also observed that these polymers exhibit one line esr signal with g value 2.00281, 2.00294 and 2.00286 respectively (Figure 3).<sup>19</sup>



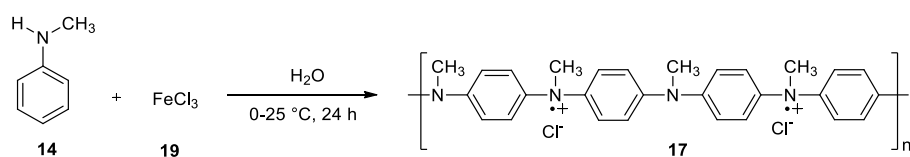
**Figure 2.** FT-IR Spectra of (a) polyaniline **16** (b) poly(*N*-methylaniline) **17** (c) poly(*N*-ethylaniline) **18** prepared using  $(\text{NH}_4)_2\text{S}_2\text{O}_8$ .



**Figure 3.** ESR spectra of radical cations of (a) polyaniline **16** (b) poly(*N*-methylaniline) **17** (c) poly(*N*-ethylaniline) **18** prepared using  $(\text{NH}_4)_2\text{S}_2\text{O}_8$ .

We have also prepared PNMA using  $\text{FeCl}_3$  as oxidant (Scheme 3).<sup>20</sup>

### Scheme 3





### III. 2.2 Preparation of Lewis base borane complexes using the PNMA/NaBH<sub>4</sub> system.

Although, in earlier reports only the structure **17** was proposed with the structure **20** as repeating unit, presence of other structures like **17a** and **17b** can not be ruled out (Figure 4). The structure **20** can be considered as a repeating unit of polymer to estimate the number of cation radical sites in the PNMA polymer. This would imply that 1 g of **17** would contain approximately 4.06 mmol of the repeating unit **20**.

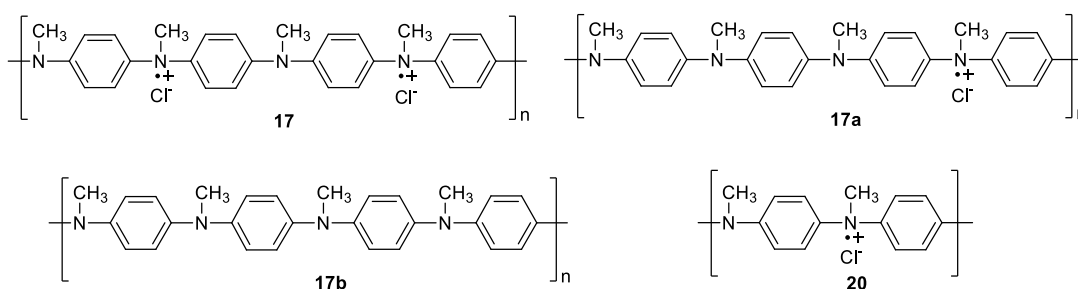
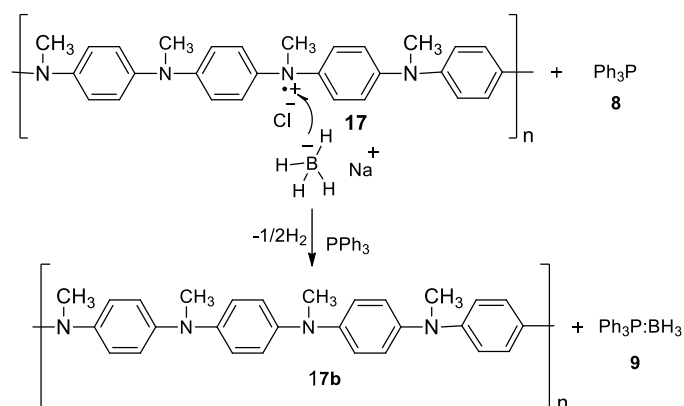


Figure 4

It was of interest to develop a method to estimate the number of radical cationic sites **20** in the poly(N-methylaniline) sample. Accordingly, we have carried out the reaction of NaBH<sub>4</sub> with PNMA in the presence of PPh<sub>3</sub> in THF and isolated the PPh<sub>3</sub>:BH<sub>3</sub> complex. A tentative mechanism for the formation of PPh<sub>3</sub>:BH<sub>3</sub> complexes can be considered involving the reduction of cation radical site by NaBH<sub>4</sub> by single electron transfer (SET) process to give PPh<sub>3</sub>:BH<sub>3</sub> and neutral polymer (Scheme 4).

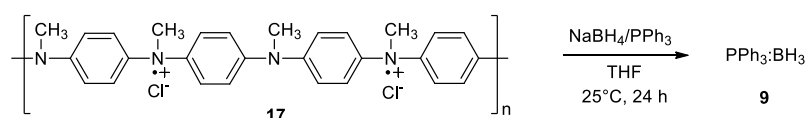
Scheme 4



When the reaction was carried out using PNMA (1 g, approximately 4.06 mmol of the cation radical **20**), NaBH<sub>4</sub> (5 mmol) and PPh<sub>3</sub> (5 mmol), PPh<sub>3</sub>:BH<sub>3</sub> (0.317 g, 1.15 mmol) was

isolated indicating the presence of only about 28% ( $1.15/4.06 \times 100$ ) of radical cation sites present in 1 g of the PNMA (Scheme 5).

### Scheme 5



We have also carried out the reaction using PNMA (2 g, 2.30 mmol cation radical sites) to obtain  $\text{PPh}_3:\text{BH}_3$  in 93% yield (Table 1, entry 1). Further, reactions using 3 and 4 g of PNMA gave  $\text{PPh}_3:\text{BH}_3$  with 87 and 72% yield respectively (Table 1, entry 2 and 3).

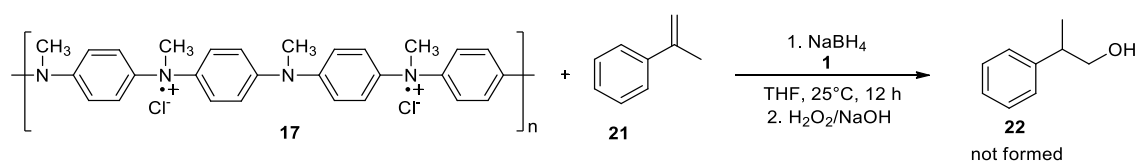
**Table 1.** Preparation of triphenyl phosphine-borane complex<sup>a</sup>

Entry	PNMA (g) (mmol radical cation sites)	$\text{PPh}_3$ (mmol)	$\text{NaBH}_4$ (mmol)	$\text{PPh}_3:\text{BH}_3$ Yield <sup>b,c</sup>
1	2 (2.30)	5	5	93
2	3(3.45)	5	5	87
3	4(4.60)	5	5	72

<sup>a</sup>All reactions were carried out using poly(*N*-methylaniline) (2 to 4 g),  $\text{PPh}_3$  (1.31 g, 5 mmol) and  $\text{NaBH}_4$  (0.189g, 5 mmol) in dry THF (20 mL). <sup>b</sup>Yields are of isolated products based on radical cation available for reaction with  $\text{NaBH}_4$ . <sup>c</sup>Products were characterized by spectral data (IR,  $^1\text{H}$ -NMR, and  $^{13}\text{C}$ -NMR).

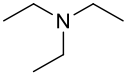
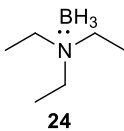
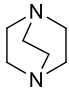
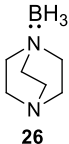
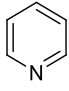
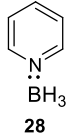
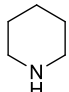
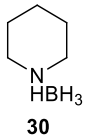
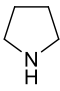
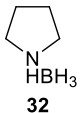
As discussed earlier that the  $\text{I}_2/\text{NaBH}_4$  system in THF hydroborates olefins. It was of interest to examine whether the PNMA/ $\text{NaBH}_4$  system would hydroborate olefins. In order to examine this possibility, we carried out an experiment using  $\alpha$ -methyl styrene as an olefin. Surprisingly, the corresponding alcohol was not isolated after  $\text{H}_2\text{O}_2/\text{NaOH}$  oxidation, indicating the expected PNMA- $\text{BH}_3$  complex does not hydroborates olefin (Scheme 6).

### Scheme 6



However, the reaction of PNMA with  $\text{NaBH}_4$  in the presence of amines gave the corresponding stable amine:borane complexes in 17-35% yield. The reaction is useful for the preparation of amine borane complexes from amines like triethylamine, DABCO, pyridine and aliphatic secondary amines. The results are presented in Table 2.

**Table 2.** Preparation of amine borane complex<sup>a</sup>

Entry	PNMA (g) (mmol radical cation sites)	Amine (mmol)	$\text{NaBH}_4$ (mmol)	Amine: Borane	Yield <sup>b,c</sup>
1	5 (5.75)	 23	5	 24	34
2	5 (5.75)	 25	5	 26	18
3	5 (5.75)	 27	5	 28	23
4	5 (5.75)	 29	5	 30	35
5	5 (5.75)	 31	5	 32	30

<sup>a</sup>All reactions were carried out using poly(*N*-methylaniline) (5 g), amine (5 mmol) and  $\text{NaBH}_4$  (5 mmol) in dry THF (20 mL). <sup>b</sup>Yields are of isolated products. <sup>c</sup>Products were characterized by spectral data (IR,  $^1\text{H}$ -NMR, and  $^{13}\text{C}$ -NMR).

### III. 3 Conclusions

---

We have developed a simple method for the synthesis of Lewis base:borane complexes using the PNMA/ $\text{NaBH}_4$  system. The borane complexes were obtained in moderate to good yields (72-93%). Although, the PNMA/ $\text{NaBH}_4$  system does not hydroborate olefins in THF, it is useful for the preparation of amine boranes in 17-35% yield. It is of interest to note that the triethyl amine borane is useful for hydroboration of olefins at  $>70^\circ\text{C}$ .

### III. 4 Experimental Section

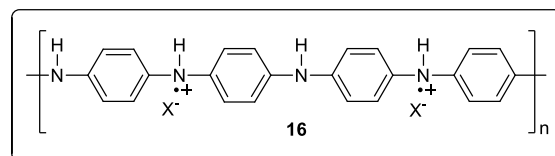
#### III. 4. 1 General informations

Most of the information given in the experimental section of the chapter 1 is also applicable to the experiments described in this chapter. Aniline, N-methyl aniline and N-ethyl aniline were purchased from commercial sources and distilled prior to experiments. The  $\text{NaBH}_4$ ,  $\text{Na}_2\text{S}_2\text{O}_8$  and  $\text{FeCl}_3$  reagents were purchased from commercial sources and were used as received. The THF was dried on sodium benzophenone-ketyl.

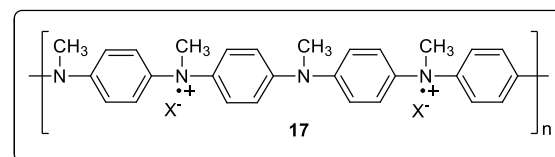
#### III. 4. 2 General procedure for the synthesis of polymer

To solution of aniline derivatives (150 mmol) in distilled water (250 mL) was added  $\text{Na}_2\text{S}_2\text{O}_8$  (35.7 g, 150 mmol) or  $\text{FeCl}_3$  (24.30 g, 150 mmol) dissolved in 150 mL water under open air. The reaction mixture was allowed to stir for 24 h at 25 °C and filtered. The collected polymer was washed several times using distilled water to remove the oxidant.

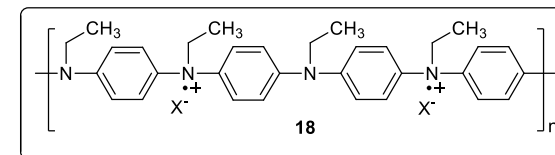
**IR (KBr)** : 1563, 1486, 1296, 1241,  
1106, 796  $\text{cm}^{-1}$



**IR (KBr)** : 1576, 1499, 1310, 1249,  
1160, 1109, 819  $\text{cm}^{-1}$



**IR (KBr)** : 1572, 1498, 1372, 1311, 1242,  
1156, 1111, 817, 616  $\text{cm}^{-1}$

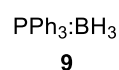


### III. 4. 3. General procedure for the synthesis of Lewis base-borane complexes

To a two neck reaction flask containing poly(N-methylaniline) and NaBH<sub>4</sub> in THF (20 mL) was added a Lewis base at 25 °C under N<sub>2</sub> atmosphere. The reaction mixture was allowed to stir for 24 h and filtered by using crucible. After removal of the solvent, the residue was subjected to chromatography on silica gel using 2-5% ethyl acetate in hexane to elute the corresponding borane complex.

#### Triphenylphosphine borane complex (9)

**Yield** : 0.590 g (66%); White solid



**<sup>1</sup>H NMR** : (400 MHz, CDCl<sub>3</sub>):  $\delta$  6.85-6.79 (m, 6H), 6.75-6.65 (m, 9H)

**<sup>13</sup>C NMR** : (100 MHz, CDCl<sub>3</sub>):  $\delta$  132.5, 132.4, 130.5, 128.7, 128.1, 127.9

**<sup>31</sup>P** : (162 MHz, CDCl<sub>3</sub>):  $\delta$  19.8

**<sup>11</sup>B** : (128.3 MHz, CDCl<sub>3</sub>):  $\delta$  -38.5

#### Triethylamine borane complex (24)

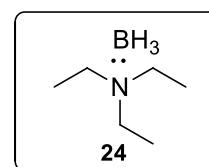
**Yield** : 0.230 g (34%)

**IR (Neat)** : 2953, 2389, 2334, 2268, 1391, 1161, 800 cm<sup>-1</sup>

**<sup>1</sup>H NMR** : (400 MHz, CDCl<sub>3</sub>):  $\delta$  2.79 (q,  $J$  = 8 Hz, 6H), 1.19 (t,  $J$  = 8 Hz, 9H)

**<sup>13</sup>C NMR** : (100 MHz, CDCl<sub>3</sub>):  $\delta$  52.3, 8.6

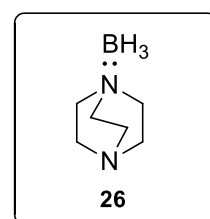
**<sup>11</sup>B** : (128.3 MHz, CDCl<sub>3</sub>):  $\delta$  -13.8



#### DABCO borane complex (26)

**Yield** : 0.135 g (18%); White solid

**IR (KBr)** : 2950, 2381, 2333, 2262, 1393, 1164, 807 cm<sup>-1</sup>



**$^1\text{H}$  NMR** : (400 MHz,  $\text{CDCl}_3$ ):  $\delta$  2.21-2.18 (m, 12 H)

**$^{13}\text{C}$  NMR** : (100 MHz,  $\text{CDCl}_3$ ):  $\delta$  50.9, 45.5

**$^{11}\text{B}$**  : (128.3 MHz,  $\text{CDCl}_3$ ):  $\delta$  -12.2

**Pyridine borane complex (28)**

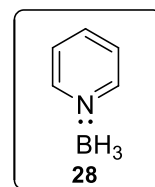
**Yield** : 0.125 g (23%)

**IR (Neat)** : 2964, 2389, 2334, 2268, 1391, 1161, 800  $\text{cm}^{-1}$

**$^1\text{H}$  NMR** : (400 MHz,  $\text{CDCl}_3$ ): 8.52 (s, 2H), 7.91 (s, 2H), 7.52 (s, 1H)

**$^{13}\text{C}$  NMR** : (100 MHz,  $\text{CDCl}_3$ ):  $\delta$  147.3, 134.3, 125.4

**$^{11}\text{B}$**  : (128.3 MHz,  $\text{CDCl}_3$ ):  $\delta$  -12.0



**Piperidine borane complex (30)**

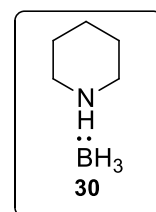
**Yield** : 0.204 g (35%); White solid

**IR (Neat)** : 3189, 2936, 2383, 2339, 2317, 2257, 1452, 1172,  
876  $\text{cm}^{-1}$

**$^1\text{H}$  NMR** : (400 MHz,  $\text{CDCl}_3$ ):  $\delta$  3.80 (brs, 1H), 3.23 (d,  $J$  = 8 Hz, 2H), 2.53-2.47  
(m, 2H), 1.78- 1.48 (m, 6H)

**$^{13}\text{C}$  NMR** : (100 MHz,  $\text{CDCl}_3$ ):  $\delta$  53.3, 25.3, 22.5

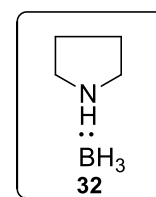
**$^{11}\text{B}$**  : (128.3 MHz,  $\text{CDCl}_3$ ):  $\delta$  -15.0.



**Pyrrolidine borane complex (32)**

**Yield** : 0.144 g (30%)

**IR (Neat)** : 3227, 2931, 2854, 2389, 2356, 2279, 1452,



1358, 1331, 1276, 1161, 1134, 1106  $\text{cm}^{-1}$

**$^1\text{H}$  NMR** : (400 MHz,  $\text{CDCl}_3$ ):  $\delta$  3.28-3.25 (m, 2H), 2.79-2.74 (m, 2H),

2.03-1.91 (m, 2H), 1.85-1.79 (m, 2H)

**$^{13}\text{C}$  NMR** : (100 MHz,  $\text{CDCl}_3$ ):  $\delta$  54.2, 24.6

**$^{11}\text{B}$**  : (128.3 MHz,  $\text{CDCl}_3$ ):  $\delta$  -15.1

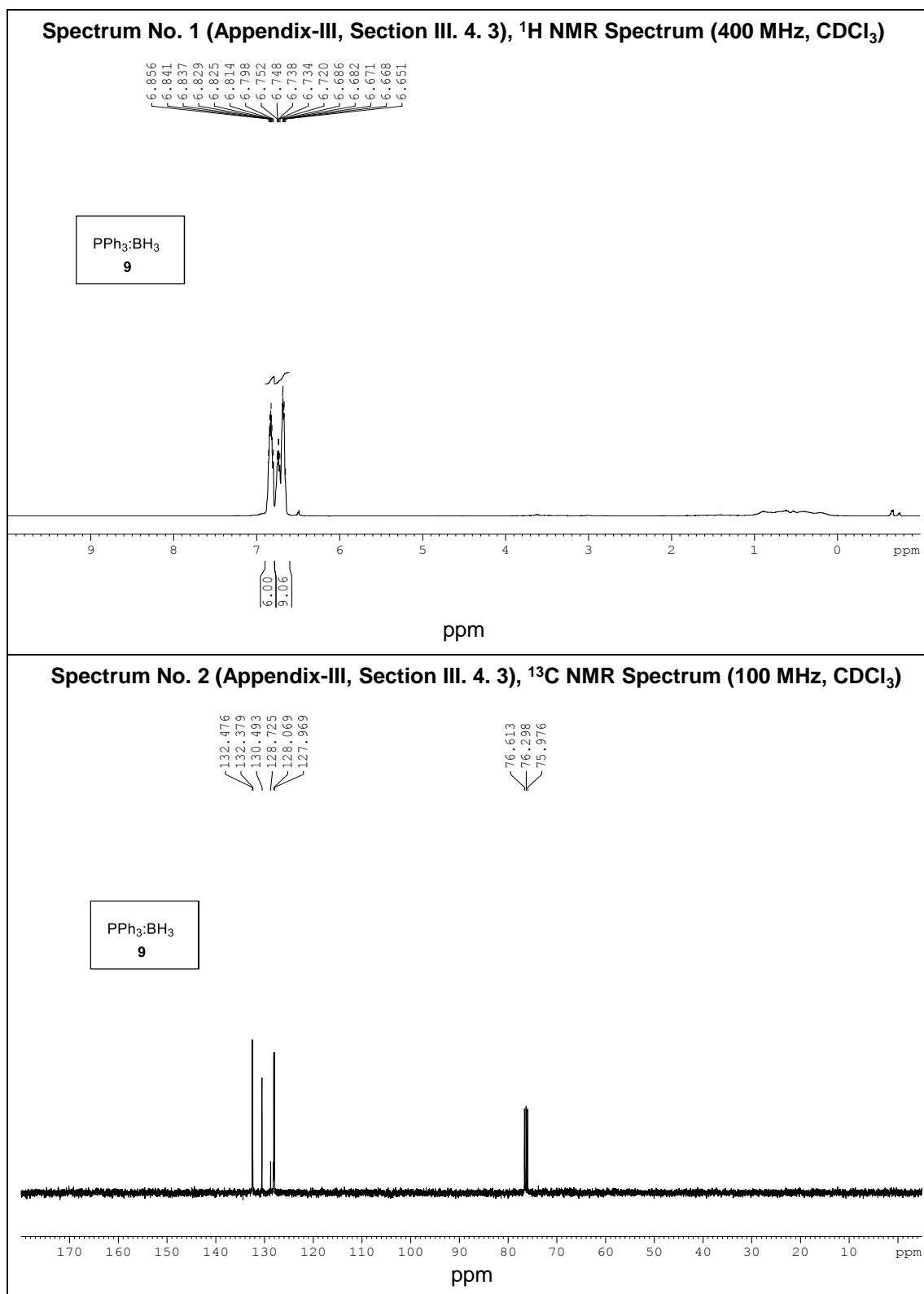


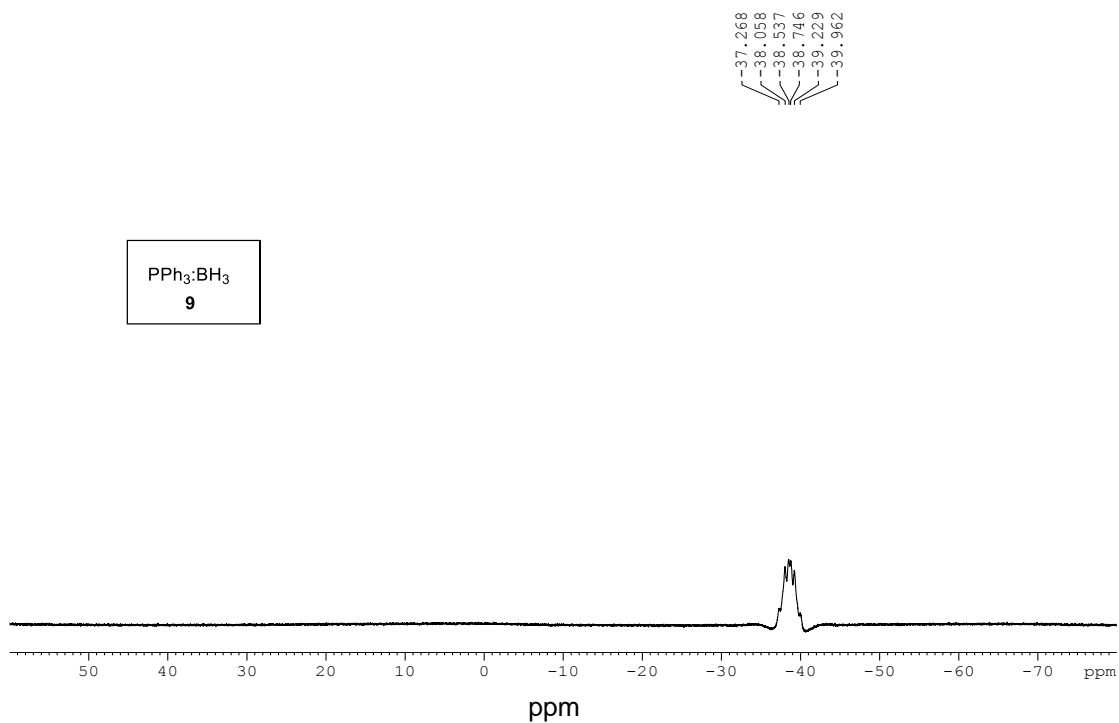
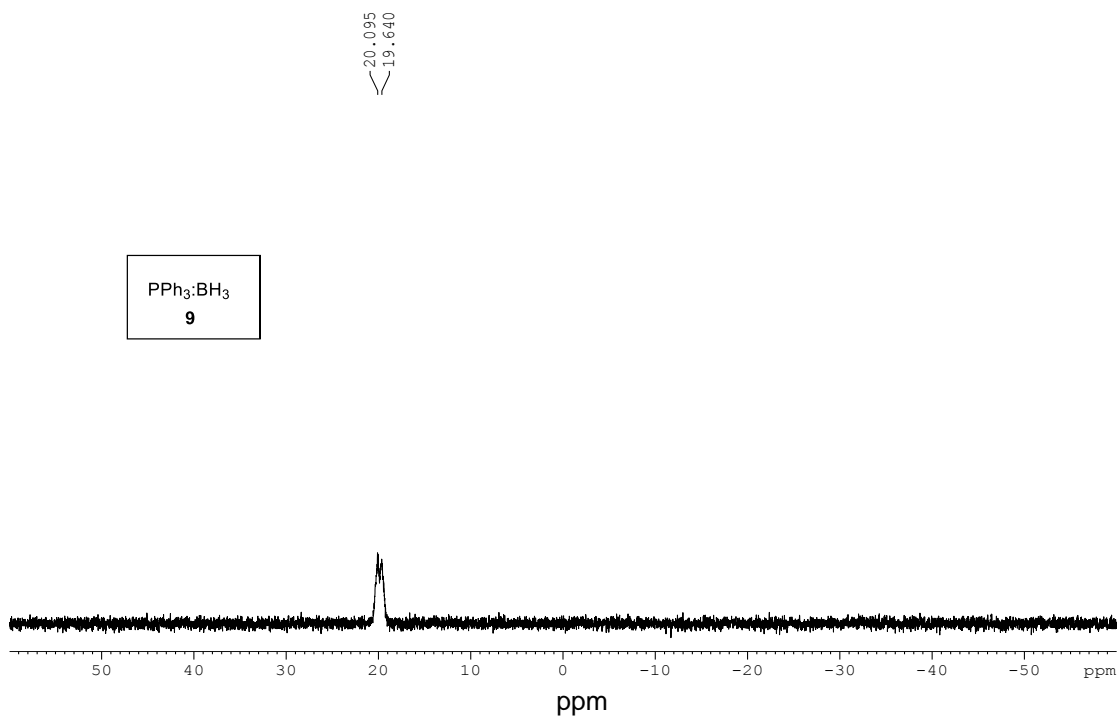
### III. 5 References

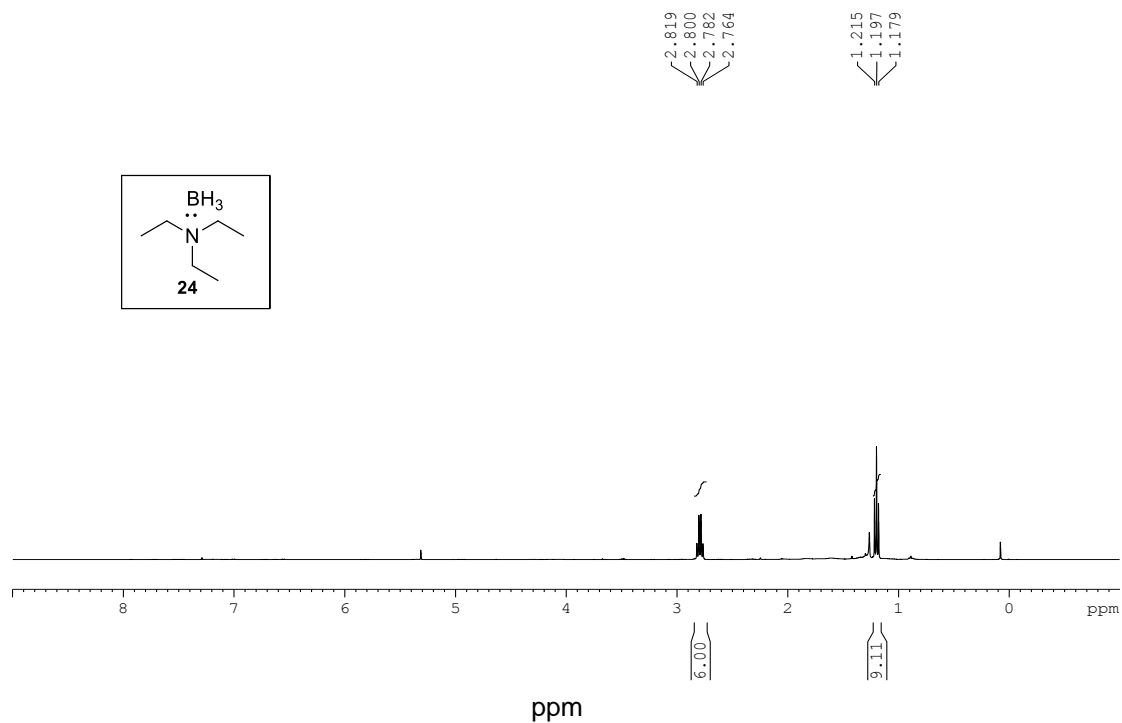
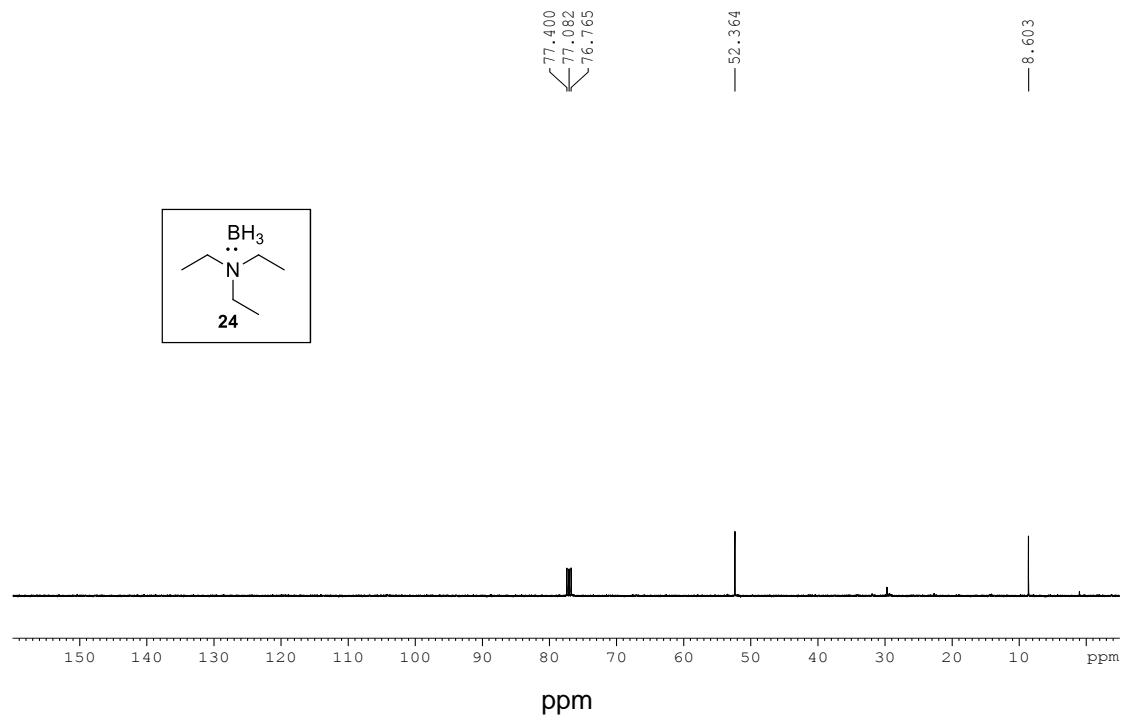
---

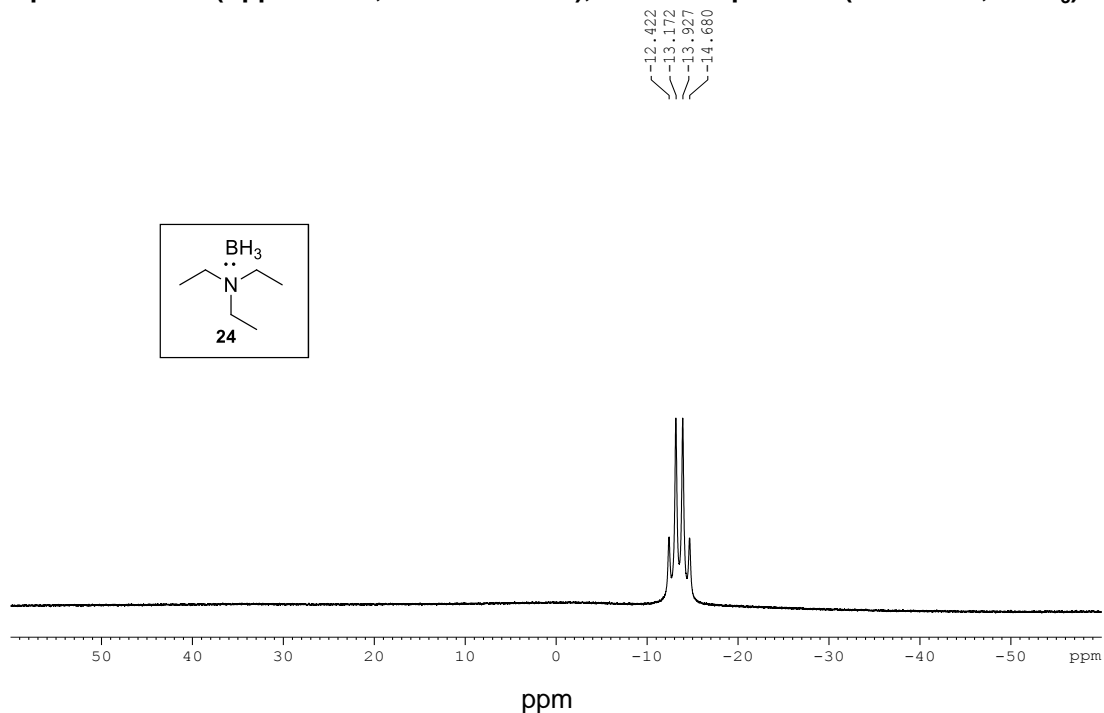
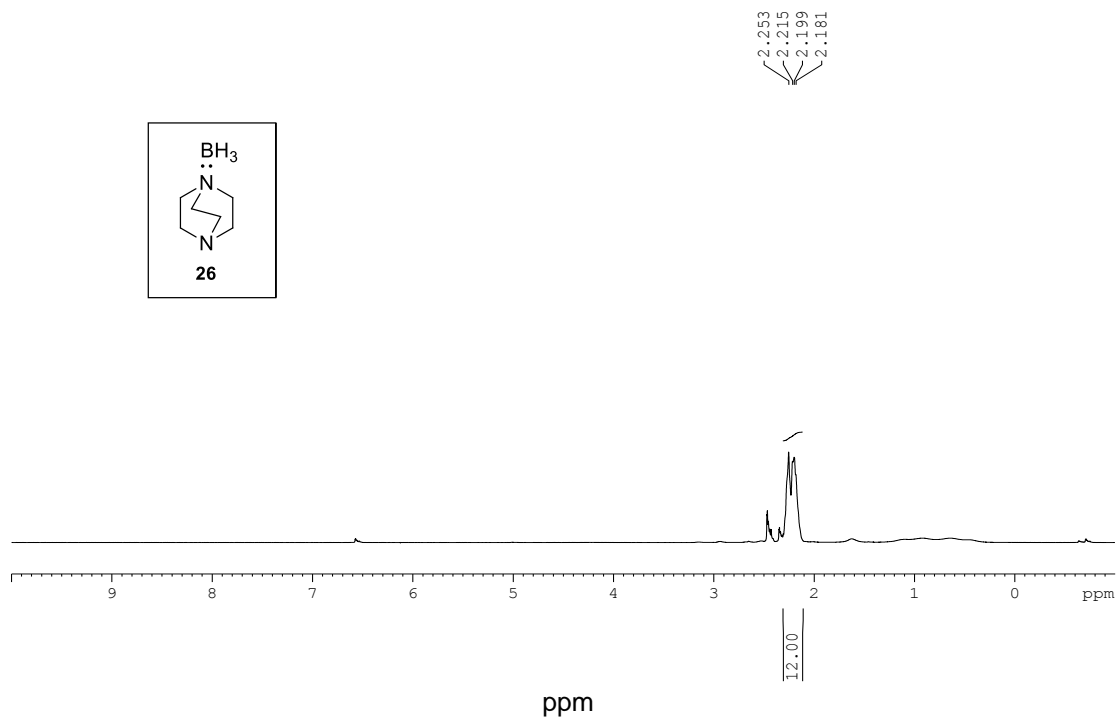
1. Freeguard, G. F.; Long, L. H. *Chem. Ind.*, **1965**, 471.
2. Narayana, C.; Periasamy, M. *J. Organomet. Chem.*, **1987**, 323, 145.
3. Periasamy, M.; Muthukumaragopal, G. P.; Sanjeevakumar, N. *Tetrahedron Lett.* **2007**, 48, 6966.
4. Narayana, C.; Periasamy, M. *Chem. Commun.* **1987**, 1857.
5. Periasamy, M.; Kishan Reddy, Ch.; Bhaskar Kanth, J. V. *J. Indian Inst. Sci.* **1994**, 74, 149.
6. Anwar, S.; Periasamy, M. *Tetrahedron: Asymmetry* **2006**, 17, 3244.
7. Bhaskar Kanth, J. V.; Periasamy, M. *J. Org. Chem.* **1991**, 56, 5964.
8. Kanth, J. V. B.; Periasamy, M. *J. Chem. Soc. Chem. Commun.*, **1990**, 1145.
9. Reddy, Ch. K.; Kanth, J. V. B.; Periasamy, M. *Synth. Commun.* **1994**, 243, 313.
10. Reddy, Ch. K.; Periasamy, M. *Tetrahedron Lett.* **1990**, 31, 1919.
11. Reddy, Ch. K.; Periasamy, M. *Tetrahedron Lett.* **1989**, 30, 5663.
12. Reddy, Ch. K.; Periasamy, M. *Tetrahedron* **1992**, 48, 8329.
13. Periasamy, M. *Current Science* **1995**, 68, 883.
14. a) Reddy, P. O. Ph. D. Thesis **2014**, University of Hyderabad. b) Periasamy, M.; Shanmugaraja, M.; Ramusagar, M. *unpublished results*.
15. a) MacDiarmid, A. G.; Chiang, J. C.; Richter, A. F.; Epstein, A. J. *Synth. Met.* **1987**, 18, 285. b) Kang, E. T.; Neoh, K. G.; Tan, K. L. *Surf. Interf. Anal.* **1992**, 19, 33. c)

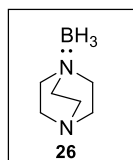
- Golczak, S.; Kanciurzevska, A.; Fahlman, M.; Langer, K.; Langer, J. J. *Solid State Ionics* **2008**, 179, 2234. d) Wessling, B. *Synth. Met.* **1998**, 93, 143.
16. MacDiarmid, A. G.; Epstein, A. J. *Faraday Discuss. Chem. Soc.* **1989**, 88, 317.
17. a) Willstatter, R.; Dorogi, S. *Ber.* **1909**, 42, 4118. b) Mohilner, D. M.; Adams, R. N. Argersinger, W. J. *J. Am. Chem. Soc.* **1962**, 84, 3618
18. Trchova, M.; Sedenkova, I.; Tobolkova, E.; Stejskal, J. *Polym Degrad Stab.* **2004**, 86, 179.
19. Watanabe, A.; Mori, K.; Iwabuchi, A.; Iwasaki, Y.; Nakamura, Y.; Ito, O. *Macromolecules* **1989**, 22, 3521.
20. Davied, S.; Nicolau, Y. F.; Melis, F.; Revillon, A. *Synth Met.* **1995**, 69 125.



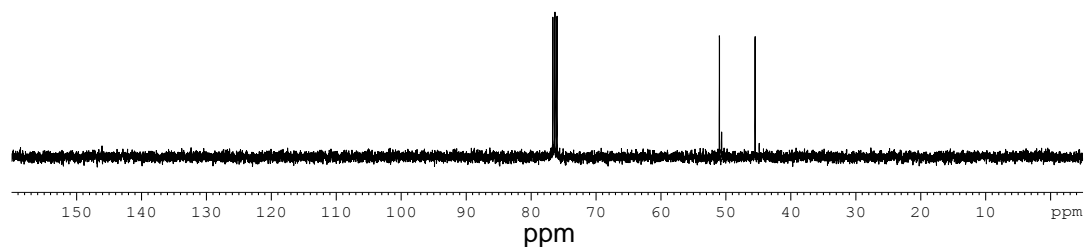
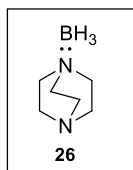
**Spectrum No. 3 (Appendix-III, Section III. 4. 3),  $^{11}\text{B}$  NMR Spectrum (128.3 MHz,  $\text{CDCl}_3$ )****Spectrum No. 4 (Appendix-III, Section III. 4. 3),  $^{31}\text{P}$  NMR Spectrum (162 MHz,  $\text{CDCl}_3$ )**

**Spectrum No. 5 (Appendix-III, Section III. 4. 3),  $^1\text{H}$  NMR Spectrum (400 MHz,  $\text{CDCl}_3$ )****Spectrum No. 6 (Appendix-III, Section III. 4. 3),  $^{13}\text{C}$  NMR Spectrum (100 MHz,  $\text{CDCl}_3$ )**

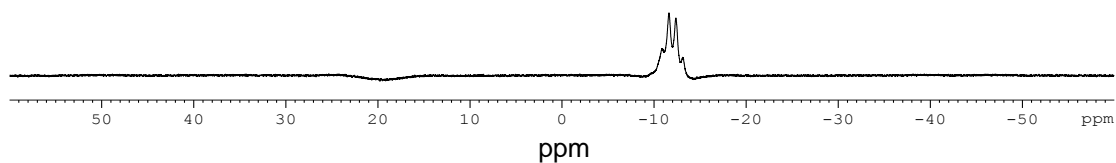
**Spectrum No. 7 (Appendix-III, Section III. 4. 3),  $^{11}\text{B}$  NMR Spectrum (128.3 MHz,  $\text{CDCl}_3$ )****Spectrum No. 8 (Appendix-III, Section III. 4. 3),  $^1\text{H}$  NMR Spectrum (400 MHz,  $\text{CDCl}_3$ )**

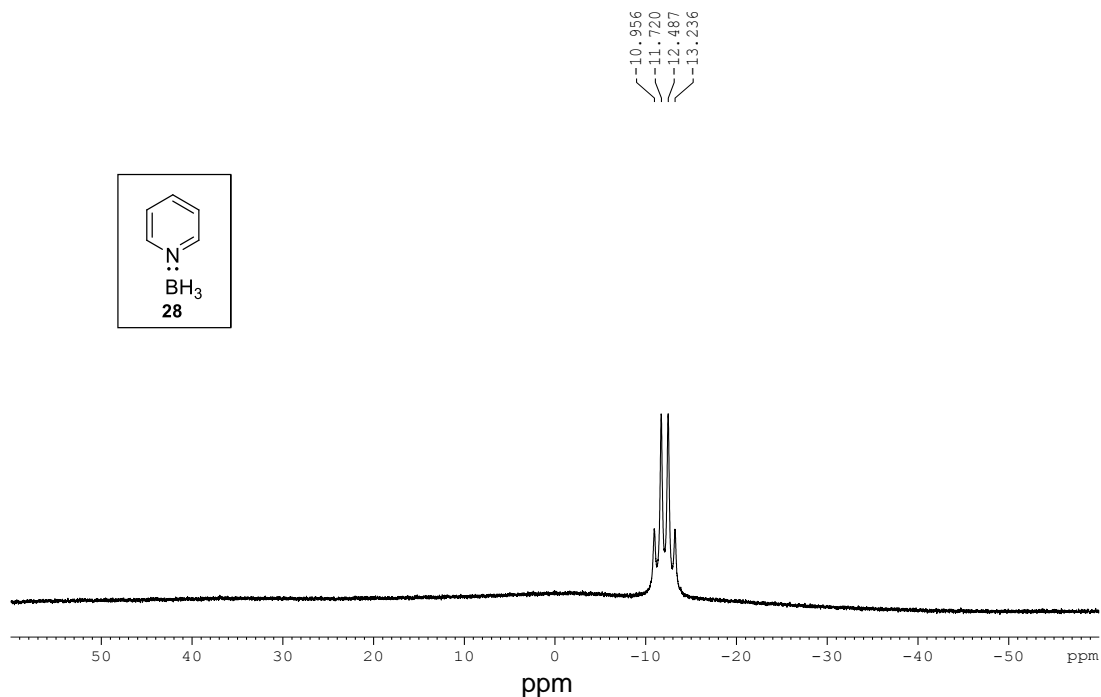
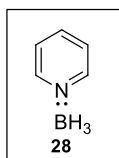
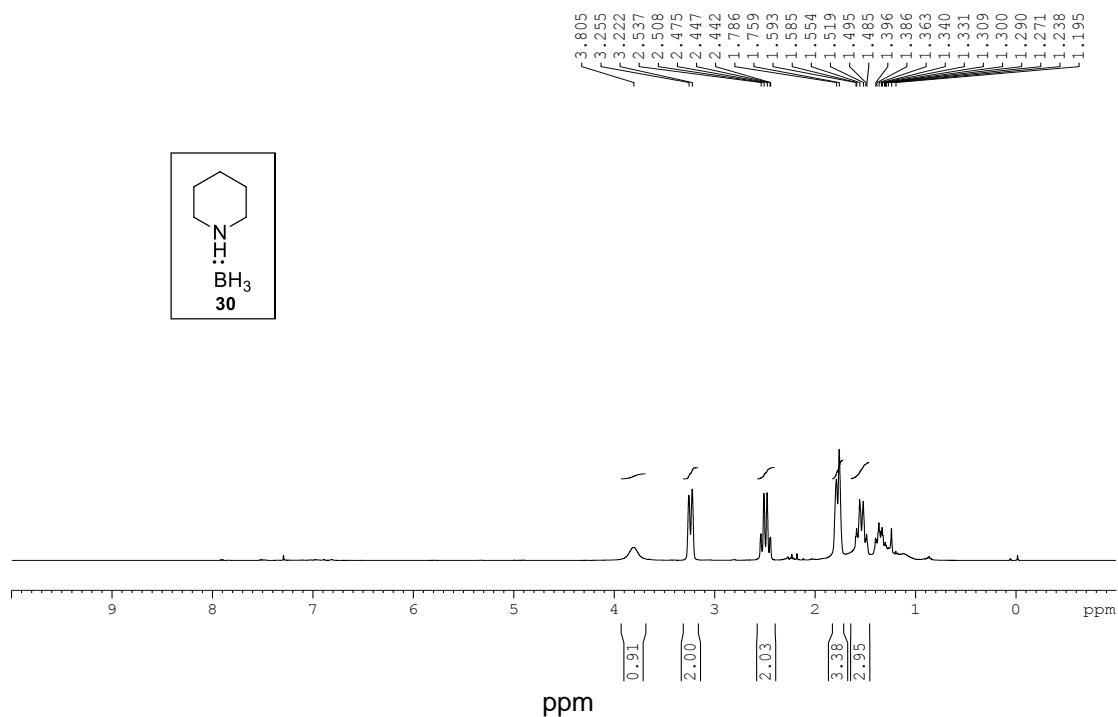
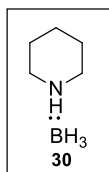
**Spectrum No. 9 (Appendix-III, Section III. 4. 3),  $^{13}\text{C}$  NMR Spectrum (100 MHz,  $\text{CDCl}_3$ )**

76.645  
76.326  
76.006  
50.986  
45.497

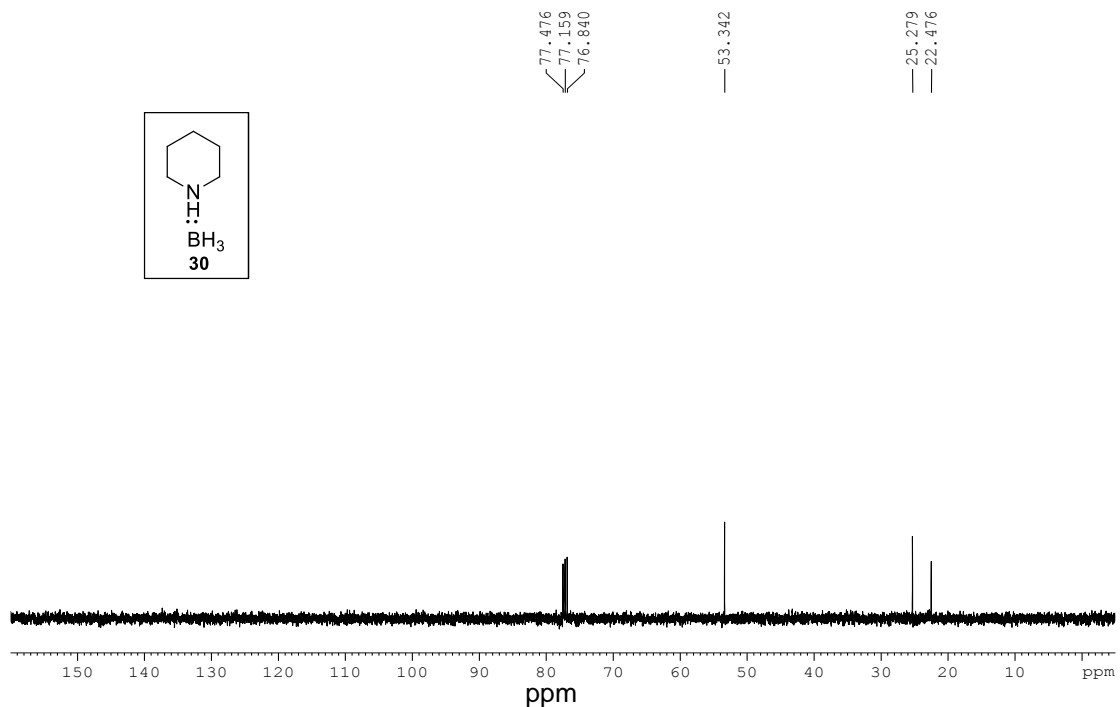
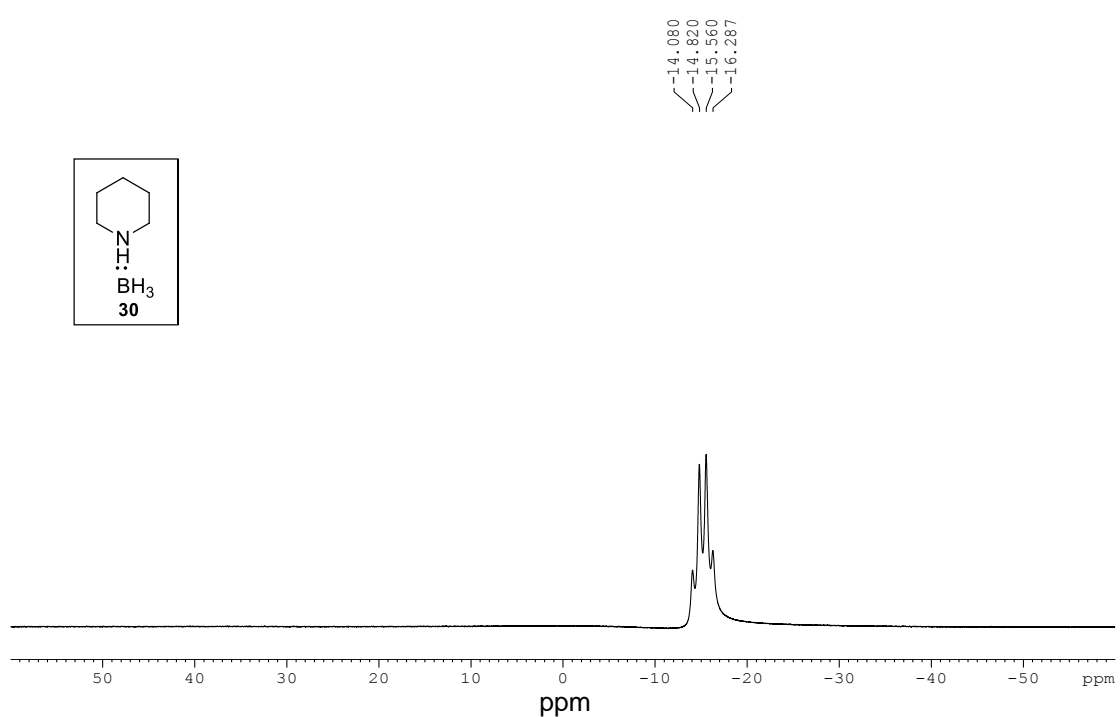
**Spectrum No. 10 (Appendix-III, Section III. 4. 3),  $^{11}\text{B}$  NMR Spectrum (128.3 MHz,  $\text{CDCl}_3$ )**

-10.917  
-11.624  
-12.399  
-13.116



**Spectrum No. 11 (Appendix-III, Section III. 4. 3),  $^{11}\text{B}$  NMR Spectrum (128.3 MHz,  $\text{CDCl}_3$ )****Spectrum No. 12 (Appendix-III, Section III. 4. 3),  $^1\text{H}$  NMR Spectrum (400 MHz,  $\text{CDCl}_3$ )**



**Spectrum No. 13 (Appendix-III, Section III. 4. 3),  $^{13}\text{C}$  NMR Spectrum (100 MHz,  $\text{CDCl}_3$ )****Spectrum No. 14 (Appendix-III, Section III. 4. 3),  $^{11}\text{B}$  NMR Spectrum (128.3 MHz,  $\text{CDCl}_3$ )**

### List of publications

1. Synthesis of new derivatives from a Tröger base *via* exchange of the methano bridge with carbonyl compounds; Periasamy, M.; **Suresh, S.**; Satishkumar, S.; *Tetrahedron: Asymmetry* **2012**, 22,108.
2. Convenient methods for the Synthesis of Chiral Amino Alcohol and Amines; Periasamy, M.; Gurubrahamam, R.; Sanjeevakumar, N.; Dalai, M.; Laxhmaiah, A.; Reddy, P. O.; **Suresh, S.**; Satishkumar, S.; Padmaja, M.; Reddy, M. N; Suresh, S.; Anwar, S.; Muthukumaragopal, G. P.; Vairaprakash, P.; Seenivasaperumal, M.; *Chimia* **2013**, 67, 23.
3. Synthesis of enantiopure 2,4,8,10-tetrasubstituted Tröger base derivatives; **Suresh, S.**; Periasamy, M. *Tetrahedron: Asymmetry* **2015**, 26, 203.
4. Resolution of *ortho*-methoxy-substituted Tröger base derivative; **Suresh, S.**; Periasamy, M. (to be communicated).
5. Reaction of Tröger base with aryne intermediates; **Suresh, S.**; Periasamy, M. (to be communicated).
6. Stereoselective exchange of methylene bridge of *ortho*-methyl Tröger base with formamides, **Suresh, S.**; Periasamy, M. (to be communicated).
7. Synthesis of Lewis base-borane complexes using PNMA/NaBH<sub>4</sub> reagent system; **Suresh, S.**; Periasamy, M. (to be communicated).

### Poster/Paper presented in symposia

1. Synthesis of new derivatives from a Tröger base via exchange of the methano bridge with carbonyl compounds; **Suresh.; S** Periasamy, M. Oral presentation in the “8<sup>th</sup> J-NOST” national symposium held at IIT Guwahati, Dec 2012.
2. Synthesis and resolution of Tröger base derivatives; **Suresh.; S** Periasamy, M. Oral presentation in the *Chemfest 2013* held at School of Chemistry, University of Hyderabad.
3. Synthesis and resolution of Tröger base derivatives; **Suresh.; S** Periasamy, M. Poster presentation in the *Chemfest 2013* held at School of Chemistry, University of Hyderabad.